Vol. 58 JANUARY, 1954 No. 1

259-

THE JOURNAL OF PHYSICAL CHEMISTRY

(Registered in U. S. Patent Office)

SYMPOSIUM ON THE CHEMISTRY OF CERTAIN LESS FAMILIAR ELEMENTS

THE JOURNAL OF PHYSICAL CHEMISTRY will appear monthly in 1954
After January 1, 1954, Notes and Communications to the Editor
will be accepted for publication.

THE JOURNAL OF PHYSICAL CHEMISTRY

(Registered in U. S. Patent Office)

Published monthly by the American Chemical Society at 20th and Northampton Sts., Easton, Pa.

Entered as second-class matter at the Post Office at Easton, Pennsylvania.

The *Journal of Physical Chemistry* is devoted to the publication of selected symposia in the broad field of physical chemistry and to other contributed papers.

Manuscripts originating in the British Isles, Europe and Africa should be sent to F. C. Tompkins, The Faraday Society, 6 Gray's Inn Square, London W. C. 1, England.

Manuscripts originating elsewhere should be sent to W. Albert Noyes, Jr., Department of Chemistry, University of Rochester, Rochester 3, N. Y.

Correspondence regarding accepted copy, proofs and reprints should be directed to Assistant Editor, Allen D. Bliss, Department of Chemistry, Simmons College, 300 The Fenway, Boston 15, Mass.

Business Office: American Chemical Society, 1155 Sixteenth St. N. W., Washington 6, D. C.

Advertising Office: American Chemical Society, 332 West 42nd St., New York 36, N. Y.

Articles must be submitted in duplicate, typed and double spaced. They should have at the beginning a brief Abstract, in no case exceeding 300 words. Original drawings should accompany the manuscript. Lettering at the sides of graphs (black on white or blue) may be pencilled in, and will be typeset. Figures and tables should be held to a minimum consistent with adequate presentation of information. Photographs will not be printed on glossy paper except by special arrangement. All footnotes and references to the literature should be numbered consecutively and placed on the manuscript at the proper places. Initials of authors referred to in citations should be given. Nomenclature should conform to that used in *Chemical Abstracts*, mathematical characters marked for italic, Greek letters carefully made or annotated, and subscripts and superscripts clearly shown. Articles should be written as briefly as possible consistent with clarity and should avoid historical background unnecessary for specialists.

Symposium papers should be sent in all cases to Secretaries of Divisions sponsoring the symposium, who will be responsible for their transmittal to the Editor. The Secretary of the Division by agreement with the Editor will specify a time after which symposium papers cannot be accepted. The Editor reserves the right to refuse to publish symposium articles, for valid scientific reasons. Each symposium paper may not exceed four printed pages (about sixteen double spaced typewritten pages) in length except by prior arrangement with the Editor.

Remittances and orders for subscriptions and for single copies, notices of changes of address and new professional connections, and claims for missing numbers should be sent to the American Chemical Society, 1155 Sixteenth St., N. W., Washington 6, D. C. Changes of address for the *Journal of Physical Chemistry* must be received on or before the 30th of the preceding month.

Claims for missing numbers will not be allowed (1) if received more than sixty days from date of issue (because of delivery hazards, no claims can be honored from subscribers in Central Europe, Asia, or Pacific Islands other than Hawaii), (2) if loss was due to failure of notice of change of address to be received before the date specified in the preceding paragraph, or (3) if the reason for the claim is "missing from files."

Subscription Rates: to members of the American Chemical Society, $8.00 for 1 year, $15.00 for 2 years, $22.00 for 3 years; to nonmembers, $10.00 for 1 year, $18.00 for 2 years, $26.00 for 3 years. Postage free to countries in the Pan American Union; Canada, $0.40; all other countries, $1.20. Single copies, $1.25; foreign postage, $0.15; Canadian postage $0.05.

THE JOURNAL OF
PHYSICAL CHEMISTRY
(Registered in U. S. Patent Office) (Copyright, 1954, by the American Chemical Society)

VOLUME 58 JANUARY 22, 1954 NUMBER 1

THE UNCATALYZED EXCHANGE OF Cl^- AND $AuCl_4^-$

BY RONALD L. RICH[1] AND HENRY TAUBE

Contribution from the George Herbert Jones Laboratories of the University of Chicago

Received May 26, 1953

The rate law for the reaction carrying exchange between $AuCl_4^-$ and Cl^- is $R = k_1(AuCl_4^-) + k_2(AuCl_4^-)(Cl^-)$. Neither k_1 nor k_2 depend on acidity, but a term depending on acidity enters when this is made sufficiently small. The values of E corresponding to the two paths are 4.5 and 16.5 kcal., respectively, and of pz are 10^3 min.$^{-1}$ and 2×10^{14} l. mole^{-1} min.$^{-1}$, respectively. The mechanism corresponding to the second term is of the S_N2 type. The mechanism corresponding to the first term may also be, but is not proven to be of the S_N2 type, nor is its relation to the rate of net hydrolysis settled.

Introduction

Kinetic studies on substitution reactions with complex ions have for the most part been conducted only for hexa-coördinated ions. Even in this field evidence contributing to a definite conclusion about mechanism has been presented only in a few cases. For square planar complex ions, which would seem to afford most interesting possibilities for composition and configuration of the activated complex, not only proofs of mechanism but even rate laws are lacking although there has been considerable speculation about mechanisms.

The kinetic data offered here for the reaction $AuCl_4^- + Cl^{*-} \rightarrow AuCl_4^{*-} + Cl^-$ make a beginning in this field. Some advantages of an exchange process in measuring the lability of a chemical system already have been discussed.[2] An additional feature of interest is that although the exchange may proceed by a path which involves ordinary chemical reactions (for example, exchange carried by a hydrolytic equilibrium), paths may exist which can be discovered only by the use of labeled atoms. The significance of these paths for the field of reaction kinetics and mechanisms is as great as that of the ordinary chemical paths.

Reagents.

Water.—It was found that ordinary distilled water, except in the precipitant solutions, induced some initial exchange. Therefore redistilled water was used in all but the earlier experiments.

$RbAuCl_4$.—The rubidium salt was used because of its fair solubility and its ease of recrystallization. Pure $HAuCl_4 \cdot 3H_2O$ and a 50% excess of C.P. RbCl were dissolved in hot water with subsequent cooling by ice. The resulting crystals of $RbAuCl_4$ were dissolved in hot water and the solution was filtered through a sintered glass filter while hot. After slow cooling and crystallization the excess solution was removed by suction and the $RbAuCl_4$ was dried at 110°. 4.244 g. of $RbAuCl_4$ and 2 ml. of 0.502 *f* HCl (to repress hydrolysis) were diluted to 100 ml. of stock solution 0.01004 *f* in HCl and presumably 0.1000 *f* in $RbAuCl_4$. By addition of excess KI to a portion of the stock and titration of the triiodide with thiosulfate the $RbAuCl_4$ was found to be 0.0992 *f*.

Other Salts and Acids.—Concentrated A.R. HCl, HNO_3, H_2SO_4 and $HClO_4$ were diluted to the desired volume and titrated with NaOH or Na_2CO_3. Solutions of NaCl, KNO_3 and $NaNO_3$ were similarly prepared from the purest salts with concentrations calculated from the weights taken.

Radioactive Chloride.—The Atomic Energy Commission at Oak Ridge supplied a sample of hydrochloric acid described as 1.2 ml. at 1.66 *f* concentration containing 10 microcuries of Cl^{36} (analysis showed the concentration of acid to be almost twice that stated.) This isotope emits 0.66 Mev. β-rays and has a half-life of about 10^5 years. The solution was diluted altogether about 1000-fold to give stock solutions. Experiments 1.13, 1.14 and 1.21 included 0.00122 *f* HCl from this source. Experiments 1.15, 1.22 and 1.23 similarly included 0.00106 *f* active HCl. Experiments 1.11 and 1.12 included 0.00070 *f* active HCl from an older source.

Precipitants.—Separation of chloroaurate and chloride at the end of exchange experiments was accomplished by precipitating the former as salt, $(C_6H_5)_4AsAuCl_4$. The precipitant used first, $((C_6H_5)_4As)_2SO_4$, was prepared by heating 100 g. of $(C_6H_5)_4AsCl$ with 40 ml. of concd. H_2SO_4 on the steam-bath until complete evolution of HCl and liquefaction, and by subsequent crystallizations with an addition of $BaCO_3$ to change bisulfate to sulfate. A later experiment (to determine whether coprecipitation of chloride was causing zero time exchange to appear larger than zero) showed

---

[1] Atomic Energy Commission Predoctoral Fellow.

[2] H. Taube, *Chem. Revs.*, **50**, 76 (1952).

that even 0.5 *f* NaCl in the precipitant had a negligible effect on results. Thereafter $(C_6H_5)_4AsCl$ was used as the precipitant in about twice the concentration required by stoichiometry. Saturated C.P. $MgSO_4$ was usually used as a coagulant.

Experimental Procedure.

The Exchange Experiments.—Nearly all except the earlier experiments were carried out as follows. The reaction vessels were round-bottom 50-ml. flasks which had been partially divided, after heating the bottom of the bulb, by pushing in with the edge of a triangular file. On one side of the division was placed a total of 3 ml. of solutions containing the chloroaurate and acids or salts (HCl, NaCl, HNO_3 except where indicated otherwise) to adjust the chloride concentration, acidity and ionic strength. On the other side was placed 1 ml. of active HCl. The bulb of the (stoppered) flask was then immersed in ice and water or in water at 10 or 20°. After 15 minutes, found to be more than adequate for complete cooling, the vessel was shaken from side to side a few times to mix the solutions at time 0. At time *t* a mixture of 1 ml. of saturated $MgSO_4$ and 1 ml. of the precipitant was poured in, with immediate shaking to quench the reaction. This mixture was previously cooled for 10 minutes (to 0°) in a small glass tube whose surface had been exposed to the vapor of Dri-Film, coating the tube with a water repellent silicone layer that provided a reproducible pouring volume. The precipitated mixture was quickly filtered through porous porcelain crucibles and the filtrate was collected for counting of activity. The magnesium sulfate appeared to improve the filtering speed greatly, at least at 0°. Only one result, and that obtained by the slower centrifugation rather than filtration, indicated exchange between precipitate and solution.

The radioactivity of the filtrates was determined directly in a solution counter having a very thin glass wall between the solution and the counting chamber. The counting efficiency was about 5%. It was necessary neither to have quite complete filtration nor to dilute the filtrate since the counter tube required only 4.5 ml. of solution. Loss of counts due to coincidence was negligible with the counter used. Counting was long enough to give a standard deviation less than 1% of the count. After subtraction of background and the value found for "infinite" time the results were usually plotted *versus* time on semilog graph paper and half-times were determined graphically. Measurements of time were made with a stop watch, times 0 and *t* being taken, respectively, at the beginning of mixing and at the beginning of pouring of the precipitant.

The very insoluble $(C_6H_5)_4AsAuCl_4$ in the filtering crucibles was reduced to Au with $N_2H_5HSO_4$ and Na_2CO_3 and then removed with aqua regia. The reaction flasks were also treated first with a hydrazine solution but then with the usual dichromate cleaning solution. The counter tube was rinsed with water, methanol, ether and a current of air.

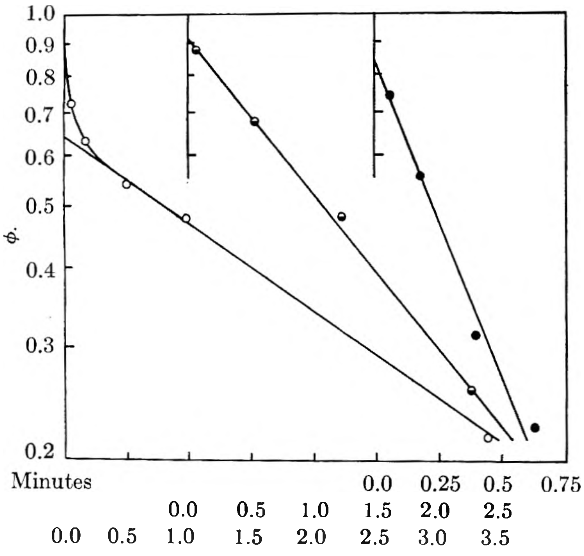

Fig. 1.—Three exchange experiments at the extremes of temperature and concentration: ○, conditions as in exp. 1.13 but with ordinary distilled water; ◒, exp. 1.12; ●, exp. 1.23.

Kinetics of Hydrolysis.—Here the reaction vessels were ordinary 200-ml. round-bottom flasks. Into each of these was placed 2 ml. of a solution 0.0328 *f* in HCl and 0.0451 *f* in $RbAuCl_4$. The chloride included the active isotope which had several days to reach isotope equilibrium with the inactive chloride. Another flask, containing 100 ml. of 0.0884 *f* KNO_3, was cooled in ice-water at least 45 minutes, which was found sufficient to cool the contents to 0.0°. After similarly cooling the other flask the KNO_3 solution was quickly poured into it. After time *t* in the ice-bath a cold mixture of 25 ml. of sat. $MgSO_4$, 1 ml. of 0.3 *N* $((C_6H_5)_4As)_2SO_4$ and 10 ml. of water was poured into the flask to quench the reaction. A stopwatch was punched at the beginning of both pourings. The first several samples were filtered after half a minute through a large sintered glass filter. In the more hydrolyzed samples, however, a later clouding occurred which was found to increase the final count appreciably. The reported data are based on filtrations after six minutes, which gave filtrates remaining almost completely clear. Since no exchange with the precipitate was observed in exchange experiments we believe that these precipitates also remained unaltered after their formation. Five ml. of 0.1 *f* $AgNO_3$ was added to each filtrate. After coagulation and one washing of the AgCl it was dissolved in 5 ml. of 2 *f* NH_4OH and counted in solution. The proportionality between observed radioactivity and final free chloride concentration was used (as in equilibrium studies also) with the values calculated for no hydrolysis to determine the amount of hydrolysis.

Equilibrium of Hydrolysis.—The reaction volume for these experiments was 4 ml. as in the exchange studies. The temperature was 0.0°, exchange was complete, but the acidity was varied while keeping initial ionic strength at 0.088. The precipitant was added to the mixture after several hours or days. Complete precipitation of gold complexes in these experiments was shown by the absence of color or clouding in the final solution and by a negative stannous chloride test. ($AuCl_3OH_2$, for example, may be precipitated as $(C_6H_5)_4AsAuCl_3OH$). The first set of runs indicated that equilibrium was not quite established in 1.5 to three hours. A later series, in which equilibrium was established in half a day to two days, is reported among the results.

Equations

The general equations for isotope exchanges[3] can be written as follows for our case, assuming chemical equilibrium and the equivalence of the four chlorides in chloroaurate

$$\phi \equiv \frac{(Cl^{*-})_t - (Cl^{*-})_\infty}{(Cl^{*-})_0 - (Cl^{*-})_\infty} = e^{-k_{ex}t} \tag{1}$$

$$k_{ex}t_{1/2} = \ln 2 \tag{2}$$

$$R = \frac{(Cl^-)(Cl_c)}{(Cl_c) + (Cl^-)} k_{ex} \tag{3}$$

where $(Cl^{*-})_t$ is the concentration of active free chloride at time *t*, (Cl^-) is the total concentration of free chloride, (Cl_c) is the concentration (equivalent) of the complexed chloride, k_{ex} is, under constant conditions, a constant defined in equation 1, $t_{1/2}$ is the half-time for the exchange and *R* is the chemical rate of exchange of chloride, active plus inactive, between the free and the complexed states. The results of some selected runs are shown in Fig. 1.

We find that the experimental values of *R* obtained in a fair range of conditions can be correlated by the equation

$$R = k_1'(Cl_c) + k_2'(Cl_c)(Cl^-) \tag{4}$$

---

[3] G. Friedlander and J. W. Kennedy, "Introduction to Radiochemistry," John Wiley and Sons, Inc., New York, N. Y., 1949, pp. 285-288.

TABLE I

RATE OF $AuCl_4^-$–Cl^- EXCHANGE AS A FUNCTION OF CONCENTRATIONS AND TEMPERATURE

No.	Formal concentrations			Misc.	μ	T, °C.	$t_{1/2}$ obs., min.	$t_{1/2}$, calc.	$\frac{(Cl^-)k_{ex}}{(Cl_c)+(Cl^-)}$
	Cl^-	$AuCl_4^-$	H^+						
1.11	0.0760	0.0124	0.076		0.088	0.0	1.64 ± 0.02		0.256
1.12	.0760	.0124	.076	0.160 KNO_3	.248	.0	1.25 ± .01		.336
1.13	.00351	.00310	.083		.088	.0	2.64 ± .05		.0576
1.14	.0167	.00620	.067		.088	.0	2.89 ± .03		.0969
1.15	.0162	.00310	.070		.088	.0	4.17 ± .04	4.15	
1.21	.0470	.0119	.032		.088	10.0	0.77 ± .01		.448
1.22	.00813	.00372	.077		.088	10.0	1.85 ± .04		.132
1.23	.0469	.0119	.032		.088	20.0	0.30 ± .01	0.31	
1.31	.021,[a] 0.028[b]	.0050	1.4	1.4 H_2SO_4	1.5	0.0	0.7 ± .2	3.3	
1.32	.035,[a] 0.036[b]	.0083	0.05	0.04 H_2SO_4	0.1	.0	2.15 ± .1	2.45	
1.33	.035	.0083	0.0018		0.043	.0	2.07 ± .02	2.45	
		Study of rate of hydrolysis							
1.4	0.000660[c]	0.000884	0.00066	0.0866 KNO_3	0.088	.0			
	0.001013[d]						1.6 ± .1		

[a] Calculation. [b] Observation. [c] At t = 0. [d] At t = 30.

Combining 3 and 4 we have

$$\frac{(Cl^-)k_{ex}}{(Cl_c) + (Cl^-)} = k_1' + k_2'(Cl^-) \qquad (5)$$

The rate law was tested in this form (Fig. 2). We can rewrite 4 as

$$R = k_1(AuCl_4^-) + k_2(AuCl_4^-)(Cl^-) \qquad (6)$$

where $k_1 = 4k_1'$ and $k_2 = 4k_2'$ since (Cl_c) is four times $(AuCl_4^-)$.

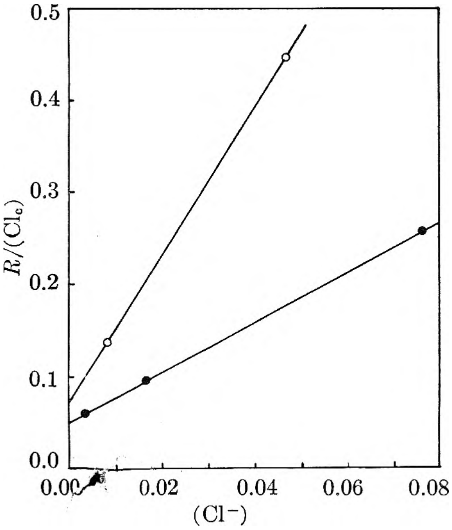

Fig. 2.—Evaluation of k_1 and k_2: ●, 0°; ○, 10°. Recalculation raises very slightly the intermediate point for 0°.

Results

Dependence on Chloride, Chloroaurate and Acid.—Table I summarizes the data on the kinetics of exchange between Cl^- and $AuCl_4^-$. In the concentration range studied a negligible amount of $AuCl_4^-$ is hydrolyzed. This was shown by the agreement of the activity found as free chloride at infinite time (over 30 minutes) with that calculated assuming the precipitate to be $(C_6H_5)_4AsAuCl_4$. The plot in Fig. 2 of the quantity in the last column of Table I permits evaluation of the parameters k_1 and k_2 of equation 6 at 0 and 10°. Experiment 1.15 (*cf.* $t_{1/2}$ calcd. and $t_{1/2}$ obs.), was performed to test the dependence of rate on $(AuCl_4^-)$ with this as the only variable. The rate law of equation 7 in unambiguously established by the data for the concentration range investigated.

Experiments 1.31, 1.32 and 1.33 were designed to determine the influence of acidity on rate. Only experiment 1.33 allows a definite conclusion to be drawn. The half-time observed is slightly shorter than that calculated using the values of k_1 and k_2 appropriate to 0° and somewhat higher ionic strength. It must be concluded therefore that at sufficiently low (H^+) a path inverse in (H^+) does contribute. However the increase in rate produced by lowering (H^+) 37-fold below the lowest concentration used to evaluate k_1 and k_2 at 0° is so slight that k_1 and k_2 are demonstrated to describe paths which are independent of (H^+).

The Effect of Oxy-anions.—The agreement in $t_{1/2}$ between experiments 1.32 and 1.33 must be construed as due to fortuitous cancellation of opposing effects, produced by variation in (H^+), μ and $(SO_4^=)$. Sulfate ion was observed to affect the stoichiometry. In experiment 1.31 the radioactivity in the free chloride after complete exchange corresponded to 0.028 M (Cl^-) rather than the 0.021 M (Cl^-) contributed by the original reagents. This suggests that Au(III) was precipitated partly as a sulfato complex, leaving additional free chloride to be counted. Participation of an equilibrium such as, $AuCl_4^- + SO_4^= \rightleftarrows AuCl_2SO_4^- + 2Cl^-$ would increase the exchange rate and may contribute to the results in experiments 1.31 and 1.32. The contribution by this path may be similar in 1.31 and 1.32 since $(SO_4^=)$ must be nearly the same in both; the greater rate in 1.31 may be due mainly to the change in μ. Another, but slower, equilibrium could contribute to the greatly altered stoichiometry in 1.31. The considerable kinetic irreproducibility observed in the presence of sulfuric acid is probably due to an accidental impurity in the acid.

Other early experiments showed that, within the error introduced by the precipitation of much $(C_6H_5)_4AsClO_4$, HNO_3 and $HClO_4$ are equivalent in the exchange studies.

Ionic Strength.—The term $k_2(AuCl_4^-)(Cl^-)$ in the rate law shows that two anions are combined in the corresponding activated complex. We then expect k_2 to vary with the ionic strength. The limiting law[4] describing this variation is

$$\log k_{2b} - \log k_{2a} = 2(0.49)Z_{Cl} - Z_{AuCl_4} - (\sqrt{\mu_b} - \sqrt{\mu_a})$$

Experiments 1.11 (= *a*) and 1.12 (= *b*) in Table I show the effect of raising the ionic strength at a chloride concentration such that the k_2 path contributes 80% of the total rate at the lower μ. Assuming k_1 to be unchanged we calculate that k_2 has increased from 10.9 to 15.0. The left side of the equation is then found to be 0.14 while the right side is calculated to be 0.20, showing that the variation with ionic strength is consistent with the ionic type of the k_2 path of equation 6.

The Influence of Light and Impurities.—The observation that the rate of exchange in the system $PtCl_6^=$–Cl^- is greatly increased even by diffuse daylight led us to test the effect of diffuse daylight on the $AuCl_4^-$–Cl^- exchange. No effect was observed. A rapid initial exchange was noted especially at low (Cl^-) (Fig. 1), when ordinary distilled water was used in the solutions. After the initial induced reaction the specific rate was reproducible and consistent with the rate law reported. This and other examples of catalysis and induced exchange are described in the following paper.

Variation with Temperature.—Table II summarizes the relevant data. The values recorded for 20° were obtained by graphical extrapolation since the exchange was too irreproducible at low (Cl^-) to get good separation of the constants. These extrapolated values lead to a good calculated half-time for experiment 1.23 in which the k_1 path should account for 8% of the rate. The activation energy and *pz* factor for each path were calculated using the equation

$$\log k = \log pz - \frac{0.4343E}{RT}$$

TABLE II

A SUMMARY OF CONSTANTS

	T, °C.	k_1, min.$^{-1}$	k_2, l. mole min.$^{-1}$	k_h, min.$^{-1}$
	0.0	0.200	11.0	0.17
	10.0	0.270	32.4	
extrap.	20.0	0.36	88	
	E, kcal.	4.5	16.5	
	log *pz*	2.9	14.3	

Rate of Hydrolysis.—The term $k_1(AuCl_4^-)$ in the rate law suggests an exchange mechanism involving loss of chloride from the complex as the first step. Such a dissociation of chloroaurate might involve hydrolysis. The last two rows of Table I describe the initial and final (after 30 minutes) conditions in a direct study of the reaction by observing the increase of (Cl^-) with time. A graph of $\log ((Cl^-)_\infty - (Cl^-)_t)$ *versus* *t* was found not to be quite straight, due to the reverse reaction, although the forward reaction is presumably first order and characterizable by a half-time. Experimental errors were fairly great. The initial rate was used to calculate k_h (= 0.17 min.$^{-1}$) in Table II, assuming this rate to be equal to $k_h(AuCl_4^-)$ minus rate of reversal.

Equilibrium of Hydrolysis.—Three kinds of experiments yielded information on the hydrolytic equilibrium: (1) infinite time results from exchange studies, (2) final results from the study of rate of hydrolysis and (3) the separate investigation of the equilibrium. The data show that the behavior of the system is complex, and further study is necessary. The post-precipitation observed in experiment 1.4 suggests the formation of polynuclear complexes. The variation of hydrolysis with acidity shows that aquo complexes cannot be the only important hydrolyzed forms. Bjerrum's use of hydroxy complexes[5] to explain the data is also inadequate, as are some hypotheses employing binuclear complexes, alone or with mononuclear forms. It may be noted that Bjerrum determined (H^+) by electrode potentials, that ionic strength was not constant and that small differences of large numbers were used.

Mercury and Thallium Complexes.—Some preliminary experiments had been performed to determine whether chloro-complexes of mercury, thallium, or gold had measurably slow exchange rates. The temperature was about 25°. After separation the radio-activity of the aqueous solutions was determined. Table IV shows the results. The exchanges may have been complete also in the first two experiments, in spite of the lower values of the apparent % exchange recorded. The high concentrations in the first solution, necessary to prevent dissociation of the complex, produced an extremely bulky precipitate and a very messy separation. The extraction of mercuric chloride from the second solution by phenylacetonitrile was known to be incomplete. From the known chemistry of these elements it seemed that gold offered the greatest possibilities for further investigation. About the mercury and thallium complexes we can say only that exchange is fast, but not necessarily immeasurably fast.

Discussion

The rate law for the k_2 path proves the presence of Cl^- and of $AuCl_4^-$ in the activated complex, and shows the mechanism of replacement of Cl^- by Cl^- by this path to be of the S_N2 type. This type of mechanism for a square planar complex ion, which has open coördination positions as well as a fairly stable vacant orbital (p), may prove to be fairly general for these ions. Such a path has in no case been proven for hexa-coördinated complex ions of the electronic structure type of Co(III), nor in fact has any simple net replacement of one anion for another been observed in these cases.

It will be recalled from the results that the *pz* factor for the k_2 path is normal. An entropy decrease would be expected for association of charges of the same sign in a dielectric medium. However, if in the activated complex the entering Cl^- and that being replaced are on opposite sides of the molecule $AuCl_5^=$, such an effect would be quite

---

[4] The value of the constant at 0° from H. S. Harned and B. B. Owen, "The Physical Chemistry of Electrolytic Solution," Reinhold Publ. Corp., N. Y., 1943, p. 119.

[5] N. Bjerrum, *Bull. soc. chim. Belg.*, **57**, 432 (1948).

TABLE III[a]

HYDROLYSIS OF $AuCl_4^-$

No.	Initial (Cl^-)	Formal concentrations Final (Cl^-)	 Final ($AuCl_4^-$)	(Au_{hyd})[b]	Initial (H^+)	t	K[c]
1.13	0.00351	0.00353	0.00308	0.00002	0.083	30 min.	
1.4	.000660	.001013	.000531	.000353	.000660	30 min.	6.8×10^{-7}
3.1	.001845	.00246	.005585	.000615	.0833	1.6 days	2.3×10^{-5}
3.2	.001845	.00308	.00496	.00124	.0222	1.7 days	1.8×10^{-5}
3.3	.001845	.00358	.00447	.00173	.00694	1.8 days	1.2×10^{-5}
3.4	.001845	.00365	.00440	.00180	.00185	1.5 days	0.5×10^{-5}

[a] Ionic strength kept very nearly equal to 0.088. [b] (Au_{hyd}) = final (Cl^-) minus initial (Cl^-). [c] Assuming $K = (H^+)(Cl^-)(AuCl_3OH^-)/(AuCl_4^-)$ represents the only important equilibrium.

TABLE IV

EXPLORATORY EXPERIMENTS

Formal concentrations Cl^-	 Complex	 Misc.	t, min.	Separation	Apparent % exchange[a]
1.0 NaCl	0.3 Na_2HgCl_4		1	Ppt. $((C_6H_5)_4As)_2HgCl_4$	90
0.0002 HCl	.001 $HgCl_2$	0.05 Na_2SO_4	1	Ext. $HgCl_2$ by $C_6H_5CH_2CN$	70
.05 HCl	.025 $HTlCl_4$	.025 HNO_3	1	Ppt. $(C_6H_5)_4AsTlCl_4$	100
.004 HCl	.03 $RbAuCl_4$		30	Ppt. $(C_6H_5)_4AsAuCl_4$	100
.004 HCl	.03 $RbAuCl_4$	1.4 H_2SO_4	4	Ppt. $(C_6H_5)_4AsAuCl_4$	100

[a] % ex. ≡ 100(1 − ϕ).

small. In view of the p-orbital available in the ion $AuCl_4^-$, it seems likely that the configuration of the activated complex approaches that of a trigonal bipyramid, the entering group and that being replaced occupying the apical positions.

No definite conclusion can be drawn about the mechanism by the k_1 path. The very low value of the pz factor suggests hydrolysis by an SN2 path as the rate determining act (in many systems SN2 solvolyses have been observed to occur with pz factors *ca.* 10^4 lower than corresponding reactions by SN1 mechanisms[6]). Mere analogy, however, does not explain the phenomenon, does not bridge the large defect of pz from the normal values, nor explain the low activation energy observed. It is tempting to try to relate the special features of the k_1 path to the circumstance that two vacant coordination positions are open, and that two solvent molecules can be directly bound in the activated complex. To explain the large entropy decrease on activation, (*ca.* −50 e.u.) a large entropy decrease must be imposed on the solvent water, in addition to the decrease involved in the transfer of two water molecules from the solution to coordination positions about Au(III).

An important feature of the k_1 path is its relation to the net hydrolysis of $AuCl_4^-$. An SN2 mechanism for the exchange yielding hydrolyzed product would suggest that the rate of net hydrolysis and the exchange rate are directly related. It is difficult to study the rate of net hydrolysis under the conditions of the exchange experiments, because these conditions were purposely chosen to minimize hydrolysis. If the first-order specific rate of exchange corresponding to the conditions of the single experiment on rate of hydrolysis is computed, making use of the dependence on OH^- indicated by experiment 1.33 and estimating the correction for ionic strength, a value of 0.76 is calculated. The results are inaccurate enough so that the relation is consistent with the interpretation that the rate of exchange is just four times the rate of hydrolysis (this is the ratio expected if each $AuCl_3OH^-$ exchanges completely before returning to $AuCl_4^-$). However, an SN1 mechanism could lead to an accidental ratio of 4. Further work is in progress to define better the relation between the two processes.

REMARKS

W. K. WILMARTH (University of Southern California) raised the question of whether a difference in rate of exchange is observed corresponding to the change in the principal hydrolyzed form from $AuCl_3OH^-$ to $AuCl_3H_2O$. In response, we can only say that the rate of exchange is very little sensitive to acidity over the range 0.002 to 0.076 *M*. There are no data outside of our work on net hydrolysis indicating that $AuCl_3H_2O$ is a weak acid, and the assumption is usually made that it is strong. Further work on the hydrolysis, and on the relation of rates of hydrolysis and exchange may lead to a more satisfactory answer.

---

[6] B. K. Morse and D. S. Tarbell, *J. Am. Chem. Soc.*, **74**, 416 (1952).

THE INDUCED EXCHANGE OF Cl^- AND $AuCl_4^-$. EVIDENCE FOR Au(II)

BY RONALD L. RICH[1] AND HENRY TAUBE

Contribution from the George Herbert Jones Laboratories of the University of Chicago, Chicago, Illinois

Received May 26, 1953

The reduction of $AuCl_4^-$ by Fe^{++} induces a rapid exchange of Cl^- and $AuCl_4^-$. Under the conditions studied a turnover of Cl^- per Fe^{++} of the order of 10^4 has been observed. Sn(II) and Sb(III), though oxidized by $AuCl_4^-$, are much less efficient inducing agents, and may in fact have no direct effect. Au(I) induces, at most, only a slow exchange. V(IV) is fairly effective, but its efficiency is diminished by accumulation of V(V). It is concluded that a form of Au(II) is the active catalyst. This is generated efficiently by one-electron reducing agents, but not by the agents Sn(II) and Sb(III), which apparently bypass Au(II) in reducing $AuCl_4^-$. The kinetics of the reaction induced by Fe^{++} are consistent with a mechanism in which Au(II) is generated by a second-order reaction of $AuCl_4^-$ and Fe^{++} (specific rate, k_1), Au(II) exchanges associated chloride very rapidly with Cl^-, undergoes rate-determining exchange with Au(III) (k_3), and is destroyed by disproportionation (k_4). The specific rate k_1 was measured as 1.8×10^4 l. mole^{-1} min.$^{-1}$, and lower limits of 10^8 and 10^{10} l. mole^{-1} min.$^{-1}$ have been set on k_3 and k_4, all at 0°.

Introduction

In a separate article,[2] the rate characteristics of the spontaneous exchange of $AuCl_4^-$ and Cl^- are described. Observations made in the course of that work, on the exchange induced by an unknown impurity in ordinary distilled water, led to an investigation of the exchange induced by various reducing agents, and exposed the extraordinary sensitivity of the system to certain reducing agents, notably Fe^{++}. This paper describes the results of exploratory experiments with a variety of reducing agents, as well as results of a more detailed kinetic study made with Fe^{++}.

Reagents.—Many of the reagents are the same as described in the previous paper. The others were prepared from the purest available reagents and redistilled water as follows, the concentrations being calculated from the amounts of reagents used.

Solutions of $K_4Fe(CN)_6 \cdot 3H_2O$, $K_3Fe(CN)_6$, HVO_3 (from V_2O_5), $KSbOC_4H_4O_6$, $NaKC_4H_4O_6$ and KCN were prepared directly. The hexacyanoferrate solutions were freshly prepared before use.

The $NaClO_2$ was recrystallized before being used.

Solutions of Fe(*o*-phen)$_3$SO$_4$ were prepared by dissolving nearly equivalent quantities of $Fe(NH_4)_2(SO_4)_2 \cdot 6H_2O$ and 1:1 of phenanthroline in water.

$Fe(NH_4)_2(SO_4)_2 \cdot 6H_2O$ (hereafter implied where $FeSO_4$ is written), $Fe(NO_3)_3 \cdot 9H_2O$ and $SnCl_2 \cdot 2H_2O$ were dissolved in dilute solutions of sulfuric, perchloric and sulfuric acids, respectively, to decrease oxidation or hydrolysis. The ferrous and stannous solutions were freshly prepared before use. A part of the ferrous solution was always diluted to the final strength immediately before being used.

For most of the experiments with V(IV), (able I), C.P. $VOSO_4$ was weighed out quickly and dissolved. For the other experiments a solution was prepared as follows: A mixture containing 9.106 g. of V_2O_5, 20 ml. of concd. H_2SO_4 and some water was warmed and treated with SO_2 gas until half an hour after all the V_2O_5 had dissolved. Nitrogen was passed through the solution on the steam-bath overnight and the solution was filtered and diluted to 100 ml. of 1.00 *f* $VOSO_4$, 3.1 *f* H_2SO_4.

Experimental Procedure.—The procedure was usually as described in the previous paper except that the catalyst and/or inhibitor (included in the 4 ml. total volume during exchange unless otherwise specified) was first added sometimes to the chloroaurate and sometimes to the radioactive solution in the divided flask.

Definitions and Derivations

This section contains derivations of the equations for the exchange induced by the reaction of Fe^{++} with $AuCl_4^-$, based on the mechanism presented in the discussion. A system of this type differs from that ordinarily discussed in which R, the rate of the reaction carrying the exchange, is constant. Here R decreases with time, since the inducing agent is consumed during the time of the exchange.

Let $F \equiv (Fe^{++})$, $A \equiv (Au(III))$, $G \equiv (Au(II))$, $b \equiv$ equivalent concentration of complexed chloride $\equiv (Cl_c) + (Cl_c^*) = 4A$, $a \equiv (Cl^-) + (Cl^{*-})$, $C \equiv (Cl_c^*) + (Cl^{*-})$, $x \equiv (Cl_c^*)$, $y \equiv (Cl^{*-})$, $n \equiv$ the number of chlorides changing association from Au(II) to Au(III) as a result of each exchange between the latter. Probably $n = 3$ or 4. Also let $\phi = (y - y_{eq})/(y_0 - y_{eq})$ and $\theta = (y - y_{eq})/(y_f - y_{eq})$. The subscript 0 refers to initial conditions, eq. to complete isotope equilibrium (infinite time for all paths), *f* to completion of the ferrous-induced exchange (infinite time for this path alone).

Assuming, for ferrous-induced exchange, the mechanism proposed in this paper (see Discussion), we can abbreviate the rates for steps 1, 3 and 4, respectively, as k_1AF, k_3AG and k_4G^2.

Set $A_0 \gg F_0$ (actually $3.2 \times 10^2 < (A_0/F_0) < 5.2 \times 10^4$). Then

$$\frac{dF}{dt} = -k_1A_0F \text{ and } F = F_0e^{-k_1A_0t} \qquad (I)$$

$$\frac{dG}{dt} = k_1A_0F - k_4G^2 = k_1A_0F_0e^{-k_1A_0t} - k_4G^2$$

Assume a steady state is quickly reached, *i.e.*, $dG/dt \approx 0$. Then

$$G = \sqrt{\frac{k_1A_0F_0}{k_4}}\, e^{-1/2(k_1A_0t)}$$

$$\frac{dy}{dt} = -nk_3A_0G\left(\frac{y}{a} - \frac{x}{b}\right) \qquad (II)$$

$$= -nk_3A_0G\left(\frac{y}{a} + \frac{y}{b} - \frac{c}{b}\right)$$

$$dy\Big/\left[\left(\frac{1}{a} + \frac{1}{b}\right)y - \frac{c}{b}\right] = -nk_3A_0\sqrt{\frac{k_1A_0F_0}{k_4}}\, e^{-1/2(k_1A_0t)}\, dt$$

$$\frac{ab}{a+b}\ln\left(\left(\frac{1}{a} + \frac{1}{b}\right)y - \frac{c}{b}\right) = 2nk_3\sqrt{\frac{A_0F_0}{k_1k_4}}e^{-1/2k_1A_0t} + \text{Const.}$$

In our experiments $y_0 = c$, therefore Const. $= (ab/a + b)\ln(c/a) - 2nk_3\sqrt{A_0F_0/k_1k_4}$

$$\ln\left(\frac{a+b}{ab}y - \frac{c}{b}\right) = \ln\frac{c}{a} - \frac{a+b}{ab}2nk_3\sqrt{\frac{A_0F_0}{k_1k_4}}\left(1 - e^{-1/2(k_1A_0t)}\right) \qquad (III)$$

---

[1] Atomic Energy Commission Predoctoral Fellow.

[2] R. L. Rich and H. Taube, THIS JOURNAL, **58**, 1 (1954).

Since $b = 4A_0$ we define

$$\frac{a+b}{2a} nk_3 \sqrt{\frac{F_0}{k_1k_4A_0}}\,(1 - e^{-1/2(k_1A_0t)}) \equiv \alpha$$

then

$$\frac{a+b}{ab} y - \frac{c}{b} = \frac{c}{a} e^{-\alpha} \text{ and } y = \frac{c}{a+b}(a + b\,e^{-\alpha})$$

In any case $y_{eq} = (a/a + b)c$ necessarily. $y - y_{eq} = (bc/a + b)e^{-\alpha}$.

$$y_0 - y_{eq} = c - \frac{ac}{a+b} = \frac{bc}{a+b}$$

$$\phi \equiv \frac{y - y_{eq}}{y_0 - y_{eq}} = e^{-\alpha} \qquad \text{(IV)}$$

Let $t \rightarrow \infty$ (only induced exchange occurring), then

$$\alpha_f \equiv (a + b/2a)\, nk_3\sqrt{F_0/k_1k_4A_0} \qquad \text{(V)}$$

and

$$\phi_f \equiv \frac{y_f - y_{eq}}{y_0 - y_{eq}} \qquad \text{(VI)}$$

We see that $\alpha/\alpha_f = 1 - e^{-1/2(k_1A_0t)}$.

Treatment of Data at Finite t.

$$1/2(k_1A_0t) = -\ln\left(1 - \frac{\alpha}{\alpha_f}\right) = \ln \alpha_f - \ln(\alpha_f - \alpha) =$$

$$\ln \alpha_f - \ln \ln \frac{\phi}{\phi_f} = \ln \alpha_f - \ln \ln \frac{y - y_{eq}}{y_f - y_{eq}} \equiv \ln \alpha_f -$$

$$\ln \ln \theta = (\ln \alpha_f - \ln \ln 10) - \ln \log \theta$$

Or

$$\ln \log \theta = \text{const.} - 1/2(k_1A_0t) \qquad \text{(VII)}$$

Limitations Implied by the Steady State Assumption.—The assumption $\mathrm{d}G/\mathrm{d}t \approx 0$ implies $|\mathrm{d}G/\mathrm{d}t| \ll k_1A_0F_0\, e^{-K_1A_0t} \approx k_4G^2$.

Since

$$G \approx \sqrt{\frac{k_1A_0F_0}{k_4}}\, e^{-1/2(k_1A_0t)}$$

$$1/2(k_1A_0)\sqrt{\frac{k_1A_0F_0}{k_4}}\, e^{-1/2(k_2A_0t)} \ll k_1A_0F_0\, e^{-k_1A_0t} \qquad \text{(VIII)}$$

The exchange depends on $e^{-1/2(k_1A_0t)}$. The linearity of Fig. 1 suggests the validity of the inequality at least until $e^{-1/2(k_1A_0t)}$ becomes less than 0.1 for all points on the graph. Therefore $1/2(k_1A_0)\sqrt{k_1A_0F_0/k_4} < 0.1k_1A_0F_0$ and $(k_1/k_4) < (F_0/25A_0)$. For Fig. 1 the smallest experimental F_0/A_0 is 6.9×10^{-5} and

$$k_4/k_1 > 3.6 \times 10^5 \qquad \text{(IX)}$$

Exploratory Experiments.—In Table I the total volume of solution was usually 4.25 ml. The 0.25 ml. of catalytic solution was added to the side of the divided flask containing radioactive chloride except where indicated otherwise. The temperature during the exchange in these and other experiments was always 0.0°. Concentrations of the inducing agent, etc., are given for the final mixed solution. Other final conditions, except where indicated otherwise, were: $(AuCl_4^-) = 0.00584\ f$, $(Cl^-) = 0.0154\ f$, $(H^+) = 0.069\ f$, ionic strength $\mu = 0.088$ neglecting the varying small catalyst concentrations. Under these conditions the expected half-time for the uncatalyzed exchange is 2.96 minutes so that in 10 seconds we should have 4% exchange and in 30 seconds 11%. The tabulated data are uncorrected.

The % exchange is defined as: % ex. $\equiv$ 100 $(1 - \phi) \equiv 100(y_0 - y/y_0 - y_{eq})$ where y_0 was chosen to include the effect of the catalyst in the water.

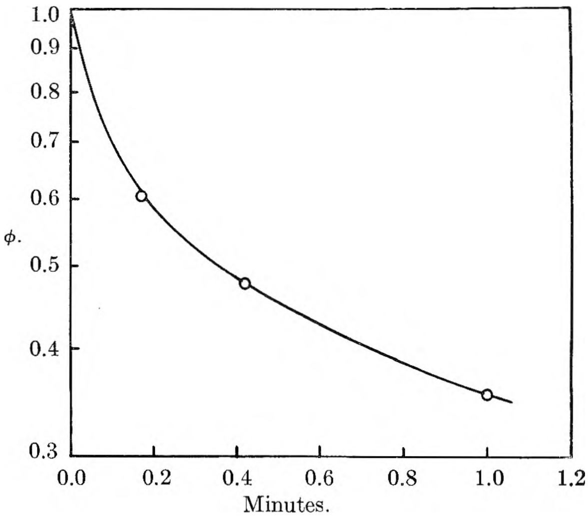

Fig. 1.—Exchange induced by vanadyl. Conditions as in exp. 1.14 of the previous paper with addition of 2.5×10^{-5} $VOSO_4$.

A short spectrophotometric study (see Discussion) was made of a solution which initially contained $0.00763\ f\ RbAuCl_4$, $0.00077\ f\ KSbOC_4H_4O_6$, $0.00077\ f$ HCl, $0.0183\ f$ NaCl, $0.088\ f\ HNO_3$ and $0.0019\ f\ NaKC_4H_4O_6$. The temperature was about 26°. The optical density at 4600 Å. varied as shown in Table II. The difference between the first and last values is that expected if the yellow $AuCl_4^-$ was reduced to the colorless $AuCl_2^-$ since the antimony was equivalent to one-tenth of the gold. The following day gold flakes appeared and the optical density rose gradually to 0.359, or higher when stirred. When excess antimony(III) was added to a similar solution the mixture eventually became colorless and much later also deposited gold flakes.

Ferrous Induced Reaction.—Table III shows the results of a study of the exchange induced by ferrous ion. The significance of the entries in the last two columns is dealt with in the Discussion section.

Discussion

Experiments 1.11–1.15 show that Fe^{++} is very efficient in inducing the exchange of $AuCl_4^-$ and Cl^-; thus 6×10^{-7} M $FeSO_4$ carries a solution 6×10^{-3} M in $AuCl_4^-$ and 15.4×10^{-3} M in Cl^- about 50% of the way to exchange equilibrium. The effect of Fe^{++} under the conditions of experiments 1.14 and 1.15 is essentially complete after 5 sec. Sn(II)- and Sb(III)-tartrate are fairly rapidly oxidized by $AuCl_4^-$. These substances are, however, much less effective in inducing the exchange than is Fe^{++}. The experiments performed with Sb(III) (1.31 to 1.35) afford a definite conclusion as to the oxidation state of Au (in the active catalyst) formed by the inducing agent. The change of optical density with time observed in the reaction of excess $AuCl_4^-$ with Sb(III) (*cf.* Table II) shows that formation of Au(I) is the primary net change, and that this stage is complete

TABLE I

EFFECT OF VARIOUS SUBSTANCES IN INDUCING THE EXCHANGE OF $AuCl_4^-$ WITH Cl^-

No.	$10^4 \times$ concn. (*f*)		Time, sec.	% ex.	Misc.
	Catalyst	Other			
1.11	0.06 $FeSO_4$	15 $Fe(NO_3)_3$	10.1	90	
1.12	0.06 $FeSO_4$		9.6	87	0.078 H^+, $\mu = 0.106$
1.13	0.006 $FeSO_4$		10.0	53	
1.14	0.006 $FeSO_4$		5.1	52	
1.15	0.006 $FeSO_4$		10.0	51	0.018 H^+
1.21	0.1 $SnCl_2$		9.5	8	
1.31	6 $KSbOC_4H_4O_6$	15 $NaKC_4H_4O_6$	9.7	34	
1.32		30 $NaKC_4H_4O_6$	9.6	26	
1.33	6 $KSbOC_4H_4O_6$	15 $NaKC_4H_4O_6$	9.5	16	Cat. in $AuCl_4^-$ 3 hr. at 29°
1.34	6 $KSbOC_4H_4O_6$	1.5 $NaKC_4H_4O_6$	10.0	18	Cat. in $AuCl_4^-$ 3 hr. at 29°
1.35	Same as 1.34 + 0.2 $FeSO_4$		10.1	98	Tart. alone in $AuCl_4^-$ 2 hr. at 29°
1.36	Same as 1.35		10.1	97	(Cat. mixture all in HCl*)
1.41	1 $VOSO_4$		10.4	28	
1.42	1 $VOSO_4$		10.0	46	0.018 H^+
1.43	1 $VOSO_4$		29.7	*ca.* 58	
1.44	1 $VOSO_4$	1 HVO_3	29.6	32	
1.45	1 $VOSO_4$		29.7	30	Cat. in $AuCl_4^-$ during 15′ cooling
1.51	0.25 $VOSO_4$		5.0	18[a]	0.00620 $AuCl_4^-$,
1.52	.064 $FeSO_4$		4.9	85	0.0163 Cl^-, 0.0667 H^+
1.53	.064 $FeSO_4$ + 0.25 $VOSO_4$		5.0	78	pure VO^{++}, 4 ml. vol.
1.61	.07 $K_4Fe(CN)_6$		3.4	27	
1.62	.07 $K_4Fe(CN)_6$		9.9	52	
1.63	.08 $K_4Fe(CN)_6$ + 2.5 $K_3Fe(CN)_6$		10.1	43	
1.64	25 × concn. of 1.63		9.6	42	$\mu = 0.126$
1.65	Same as 1.63		9.4	54	0.018 H^+
1.71	0.6 Fe(*o*-phen)$_3$SO$_4$		9.8	100	Slight excess $FeSO_4$
1.72	0.6 Fe(*o*-phen)$_3$SO$_4$		10.4	*ca.* 0	Slight excess *o*-phen.
1.81	5 $NaClO_2$		10.3	3	

[a] Estimated from Fig. 1.

TABLE II

REACTION OF Sb(III) WITH $AuCl_4^-$

t, min.	Density	*t*, min.	Density
0.4	0.362	27.5	0.3425
1.4	.360	29.0	.3415
3.0	.358	39	.3365
6.0	.355	50	.334
12.5	.350	70	.331
18.0	.348	110	.326
23.0	.345		

TABLE III

KINETICS OF THE EXCHANGE INDUCED BY Fe^{++}

($\mu = 0.088$, $T = 0.0°$, $t = 5$ sec.)

	3.1	3.2	3.3	3.4
(Cl^-)	0.01718	0.01655	0.01624	0.00664
$(AuCl_4^-)_0$	0.01240	0.00620	0.00310	0.00620
$(Cl^-) + (Cl_c)$	0.0668	0.0414	0.0286	0.0314
(H^+)	0.0609	0.0667	0.0701	0.0690
$[(Cl^-) + (Cl_c)]/[(Cl^-)\sqrt{(AuCl_4)_0}]$	34.9	31.7	31.7	60.1
$-\Delta \ln \phi_f/\Delta\sqrt{(Fe^{++})_0}$	864 ± 40	750 ± 7	656 ± 70	1310 ± 20
$-[\Delta \ln \phi_f/\Delta(Fe^{++})_0]/[(Cl^-) + (Cl_c)/(Cl^-)\sqrt{(AuCl_4^-)_0}]$	24.7	23.6	20.7	21.8

after 2 hours. Eventually $AuCl_4^-$ is partially restored and Au is formed by the disproportionation reaction 3Au(I) = Au(III) + 2Au. Au(I) was pre-formed in experiments 1.33 to 1.34 using Sb(III) as the reducing agent. The comparison of the exchange results in these experiments with those obtained using Fe^{++} as the inducing agent shows that Au(I) is not the active catalyst. Since Fe^{++} still is active in a solution such as was prepared for experiment 1.34, it cannot be argued that Au(I) is the active agent but that its effect is suppressed by some other component of the solution. The slight induced exchanges observed in experiments 1.33 and 1.34 can be attributed to the effects of tartrate (*cf.* exp. 1.32) and probably of Au(I) in generating the catalyst. The conclusion seems unavoidable that this catalyst is Au in the oxidation state +2, and that it is generated efficiently by Fe^{++}, but much less efficiently by the $2e^-$ reducing agents Sn(II) and Sb(III).

The experiments with the one-electron reducing agent VO^{++} provide further support for the conclusions. Although VO^{++} is oxidized only very slightly, it is a fairly effective inducing agent. Because of the low rate of oxidation of VO^{++} by $AuCl_4^-$, the system seemed a promising one for a thorough kinetic study but it proved disappointing in this respect. Figure 1, in which the exchange induced by VO^{++} is displayed as a function of time, shows that its efficiency decreases markedly as time progresses. This decline is not due to net consumption of VO^{++} which can be only very slight, and is apparently due to the accumulation of V(V). Such an effect for V(V), operating by reversal of the reaction, Au(III) + V(IV) = Au(II) + V(V), is not surprising for a couple as weakly reducing as V(IV)–V(V). This interpretation of the cause of the decline is supported by the increased inducing effect of V(IV) at lower acidity (exp. 1.42 compared to 1.41), by the observed inhibitory effect of HVO_3 (exp. 1.44 compared to 1.43), and by the decrease in the efficiency of VO^{++} when it is left in contact with $AuCl_4^-$ before radioactive chloride is added (exp. 1.45 compared to 1.43). V(V) freshly formed by oxidation of VO^{++} is much more effective than HVO_3 prepared as outlined in the experimental part. Its efficiency depends on its history and is improved by heating in dilute solution. These complexities presumably are due to slow condensation equilibria involving V(V), and because of them, a more detailed kinetic study was not undertaken. Experiments 1.51, 1.52 and 1.53 show that a mixture of V(IV) and Fe^{++} induces less exchange than would be expected for the substances acting independently, and in fact less than does Fe^{++} alone. The result suggests that VO^{++}, being left at high concentration, partially destroys Au(II), reducing it to Au(I).

Although ClO_2^- can function as a one-electron reducing agent, it is entirely without effect as an inducing agent. The value of E^0 for ClO_2^-–ClO_2 is −1.2 v., and ClO_2^- may be too weak as a reducing agent to generate Au(II) at sufficiently high concentration.

The kinetic data obtained with Fe^{++} as inducing agent support the conclusion that Au(II) is the catalyst. The observations recorded in Table I show that the inhibition by Fe^{+++} formed in the reaction can only be very slight, and that a fourfold change in acidity is also without effect. It will be convenient to discuss the data of Table III on the variation of the induced exchange with concentration of Fe^{++}, Cl^- and $AuCl_4^-$, referring to the following mechanism for the mode of action of Au(II).

Rate

$$Fe^{++} + AuCl_4^- \longrightarrow Fe(III) + Au(II) \qquad k_1(Fe^{++})(AuCl_4^-) \qquad (1)$$

$$Au^{II}_{Cl^-} + Cl^{*-} = Au^{II}_{Cl^{*-}} + Cl^- \qquad \text{Very rapid} \qquad (2)$$

$$Au^{II}_{Cl^{*-}} + AuCl_4^- \longrightarrow Au^{II}_{Cl^-} + AuCl_4^{*-} \qquad k_3(Au(II))(AuCl_4^-) \qquad (3)$$

$$2Au(II) \longrightarrow Au(I) + Au(III) \qquad k_4(Au(II))^2 \qquad (4)$$

If the chains are long (as is certainly true since the turnover of Cl^- is very large compared to the amount of Fe^{++} consumed), the mechanism leads (see equations) to the rate law

$$\ln \frac{(Cl^{*-}) - (Cl^{*-})_{eq}}{(Cl^{*-})_0 - (Cl^{*-})_{eq}} \equiv \ln \phi = - \frac{(Cl^-) + (Cl_c)}{2(Cl^-)} nk_3 \sqrt{\frac{(Fe^{++})_0}{k_1k_4(AuCl_4)_0}} (1 - e^{-1/2k_1(AuCl_4^-)_0t})$$

where (Cl^-) and (Cl_c) now represent the total concentrations of free chloride and complexed chloride and n is 3 or 4. The entries for each row in Table III were obtained by measuring the total exchange induced by Fe^{++} acting for 5 seconds, using various initial concentrations of Fe^{++} at fixed values of $(AuCl_4^-)$, (Cl^-) and (H^+) as shown in Fig. 2. The consumption of Fe^{++} is sufficiently complete in 5 seconds, except at the lowest concentration of $AuCl_4^-$, so that the term $(1 - e^{-1/2k_1(AuCl_4^-)_0t})$ is essentially equal to unity, with the one exception. Figure 2 shows the variation of $\ln \phi_f$ (f implies $t \rightarrow \infty$) with $\sqrt{(Fe^{++})_0}$ for exp. 3.2. The relation demanded by the mechanism is followed strictly, and the line through the points covering a 15-fold range in $(Fe^{++})_0$ extrapolates well at $(Fe^{++}) = 0$ to the spontaneous exchange expected in five seconds. Similar data provided the bases for other entries in column 7 of Table III. The figures in the last column of Table III should be a constant if the proposed mechanism accounts also for the influence on the induced exchange of varying the concentration of $AuCl_4^-$ and Cl^-. The agreement of the values, with some apology for the experiment at lowest $AuCl_4^-$, is satisfactory.

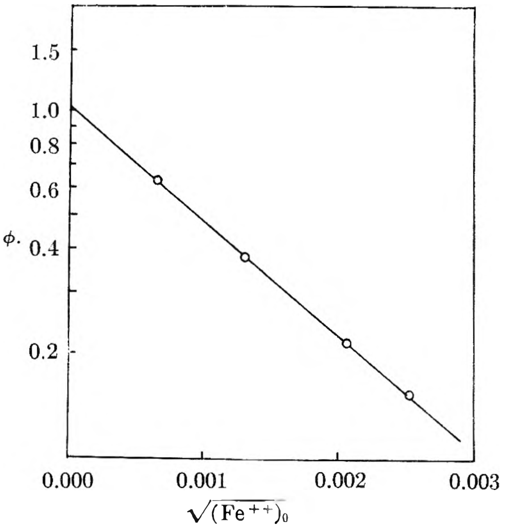

Fig. 2.—Induced exchange as a function of square root of ferrous concentration, exp. 3.2.

It should be noted that the data do not establish the formula of the catalyst $Au^{II}_{Cl^-}$. On this point they require merely that the rate-determining reaction 3 and the disproportionation reaction 4 in combination do not introduce dependence on chloride ion concentration. Reasonable formulations for the catalyst would appear to be $AuCl_4^=$ or $AuCl_3^-$. On the former assumption, reaction 3 becomes an electron transfer process; on the latter, it requires transfer of Cl. In any event, it seems likely that the very great lability of $Au^{II}Cl^-$ as compared to $AuCl_4^-$ is due to the possibility of states of different coördination number for Au(II) having nearly the same energy. The electronic structures for $AuCl_4^=$ and $AuCl_3^-$ can be represented as DSPPp′ and DSPp′. Some compensation in energy for the loss of Cl^- is expected from the increase in average stability of the hybridized orbitals, from increase in stability of the electron in the atomic orbital, and from the decrease in repulsion of negative ions. The phenomenon of an intermediate oxidation state having extraordinary lability with respect to substitution is not unique for Au, but appears to be the explanation for some induced exchanges observed with $PtCl_6^=$ (to be published), with $Pt^{III}Cl^-$ being much more labile than $PtCl_4^=$ or $PtCl_6^=$.

Equations III and VIII show that by measuring the induced exchange at times short enough so that the consumption of Fe^{++} is not complete, it is possible to obtain the value of k_1. An attempt to do this has been made. Low chloroaurate concentration was chosen to prolong the life of the inducing agents. Its concentration and that of H^+ and Cl^- were the same as in experiment 3.3. The initial concentration of Fe^{++} was 2.43×10^{-6} *f*. The relation pertinent to these results is equation (VII)

$$\ln \log \theta = \ln \log \frac{(\text{Cl}^{*-}) - (\text{Cl}^{*-})_{\text{eq}}}{(\text{Cl}^{*-})_{\text{f}} - (\text{Cl}^{*-})_{\text{eq}}} = \text{const.} - 1/2k_1(\text{AuCl}_4^-)_0 t$$

Figure 3 shows a logarithmic plot of log θ *vs.* *t*. From the slope of the line, taking account of the concentration of $AuCl_4^-$, k_1 is found to be 1.8×10^4 l. mole^{-1} min.$^{-1}$. It can be seen that the half-time for log θ is 1.5 sec., and that of the controlling oxidation–reduction reaction is 0.75 sec. The measured value of k_1 combined with the average value of the function in the last column of Table III yields, using eq. V and VI, for nk_3/k_4 the value 6×10^3 l.$^{1/2}$ mole$^{-1/2}$ min.$^{-1/2}$. The experimental results provide no basis for making accurate estimates of k_3 or k_4 separately. Only lower limits can be set. Using inequality (IX) and our value of k_1 we find $k_4 > 6 \times 10^9$ l./mole min., then $nk_3 > 5 \times 10^8$ l. mole^{-1} min.$^{-1}$. The lower limit for k_3 is useful in demonstrating a very high specific rate for the Au(II)–Au(III) exchange process, whether by electron or atom transfer.

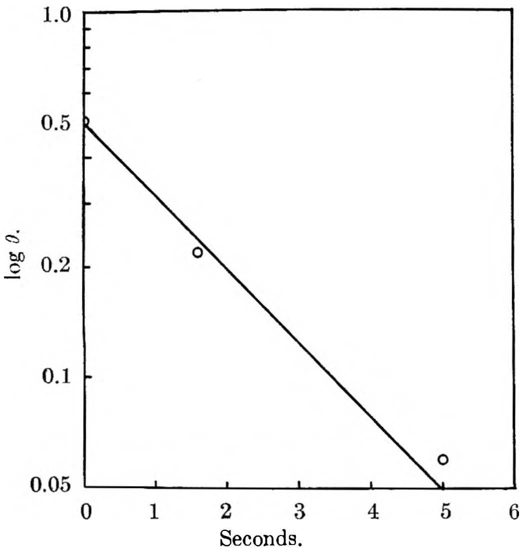

Fig. 3.—Rate of ferrous-induced exchange. Conditions in text.

The experiments with $Fe(o\text{-phen})_3^{++}$ were performed in the hope of fixing a lower limit of E^0 for Au(II)–$AuCl_4^-$, but led to no definite conclusions on this point. Experiment 1.71 shows that Fe^{++} is an effective inducing agent in the presence of $Fe(o\text{-phen})_3^{++}$. Evidently the reaction, $Fe(o\text{-phen})_3^{++} + Au(II) \rightarrow Fe(o\text{-phen})_3^{+++} + Au(I)$, is not rapid compared to exchange between Au(II) and $AuCl_4^-$. The absence of an induced exchange in experiment 1.72 may be due to slowness in forming Au(II) (unfavorable equilibrium in the first step), or to an inhibitory effect of 1:10 phenanthroline.

The behavior of $Fe(CN)_6^{==}$ as an inducing agent is complex. The measurably slow exchange indicated by experiments 1.61 and 1.62 has other causes than a slow reduction of $AuCl_4^-$ by $Fe(CN)_6^{==}$. The net change was studied directly, using the release of Cl^- ($AuCl_4^- + 2e^- \rightarrow AuCl_2^- + 2Cl^-$) measured by its radioactivity as index of the extent of reaction. There was an initial rapid release of Cl^-, half completed in 2 or 3 seconds, and following this, a slow continued liberation proceeding beyond what could be produced by complete oxidation of $Fe(CN)_6^{==}$ to $Fe(CN)_6^{\equiv}$. This shows that $Fe(CN)_6^{==}$ is in part disrupted by $AuCl_4^-$, and that CN^- also produces Cl^- in the system. An independent experiment showed that KCN also releases Cl^-. The amount of Cl^- released is increased by $Fe(CN)^{\equiv}$, both with $Fe(CN)_6^{==}$ and with CN^-, although $Fe(CN)_6^{\equiv}$ alone causes no release. The results indicate CN^- transfer during oxidation of $Fe(CN)_6^{==}$, and the reaction seems worthy of further study.

The agents inducing the exchange are not limited to the metal ions mainly dealt with thus far. Tartrate induces a slow exchange, and CN^-, a fairly rapid exchange. Acetaldehyde has no effect.

The agent in distilled water which led to the discovery of the induced exchange processes is believed to be Fe^{++}, especially in view of work done partly since the symposium. The rate of disappearance of the agent after mixing with $AuCl_4^-$ is similar to that of Fe^{++}. The agent is destroyed also by air in basic solution, less effectively by O_2 in neutral solution and very effectively by 0.0004 *M* 1:10 phenanthroline, O_3 and H_2O_2. Even redistilled water, kept in an ordinary greenish glass container (color presumably due to ferrous), induced some exchange.

A point of general interest in the results is concerned with the mechanism of reduction of $AuCl_4^-$ by various reducing agents. The results show without question that the catalytic intermediate Au(II) is present at much lower steady state concentration when the $2e^-$ reducing agents Sb(III) and Sn(II) react, than when Fe^{++} reacts. This comparison suggests the conclusion that the intermediate is not formed by the two-electron reducing agents, or is formed in a much smaller fraction of the acts of reduction for the former substances than for Fe^{++}. To meet the objection that Sb(III), although it may generate Au(II), reacts much more rapidly with it than does Fe^{++}, an experiment was performed in which the effect of Fe^{++} as inducing agent was tested for a solution also containing Sb(III) (exp. 1.36). This experiment shows that the Au(II) is not appreciably destroyed by Sb(III). The possibility that Sb(IV) and Au(II) are formed by interaction of Au(III) and Sb(III), but that the specific rate of further interaction of these products is much greater than any other changes for them is rendered unlikely if not completely ruled out by noting that the disproportionation of Au(II) proceeds at a rate nearly equal to the collision frequency. An extraordinary selectivity of Au(II) and Sb(IV) exercised in competition with a high disproportionation rate and even in the presence of Fe^{++}, can be understood only if the Au(II) and Sb(IV) are not separated from each other, *i.e.*, if Au(II) is not a true intermediate. The classification of a reaction as a one- or two-electron change is concerned with the question of whether intermediates (or immediate products) characteristic of one or other process are formed, and not with the mechanism of electron transfer in the activated complex. We conclude that the reduction of Au(III) by Sb(III) (and probably by Sn(II)) does in fact bypass Au(II).

A second question of fairly general interest is whether reaction 3 takes place by electron transfer or atom transfer. The former process is indicated if Au(II) participates in the reaction in the form $AuCl_4^=$, the latter if as $AuCl_3^-$. It is hoped that some evidence about the formula can be obtained from a study of the exchange catalyzed by Au(I). In this system Au(II) may exist in equilibrium with Au(I) and Au(III).

REMARKS

HAROLD L. FRIEDMAN (University of Southern California): Do you know that the active catalyst produced by the inducing agent is not atomic chlorine?

HENRY TAUBE (communicated in part): We cannot rule out this possibility definitely, but we believe it is rather unlikely. In any case, we can make a simple experimental test by looking for exchange induced in the system $AuCl_4^-$–Cl^- by light acting on molecular chlorine. Our reasons for considering it unlikely are: no exchange is induced by light acting on $AuCl_4^-$ (in the system $PtCl_6^=$–Cl^-, laboratory light produces rapid exchange); in the latter system, the induced exchange is wiped out by Cl_2, proving Cl not to be the intermediate, and leaving Pt(III) as the likely choice, analogous to Au(II) discussed in the present system; Au(II) cannot be powerful enough as an oxidizing agent to generate Cl from Cl^-. An assignment of values of E^0 consistent with the known over-all value[3] of E^0 for Au–$AuCl_4^-$, with the instability of Au(I) (probably only slight by analogy to Au(I)) in presence of Br^-) is

$$\underbrace{\mathrm{Au}\overset{-1.10}{\text{———}}\mathrm{AuCl_2^-}\overset{-0.95}{\text{———}}\mathrm{AuCl_4^-}}_{-1.00}$$

For Fe^{++} to be efficient in generating Au(II), even in the presence of much Fe^{+++}, E^0 for $Au^{II}_{Cl^-}$–$AuCl_4^-$, must be < -0.5, and this means that E^0 for $AuCl_2^-$–$Au^{II}_{Cl^-}$ > -1.4, hence $Au^{II}_{Cl^-}$ cannot generate Cl efficiently from Cl^- ($E^0 \sim -2.3$).

Since the symposium it has been found that no exchange is induced in the presence of 10^{-4} *M* Cl_2 and a bright fluorescent light.

---

[3] W. M. Latimer, "Oxidation Potentials," 2nd Ed., Prentice-Hall, Inc., New York, N. Y., 1952, p. 194.

ANION-EXCHANGE STUDIES. IX.[1,2]

ADSORBABILITY OF A NUMBER OF METALS IN HYDROCHLORIC ACID SOLUTIONS

By KURT A. KRAUS, FREDERICK NELSON AND GILBERT W. SMITH

Oak Ridge National Laboratory Chemistry Division, Oak Ridge, Tenn.

Received June 1, 1953

The results of anion-exchange studies in hydrochloric acid solutions of the alkali metals, ammonium ions, alkaline earths, elements of Group III, titanium and vanadium, and of palladium, iridium and platinum are given. Negligible adsorption is shown by the alkali metals, ammonium ions, alkaline earths, Al(III), Y(III) and rare earths. Ti(III), V(III), V(IV) and Sc(III) are slightly adsorbed from concentrated HCl, while Ti(IV) and V(V) show considerable adsorption under these conditions. In(III) shows some adsorption between 0.5 and 12 *M* HCl, and Ga(III) excellent adsorption, with adsorption increasing to 7 *M* HCl and decreasing beyond this molarity. Tl(III), Pd(II) and Pt(IV) show excellent adsorption between 0.1 and 12 *M* HCl with adsorption generally decreasing in this range. Ir(III) is negligibly adsorbed in the same range, but adsorbs at very low HCl concentrations. Some implications of these results on separations are illustrated. A striking parallel between anion-exchange adsorption and solvent extraction by ethers is discussed.

In a series of earlier papers from this Laboratory it was demonstrated that anion exchange of metal complexes is a powerful new tool for the separation of ions, as well as for the study of complexing reactions. The investigations at the present time have included a number of the less familiar "elements" which are of interest in this symposium. Some of our results, particularly from the analytical point of view, for the elements titanium and vanadium, scandium and yttrium; gallium, indium and thallium; palladium, iridium and platinum, will be given in this summary. In order to demonstrate the wide applicability of the method, studies are included of a number of elements which were not expected to form negatively charged complexes, namely, the alkali metals, alkaline earths and the remaining elements of Group III.

Experimental

The adsorbability of the elements was studied by both the equilibrium and the column methods.[3] In the equilibrium method, measured amounts of resin and solution are agitated, usually for several days, and the resulting decrease in concentration of the metal in the solution used to compute the distribution coefficient *D* (amount per kg. resin/amount per liter solution).

All distribution coefficients *D* are calculated with resin

---

[1] This document is based on work performed for the Atomic Energy Commission at the Oak Ridge National Laboratory.

[2] Previous paper, K. A. Kraus and F. Nelson, *J. Am. Chem. Soc.*, **75**, 3273 (1953).

[3] (a) K. A. Kraus and G. E. Moore, *ibid.*, **73**, 9 (1951); (b) **75**, 1460 (1953).

weights expressed in terms of resin dried to constant weight at 60° over Anhydrone. This method yields constant weights within 24 hours and an apparently water-free product. Because of its speed, this method is preferred over that used earlier,[3b] which involved drying over Anhydrone at room temperature.

In the column method the volume V (cc.) is measured, which is necessary to move an adsorption band (adsorption maximum) under essentially equilibrium conditions through a known distance d (cm.) in a column of known cross-sectional area A (cm.^{2}). From these data the elution constant E is calculated by the equation[3a]

$$E = dA/V \qquad (1)$$

Two modifications of the method were used. In one, d is small compared with the length of the column, and V and d are measured simultaneously. This method is particularly applicable for more strongly adsorbable ions. In the other method the band is moved through the whole column, and the effluent volume measured at which the element in question appears in maximum concentration. Under these conditions d becomes equal to the length of the column. Quantitative analysis of the effluent is desirable to obtain information on the shape of the elution band. However, qualitative analysis, *e.g.*, by spot tests, is often sufficient to determine the volume at which the band maximum appears in the effluent. This qualitative method is quite successful with elements which show little or no adsorption and permits essentially a quantitative description of adsorbability by a series of qualitative tests.

Flow rates varied from *ca.* 0.2 to 1 cm./minute. In most of the experiments, the columns were apparently operated near equilibrium since the elution bands were reasonably symmetrical.

The resin was from the same batch of relatively highly cross-linked "strong base" anion-exchange resin (polystyrene–divinylbenzene quaternary amine resin, Dowex-1, 200–230 mesh) which was used in the earlier work. The experiments were carried out at room temperature (25 ± 2°).

Further details of the experimental procedure will be given in connection with the discussion of the various elements.

Results and Discussion

1. Alkali Metals, Ammonium Ions and Alkaline Earths.—The alkali metals, lithium to cesium, ammonium ions and the alkaline earths, beryllium to barium, were studied by the column technique using 40 cm. × 0.04 cm.^{2} glass columns. A small volume (0.02 to 0.05 ml.) of the metal solution (*ca.* 0.1 M) in the appropriate acid was permitted to seep into the columns. The eluant was then added through a buret and the effluent collected in drops and analyzed by standard spot tests[4] or by evaporation on a black spot plate followed by confirmatory tests.[4] Significant concentrations of the salt in the effluent occurred in only a few drops and hence the band maxima could be determined to approximately ±1 drop. The results of the experiments are summarized in Table I.

TABLE I

ELUTION CONSTANTS OF ALKALI METALS, AMMONIUM IONS, ALKALINE EARTHS AND SOME ELEMENTS OF GROUP III

	E in			E in			E in	
	7 M HCl	12 M HCl		7 M HCl	12 M HCl		7 M HCl	12 M HCl
Li	2.1	2.2	Be	2.0	2.1	Al	2.4	2.5
Na	2.4	2.4	Mg	2.3	2.5	Sc	1.5	0.7
K	2.3	2.5	Ca	2.4	2.5	Y	2.2	2.4
Rb	2.4	2.4	Sr	2.3	2.6	La	2.3	2.5
Cs	2.3	2.5	Ba	2.4[a]	...	Yb	2.4	2.5
NH_4	2.2	2.4						

[a] Measured in 5 M HCl.

Inspection of this table shows that the elution constants E for most of these elements are near 2.3 and 2.5 in 7 and 12 M HCl, respectively. These are probably the maximum values of E when only negligible adsorption takes place.

It has been shown earlier[3a] that

$$E = 1/(i + D_v) \qquad (1)$$

where i is the fractional interstitial space of the columns and D_v the volume distribution coefficient (amount per liter bed/amount per liter solution).[5]

Thus E should approach the maximum value $1/i$ as D_v approaches zero, *i.e.*, when no adsorption takes place. Conditions for which $D_v = 0$, however, are not realizable since for all components some partitioning between the two phases must always take place. This partitioning is sensitive to the hydrochloric acid concentration since it affects the activity of the components in both phases. However, without some detailed knowledge on the behavior of the activity coefficients, no quantitative comparisons can be made. Setting $D_v = 0$ thus yields maximum values of i which for $E = 2.3$ or 2.5 are $i = 0.43$ or 0.40. In addition, small differences in i between various columns are also expected, since the columns are apparently loosely packed ($i = ca.$ 0.27 for close-packed spheres of uniform size) and thus i should be sensitive to the method of preparation of the columns, to their age and history, and to density difference between resin and solution.

If the definition $E = 2.3$ or 2.5 is made for "non-adsorbable ions" for the columns used here, one concludes that lithium and beryllium are very slightly adsorbed. Some adsorption of these elements might be expected, since they are the smallest ions of their valence type and might be considered the most likely elements of their groups to form complexes.

By extrapolation to the last row of the periodic table, negligible adsorption is predicted for Fr(I) and Ra(II).

2. Scandium, Yttrium and Rare Earths.—The adsorbability of these elements was determined in 7 and 12 M HCl by the column method. Of the rare earths, only lanthanum and ytterbium were studied. These two elements should be representative of all the rare earths since they are the first and next to last elements of the series. The results of the experiments are included in Table I. Except for Sc(III) these elements (and probably Ac(III)) show negligible adsorption.

The slight adsorbability of Sc(III), particularly in 12 M HCl, is sufficient to permit separation of this element from elements which show no adsorption and from elements which are strongly adsorbed, since the volume of eluant necessary to remove scandium from the column under these conditions is not excessive. To illustrate these separations, a column experiment was carried out in which 0.065 ml. of a 12 M HCl solution containing 0.5 M scandium (with 85 day Sc^{46}) and 0.027 M yttrium (with 57 day Y^{91}) in 12 M HCl were placed on a 40 cm. × 0.4 cm.^{2} column, eluted

---

[4] F. Feigl, "Spot Tests," 3rd Ed., Elsevier Publishing Co., New York, N. Y., 1946.

(5) The distribution coefficients D which are determined by the equilibrium method and expressed in the units (amount per kg. dry resin/amount per liter solution) are approximately a factor of 2 larger than the values of D_v because of the difference in the units used. The conversion factor between the two is essentially the bed density, which was found to be(3b) 2.2 liters of bed per kg. of dry resin.

with 12 M HCl at a flow rate of *ca.* 0.3 cm./min. and samples analyzed radiometrically. As shown in Fig. 1, separation of Sc(III) and Y(III) is satisfactory. Had a more strongly adsorbable element been included under these conditions, it would have remained on the column.

It is interesting to note that scandium is the only element of oxidation number three in the series, Al, Sc, Y and rare earths, which shows adsorption. This slight adsorbability of Sc(III) is paralleled by other unusual complexing properties of this element. The extraction constant of Sc(III) into thenoyltrifluoroacetone (TTA)-benzene systems is larger than that of Al(III), Y(III), La(III) and Ac(III) by factors of 10^5, 10^7, 5×10^9 and 10^{11}, respectively, as shown by the work of Bolomy and Wish, Broido, Hagemann and Suttle.[6] Similarly, extractability of Sc(III) by ether from thiocyanate solutions is unusually high.[6]

3. Titanium. (a) **Ti(IV).**—The adsorbability of Ti(IV) from strong HCl solutions was studied by the equilibrium method with (initially) 1.3×10^{-3} M Ti(IV) solutions. The Ti(IV) solutions were prepared from "Analytical Grade" Ti(III) chloride solutions by oxidation with peroxide and back-titration with Ti(III). Titanium concentrations were determined before and after equilibration (*ca.* 62 hours) by the peroxide method[7] with a Beckman Model DU spectrophotometer, measuring optical density of the solutions near 410 mμ.

The observed distribution coefficients were $D = 0.6$, 2.6, 14.3 and 66 for 8.9, 9.9, 10.8 and 11.7 M HCl solutions, respectively. These experiments were carried out at less than 3% loading (L), where L is defined by the equation $L = nm_r/C$, where n is the charge of the adsorbed ion (assumed $n = 1$), m_r is the concentration of the ion in the resin phase and C the capacity of the resin in the same units as m_r. No distribution experiments were carried out below 8.9 M HCl, since at low hydrochloric acid concentrations Ti(IV) tends to precipitate, probably due to hydrolysis. No slow precipitation was found above 9 M HCl after standing several days. At these high hydrochloric acid concentrations the titanium solutions are yellow, the intensity of the color increasing with M HCl, probably due to the increased concentration of chloride complexes. In column experiments it was found that titanium adsorbs as a yellow band, indicating that the adsorbed negatively charged complex (or complexes) is also yellow.

(b) **Ti(III).**—The adsorbability of Ti(III) was studied by the column method in 9 and 12 M HCl, determining Ti concentrations in the effluent by the peroxide method. Ti(III) was found to be very slightly adsorbed. Thus $E = 1.1$ was found in 12 M HCl using a 17.2 cm. $\times$ 0.21 cm.^{2} column. Although Ti(III) is slowly oxidized to Ti(IV), such reaction has negligible influence on the determination of E of Ti(III), since Ti(IV) is strongly adsorbed under these conditions and remains as a yellow band at the top of the column.

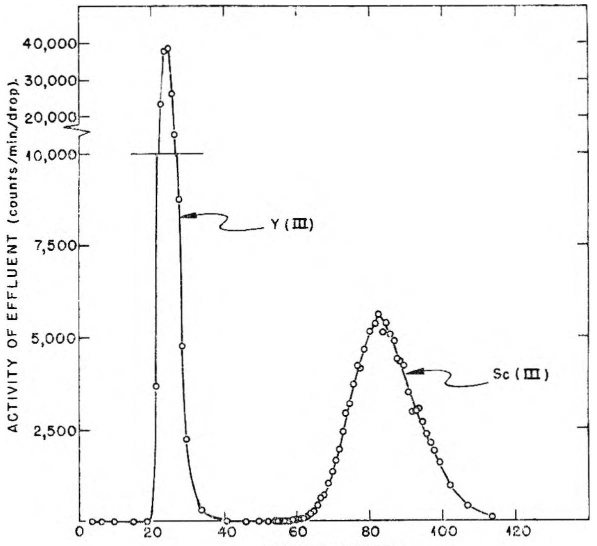

Fig. 1.—Anion-exchange separation of scandium and yttrium in 12 M HCl (average volume per drop 0.0232 ml.).

4. Vanadium. (a) **V(V).**—Vanadium(V) solutions were prepared by dissolving ammonium vanadate in HCl or by dissolving vanadium metal in aqua regia and fuming repeatedly with HCl. In the latter case large amounts of V(IV) are formed. In strong hydrochloric acid solutions V(V) forms an intensely brown solution. When vanadium is in the form of this brown complex, it can be strongly adsorbed by the anion-exchange resin yielding a dark brown band. Estimates of the elution constant of V(V) in 9 and 12 M HCl were obtained by first adsorbing a large amount of V(V) on a 4.0 cm. $\times$ 0.25 cm.^{2} column, eluting with 9 or 12 M HCl and averaging the distance that the upper and lower adsorption edges traveled. The approximate values $E = 0.02$ and 0.005 were found for 9 and 12 M HCl solutions, respectively. These correspond to distribution coefficients on a weight basis of 100 and 400, respectively.

(b) **V(IV).**—The adsorbability of V(IV) was studied in the range 1 to 12 M HCl and no region was found where considerable adsorption occurred. Best adsorption was found in 12 M HCl where E of V(IV) is approximately 1.15. This adsorption is sufficient to permit separation from non-adsorbable elements, if relatively long columns (*e.g.*, 50 cm. long) are used.

The V(IV) solutions were prepared by permitting V(V) solutions to reduce partially with concentrated HCl and then separating the oxidation states by passing the mixture through a small Dowex-1 column. Unreduced V(V) remained on the column, while the effluent was a pure V(IV) (blue) solution. The reduction of V(V) by HCl appears to be increased when adsorption by the resin takes place. Passing concentrated HCl solutions over the V(V) bands causes relatively rapid and complete reduction. This effect is probably connected with the fact that chlorine (as well as other halogens) is strongly adsorbed by the resin, while V(IV) is not appreciably adsorbed.

(c) **V(III).**—Solutions of V(III) were prepared by reduction of V(IV) solutions with stannous

(6) See, for example, H. M. Irving, *Quart. Revs.* (*London*), **5**, 200 (1951), where individual references are given.

(7) See, *e.g.*, N. L. Allport, "Colorimetric Analysis," Chapman and Hall, Ltd., London, 1945.

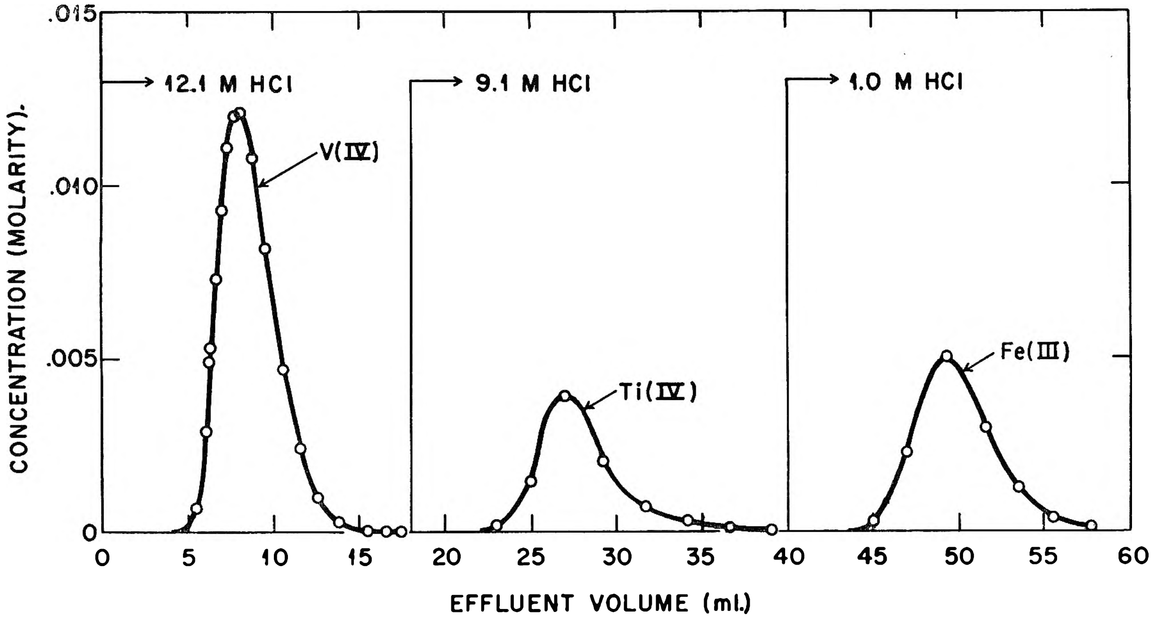

Fig. 2.—Separation of V(IV), Ti(IV) and Fe(III) by anion exchange (18.6 cm. × 0.49 cm.^{2} column (Dowex-1)); 1 ml.-0.05 *M* V(IV), 0.018 *M* Ti(IV), 0.025 *M* Fe(III) in 12 *M* HCl.

chloride. The adsorbability of V(III) was studied by the column method. Only slight adsorption occurred. In 12 *M* HCl, $E = 1.3$ was found.

5. Separation of Titanium, Vanadium and Iron.—As described in section 3, titanium is sufficiently strongly adsorbed to permit its ready separation from other elements. To demonstrate the procedure, the separation of titanium, vanadium and iron was carried out using an 18.6 cm. × 0.49 cm.^{2} column of Dowex-1, adding to it a 1-ml. sample containing 0.05 *M* V(IV), 0.018 *M* Ti(IV) and 0.025 *M* Fe(III) in 12 *M* HCl. As shown in Fig. 2, the separation of these three elements is satisfactory, V(IV) appearing rapidly in the effluent in 12.1 *M* HCl, Ti(IV) being eluted in a reasonably narrow band near 9 *M* HCl, under which condition Fe(III) is still held strongly on the column.[8] Fe(III) was removed with 1.0 *M* HCl.

6. Palladium, Iridium and Platinum.—Some of the earliest experiments on anion exchange of negatively charged complexes were carried out with the platinum elements by Nachod and Sussman[9,10] who suggested this method for the isolation of certain elements. They found that platinum, gold and other elements which form very stable negatively charged complexes are adsorbed by various anion-exchange materials, including certain weak-base synthetic exchangers. Most of the complexes which have been discussed in the present and earlier papers were relatively weak and could be decomposed by decreasing (or changing) the concentration of the ligand. Thus a simple method for controlling the degree of adsorption became available, since a minor change in the composition of the solution can cause a change from strong adsorption to rapid elution. The complexes studied by Nachod and Sussman were very stable and usually were not in rapid equilibrium with neutral or positively charged species. Hence, for those elements the removal of the complexes from the resin by decreasing the ligand concentration is essentially precluded. Instead, a decrease in the concentration of the ligand generally will cause an increase in adsorbability.

(a) **Pd(II)**.—The adsorbability of Pd(II) was studied by the equilibrium method in the range 0.1 to 12 *M* HCl using a spectrophotometric method of analysis. Pd(II) has an absorption band in the visible region with maximum located near 475 mμ for HCl concentrations from 1 to 12 *M*. In this HCl range the spectrum is essentially constant, showing only minor changes in the extinction coefficients of this band with *M* HCl. Below 1 *M* HCl the spectrum is different, indicating a change in species. The absorption maximum is located near 450 mμ in 0.1 *M* HCl and near 420 mμ in 0.002 *M* HCl. In addition, at low acidities the spectrum changes slowly with time.

Pd(II) was found to be strongly adsorbed throughout the experimental range, as shown in Table II, with distribution coefficients *D* decreasing with increasing hydrochloric acid concentration. Unfortunately, even in concentrated hydrochloric acid the adsorbability of this element is still suffi-

Table II

Adsorption of Pd(II) and Pt(IV) from HCl Solution

	Pd(II)		Pt(IV)	
M HCl	*D*	Loading,[a] %	*D*	Loading,[a] %
0.10	1,600	85	>10,000	55
1.0	870	50	5,560	26
4.0	300	20	2,480	28
7.9	79	5	914	16
11.6	40	3	440	10

[a] For definition of loading *L*, see section 3a. *D* is expected to increase considerably with decreasing *L* when *L* is larger than a few hundredths. For calculation of *L* assumed charge $n = 2$.

---

[8] G. E. Moore and K. A. Kraus, *J. Am. Chem. Soc.*, **72**, 5792 (1950).

[9] F. C. Nachod, U. S. Patent 2,371,119 (March 6, 1945) to Permutit Co.

[10] S. Sussman, F. C. Nachod and W. Wood, *Ind. Eng Chem.*, **37**, 618 (1945).

ciently large to preclude its easy removal from the resin. The continued rapid decrease of D_{Pd} suggests that reasonably rapid elution might be achieved with more concentrated hydrochloric acid solutions, *e.g.*, solutions where the partial pressure of HCl is greater than one atmosphere.

The removal of Pd in a relatively narrow band without excessive tailing was achieved by displacement with other strongly adsorbed complexes, *e.g.*, cadmium chloride[11] in HCl or zinc chloride[3b] in HCl. Thus, using 1 *M* $CdCl_2$ in 6 *M* HCl, palladium was essentially completely removed from a 4 cm. × 0.25 cm.^{2} column in about seven column volumes at 88°.

(b) **Pt(IV).**—The adsorbability of Pt(IV) was studied by the equilibrium method in the range 0.1 to 12 *M* HCl using a spectrophotometric method of analysis, utilizing the absorption region between 350 and 450 mμ. The position of the absorption maximum, which lies below 350 mμ, was not investigated.

Pt(IV) was strongly adsorbed throughout the whole experimental range and, as in the case of of Pd(II), the distribution coefficients decreased with increasing hydrochloric acid concentration (see Table II). The adsorbability of Pt(IV) was considerably larger than that of Pd(II).

The decrease of distribution coefficients with increasing hydrochloric acid concentration is characteristic of elements for which the concentration of adsorbable species does not increase with *M* HCl and results from the "displacing" effect of the chloride ions and the effect of the hydrochloric acid on the activity coefficient quotient of the adsorption equilibrium, as will be discussed in another paper.[12]

(c) **Iridium. Separation of Iridium from Palladium and Platinum.**—The adsorbabilities of Ir(III) and Ir(IV) were studied in the range 0.1 to 11.5 *M* HCl by the equilibrium and column methods using spectrophotometric and radiometric (Ir^{142}) methods of analysis.

Ir(IV) was found to be strongly adsorbed throughout this hydrochloric acid concentration range. Ir(III), on the other hand, showed negligible adsorption in this range, but some adsorption at lower hydrochloric acid concentrations.

The low adsorbability of Ir(III) intrinsically permits the separation of this element from other "platinum elements," and several experiments were carried out to demonstrate this. For example, a 0.03 *M* Pt solution was heated with iridium tracer (using Ir^{192}) in aqua regia, then fumed with hydrochloric acid to remove the nitric acid. During the fuming Ir(III) apparently is formed. After making the solution 10 *M* in HCl, a 0.5-ml. sample was placed on a 8.0 cm. × 0.25 cm.^{2} column. Approximately 99% of the iridium tracer appeared in the first few column volumes of effluent, while Pt(IV) was held tightly as an orange band at the top of the column. Similar results were found with a 10 *M* HCl solution which was 0.03 *M* in Pd(II) and contained Ir^{192} tracer. Only about 1% of the iridium remained on the column after three column volumes of 10 *M* HCl had been passed through it, as determined by counting the small column directly in a "re-entrant hole" sodium iodide scintillation counter.[13]

7. **Aluminum, Gallium, Indium and Thallium.**—Aluminum has been reported[8] not to be adsorbed from concentrated hydrochloric acid solutions. Additional column experiments (Table I) verified this result.

The adsorbability of Ga(III) at loadings of less than 1% was determined by the equilibrium method, as will be described in another paper. The data have been included here mainly for the sake of comparison.

The adsorbability of In(III) was determined by measuring with an automatic scanner[3a] the elution rate of an indium band containing In^{114} tracer. The distribution coefficients of In(III) were obtained from the elution constants by using as conversion factor the bed density.[5]

The adsorbability of Tl(III) at loadings of less than 1% was studied by the equilibrium method using radiometric analysis with Tl^{204} tracer. The Tl(III) solutions were prepared from Tl(I) solutions by oxidation with chlorine. For analysis, samples were either evaporated on platinum plates and counted in a windowless β-proportional counter[14] or were counted directly as liquid samples in small (*ca.* 5 mm. diameter) Lusteroid test-tubes with a Geiger–Müller counter. To minimize possible reduction to Tl(I), the equilibrations were carried out in the presence of chlorine. In separate experiments it was shown that although Tl(I) can be adsorbed by the anion-exchange resin, its adsorbability under all conditions studied is considerably less than that of Tl(III).

The adsorbabilities of these elements differ strikingly from each other, as shown in Fig. 3. Thus while Al(III) is negligibly adsorbed, Ga(III) is strongly adsorbed in concentrated HCl, shows a rapid decrease of *D* with decreasing HCl concentration below 7 *M* HCl and has negligible adsorption at low hydrochloric acid concentration. This behavior permits excellent separation of gallium from a large number of elements.

In(III), though showing appreciable adsorption above 0.5 *M* HCl, is never very strongly adsorbed. For *M* HCl < 2 the adsorbability of In(III) decreases rapidly, probably as in the case of Ga(III), because of a rapid decrease of the fraction of the element in the form of an adsorbable complex. The adsorption of In(III) is sufficiently small throughout the whole experimental range to necessitate some caution in its separation from large volumes of solutions containing non-adsorbable elements such as Al(III).

Tl(III) is strongly adsorbed and, in general, its distribution coefficients decrease with increasing hydrochloric acid concentration. Since the adsorbability of Tl(III) shows no region where *D* decreases with decreasing *M* HCl, some difficulties

---

[11] Cadmium chloride has been found (F. Nelson and K. A. Kraus, unpublished results) to be strongly adsorbed from dilute and concentrated HCl solutions in a manner similar to Zn(II)[(3b)], although its adsorption starts at a lower *M* HCl than that of Zn(II).

[12] K. A. Kraus and F. Nelson, *J. Am. Chem. Soc.*, in press.

[13] In this instrument the samples are placed in a re-entrant hole in the sodium iodide crystal, hence permitting direct γ-counting of solutions in small test-tubes. The instrument was developed at the ORNL Chemistry Division by C. J. Borkowski (Report ORNL-1153).

[14] C. J. Borkowski, *Anal. Chem.*, **21**, 348 (1949).

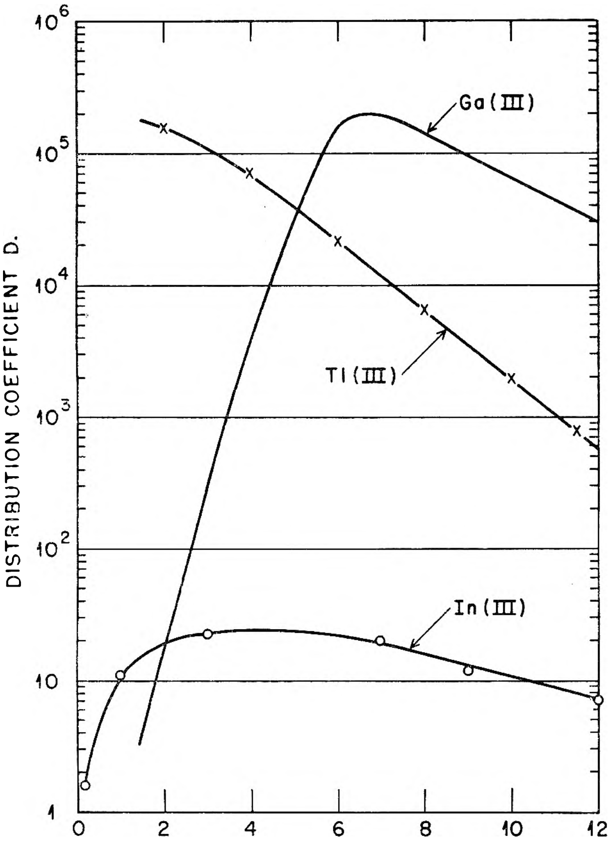

Fig. 3.—Anion-exchange adsorption of Ga(III), In(III) and Tl(III).

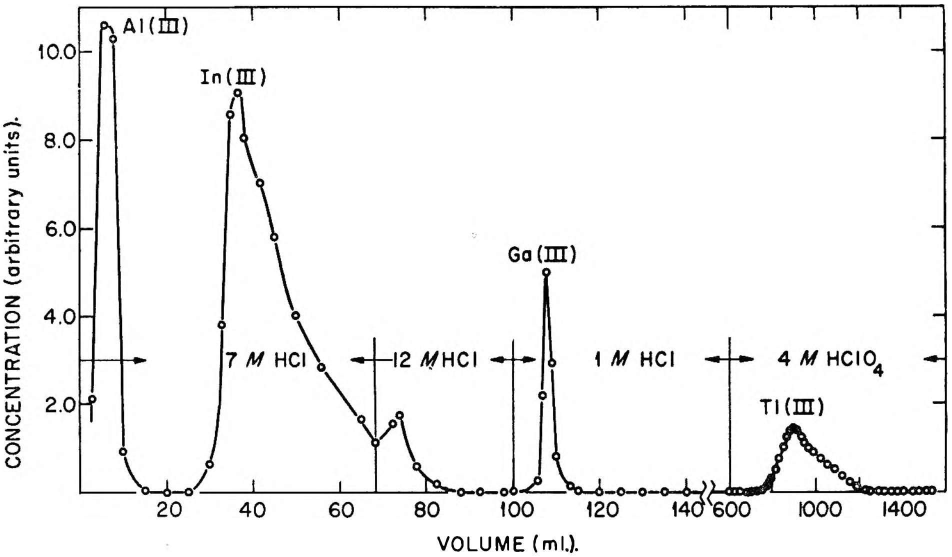

Fig. 4.—Separation of Al(III), Ga(III), In(III), and Tl(III) (Dowex-1, room temperature, column 20 cm. × 0.4 cm.^{2} flow rate 0.3–0.8 cm./min.).

will be encountered in its elution. For its successful removal from columns, chloride-free media appear necessary. These solutions probably need to be sufficiently acidic to prevent hydrolysis of Tl(III).

The following experiments illustrate the utilization of these distribution coefficient measurements for separations:

(a) **Adsorption of Ga(III) from Aluminum Chloride Solutions.**—A 10^{-4} *M* Ga(III) solution containing 14-hour[15] Ga^{72} in 2 *M* $AlCl_3$ and 3.5 *M* HCl was passed through a 10 cm. × 0.04 cm.^{2} column. After passage of 40 ml. of solution, Ga could be detected only in the upper one centimeter of the column and no detectable amount of gallium appeared in the effluent, indicating that very large volumes of solution could be processed in this way with small amounts of resin.

(b) **Separation of the Group Al(III), Ga(III), In(III) and Tl(III).**—Approximately 4 ml. of a 7 *M* HCl solution containing 0.5 *M* Al(III), 0.15 *M* Ga(III), 0.15 *M* In(III) and 0.15 *M* Tl(III) were passed into a 20 cm. × 0.4 cm.^{2} Dowex-1 column. To facilitate analysis, the solution contained Ga^{67}, In^{114} and Tl^{204} tracers. As shown in Fig. 4, elution with 7 *M* HCl caused immediate appearance of Al(III) in the effluent in concordance with the large elution constant given in Table I. The Al(III) was satisfactorily separated from In(III) which in 7 *M* HCl slowly elutes and shows some tailing. Its rate of elution, however, can be considerably increased by the use of 12 *M* HCl. Ga(III) in this experiment was eluted with 1 *M* HCl and Tl(III) with 4 *M* $HClO_4$. The elution of Tl(III), even in this medium, was unexpectedly slow. The use of nitric acid for the elution of Tl(III) was found to be[16] more successful. Considerable tailing still occurred, which is believed to be connected with difficulties in removing the last traces of chloride ions from the column.

(c) **Separation of Cadmium and Indium.**—Since cadmium is very strongly adsorbed from hydrochloric acid solutions,[11] it can readily be separated from indium. The following experiment illustrates

---

[15] The half-life of Ga^{72} after anion-exchange purification was found to be 14.08 ± 0.05 hours during more than 6 half-lives decay. This value is in good agreement with the half-life most recently reported in the literature, $T_{1/2}$ = 14.08 hours (Nuclear Data, Circ. National Bureau of Standards, 499, Supplement 1, April 1951).

[16] H. H. Rowley, summer participant at ORNL, summer, 1952, unpublished results.

the procedure. A sample of a cadmium solution (0.25 ml.) in 1 *M* HCl containing the tracer Cd^{115} in radioactive equilibrium with its daughter In^{115} was placed on a 12.2 cm. × 0.075 cm.^{2} column. Elution was carried out with 1 *M* HCl, which removed In^{115} within *ca.* 10 column volumes. Although more rapid elution of In^{115} could have been achieved with less concentrated HCl without danger of contamination with cadmium, the conditions used permitted additional purification from non-adsorbable elements. Cadmium was removed from the column with 10^{-4} *M* HCl in a narrow band with little tailing. The half life of the In^{115} isolated in this manner ($T_{1/2}$ = 4.56 hours) is in satisfactory agreement with the values given in the literature, 4.50 and 4.53 hours.[17]

8. Comparison between Anion-exchange and Solvent Extraction.—The adsorbability of the elements, Al(III), Ga(III), In(III) and Tl(III), described in section 7 is very closely paralleled by their extractability into ethers from hydrochloric acid solutions. Thus Irving in his summary[6] reports that the per cent. extractability from 6 *M* HCl is 0% for Al(III), 97% for Ga(III), trace for In(III) and 90 to 95% for Tl(III). The extractability of In(III), though small, is unequivocally established, however.[18,19]

This extremely close parallel between anion-exchange adsorption and extraction by ethers leaves little doubt that extractability in the two methods is, in some cases at least, due to the presence of similar complexes in the aqueous phase. On the basis of work with Fe(III)[6,20] and Ga(III)[6,21] especially, it appears that ethers tend to extract the component $HMCl_4$. Hence, one might tentatively assume that extractability by ethers generally increases when, in the aqueous phase, the fraction of the metal in the form of the species MCl_4^- increases. Similarly, the adsorbability by anion-exchange resins of the species MCl_4^- is particularly high, as demonstrated by the excellent adsorption at high HCl concentrations of Fe(III)[8] and Ga(III). Hence, one might explain the low extractability and adsorbability of In(III) by assuming that a complex of charge minus one ($InCl_4^-$) does not exist in large concentration. The lack of extraction of Al(III) by either resins or ethers indicates that it does not form negatively charged complexes in hydrochloric acid solutions.

The parallel between solvent extraction and anion exchange must be applied with caution since apparently anions of charge minus two can be strongly adsorbed, (*e.g.*, Pd(II) and Pt(IV) are probably adsorbed as $PdCl_4^{--}$ and $PtCl_6^{--}$) while such anions show apparently negligible extractability by ethers. Thus in the summary by Irving,[6] extractability of Pd is given as 0% and that of Pt(IV) as trace.

Since the adsorption of In(III) goes through a maximum, it is believed that negatively charged species become predominant at high HCl concentrations. In view of the good adsorbability of at least some complexes of charge minus two, the low adsorbability of In(III) might be explained by assuming that it tends to form a complex of charge minus three (*e.g.*, $InCl_6^{---}$). The small amount of solvent extractability and adsorbability would then be due to a small fraction of indium in the form $InCl_4^-$, which is in equilibrium with the other species. The inherent low adsorbability of complex ions of charge minus three, which has been postulated, is supported by the results with Ir(III) (see section 6c) which showed negligible adsorption and for which the complex $IrCl_6^{---}$ is usually written.

One might thus generally conclude that anion-exchange adsorption will occur for elements which show good ether extraction. However, the reverse is not true and excellent adsorption is possible without concordant ether extraction.

Acknowledgment.—The authors are indebted to Mrs. L. W. Magnusson, Jr., for valuable technical assistance.

---

[17] Nuclear Data, Circular of the National Bureau of Standards, 499 (1950).

[18] K. L. Knox and J. W. T. Spinks, *Can. Chem. Process Ind.*, **30**, 85 (Nov., 1946).

[19] H. M. Irving, F. J. C. Rossotti and J. G. Drysdale, *Nature*, **169**, 619 (1952).

[20] R. W. Dodson, G. J. Forney and E. H. Swift, *J. Am. Chem. Soc.*, **58**, 2573 (1936); W. H. Nachtrieb and J. G. Conway, *ibid.*, **70**, 3547 (1948); R. J. Meyers, D. E. Metzler and E. H. Swift, *ibid.*, **72**, 3767 (1950).

[21] E. H. Swift, *ibid.*, **46**, 2375 (1924); N. H. Nachtrieb and R. E. Fryxell, *ibid.*, **71**, 4035 (1949).

THE PREPARATION OF A SOLID RHENIDE[1]

BY JUSTO B. BRAVO, ERNEST GRISWOLD AND JACOB KLEINBERG

Contribution from the Chemical Laboratory of the University of Kansas, Lawrence, Kansas

Received May 22, 1953

The reduction of potassium perrhenate in ethylenediamine–water solutions by means of potassium metal yields a white solid containing uninegative rhenium (rhenide) mixed with potassium hydroxide. Under optimum conditions of reduction an apparent conversion of up to 90% of the perrhenate to solid rhenide is obtained. A number of extractions of the solid with isopropyl alcohol results in the removal of a large proportion of the potassium hydroxide and in the formation of a colloidal brown liquid which contains potassium hydroxide, isopropyl alcohol and rhenium, the latter almost entirely in the uninegative state. Fractional extraction of this brown liquid finally gives a gray solid usually containing between 55–60% rhenium, all as potassium rhenide. Analysis of the gray solid shows the presence of small amounts (about 5%) of potassium hydroxide as impurity and also the presence of approximately four molecules of water per rhenide ion. Magnetic measurements demonstrate that the rhenide compound is slightly paramagnetic, the degree of paramagnetism being even less than that required for a substance with one unpaired electron. Inasmuch as the rhenium atom possesses five unpaired electrons, the magnetic evidence indicates that the formation of the rhenide ion involves a considerable modification in electronic configuration. The magnetic data do not distinguish between two alternative structures: one in which the rhenide ion has a halide configuration, and the other in which the rhenium exists in a hydrated complex having four water molecules coördinated at the corners of a square. From energy considerations the latter structure appears to be the more plausible.

The discovery by Lundell and Knowles[2] in 1937 of the existence of uninegative rhenium (rhenide) has been confirmed by other investigators[3-6]; up to the present, however, no solid substance containing the rhenide ion has been prepared. In a preliminary communication from this Laboratory[7] the production for the first time of a solid rhenide material in admixture with potassium hydroxide was reported. The current communication describes the preparation and some properties of potassium rhenide tetrahydrate, which has been obtained in greater than 90% purity. This compound was extracted from a mixture consisting essentially of potassium rhenide and potassium hydroxide, which had been prepared by the reduction of potassium perrhenate in ethylenediamine–water solutions by means of potassium metal.

The Reduction of Potassium Perrhenate

Materials.—Potassium perrhenate obtained from the University of Tennessee and of 99.8% purity was used without further purification. The potassium sticks were obtained from Baker and Adamson. The ethylenediamine employed was of Eastman Kodak Co. white label quality. The water content of this material was determined by titration with Karl Fischer reagent,[8] which was purchased with the water-in-methanol standard from Hartman-Leddon Co. Spent ethylenediamine was recovered by distillation from potassium hydroxide sticks. Anhydrous ethyl ether was produced by drying special drum ether from Carbide and Carbon Chemicals over sodium.

The Reduction Procedure.—The apparatus employed for the reduction of potassium perrhenate is shown in Fig. 1. The reaction chamber was about 3.5 cm. in diameter and approximately 15 cm. high. Sampling bulbs A and B were inserted in the reaction chamber through ground glass joints. The nitrogen delivery tube extended close to the bottom of the reaction chamber in order that the gas would have a stirring effect on the reaction mixture. The presence at C of a large standard taper joint permitted the removal of the lower part of the reaction chamber for sampling purposes. An ultrafine fritted glass disk sealed into the bottom of the reaction chamber served, after removal of the solvent into the filter trap by means of an aspirator, to hold the insoluble white product formed in the reduction reaction.

Prior to each reduction the several pieces of the reaction chamber assembly were cleaned and dried in an oven at 110°. The apparatus was then assembled except for the sampling bulbs. The openings for the bulbs were stoppered with standard taper plugs and dry, oxygen-free nitrogen was passed through the system for at least 10 min. to sweep out the air. The sampling bulb A was then charged with a weighed quantity (2 or 4 g.) of potassium, which had been cut and weighed under benzene. Bulb B was charged with 50 or 100 ml. of 3 m*M* potassium perrhenate solution in ethylenediamine–water solution containing 9.8% water. After the sampling bulbs had been connected with the reaction chamber, bulb A was rotated and the potassium metal dropped into the chamber. This was followed by the introduction of the perrhenate solution.

Usually from 2 to 10 min. was required for complete reaction of the potassium, during which time the temperature of the reaction mixture rose to about 70°. When the reaction was complete, the white solid product was filtered by aspiration and twice washed with anhydrous ethyl ether, being stirred at the same time. After a final rinse with ether the solid was dried thoroughly by means of a stream of dry, oxygen-free nitrogen and was then dissolved in distilled water and made up to volume. Separate aliquots of the solution were analyzed for rhenium content, and for reducing power in terms of the number of g. equivalents of standard oxidizing agent required to oxidize 1 g. atom of rhenium to the perrhenate state.

Analytical Methods.—The reducing power of the rhenium was determined by the addition of an aliquot of the solution described above to a measured quantity of an excess of standard dichromate solution in a considerable excess of 4 *N* sulfuric acid; a measured quantity of standard iron(II) sulfate was then added, and the excess iron(II) sulfate was titrated with standard dichromate in the presence of diphenylaminesulfonic acid indicator. A suitable correction was made for reaction of the indicator with the dichromate.[9]

Rhenium was determined in the following manner. An aliquot of the solution was digested with 2 ml. of 30% hydrogen peroxide and sufficient 1:1 hydrochloric acid to make the final solution acidic. Digestion was continued until excess hydrogen peroxide had been destroyed. The perrhenate formed was then converted to $ReO(CNS)_4$ by treatment with potassium thiocyanate and tin(II) chloride, and the oxythiocyanate determined spectrophotometrically as de-

---

[1] Constructed from a thesis submitted by Justo B. Bravo in partial fulfillment of the requirements for the degree of Doctor of Philosophy, January, 1953.

[2] G. E. F. Lundell and H. B. Knowles, *J. Research Natl. Bur. Standards*, **18**, 629 (1937).

[3] O. Tomíček and F. Tomíček, *Collection Czech. Chem. Communs.*, **11**, 626 (1939).

[4] (a) J. J. Lingane, *J. Am. Chem. Soc.*, **64**, 1001 (1942); (b) *ibid.*, **64**, 2182 (1942).

[5] E. K. Maun and N. Davidson, *ibid.*, **72**, 3509 (1950).

[6] C. L. Rulfs and P. J. Elving, *ibid.*, **73**, 3287 (1951).

[7] E. Griswold, J. Kleinberg and J. B. Bravo, *Science*, **115**, 375 (1952).

[8] J. Mitchell and D. M. Smith, "Aquametry: Application of the Karl Fischer Reagent to Quantitative Analysis Involving Water," Interscience Publishers, Inc., New York, N. Y., 1948.

[9] I. M. Kolthoff and E. B. Sandell, "Textbook of Quantitative Inorganic Analysis," The Macmillan Co., New York, 1947, pp. 493–494.

scribed by Sandell.[10] A Model DU Beckman spectrophotometer was employed.

Results.—The results of typical reduction experiments are summarized in Table I. It should be emphasized that the conditions of reduction as listed in the table are those which, after many preliminary experiments, were found to give excellent conversions of perrhenate to rhenide. It is seen that under optimum conditions up to 90% of the initial perrhenate apparently is converted to solid rhenide. The solid mixture of potassium hydroxide and rhenide which is formed contains about 0.5% rhenium. In almost every case, the filtrate possessed some reducing power, indicating that it also contained rhenide.

TABLE I

REDUCTION OF POTASSIUM PERRHENATE BY POTASSIUM IN ETHYLENEDIAMINE–WATER SOLUTION

(Concn. of $KReO_4$, 3 m*M*; 9.8% H_2O)

Rhenium titrated, mmoles	Ml. of 0.1 *N* $K_2Cr_2O_7$ required	Valence no. change; theoretical, 8	Total rhenium in solid, mg.	Conversion to rhenide, %
0.0376	3.00	7.99	8.40	30.0[a,c]
.0311	2.48	7.97	6.96	24.9[a,c]
.0365	2.89	7.92	8.16	29.2[a,c]
.0174	1.39	7.97	5.02	18.0[a,c]
.0651	5.32	8.16	14.50	52.0[a]
.0681	5.33	7.82	15.26	54.7[a]
.1014	8.44	8.30	37.80	67.6[b]
.1356	11.02	8.13	50.50	90.4[b]
.1390	11.38	8.18	51.76	92.5[b]

[a] Fifty milliliters of perrhenate sample and 2.00 (±0.05) g. of potassium were used in these experiments. [b] One hundred milliliters of perrhenate sample and 4.00 (±0.05) g. of potassium were used in these experiments. [c] Initial reaction temperature 15°; all other experiments were carried out at an initial temperature of about 25°.

It is questionable that potassium metal itself is the actual reducing agent. The reaction of the metal with the water present in the ethylenediamine gives rise to hydrogen, and it is possible that this is the agent responsible for the reduction of the perrhenate.

The Separation of Potassium Rhenide

Preliminary Experiments.—Exploratory efforts to extract potassium hydroxide from the solid mixture produced by reduction of perrhenate demonstrated that, of the various solvents tested (liquid ammonia, ethyl alcohol, dioxane, cellosolve, *n*-amyl alcohol, *n*-butyl alcohol and isopropyl alcohol), isopropyl alcohol was the most satisfactory. This solvent dissolves potassium hydroxide and has practically no solvent action on the rhenide. However, in the course of treatment of the mixture with isopropyl alcohol two liquid layers are formed. The upper colorless layer, formed in greater volume, contains much potassium hydroxide but no rhenide. The lower layer, brown in color and colloidal in nature, contains potassium hydroxide and all of the rhenium.[11] Further extractions of this brown liquid with isopropyl alcohol, continued until the brown layer has almost disappeared, yield a grayish white solid containing in most cases approximately 20% of rhenium, nearly all of which is apparently in the uninegative state.

In an effort to concentrate the rhenide further, the grayish white solid was subjected to further extractions with isopropyl alcohol. In most of these experiments the solid became darker and, although its rhenium content increased, the reducing power was found to have undergone some diminution. This fact, indicating oxidation of part of the rhenium during extraction, suggested that the brown liquid layer might contain some unreduced perrhenate, which appears in the grayish white solid obtained by complete extraction of the brown layer, and, with decrease in concentration of hydroxide during further extraction of the solid, interacts with the rhenide to form metallic rhenium.

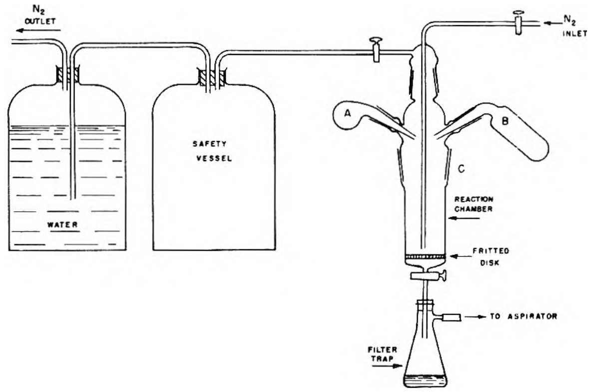

Fig. 1.—Apparatus for reduction of potassium perrhenate solution with metallic potassium.

In order to test this hypothesis, a series of fractional extractions of the brown liquid layer were carried out. The procedure employed was as follows, all operations involving transfer being carried out in a dry-box.

Two reductions were performed as previously described, each with 100 ml. of 3 m*M* potassium perrhenate solution in ethylenediamine–water mixture containing 10.8% water; 6.00 (±0.05) g. of potassium was used as reducing agent and the reaction was carried out at an initial temperature of about 25°.

The white solid products from these reductions were transferred to a single 60-ml. glass stoppered centrifuge tube. The tube was filled with oxygen-free anhydrous isopropyl alcohol (obtained by the fractionation from sodium of 98% Baker and Adamson material in a nitrogen atmosphere) and then shaken on a mechanical shaker for 1 hr. After centrifugation, the alcoholic extract was discarded. A total of three extractions usually resulted in the formation of the two layers previously described. The brown layer (plus any white solid which may have been present) was extracted once with isopropyl alcohol. Invariably there appeared at this stage a small amount of white solid. The clear alcohol layer was drained off and the brown layer was separated by decantation to another 60-ml. glass stoppered centrifuge tube. The solid phase was extracted once again with the alcohol, washed with anhydrous ether, and dried in a stream of nitrogen. The rhenium content and reducing power were then determined as previously described, except that the solid was dissolved in 10% potassium hydroxide solution rather than in distilled water. The results of typical experiments are given in the rows marked A in Table II.

The brown liquid phase was subjected to three additional extractions with isopropyl alcohol, each of which gave a deposit of a gray solid. The small amount of brown liquid still remaining was drained off, and the solid which had been

TABLE II

FRACTIONAL EXTRACTION OF RHENIDE–POTASSIUM HYDROXIDE BROWN LIQUID PHASE[a]

Expt. no.		Wt. of solid, mg.	Total rhenium content, mg.	Rhenium, %	Valence no. change; theoretical, 8
1	A	22.7	11.7	51.5	3.85
	B	86.2	48.8	56.6	8.16
2	A	15.6	8.1	52.0	5.42
	B	157.1	70.5	44.8	7.72
3	A	18.7	8.5	45.4	6.56
	B	146.7	79.0	53.8	8.17
4	A	15.2	8.9	58.7	5.62
	B	162.7	76.0	46.8	8.14
5	A	39.9	7.9	19.7	6.16
	B	147.4	77.1	52.4	8.02
6	A	15.2	7.1	46.7	5.47
	B	190.9	85.3	44.7	8.00

[a] The original reductions were carried out with 100 ml. of 3 m*M* $KReO_4$ solution in ethylenediamine–water mixture containing 10.8% water; 6.00 (±0.05) g. of potassium was used as reducing agent. Each extraction experiment was performed on two batches of reduction product.

---

(10) E. B. Sandell, "Colorimetric Determination of Traces of Metals," Interscience Publishers, Inc., New York, 1944, pp. 375–383.

(11) Occasionally a small amount of white solid remained when the two layers were formed. The white solid was combined with the lower brown layer and the mixture further extracted as described for the brown layer alone.

deposited was extracted once again, washed with ether, dried and analyzed after dissolution in 10% potassium hydroxide solution. The results appear in the rows labeled B in Table II.

The results shown in Table II are in agreement with the hypothesis that a small amount of unreduced perrhenate is present in the original brown layer. The perrhenate apparently is thrown out in the first small amount of solid deposit when the brown layer is treated with isopropyl alcohol, so that all of the remaining rhenium is in the uninegative state.

The Isolation of Potassium Rhenide Tetrahydrate.—A series of experiments was performed to determine the maximum rhenide content obtainable in the solid. The gray solid material, which had been freed of perrhenate by the method just described, was further extracted with isopropyl alcohol until two successive extracts (each the product of one hour's treatment) gave no test for potassium hydroxide. Approximately twenty extractions were required. Prior to each extraction, after the fifth one, the solid was crushed and stirred with a glass rod. The solid was finally washed with ether, dried and analyzed for rhenium content and reducing power. The data obtained from these experiments are given in Table III. It is seen that the maximum rhenium content of the solid approximates 61%. It should be pointed out that the solids analyzed still contained small amounts of potassium hydroxide, as evidenced by the fact that long contact (about 10 hr.) with isopropyl alcohol resulted in additional extraction of base.

Table III

The Separation of Rhenide from Admixture with Potassium Hydroxide[a]

Expt. no.	Wt. of solid, mg.	Total rhenium content, mg.	Rhenium, %	Valence no. change; theoretical, 8
1	140.0	83.4	59.6	7.96
2	122.1	75.1	61.5	7.98
3	84.7	51.6	60.9	8.07
4	99.2	59.2	59.6	8.06
5	49.2[b]	26.9	54.6	8.14
6	102.4	54.2	52.9	8.10
7	102.6	55.4	54.0	8.21
8	41.0[b]	23.7	57.7	8.07

[a] The original reductions were carried out under the identical conditions described in Table II. Each extraction experiment was performed on two batches of reduction product. [b] This does not represent the total quantity of solid obtained, a portion having been used for analysis for C, H and N.

Portions of two of the solids (see Table III) were analyzed for carbon, nitrogen and hydrogen.[12] The amounts of carbon and nitrogen were found to be insignificant, whereas the hydrogen contents, as is shown below, correspond closely to that calculated for a tetrahydrate.

Re, %	H, %	Atomic ratio, H:Re
57.7	2.50	8.0
54.6	2.33	8.0
	2.14	7.3

This result is entirely consistent with the fact that the maximum rhenium content found in the extracted solid was 61.5%, the theoretical value for the tetrahydrate being 62.6%. It is somewhat surprising that, although it was prepared in a medium rich in the excellent coördinator ethylenediamine, the rhenide compound nevertheless combined preferentially with water molecules.

Additional samples of the rhenide compound were prepared, extracted as previously described, and analyzed for both rhenium and potassium.[13] From the excess of potassium beyond that required for potassium rhenide formation, the percentage of potassium hydroxide present as impurity was calculated; the water content was obtained as the difference between the total quantity of material and the sum of the potassium rhenide and potassium hydroxide present. The results which are shown in Table IV, also definitely indicate that potassium rhenide is formed as a tetrahydrate. The actual percentages of water and the water:rhenium ratios are a little lower than those which appear in the table, since the small and variable (about 1–2%) content of organic material, presumably ethylenediamine, has been neglected in the calculations.

Table IV

Analysis of Potassium Rhenide[a]

Rhenium, %	Potassium, %	Potassium hydroxide, %	Water, %	H_2O:Re ratio
58.4	17.8	7.9	21.4	3.8
55.8	16.6	7.0	25.5	4.7
57.2	15.6	5.1	25.6	4.6
57.9	15.5	4.8	25.1	4.5

[a] The product was washed with anhydrous ether and treated with a stream of dry nitrogen.

Some Properties of Potassium Rhenide Tetrahydrate

Magnetic measurements by means of a Gouy balance demonstrate that the solid rhenide is slightly paramagnetic, giving values at 20° of 254×10^{-6} and 223×10^{-6} c.g.s., respectively, for the molar susceptibility of $KRe \cdot 4H_2O$ in two different samples, after correction for the diamagnetism of the potassium hydroxide impurity. This degree of paramagnetism is even less than that (about 1300×10^{-6} c.g.s.) required for a substance with one unpaired electron. Inasmuch as the rhenium atom possesses five unpaired electrons, the magnetic evidence indicates that the formation of the rhenide ion involves a considerable modification in electronic configuration.

A number of possible structures may be assigned to the rhenide ion. Lingane[4b] has suggested the following possibilities for electronic distribution in significant orbitals

A $5s^25p^65d^66s^2$

B $5s^25p^66s^26p^6$

The structure

C $5s^25p^65d^8$

must also be considered.

In addition, Pauling[14] has suggested the likelihood of the existence of a tetrahydrate of a square planar structure, involving dsp^2 bonds

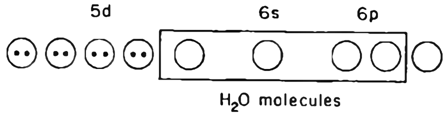

The magnetic evidence definitely eliminates structures A and C, which possess four and two unpaired electrons, respectively. Structure B which requires promotion of the 5d electrons to 6p orbitals is unreasonable in that there is a large amount of promotion energy involved.[15] The possibility that the rhenium exists in a hydrated complex having four water molecules coördinated at the corners of

---

[12] Sample no. 5, Table III, was analyzed by Dr. G. Weiler and Dr. F. B. Strauss, Microanalytical Laboratory, Oxford, Eng., and sample no. 8 by Micro-Tech Laboratories, Skokie, Ill.

[13] Potassium was determined by means of flame photometry, according to directions contained in the "Instruction Manual, Flame Photometer," Model 52-C, The Perkin-Elmer Corp., Norwalk, Conn., 1952.

[14] L. Pauling, *Chem. Eng. News*, **25**, 2970 (1947).

[15] L. Pauling, private communication.

a square is consistent with energy considerations, and also with the magnetic data.[16]

Although potassium rhenide tetrahydrate, as isolated, is gray in color, it is probable that the pure substance is actually colorless, inasmuch as the original reduction product, a mixture of rhenide and potassium hydroxide, is colorless. The gray color appears after extraction from the brown, colloidal dispersion in isopropyl alcohol, and probably is attributable to the adsorption of colloidal material. That this is a reasonable explanation is seen from the fact that the compound dissolves in aqueous potassium hydroxide to give pale yellow solutions which exhibit the Tyndall effect.

Treatment of such solutions with aqueous thallium(I) nitrate gives a white precipitate which presumably is thallium(I) rhenide. Unfortunately the precipitate is unstable and soon is converted to a black substance which proved to be metallic thallium; perrhenate ion was identified in the solution.

Acknowledgment.—The authors are indebted to the Office of Naval Research for financial support of this investigation.

---

[16] In the Pauling structure, if the electrons of the water molecules are not considered, the electronic distribution may be considered to be C given above, but it must be recognized that only four 5d orbitals are available, rather than all five. The coördination of the rhenium with water molecules rather than with ethylenediamine is explained by Pauling (private communication) in the following manner: "I feel that there will be a very strong tendency for the rhenium atom to form covalent bonds. However, if the covalent bonds have too large an amount of covalent character there will be built up a very large negative charge on the rhenium atom, which would be contrary to the electroneutrality principle [see *J. Chem. Soc.*, 1461 (1948)]. Accordingly the bonds to the four ligated atoms would be expected to have a rather large amount of ionic character, although still retaining a significant amount of covalent character. For this reason bonds to oxygen would be preferred in the rhenide complex over bonds to nitrogen, which, because of the smaller electronegativity of nitrogen, would be less stable, with a large amount of ionic character, than the bonds to oxygen. I think that this provides an explanation not only of the preference of the rhenide ion for water molecules, over ethylenediamine groups, but also for the ligation of only four water molecules, rather than six.

THE PRESENT STATUS OF ELEMENTS 85 AND 87

BY EARL K. HYDE

Radiation Laboratory, University of California, Berkeley, California

Received May 22, 1953

Our present knowledge of elements 85 and 87 is reviewed with considerable emphasis on their nuclear properties. From recent studies, primarily of cyclotron produced activities, we have reliable information on 7 isotopes of francium and more than 14 isotopes of astatine. The longest lived forms are the 21-minute AcK and the 8.3-hour At^{210}, respectively. From consideration of α- and β-decay systematics it can be concluded that there is no possibility of the existence of long lived forms. Short lived isotopes can and do exist in naturally occurring radioactive ores and some recent work in this field is discussed. A brief review of the principal chemical properties is included.

Introduction

A review of our present knowledge of the heaviest alkali element, francium, and the heaviest halogen, astatine, is very properly included in a symposium dealing with the less familiar elements. In contrast with most of the other papers in this symposium the emphasis will not be on the chemical properties but on the nuclear characteristics of these elements, since the instability of these elements is their most prominent characteristic. Nevertheless we will briefly review the principal chemical properties. Also the question of the existence of these elements in nature will be discussed.

One is impressed at once with the fact that these two elements are the prime examples of trace elements. For all the other radioactive elements with the exception of berkelium and californium there is at least one isotope of half-life sufficiently long to permit isolation of weighable amounts of the element and the study of its chemical reactions and properties by more or less typical methods, subject, it is true, to some severe experimental difficulties posed in several cases by the radioactivity. This is not true for astatine which can boast of a half-life of only 8.3 hours in its longest lived form, nor of francium which puts up a losing fight for permanence with a half-life of only 21 minutes in its longest lived form. Francium has the dubious distinction of being the most unstable of the 98 known elements.

The question naturally arises whether some stable or long lived form of these elements may not yet be found; this question will be answered in the negative in the discussion to follow.

Francium

Nuclear Properties.—The presently known isotopes of francium are listed in Table I together with their principal characteristics. The best known isotope is the 21-minute beta emitter AcK discovered by M. Perey[1] in 1939. Mlle. Perey demonstrated that the 22-year Ac^{227} isotope in the U^{235} decay chain, which decays predominantly by β-emission, has a branching decay of 1.2% for the emission of α-particles. This branching decay produces Fr^{223}, which she succeeded in isolating and studying. Because she was the first to identify conclusively an isotope of element 87 she earned the right to name the element. The work done on the nuclear radiations and the chemical behavior of this isotope has recently been summarized by her.[2]

The second isotope of francium to be discovered was Fr^{221}. This appears in the decay chain of U^{233} as was shown in the wartime research on the decay chain of this isotope.[3,4]

---

[1] M. Perey, *J. phys. radium*, **10**, 435 (1939); *Compt. rend.*, **208**, 97 (1939).

[2] M. Perey, *Bull. soc. chim. France*, 779 (1951).

[3] A. C. English, T. E. Cranshaw, P. Demers, J. A. Harvey, E. P. Hincks, J. V. Jelley and A. N. May, *Phys. Rev.*, **72**, 253 (1947).

[4] F. Hagemann, L. I. Katzin, M. H. Studier, A. Ghiorso and G. T. Seaborg, *ibid.*, **72**, 252 (1947).

TABLE I

ISOTOPES OF FRANCIUM[a]

Isotope	Principal ref.	Half-life	Obsd. radiation	Energy of radiation (Mev.)	Source	Total decay energy[15]		
						α-Decay	β-Decay	EC-Decay
Fr^{223} (AcK)	1, 2 14	21 min.	β^- α ($4 \times 10^{-3}\%$)	1.2	Natural source U^{235} decay chain	5.60[b]	1.19[c]	..
Fr^{222}	8	15 min.	β^- $99^+\%$ α 0.01–0.1%	...	Th (p, spallation)	6.00[b]	2.04[b]	0.02[b]
Fr^{221}	3, 4	4.8 min.	α	6.30 (~75%) 6.05 (~25%)	Daughter Ac^{225} in U^{233} decay chain	6.42	0.24[c]	..
Fr^{220}	5, 6	27.5 sec.	α	6.69	Daughter Ac^{224} in Pa^{228} decay chain	6.81	1.27[c]	0.87
Fr^{219}	5, 6	0.02 sec.	α	7.30	Daughter Ac^{223} in Pa^{227} decay chain	7.44	Stable	Stable
Fr^{218}	5, 6	5×10^{-3} sec.[b]	α	7.85	Daughter Ac^{222} in Pa^{226} decay chain	8.00	..	1.8
Fr^{217}	7	....	α	8.3	Descendant Pa^{225} (preliminary study)	..	..	..
Fr^{212}	9, 10	19.3 min.	α 56%, EC 44%	6.409 (37%) 6.387 (39%) 6.339 (24%)	Th (p,spallation)	..	..	..

[a] Data taken from Table of Isotopes. J. M. Hollander, I. Perlman and G. T. Seaborg, *Rev. Modern Phys.*, April (1953). Estimated value. [c] Value obtained by closed cycle calculation.

At the end of the war when intensive study was begun of the products of the bombardment of thorium and uranium with the high energy protons available in the 184-inch cyclotron at Berkeley, a number of neutron deficient protactinium isotopes were found and carefully studied. In the decay chains initiated by these protactinium isotopes were found the isotopes Fr^{220}, Fr^{219} and Fr^{218} listed above.[5,6] These short lived alpha emitters were observed only in equilibrium with longer lived precursors. The work of Keyes[7] on the decay chain of Pa^{225} produced by high energy spallation of thorium provides a little information on Fr^{217}. This particular work is very preliminary in nature.

Additional work was carried out at Berkeley in which francium isotopes were sought by direct isolation of a francium fraction from a thorium target. The 15-minute[8] Fr^{222} and the 19-minute[9,10] Fr^{212} were characterized in this work. No reliable evidence was found for any other francium isotopes in the mass range 205–220, all of which were certainly produced in the bombardments, from which an upper limit of 5 minutes may be placed on the half-lives.

Using the data above we are in a position to make some general comments on the α-decay characteristics. These comments make use of the general treatment of alpha systematics given by Perlman, *et al.*,[11] and some special applications to francium systematics given by Momyer.[12] These ideas are best expressed in the form of Fig. 1 which indicates the α-disintegration energy *vs.* mass number. Several unknown values are plotted at the points where one would predict them to fall by analogy to other elements and by considerations somewhat more detailed than we shall go into here (see Momyer[12] for example).

The region from Fr^{215} upwards represents the normal trend of decreasing α-decay energy for increasing mass to be expected from any smoothed atomic mass equation of the Fermi type[13] if nuclear discontinuities are neglected. A sharp discontinuity occurs as we drop to mass numbers lower than 215. Without entering into a discussion of nuclear shell structure or its effect on α-decay in the heavy region we will point out that this discontinuity is related to the closed shell at 126 neutrons.[9,12] We can use the α-disintegration estimates of Fig. 1 to estimate partial α half-lives for many unknown isotopes. There is some uncertainty in this since α-decay in odd-odd and odd-even nuclear types can be hindered by a factor as large as several hundred over that expected by a straight application of the Gamow α-decay theory, for reasons which are not at all well understood. Even within this limitation, however, we can be certain that the half-lives of the unknown isotopes Fr^{214}–Fr^{216} are much less than one second. Fr^{213}, Fr^{210} and Fr^{211} should have half-lives of a few seconds to a few minutes. Below these mass numbers the α half-lives will get progressively shorter and the electron capture half-lives which contribute prominently even in Fr^{212} will also decrease. Hence, on α-instability and orbital electron capture instability grounds we must conclude that no forms of francium longer lived than those already reported will be observed in the mass region below 222. Toward the heavy end of Fig. 1 the α-disintegration energy decreases rapidly. The measured partial α half-life of AcK, for example,

---

(5) A. Ghiorso, W. W. Meinke and G. T. Seaborg, *Phys. Rev.*, **74**, 695 (1948).

(6) W. W. Meinke, A. Ghiorso and G. T. Seaborg, *ibid.*, **81**, 782 (1951).

(7) J. D. Keyes, Ph.D. Thesis, McGill University (1951).

(8) E. K. Hyde and A. Ghiorso, University of California Radiation Laboratory Unclassified Report UCRL-593 (February, 1950), unpublished.

(9) E. K. Hyde, A. Ghiorso and G. T. Seaborg, *Phys. Rev.*, **77**, 765 (1950).

(10) E. K. Hyde and F. Asaro, unpublished data (December, 1952).

(11) I. Perlman, A. Ghiorso and G. T. Seaborg, *Phys. Rev.*, **77**, 26 (1950).

(12) F. F. Momyer, University of California Radiation Laboratory Unclassified Report UCRL-2060 (February, 1953), unpublished.

(13) See for example, E. Fermi, "Nuclear Physics," (notes compiled by J. Orear, A. H. Rosenfeld and R. A. Schluter, University of Chicago Press, 1950, p. 6).

is of the order of one year[14] and much longer half-lives may be expected for higher mass numbers.

In this region it is β-instability that accounts for the absence of isotopes. A direct measurement of β-decay energy is available only for Fr^{223} but enough auxiliary data are available to allow the application of the method of closed cycles to the calculation of β-decay energies for Fr^{218} through Fr^{224}. One example of the method is

$$\begin{tikzcd}
{}_{88}Ra^{224} & & {}_{90}Th^{228} \arrow[ll, "E_\alpha = 5.520 \text{ Mev.}"'] \\
{}_{87}Fr^{224} \arrow[u, "E_{\beta^-} = 3.04 \text{ Mev. (calcd.)}"'] & & {}_{89}Ac^{228} \arrow[ll, "E_\alpha = 4.66 \text{ Mev.}", "\text{(est.)}"'] \arrow[u, "E_{\beta^-} = 2.18 \text{ Mev.}"']
\end{tikzcd}$$

Data calculated by Seaborg, Glass and Thompson[15] are listed in Table I. From these data and the general considerations of β-systematics it seems clear that Fr^{224} and all higher mass isotopes will be quite short lived. Since our knowledge of the spin and parity assignments and the energy separations of the ground states and low lying excited levels among the heavier nuclei is rudimentary, it is still possible that some isomer with a somewhat longer half-life than AcK may eventually be discovered among the neutron excess isotopes. At the moment the prospects for such a discovery are small and in any case will not remove the element from the category of a trace element.

Before concluding the discussion of β-instability it is interesting to observe that Fr^{219} is β-stable[15] and if it were not for α-instability, francium would appear on earth in massive quantities with the atomic weight 219.

Chemical Properties.—The chemistry of francium reduces largely to a radiochemical study of its coprecipitation behavior. Most of our knowledge on this point derives from the researches of Perey[1,2,16] and can be summarized in the statement that francium shows the behavior to be expected of the heaviest alkali element.

Since the alkalies are very soluble in most aqueous solutions and coprecipitate with but few compounds, there are not many suitable carriers for francium. This handicap can be converted partially into an aid by using some simple precipitates to scavenge radioactive impurities from solution. Metal hydroxides, carbonates, fluorides, sulfides and chromates serve well in such a scavenge capacity.

However, there are certain compounds of cesium and rubidium which may be precipitated as carriers for francium. Some examples are cesium perchlorate, cesium chloroplatinate, cesium silicotungstate, cesium chlorostannate, etc.

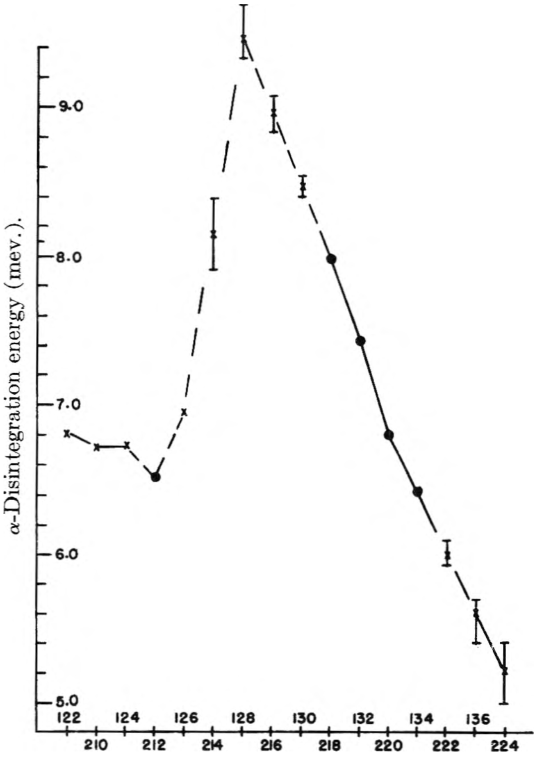

Fig. 1.—α-Disintegration energy *vs.* mass number of francium isotopes. Experimental data shown by solid dots. Predictions are shown by crosses and dotted lines.

These two general types of coprecipitation methods, *i.e.*, the one in which francium is sought in a solution after precipitating other activities away and those in which it is coprecipitated with an insoluble cesium compound, both suffer from the disadvantage that the final sample is necessarily diluted with inert solid matter. In some studies this is not too serious, but for careful work in the study of the radiations of francium isotopes it is imperative to have a carrier-free sample.

Such a chemical method has recently been introduced.[17] In this method francium is coprecipitated with free silicotungstic acid (rather than the cesium salt) which is insoluble in a saturated aqueous hydrochloric acid solution. The silicotungstic acid is then dissolved in water and separated from the francium by a simple ion exchange method.

Astatine

Nuclear Properties.—In the case of astatine as in our discussion of francium we shall not review the history of the older unsuccessful attempts to isolate the element from natural sources, but shall begin with a mention of the famous 1940 work of Corson, MacKenzie and Segrè[18] in which At^{211} was synthesized by the bombardment of bismuth with helium ions in the 60-inch cyclotron of the University of California by the reaction, $Bi^{209}(\alpha,2n)At^{211}$.

At^{211} has a half-life of 7.5 hours and a branching decay–40% by α-emission and 60% by K electron capture.

While this half-life is not ideal for radiochemical tracer studies it is long enough to make such studies very feasible, and having just acquainted ourselves with the situation in the francium case we can

---

[14] E. K. Hyde and A. Ghiorso, University of California Radiation Laboratory Unclassified Report UCRL-2019 (November, 1952); *Phys. Rev.*, **90**, 267 (1953).

[15] G. T. Seaborg, R. A. Glass and S. G. Thompson, *J. Am. Chem. Soc.*, in press.

[16] M. Perey, Ph.D. Thesis, University of Paris (1946).

[17] E. K. Hyde, *J. Am. Chem. Soc.*, **74**, 4181 (1952).

[18] D. R. Corson, K. R. MacKenzie and E. Segrè, *Phys Rev.*, **58**, 672 (1940).

TABLE II

ISOTOPES OF ASTATINE[a]

Isotope	Principal ref.	Half-life	Obsd. radiation	Measured energy of α-radiation (Mev.)	Source
At^{219}	14	0.9 min.	α, β^-	6.27	Natural source daughter AcK
At^{218}	23, 24	1.5–2.0 sec. several sec.	α	6.63	Natural source daughter RaA
At^{217}	3, 4	0.018 sec.	α	7.00	Daughter Fr^{221} in U^{233} decay chain
At^{216}	5, 6	$\sim 3 \times 10^{-4}$ sec.	α	7.79	Daughter Fr^{220} in Pa^{228} decay chain
At^{215}	5, 6	$\sim 10^{-4}$ sec.	α	8.00	Daughter Fr^{219} in Pa^{227} decay chain
	24, 29	Short	α	8.4	Natural source daughter AcA
	31	Short	α	8.02	
At^{214}	5, 6	2×10^{-6} sec.[b]	α	8.78	Daughter Fr^{218} in Pa^{226} decay chain
At^{213}	7	......	α	9.2	Descendant Pa^{225} (preliminary study)
At^{212}	22	0.25 sec.	α	....	Bi(α, n) (preliminary study)
At^{211}	18	7.5 hr.	α 40%, EC 60%	5.862	Bi(α, $2n$)
At^{210}	19	8.3 hr.	α 0.17%, EC 99+%	5.519 (32%) 5.437 (31%) 5.355 (37%)	Bi(α, $3n$)
At^{209}	21	5.5 hr.	α ~5%, EC ~95%	5.65	Bi(α, $4n$) daughter Em^{209}
At^{208}	21	6.3 hr.	EC	....	Bi(α, $5n$) daughter Fr^{212}
	14	1.7 hr.	EC 99+% α 0.5%	5.65	
At^{207}	21	2.0 hr.	EC ~90% α ~10%	5.75	Bi(α, $6n$)
At^{206}	21	2.6 hr.	EC	..	Bi(α, $7n$)
At^{205}	21	25 min.	EC, α	5.90	Bi(α, $8n$)
At^{204}	21	~25 min.	EC	..	Bi(α, $9n$)
At^{203}	21	7 min.	EC, α	6.10	Bi(α, $10n$) (preliminary study)
$At^{<203}$	21	1.7 min.	EC, α	6.35	Bi(α, xn) (preliminary study)
$At^{<202}$	21	43 sec.	EC, α	6.50	Bi(α, xn) (preliminary study)

[a] Data taken from Table of Isotopes. J. M. Hollander, I. Perlman and G. T. Seaborg, *Rev. Modern Phys.*, April (1953).
[b] Estimated value.

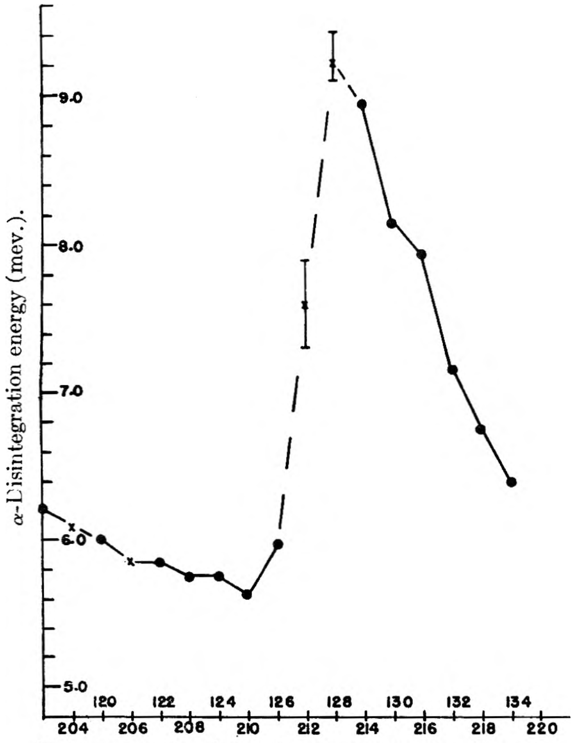

Fig. 2.—α-Disintegration energy *vs.* mass number of astatine isotopes. Experimental data are shown by solid dots. Predictions are shown by crosses and dotted lines.

regard it as quite attractive. And indeed, although we now have knowledge of some 20 different nuclear species of astatine, there is none which is more suitable for chemical studies.

Kelly and Segrè[19] several years later looked again at the products of bombardment of bismuth using helium ions of 38 Mev. and found 8.3-hour At^{210} produced by the (α,$3n$) reaction. The decay is more than 99% by electron capture although quite recent measurements by Hoff and Asaro[20] have indicated an α-branching of 0.17% and a maximum α-particle energy of 5.519 Mev. The partial α half-life is about 5.5 years. As Fig. 2 indicates this is the astatine isotope which is most stable toward α-decay in this region. However, at these low mass numbers instability toward electron capture is quite high and limits the half-lives to a few hours or less.

Barton[21] has continued the study of astatine isotopes by bombarding bismuth with the high energy helium ions of the 184-inch cyclotron and has reported the principal decay characteristics for many isotopes below mass 210. These are listed in Table II. These decay predominantly by orbital electron capture and none have half-lives greater than those of At^{210} and At^{211}.

As we cross the 126 shell line (see Fig. 2) into the higher mass region we expect to find a group of isotopes of high α-decay energy and very short

(19) E. L. Kelly and E. Segrè, *Phys. Rev.*, **75**, 999 (1949).

(20) R. W. Hoff and F. Asaro, private communication (1952), quoted by J. M. Hollander, I. Perlman and G. T. Seaborg, University of California Radiation Laboratory Report UCRL-1928 Rev. (December, 1952).

(21) G. W. Barton, Jr., A. Ghiorso and I. Perlman, *Phys. Rev.*, **82**, 13 (1951).

half-life decaying almost entirely by α-emission. From the studies of Meinke, *et al.*,[6,5] on the decay chains of the protactinium isotopes produced by high energy proton bombardments of thorium we obtain the data on At^{214} through At^{216} shown in Table II. The half-lives range from an estimated 2 microseconds up to 18 milliseconds. The short lived At^{217} appears in the U^{233} decay chain.[3,4] There are some preliminary data[22] on At^{212} and At^{213}.[7]

Perlman, Ghiorso and Seaborg[11] discussed the question whether any isotopes of astatine are β-stable, and reached the conclusion that it is borderline whether At^{213} and At^{215} are or are not. It is quite possible that astatine, like elements 43 and 61, has no β-stable form. Whatever the final decision on this, we note from Fig. 2 that At^{213} and At^{215} fall right at the maximum of α-instability. It can be shown by closed cycle systematics that by the time a high enough mass number is reached to reduce the α-instability to the point where β-instability rather than α-instability is limiting, the β-disintegration energy is very high. The possibility of an undiscovered long lived form of astatine can be discounted almost with certainty.

Astatine in Nature.—Our discussion above eliminated the possibility of the existence of stable or long lived astatine in natural sources, but did not rule out the presence of short lived forms in radioactive ores. There have been a number of interesting publications on this point in the last 10 years originating chiefly from the Viennese research team of Karlik and Bernert. These workers looked for the astatine isotopes which would form if the A products in the decay chains of uranium, actinouranium and thorium showed some β-branching.

In the uranium–radium series α-particles of 6.63 Mev. energy with a half-life of a few seconds were observed to grow into a freshly deposited sample of the 3.05-minute RaA (Po^{218}) and these were ascribed to At^{218} resulting from a β-branching of $5 \times 10^{-2}\%$ in RaA.[23 24] These experiments were repeated by Walen[25] in France with substantially the same results. The properties attributed to RaA and At^{218} are in conformity with the interpolations of α-systematics and the interpretation given to the experimental observations are probably correct, but further confirmation would be desirable. Walen claimed to have observed β-branching of 0.1% in the At^{218} itself to produce a 1.3-second Em^{218}. This report seems very doubtful to this reviewer for reasons given by Perlman, *et al.*,[11] because the half-life is greatly out of line with the regularities of even-even α-emitters and in conflict with the properties of the Em^{218} reported by Studier and Hyde[26] in a study where the identification of Em^{218} was rather certain.

Karlik and Bernert also examined the α-activity in a fresh preparation of thoron from the thorium decay series and observed some previously unreported α-particles of 7.64 Mev. These were ascribed to At^{216} arising from a $1.35 \times 10^{-2}\%$ β-branching of the 0.158-second ThA (Po^{216}) daughter of thoron.[27,24] There was no observation of a growth of these new α-particles because of the extremely short half-lives of ThA and At^{216}. Recent unpublished calculations of Seaborg, Glass and Thompson[15] indicate that At^{216} is heavier than ThA by 0.46 Mev., making the assignment of these 7.64 Mev. α-particles to At^{216} untenable.

In a third study Karlik and Bernert examined the α-activity in a weak sample of the 3.92-second actinon activity from the U^{235} series and found a small number of previously unreported 8.4 Mev. α-particles.[28,24] These were ascribed to an extremely short lived At^{215} resulting from a $5 \times 10^{-4}\%$ β-branching in AcA. As originally reported these results were open to objections on energetic grounds as discussed by Feather.[29] The work was repeated by Avignon[30] in France on a considerably larger sample with substantially the same results except that the α-particle energy was determined as 8.04 Mev. This revision of the α-energy removes one main objection to the assignment (*i.e.*, the non-equivalence of the AcA–At^{215}–AcC energy sum as compared to the AcA–AcB–AcC energy sum) and makes it possible to identify this At^{215} with the At^{215} discovered by Meinke[6] in cyclotron prepared activities. Nevertheless, more conclusive evidence is desirable on this question.

Some recent work establishes the presence of minute amounts of the $(4n + 1)$ series in uranium ores (about 2×10^{-12} parts by mass of Np^{237} to one part of U^{238}).[31] Since the 0.02-second At^{217} is a member of the $(4n + 1)$ decay chain, this report implies the existence of this astatine isotope in uranium ores and indeed the α-particles of At^{217} were observed in their α-spectrum analyses.

The most recent work on naturally occurring astatine was done at Berkeley where it was shown that At^{219} is present in U^{235} ores in minute amounts.[14] It was predicted that AcK (Fr^{223}) should show α-branching to a slight extent. Astatine was chemically separated from a pure francium fraction which in turn had been separated from a 20-millicurie source of Ac^{227}. It was shown that AcK emits α-particles with a branching ratio of 4×10^{-5} and that At^{219} has a half-life of 0.9 minute for the emission of 6.27 Mev. α-particles. This is the longest lived astatine isotope in nature and the only one long lived enough to permit chemical isolation.

Astatine Chemistry.—The principal published work on astatine chemistry is contained in two important papers. The first is the original discovery paper by Corson, MacKenzie and Segrè[18] of 1940 and the second is a postwar paper by Johnson, Leininger and Segrè.[32] Some additional in-

---

(22) M. Weissbluth, T. M. Putnam and E. Segrè, private communication (July, 1948). Quoted by J. M. Hollander, I. Perlman and G. T. Seaborg, *Rev. Modern Phys.*, April (1953).

(23) B. Karlik and T. Bernert, *Naturwissenschaften*, **31**, 298 (1943).

(24) B. Karlik and T. Bernert, *Z. Physik*, **123**, 51 (1944).

(25) R. Walen, *Compt. rend.*, **227**, 1090 (1948).

(26) M. H. Studier and E. K. Hyde, *Phys. Rev.*, **74**, 591 (1948).

(27) B. Karlik and T. Bernert, *Naturwissenschaften*, **31**, 492 (1943).

(28) B. Karlik and T. Bernert, *ibid.*, **32**, 44 (1944).

(29) N. Feather, *Nucleonics*, **5**, 22 (1949).

(30) P. Avignon, *J. Phys. Radium*, **11**, 521 (1950).

(31) D. F. Peppard, G. W. Mason, P. R. Gray and J. F. Mech, *J. Am. Chem. Soc.*, **74**, 6081 (1952).

(32) G. L. Johnson, R. F. Leininger and E. Segrè, *J. Chem. Phys.*, **17**, 1 (1949).

formation is given by Barton.[21] Also Hamilton, Garrison and others of the Division of Medical Physics at the University of California in their extensive studies of the radiobiological effects of astatine have developed useful chemical techniques for the handling of astatine.[33] We will not have time in this review to discuss the interesting biological studies with astatine.

One of the outstanding characteristics of astatine is its high volatility. The easiest way to separate it from bismuth target material is to melt the bismuth in a closed system and distil out the astatine, collecting it on a cold finger. In aqueous solution astatine is easily reduced to the free state in which condition it is readily extracted into organic solvents. This is perhaps its single most useful property. Strong reducing agents such as SO_2 or zinc reduce it to a negative oxidation state, presumably minus 1, in which condition it carries quantitatively on AgI. In these and other respects it resembles the lighter halogens. Oxidizing agents convert astatine to at least two different oxidation states, neither of which has been satisfactorily identified. Coprecipitation on $AgIO_3$ under some strongly oxidizing conditions is quantitative, suggesting an AtO_3^- ion. While astatine thus shows some strong resemblances to iodine it also shows considerable metallic character in which its resemblance to its neighboring element polonium is marked. Its quantitative coprecipitation on freshly reduced tellurium or silver is an example.

While the references quoted above give much useful and fundamental work on the chemistry of astatine, there is much yet to be learned. The identification of the oxidation states and the ionic species, the estimation of oxidation potentials and the perfection of methods for quantitative separation and recovery, await new research. The number of cyclotrons with helium ion beams of energy greater than the 21 Mev. threshold for the reaction $Bi^{209}(\alpha,2n)At^{211}$ has increased markedly in the past decade and we can expect that more nuclear chemists will initiate research on this exceedingly interesting element.

---

[33] W. M. Garrison, J. D. Gile, R. D. Maxwell, and J. G. Hamilton, University of California Radiation Laboratory Unclassified Report UCRL-741 (May, 1950), unpublished.

THE COMPLEXING OF INDIUM(III) BY FLUORIDE IONS IN AQUEOUS SOLUTION: FREE ENERGIES, HEATS AND ENTROPIES

By L. G. Hepler, John W. Kury and Z Z. Hugus, Jr.[1]

Contribution from the University of California Radiation Laboratory, and the Department of Chemistry and Chemical Engineering, University of California, Berkeley, California

Received May 22, 1953

The potential of the ferrous–ferric half-cell has been studied as a function of the concentrations of hydrofluoric acid and indium perchlorate at a total ionic strength of 0.5. The resulting data can be interpreted by assuming the existence of the ions InF^{++} and InF_2^+. Equilibrium constants for the formation of these ions are calculated at 15, 25 and 35° and the free energy, heat and entropy changes computed for the reactions: $In^{+3} + HF = InF^{+2} + H^+$ and $InF^{+2} + HF = InF_2^+ + H^+$.

Recent studies in this Laboratory on the potential of the ferrous–ferric half-cell as a function of the hydrofluoric acid concentration have provided a useful tool for the investigation of the extent of fluoride complexing of various cations.[2,3]

The experimental technique used in the present investigation of the fluoride complex ions of indium(III) is a modification of that used by Dodgen and Rollefson for their investigation of fluoride complex ions of thorium(IV).[2]

Experimental

The Cells.—The cell containers used in these experiments are similar to those previously described.[2] The interiors of the containers and the stirrers were coated with paraffin to prevent hydrofluoric acid from reacting with the glass. The electrodes were made of pure platinum sheet and wire. They were stored in distilled water when not in use.

The three half-cell containers used were connected by salt bridges in the manner A-B and B-C in order that half-cell B might serve as a reference half-cell. In an effort to minimize junction potentials, the salt bridges were made from agar–agar and 1.6 *M* sodium perchlorate solution. A carbon dioxide atmosphere was maintained over the solutions to prevent air oxidation of ferrous ion. Standard sodium fluoride solution was added from a 5-ml. buret or a "Dri-Filmed" micropipet.

Solutions.—A stock solution of sodium perchlorate was prepared by adding an excess of double vacuum-distilled 72% perchloric acid to analytical reagent sodium carbonate. The solution was boiled to expel carbon dioxide and the *p*H adjusted to 5 with carbonate-free sodium hydroxide solution. After several days this solution was diluted and filtered through sintered glass. The solution was standardized by evaporating aliquots to dryness in the presence of an excess of sulfuric acid and weighing the residue as sodium sulfate.[4]

Double vacuum-distilled 72% perchloric acid was diluted with conductivity water to yield a stock solution which was standardized against mercuric oxide using methyl red as an indicator.

A stock solution of ferrous perchlorate, ferric perchlorate and perchloric acid was prepared by treating electrolytic iron with a standard perchloric acid solution. Hydrogen peroxide was added to the resulting solution to oxidize a portion of the ferrous perchlorate to ferric perchlorate. The ferrous ion concentration was determined by titrating to a ferroin end-point with a standard ceric solution. Since the ferrous perchlorate, total iron and initial perchloric acid concentrations were known, we were able to calculate the final ferric perchlorate and perchloric acid concentrations.

C.P. sodium fluoride, which had been ignited in platinum, was dissolved in conductivity water to make a standard fluoride solution.

---

[1] School of Chemistry, University of Minnesota, Minneapolis 14, Minnesota.

[2] H. Dodgen and G. Rollefson, *J. Am. Chem. Soc.*, **71**, 2600 (1949).

[3] R. E. Connick, *et al.*, to be published.

[4] W. W. Scott, "Standard Methods of Chemical Analysis," 5th Edition, Vol. I, D. Van Nostrand Co., Inc., New York, N. Y., 1939.

Indium oxide, obtained from Indium Corporation of America, containing iron as the most important impurity, was purified in the following manner. The oxide was dissolved in concentrated hydrochloric acid and the solution then diluted. Dilute ammonium hydroxide was added to this solution to precipitate indium hydroxide. The precipitate was washed several times with hot water and then dissolved in 6 *M* acetic acid. Indium sulfide was precipitated with hydrogen sulfide from this solution. The sulfide was filtered, washed with acetic acid and dissolved in nitric acid. Indium hydroxide was precipitated with an excess of dilute ammonium hydroxide. The precipitate was washed and then dissolved in hydrochloric acid. Spongy indium was plated out with platinum electrodes from this solution. The spongy mass then served as anode; the indium being redeposited on a platinum cathode.[5,6]

Pure indium metal was dissolved in standard perchloric acid. The resulting solution was standardized by determining indium as In_2O_3.

Procedure.—Experiments were carried out at 15.00 ± 0.02°, 25.00 ± 0.01° and 35.00 ± 0.02°. Before each run the assembled cells and the stock solutions were brought to the temperature of the experiment.

One hundred-ml. aliquots of stock solution containing the desired concentrations of ferrous perchlorate, ferric perchlorate, perchloric acid and sodium perchlorate were pipetted into containers A, B and C. A known volume of standard indium perchlorate–perchloric acid solution was added to half-cell A. An equal volume of sodium perchlorate–perchloric acid solution, equivalent to the indium solution in total ionic strength and in acid concentration, was added to half-cells B and C.

The stirrers were turned on and the potentials of half-cells A and C were measured with respect to the reference half-cell B. These potentials were measured with a Rubicon type B high precision potentiometer with a d.c. spotlight galvanometer for the indication of the null point. The potentiometer was checked against a standard cell from time to time during an experiment. After the small initial potentials (usually less than 0.20 mv.) had become constant, aliquots of standard sodium fluoride solution were added to half-cells A and C. The potentials of these half-cells were then measured with respect to the reference half-cell B after each addition. The stirrers were left on when the sodium fluoride was added and while the potentials were read. The potentials became constant to within 0.02 mv. shortly after the sodium fluoride was added.

Experimental Results

The variation of potential with $\Sigma(F^-)$ for cells A-B and B-C for a typical run is given in Table I. The ferrous and ferric ion concentrations for every run were approximately 5×10^{-4} *M*.

Analysis of Results

Equilibria to Be Considered.—In analyzing the data it is necessary to consider the following equilibria

$$Fe^{+3} + HF = FeF^{++} + H^+ \qquad K_1 \qquad (1)$$

$$FeF^{++} + HF = FeF_2^+ + H^+ \qquad K_2 \qquad (2)$$

$$FeF_2^+ + HF = FeF_3 + H^+ \qquad K_3 \qquad (3)$$

$$Fe^{+++} + H_2O = FeOH^{++} + H^+ \qquad K_h \qquad (4)$$

$$HF = H^+ + F^- \qquad K_{HF} \qquad (5)$$

$$In^{+++} + HF = InF^{++} + H^+ \qquad K_4 \qquad (6)$$

$$InF^{++} + HF = InF_2^+ + H^+ \qquad K_5 \qquad (7)$$

All the *K*'s are equilibrium quotients; for example

$$K_4 = \frac{(InF^{++})(H^+)}{(In^{+++})(HF)} \qquad (8)$$

$$K_5 = \frac{(InF_2^+)(H^+)}{(InF^{++})(HF)} \qquad (9)$$

Parentheses designate concentrations in moles per liter. The concentrations of the various species were calculated using the total volume, *i.e.*, the initial volume plus the volume of the sodium fluoride solution added. The experiments were carried out at 0.50 ionic strength because the activity coefficients of many electrolytes have a small rate of change with ionic strength in this range.[2]

TABLE I

Run IV: $t = 25.00 \pm 0.01°$; $\Sigma(H^+_i) = 0.04969$; $\Sigma(In^{+3}_i) = 0.05781$; $V_{A_i} = 104.90$ ml.

V_A, ml.	E_{A-B}, mv.	$\Sigma(F^-)_A \times 10^4$, moles/l.	E_{B-C}, mv.	$\Sigma(F^-)_C \times 10^4$ moles/l.
104.94	9.54	3.74	13.83	3.78
105.05	18.67	7.47	26.32	7.55
105.12	26.55	11.19	36.65	11.31
105.20	33.41	14.91	45.17	15.07
105.40	48.29	24.88	52.57	18.83
105.60	59.86	34.80	68.22	28.77
105.80	69.45	44.69	80.24	38.68
105.99	77.75	54.54	90.29	48.55
106.19	85.21	64.36	107.32	68.18
106.59	98.48	83.87	121.46	87.66
106.99	110.18	103.24	133.84	107.00
107.38	120.73	122.48	144.98	126.20
107.98	135.20	151.20		
108.38	144.14	169.93		

The values of the constants used in this work are given in Table II.[3,7]

TABLE II

	15°	25°	35°
K_1	192	184	178
K_2	11.5	10.3	10.0
K_3	1.0	1.0	1.0
K_h	1.18×10^{-3}	1.9×10^{-3}	3.2×10^{-3}

Calculation of K_4 and K_5.—For each run the known quantities were K_1, K_2, K_3, K_h, initial total indium $\Sigma(In_i^{+3})$ and initial total acid $\Sigma(H_i^+)$. $\Sigma(Fe_i^{++})$ and $\Sigma(Fe_i^{+3})$ were also known, but, as will be shown later, are not necessary for the calculation of K_4 and K_5. The total fluoride concentration $\Sigma(F^-)$ and the potential (*E*) with respect to the reference half-cell are measured quantities. The potential (*E*) was plotted *vs.* $\Sigma(F^-)$ for both cells A-B and B-C (Fig. 1). We define $\Delta\Sigma(F^-)$ as

$$\Delta\Sigma(F^-) = \Sigma(F^-)_A - \Sigma(F^-)_C \qquad (10)$$

when $E_{A-B} = E_{B-C}$. Because half-cells A and C have

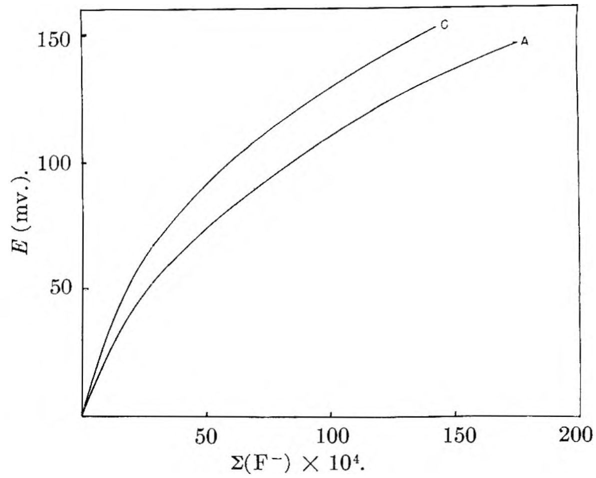

Fig. 1.—Run IV at 25°.

---

[5] E. Hattox and T. DeVries, *J. Am. Chem. Soc.*, **58**, 2126 (1936).

[6] G. P. Baxter and C. M. Alter, *ibid.*, **55**, 1943 (1933).

[7] Maak-Sang Tsao, Dissertation, University of California, Berkeley, Calif. (1952).

the same $\Sigma(H_i^+)$, $\Sigma(Fe_i^{+3})$ and $\Sigma(Fe_i^{++})$, $\Delta\Sigma(F^-)$ is a measure of the fluoride ions complexing indium.

Runs 1, 2 and 3 at each temperature were carried out at low $(HF)/(H^+)$. We therefore assume that in these cases only the first complex need be considered. Thus

$$\Delta\Sigma(F^-) = (InF^{++}) \quad (11)$$

$$\Sigma(In^{+++}) = (In^{+3}) + (InF^{++}) \quad (12)$$

Combination of 8, 11 and 12 gives

$$\frac{\Sigma(In^{+3})}{\Sigma(In^{+3}) - \Delta\Sigma(F^-)} = 1 + K_4(HF)/(H^+) \quad (13)$$

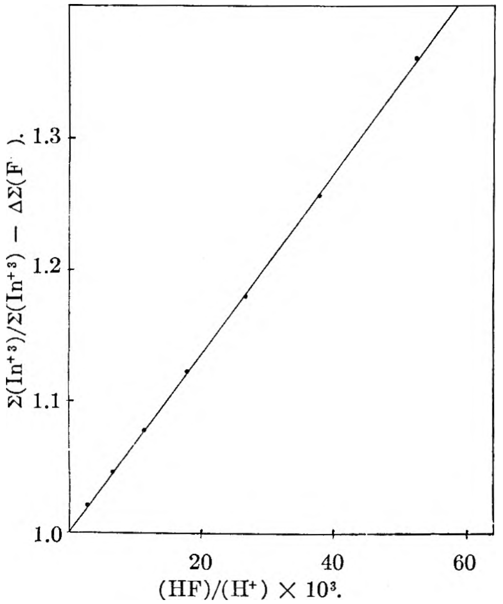

Fig. 2.—Run IV at 25°.

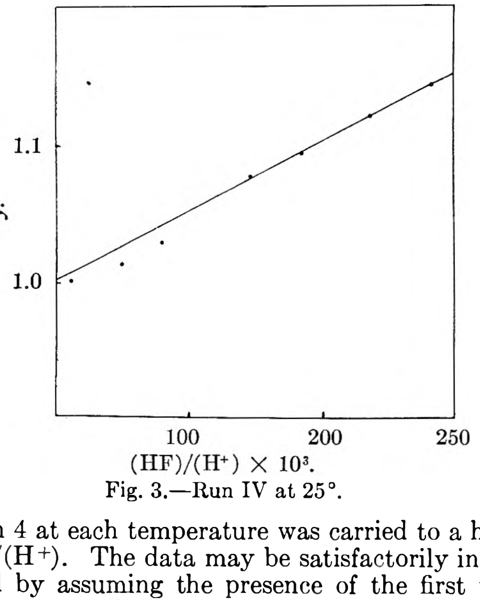

Fig. 3.—Run IV at 25°.

Run 4 at each temperature was carried to a high $(HF)/(H^+)$. The data may be satisfactorily interpreted by assuming the presence of the first two complexes of indium, InF^{++} and InF_2^+. Thus

$$\Delta\Sigma(F^-) = (InF^{++}) + 2(InF_2^+) \quad (14)$$

$$\Sigma(In^{+3}) = (In^{+++}) + (InF^{++}) + (InF_2^+) \quad (15)$$

Combination of 8, 9, 14 and 15 gives

$$\left[\frac{\Sigma(In^{+++})K_4(HF)/(H^+) + \Delta\Sigma(F^-)}{2\Sigma(In^{+++}) - \Delta\Sigma(F^-)}\right] [(H^+)/(HF)] = K_4 + K_4K_5(HF)/(H^+) \quad (16)$$

It is seen from 13 that a plot of $\Sigma(In^{+++})/[\Sigma(In^{+++}) - \Delta\Sigma(F^-)]$ *vs.* $(HF)/(H^+)$ should give a straight line of slope K_4 and intercept 1. Similarly, by using equation 16, we can obtain an estimate of K_5 (see Figs. 2 and 3); Y represents the first factor in equation 16. In order to do this we must know $(HF)/(H^+)_A$ as a function of E.

When $E_{A-B} = E_{B-C}$, the quantity $(HF)/(H^+)$ in half-cell A is equal to that in half-cell C. This is true because initially

$$\Sigma(Fe^{+3})_A = \Sigma(Fe^{+3})_C,\ \Sigma(Fe^{+2})_A = \Sigma(Fe^{+2})_C \text{ and } \Sigma(H^+)_A = \Sigma(H^+)_C$$

By utilizing the results of earlier work on fluoride complexing[2,3] of ferric ion, we can calculate $(HF)/(H^+)$ in half-cell C.

The measured potential can be expressed as

$$E = \frac{RT}{F} \ln \frac{(Fe^{+++})_B(Fe^{++})_C}{(Fe^{+++})_C(Fe^{++})_B} \quad (17)$$

Stoichiometric considerations lead to the equations

$$\Sigma(Fe^{+++})_C = (Fe^{+3})_C + (FeOH^{++})_C + (FeF^{++})_C + (FeF_2^+)_C + (FeF_3)_C \quad (18)$$

$$\Sigma(Fe^{+++})_B = (Fe^{+++})_B + (FeOH^{++})_B \quad (19)$$

Equations 18 and 19 can be expressed in terms of K_1, K_2, K_3, K_h and $(HF)/(H^+)$.

$$\frac{\Sigma(Fe^{+++})_C}{(Fe^{+++})_C} = 1 + \frac{K_h}{(H^+)_C} + K_1(HF)/(H^+) + K_1K_2(HF)^2/(H^+)^2 + K_1K_2K_3(HF)^3/(H^+)^3 \quad (20)$$

$$\frac{\Sigma(Fe^{+++})_B}{(Fe^{+++})_B} = 1 + \frac{K_h}{(H^+)_B} \quad (21)$$

Combining 17, 20 and 21 we obtain an expression from which $(HF)/(H^+)$ can be calculated.

$$(e^{EF/RT} - 1)\left(1 + \frac{K_h}{(H^+)}\right) = K_1(HF)/(H^+) + K_1K_2(HF)^2/(H^+)^2 + K_1K_2K_3(HF)^3/(H^+)^3 \quad (22)$$

The justifiable assumptions that

$$\left[1 + \frac{K_h}{(H^+)_B}\right] = \left[1 + \frac{K_h}{(H^+)_C}\right]$$

and that ferrous ion is not complexed by fluoride were made in obtaining 22.[2]

Results

The values obtained for K_4 and K_5 at each temperature are summarized in Table III. In Table IV are summarized ΔF, ΔH and ΔS for reactions 6 and 7.

TABLE III

	t = 15°		t = 25°		t = 35°	
Run	K_4	K_5	K_4	K_5	K_4	K_5
I	7.1		6.7		6.8	
II	7.3		7.1		6.7	
III	7.0		7.1		6.4	
IV	6.9	0.5	6.8	0.5	6.7	0.6
V					6.8	
Av.	7.1	0.5	6.9	0.5	6.7	0.6

TABLE IV

	ΔF_{298}, kcal.	ΔH_{298}, kcal.	ΔS_{298}, e.u.
$In^{+++} + HF = InF^{++} + H^+$	−1.144	−0.508	2.1
$InF^{++} + HF = InF_2^+ + H^+$	0.41	1.0	2

Acknowledgment.—The authors wish to express their thanks to Professors Wendell M. Latimer and R. E. Connick for helpful discussions.

KINETICS OF THE OXIDATION OF VANADIUM(II) AND VANADIUM(III) IONS BY PERCHLORATE ION[1a]

By WILLIAM R. KING, JR.,[1b] AND CLIFFORD S. GARNER

The Department of Chemistry, University of California, Los Angeles 24, California

Received May 22, 1953

Kinetic studies of the oxidation of V(II) and V(III) ions by perchlorate ion were carried out at 49.9°, leading to the following rate laws in the initial concentration range 0.050–0.15 *f* VCl_2, 0.0035–0.078 *f* VCl_3, 0.53–1.99 *f* ClO_4^-, 0.17–1.67 *f* H^+, μ adjusted to 2.5 with NaCl and $NaClO_4$, $-d(V^{++})/dt = k_1(V^{++})(ClO_4^-) + 2k_2(V^{++})(ClO_4^-)$, and in the absence of V(II) ion, $-d(V^{+++})/dt = k_2(V^{+++})(ClO_4^-)$. The latter rate law agrees with that found by Sugimoto. A decrease in the average hydrogen ion concentration from 1.65 to 0.11 *f* gave an approximately 25% decrease in the value of k_1 and a twofold decrease in the value of k_2. The former effect is not much larger than the estimated experimental error (15%), and may arise from specific electrolyte effects in maintaining constant ionic strength. At $(H^+) = 1\,f$, $k_1 = 1.3 \times 10^{-3}$ mole^{-1} liter min.$^{-1}$. Although the variation of k_2 with hydrogen ion concentration appears to be sigmoidal, a rough resolution of k_2 may be effected into two terms, $k_2 = k_2' + k_2''(H^+)$, with $k_2' = 0.17 \times 10^{-3}$ mole^{-1} liter min.$^{-1}$ and $k_2'' = 0.1 \times 10^{-3}$ mole^{-2} liter^2 min.$^{-1}$. The rate-determining step in the V(II)–ClO_4^- reaction is suggested to involve transfer of an oxygen atom from ClO_4^- to V^{++}, or possibly to be an electron transfer from V^{++} to ClO_4^-. The absorption spectrum of $V(ClO_4)_2$ in aqueous $HClO_4$ was obtained. VCl_2 solutions 0.1–1 *f* in HCl are only slowly oxidized by hydrogen ion (or water) even at 50°, although oxidation by oxygen is fairly rapid at 25°.

As is well known, aqueous perchlorate ion is remarkably inert at ordinary temperatures toward many reducing agents, including even such strong reductants as sodium amalgam, zinc and iron(II) ion. At room temperature perchlorate ion is reduced to chloride ion in aqueous acid solutions at a measurable rate by titanium(III),[2,3] vanadium (III),[2] chromium(II),[2,3] molybdenum(III),[3] ruthenium(III)[4] and europium(II)[5] ions. Bromide ion in the presence of ruthenium(III, IV)[6] and osmium(IV)[7] catalysts and tin(II) ion with molybdate catalyst[8] also reduce perchlorate ion under these conditions. However, only five kinetic investigations of oxidation by aqueous perchlorate ion appear to have been reported,[3,6–9] three of which involve catalyzed reactions.

Sugimoto[9] carried out a kinetic study of the vanadium(III)-perchlorate reaction, for which the over-all reaction may be represented by

$$8V^{+++} + ClO_4^- + 4H_2O \longrightarrow 8VO^{++} + Cl^- + 8H^+ \quad (1)$$

At 50° the oxidation of vanadium(III) ion, V^{+++} (hydrated), was first order in vanadium(III) and in perchlorate ion, with a complex dependence on hydrogen ion concentration, the nature of which may have been obscured by failure to control the ionic strength of the reaction solutions (ionic strength, μ, varied from 0.65 to 3.5).

We have undertaken a kinetic study of the vanadium(II)–perchlorate reaction, as well as a reinvestigation of the vanadium(III)–perchlorate reaction, not only to extend the knowledge of the kinetic behavior of perchlorate ion as an oxidant, but also to gain information about perchlorate oxidation of vanadium(II) and vanadium(III) ions which was of interest in connection with a study[10] of isotopic exchange reactions.

Preliminary experiments with vanadium(II) perchlorate solutions initially free of chloride ion demonstrated that chloride ion is produced according to the stoichiometry of equation 2

$$8V^{++} + ClO_4^- + 8H^+ \longrightarrow 8V^{+++} + Cl^- + 4H_2O \quad (2)$$

The study of the kinetics of this reaction was complicated by the fact that the vanadium(III) produced by this reaction reacts at a comparable rate with perchlorate ion by equation 1, forming vanadyl ion, VO^{++}, which reacts instantaneously with vanadium(II) ion to produce vanadium(III) ion

$$VO^{++} + V^{++} + 2H^+ \longrightarrow 2V^{+++} + H_2O \quad (3)$$

Experimental

Chemicals.—Stock solutions of vanadium(II) chloride were prepared by electrolytic reduction of a mixture of vanadium(V) oxide (made by igniting recrystallized ammonium metavanadate) and 0.7 *f* hydrochloric acid, the cell having a mercury cathode and an anode compartment separated by a porous cup. In addition to oxygen, chlorine was liberated at the anode, necessitating the addition of more hydrochloric acid during the reduction. Vanadium(II) perchlorate solution was prepared from vanadium(IV) perchlorate solution (1.6 *f* in $HClO_4$) by reduction with zinc amalgam at 0.5°; the vanadium(IV) perchlorate solution was made by refluxing a mixture of purified vanadium(V) oxide, perchloric acid and formic acid, adsorbing the resulting solution on Ion-X cation-exchange resin, washing out the excess formic acid with water, then eluting the vanadium(IV) with 4 *f* perchloric acid. The stock solutions were analyzed for dipositive and tripositive vanadium by a modification of the method devised by Ramsey[11] for the determination of vanadium(III). Total vanadium was determined by oxidation of an aliquot to vanadium(IV) with ammonium peroxydisulfate, followed by titration at 50° with cerium(IV) sulfate solution standardized against arsenic(III) acid, using *o*-phenanthroline iron(II) sulfate indicator. For the determination of total reducing equivalents a separate aliquot was delivered into an excess of sodium metavanadate solution (0.3 *f* in sulfuric acid), which oxidizes all the vanadium to vanadium(IV) and reduces the metavanadate to the same state in an amount dependent upon the amounts of +2 and +3 vanadium present; the vanadium(IV) thus formed was titrated as above with cerium(IV) sulfate. From the results of these two titra-

---

[1] (a) Adapted from a portion of the Ph.D. thesis of William R. King, Jr., University of California, Los Angeles, June, 1952; (b) Filtrol Corporation, Los Angeles, California.

[2] V. Rothmund, *Z. anorg. Chem.*, **62**, 109 (1909).

[3] G. Bredig and J. Michel, *Z. physik. Chem.*, **100**, 124 (1922).

[4] P. Wehner and J. C. Hindman, *J. Am. Chem. Soc.*, **72**, 3911 (1950). Ru(IV) is reported to be inert toward 1 *f* $HClO_4$ at 25° and to reduce ClO_4^- to Cl^- slowly in 6 *f* $HClO_4$ at 75°.

[5] D. J. Meier and C. S. Garner, THIS JOURNAL, **56**, 853 (1952).

[6] W. R. Crowell, D. M. Yost and J. M. Carter, *J. Am. Chem. Soc.*, **51**, 786 (1929).

[7] W. R. Crowell, D. M. Yost and J. D. Roberts, *ibid.*, **62**, 2176 (1940).

[8] G. P. Haight, Jr., and W. F. Sager, *ibid.*, **74**, 6056 (1952).

[9] R. Sugimoto, M.S. thesis, University of California, Los Angeles, 1941.

[10] W. R. King, Jr., and C. S. Garner, *J. Am. Chem. Soc.*, **74**, 3709 (1952).

[11] J. B. Ramsey, *ibid.*, **49**, 1138 (1927).

tions the concentrations of vanadium(II) and vanadium(III) were calculated (*ca.* 10% of the vanadium was present as vanadium(III) at the time of use in the rate runs). The hydrogen ion concentration was determined indirectly by a gravimetric determination of the chloride concentration, assuming that neither vanadium(II) ion nor vanadium(III) ion is hydrolyzed to any extent in these solutions.[12]

Because of the ease of air oxidation of vanadium(II) and vanadium(III), all solutions were prepared from water redistilled from an alkaline permanganate solution in an all-Pyrex still and freed from oxygen by passage of a stream of oxygen-free nitrogen through the water. All solutions were stored in all-Pyrex closed-buret systems,[13] under an atmosphere of oxygen-free nitrogen. The latter was prepared by passage of high purity tank nitrogen through a continuously regenerated chromium(II) chloride solution.[14]

The perchloric acid was C.P. grade, redistilled at 5 mm. pressure. C.P. sodium perchlorate was found to contain chlorate and iron(III) ions, and was purified by recrystallization from water until negative tests for these impurities were obtained (KSCN test for Fe(III), and $Ag^+ + NO_2^-$ for ClO_3^-). C.P. hydrochloric acid and C.P. sodium chloride were tested and found satisfactory without further purification. Sodium metavanadate solution was prepared by boiling recrystallized ammonium metavanadate with the stoichiometric amount of C.P. sodium carbonate.

Procedure.—Appropriate volumes of standardized solutions of perchloric acid, sodium perchlorate, hydrochloric acid, sodium chloride and water were delivered from their respective storage burets into a closed previously evacuated reaction vessel equipped with a buret. A calculated volume of standardized vanadium(II) chloride solution was similarly transferred to a second vessel, and both vessels were brought to temperature in a thermostated oil-bath maintained at 49.9 ± 0.1°. Then the two solutions were mixed by interconnecting the two vessels and forcing the vanadium(II) chloride solution into the reaction vessel with nitrogen. The transfer was quantitative inasmuch as the inside of the vessel containing the vanadium(II) solution was coated with Beckman "Silicote" and was not wet by the solution.

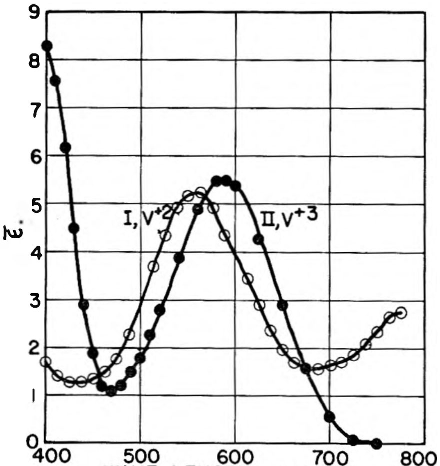

Fig. 1.—Comparison of absorption spectra of hydrated V^{+2} and V^{+3} ions in $HClO_4$, 25°: curve I, 0.07 *f* $V(ClO_4)_2$, 0.5 *f* $HClO_4$, $\mu = 0.7$; curve II, 0.073 *f* $V(ClO_4)_3$, 0.38 *f* $HClO_4$, 0.56 *f* $NaClO_4$, $\mu = 1.4$ (Furman and Garner, ref. 15).

The change in vanadium(II) concentration with time was followed by removing the reaction vessel momentarily from the oil-bath, immersing the tip below the surface of an excess of sodium metavanadate solution (0.3 *f* in sulfuric acid), and delivering a 5-ml. aliquot from the buret (another aliquot was delivered 0.5 minute later into a second metavanadate solution for a duplicate analysis). Titration with cerium(IV) sulfate, as outlined above, together with a knowledge of the total vanadium concentration, permitted calculation of the vanadium(II) concentration at that time. Two other less satisfactory methods of following the change in vanadium(II) concentration were tried. In one case, the vanadium(II) was caused to react with α,α′-dipyridyl to form a green complex, the color intensity of which was determined spectrophotometrically. In the other case, attempts were made to follow the decrease in the absorption of light by the vanadium(II) ion itself, but the absorption spectra of vanadium(II) and vanadium(III) ions were found to be too similar to make this convenient. Figure 1 gives a comparison of these spectra, the spectrum of the vanadium(III) ion being taken from the paper of Furman and Garner.[15]

In some experiments the rate of the vanadium(III)-perchlorate reaction was followed in the absence of vanadium(II) by using reaction mixtures which had stood until all the vanadium(II) had reacted, the change in vanadium(III) concentration being followed by titration as above.

Calculation of Reaction Rates.—Vanadium(II) titers of the reaction aliquots were plotted against time on large-scale graph paper for each run, the points falling on a smooth curve. Slopes were measured at various points on each curve with a Bausch and Lomb tangent meter, these values (multiplied by suitable factors) giving the rate of disappearance of vanadium(II) ion, $-d(V^{++})/dt$. Similar treatment was given the data for the vanadium(III)-perchlorate reaction. All concentrations are expressed in moles per liter of solution of 49.9°, and the time is given in minutes.

Normally the order of reaction with respect to a particular species can be determined by varying the concentration of this species while holding that of all others constant. This procedure was not possible here, but an equivalent method was used by calculating the slopes from the various curves as a function of time for various fixed concentrations of all species but the particular one. A plot of such slopes *versus* the concentration of the particular species then allowed determining the order of reaction with respect to that species. The data of all such plots were treated by the least squares method. The over-all error in the values of the rate constants is estimated to be 15%.

Results

Stability of Vanadium(II) Chloride Solutions.—Although vanadium(II) ion, V^{++} (hydrated), is thermodynamically capable of reducing hydrogen ion (or water) in acid solutions ($V^{++} = V^{+++} + e^-$, $E = +0.255$ volt[16] at 25° on the Latimer scale), we find that vanadium(II) chloride solutions 0.5–1 *f* in hydrochloric acid, prepared as described above, are comparatively inert with respect to oxidation by hydrogen ion even at 50°. Solutions 0.5 *f* in hydrochloric acid retained their vanadium(II) titer to within 1% for a month at 25°, and only a 13% decrease in vanadium(II) concentration was found for a 1 *f* hydrochloric acid solution kept at 50° for 36 days. The gas above a solution *ca.* 0.05 *f* in vanadium(II) chloride and 0.1 *f* in hydrochloric acid which had been kept at 50° for 3 days showed no trace of hydrogen when examined in a mass spectrometer. (However, hydrogen is rapidly evolved when a platinum wire is immersed in these vanadium(II) solutions.) Consequently, no correction to the rate data is required for oxidation of vanadium(II) by hydrogen ion or water.

Dependence of Rate of Vanadium(II)-Perchlorate Reaction on Vanadium(II) and Vanadium(III) Concentrations.—To find the order with respect to vanadium(II), $-d(V^{++})/dt$ was determined at fixed concentrations of vanadium(III), perchlorate

---

[12] S. C. Furman and J. T. Denison, private communication, estimated the hydrolysis constant for V^{+++} to be of the order of 2×10^{-3} at 25°.

[13] H. W. Stone, *Anal. Chem.*, **20**, 749 (1948).

[14] H. W. Stone and E. R. Skavinski, *Ind. Eng. Chem., Anal. Ed.*, **16**, 111 (1944).

[15] S. C. Furman and C. S. Garner, *J. Am. Chem. Soc.*, **72**, 1785 (1950).

[16] G. Jones and J. H. Colvin, *ibid.*, **66**, 1573 (1944).

TABLE I

SUMMARY OF KINETIC RATE RUNS AT 49.9°, μ = 2.5[a]

(H^+), f	(ClO_4^-), f	(V^{+2}), f	(V^{+3}), f	$k_1 \times 10^3$, mole^{-1} l. min.$^{-1}$	$k_2 \times 10^3$, mole^{-1} l. min.$^{-1}$
1.65	1.50	0.050	0.0035	1.33	0.35
1.62	1.50	.100	.0071	1.39	.32
1.60	1.50	.150	.0106	1.44	.35
0.98	1.50	.050	.0035	1.27	.25
.95	1.50	.100	.0071	1.21	.28
.68	0.532	.100	.0071	[b]	[b]
.65	1.50	.100	.0071	1.10	.26
.65	1.99	.100	.0071	1.10	.25
.11	1.50	.100	.0071	1.10	.17
1.62	1.49	0	.0784	..	.30
0.94	1.49	0	.0784	..	.23
.65	1.49	0	.0784	..	.23
.11	1.49	0	.0784	..	.19

[a] All concentrations are initial values, except (H^+) for which the average value is given. [b] This run was used solely to gain an additional point on the (ClO_4^-) dependence plot.

ion, and hydrogen ion (the latter varied *ca.* 3% in a given run), and these slopes were plotted against the vanadium(II) concentration. The linearity of the plot, shown in Fig. 2, indicates first-order dependence on vanadium(II) ion concentration.

Figure 2 also gives a plot of $-d(V^{++})/dt$ at fixed concentrations of vanadium(II), perchlorate ion and hydrogen ion against vanadium(III) concentration and shows that the reaction is first order in vanadium(III) ion.

Dependence of Rate of Vanadium(II)–Perchlorate Reaction on Perchlorate Ion Concentration.— Plots of $-d(V^{++})/dt$ against perchlorate ion concentration (varied from 0.53 to 1.99 f) at various fixed values of vanadium(II) concentration were made. Figure 3 displays some typical plots. The linearity of the curves and the fact that each curve extrapolates to the origin within the experimental error indicates that the entire rate expression is first order in perchlorate ion with no significant terms independent of perchlorate ion concentration.

The results presented allow the formulation of the rate expression as

$$-d(V^{++})/dt = k_1(V^{++})(ClO_4^-) + 2k_2(V^{+++})(ClO_4^-) \quad (4)$$

where any hydrogen ion dependence is included in the rate constants k_1 and k_2. The first term expresses the rate of disappearance of vanadium(II) due to direct reaction with perchlorate ion, and the second term gives the rate of disappearance because of reaction with the product (VO^{++}) of the concurrent reaction between vanadium(III) and perchlorate ions according to equations 1 and 3. Values of the rate constants are given in Table I. It is assumed that the concentrations of chloro-complexed and hydrolyzed species of vanadium(II) and vanadium(III) are negligible. Lingane and Meites[17] have shown that the polarographic half-wave potential for the reduction of vanadium(III) ion to vanadium(II) ion remains constant within the experimental error (±0.002 volt) when the perchlorate medium is replaced by chloride medium (1 f acid). Furman and Garner[15] found that the absorption spectrum of vanadium (III) perchlorate solutions was not measurably altered by the addition of chloride ion until the Cl^- concentration was at least twenty times the total vanadium concentration. The hydrolysis constant for the presumably more hydrolyzed V^{+++} ion is only *ca.* 7 × 10^{-3} at 50°, estimated from an approximate value[12] for the hydrolysis constant at room temperature and the heat of hydrolysis.[15]

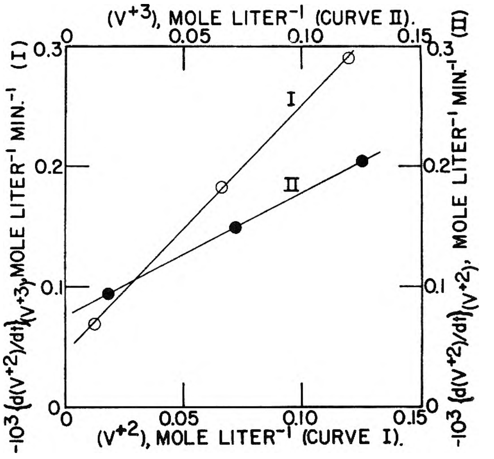

Fig. 2.—Effect of vanadium(II) and vanadium(III) ion concentrations on rate of oxidation of vanadium(II) ion, (ClO_4^-) = 1.50 f, $(H^+)_0$ = 1.62 f, 49.9°, μ = 2.5: curve I, (V^{+3}) = 0.041 f; curve II, (V^{+2}) = 0.035 f.

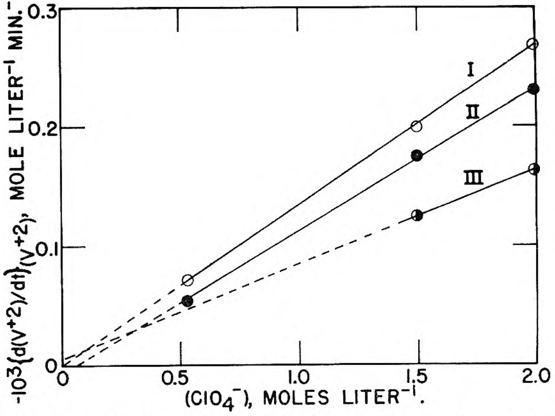

Fig. 3.—Effect of perchlorate ion concentration on rate of oxidation of vanadium(II) ion, $(H^+)_0$ = 0.70 f, 49.9°, μ = 2.5: curve I, (V^{+2}) = 0.080 f; curve II, (V^{+2}) = 0.75 f, curve III, (V^{+2}) = 0.050 f.

---

(17) J. J. Lingane and L. Meites, *J. Am. Chem. Soc.*, **70**, 2525 (1948).

Order of Rate of Vanadium(III)–Perchlorate Reaction with Respect to Reactants.—From runs made in the absence of vanadium(II), rate plots were prepared by plotting the logarithm of vanadium(III) concentration *versus* time for fixed concentrations of perchlorate ion and hydrogen ion. A typical plot is shown in Fig. 4. The linearity of these plots demonstrates the first-order dependence on vanadium(III) concentration. First-order dependence on perchlorate ion concentration was demonstrated by the fact that the entire rate expression (vanadium(II) present also) was found to be first order in perchlorate ion. These findings are in agreement with the rate law developed by Sugimoto[9] for the vanadium(III)–perchlorate reaction, namely

$$-\mathrm{d}(\mathrm{V}^{+++})/\mathrm{d}t = k_2(\mathrm{V}^{+++})(\mathrm{ClO_4}^-) \qquad (5)$$

where the hydrogen ion dependence is included in the rate constant k_2. Intercomparison of our values of k_2 with Sugimoto's values is presented below.

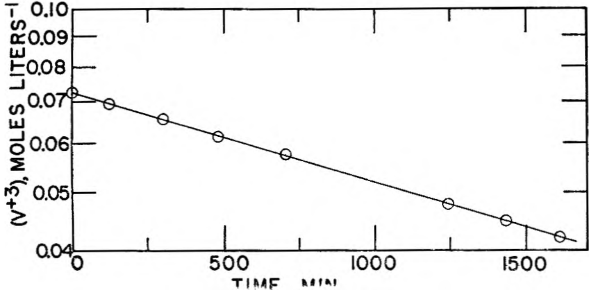

Fig. 4.—Representative semi-logarithmic plot of vanadium(III) ion concentration against time, vanadium(III)–perchlorate reaction, $(\mathrm{ClO_4}^-) = 1.49\ f$, $(\mathrm{H}^+)_0 = 0.63\ f$, 49.9°, $\mu = 2.5$.

Hydrogen Ion Dependence.—The data of Table I show that a fifteen-fold variation in hydrogen ion concentration is associated with an approximately 25% change in the value of k_1 and a twofold change in k_2, the latter holding both in the presence and absence of vanadium(II) ion. In view of the experimental error of *ca.* 15% the relatively small variation in the values of k_1 may be due to a specific electrolyte activity effect arising from the substitution of sodium ion for hydrogen ion in maintaining constant ionic strength, rather than being due to an actual hydrogen-ion dependence. The larger variation in values of k_2 suggests that there is a hydrogen ion-dependent term in the rate expression, as was proposed by Sugimoto[9] for the vanadium(III)–perchlorate reaction. In order to examine this and to permit intercomparison of our data with Sugimoto's, the values of k_2 were plotted against hydrogen ion concentration, both for the vanadium(II)–perchlorate and vanadium(III)–perchlorate reactions. These curves, although actually sigmoidal, may be treated as roughly linear, permitting an approximate resolution of k_2 into two terms

$$k_2 \cong k_2' + k_2''(\mathrm{H}^+) \qquad (6)$$

Table II gives the average values of k_2' and k_2'' so determined. In view of the experimental errors and the approximations made in computing these values, the agreement is satisfactory.

Catalysis by Light.—Some of the reactions were allowed to proceed for 30% of the run time in darkness; all others were carried out with normal laboratory illumination. There was no noticeable difference in the rate curves for the dark and light runs.

Table II

Dependence of k_2 on Hydrogen Ion Concentration

(49.9°, μ = 2.5)

$k_2' \times 10^3$, mole^{-1} l. min.$^{-1}$	$k_2'' \times 10^3$, mole^{-2}l.^{2} min.$^{-1}$	Source
0.17	0.10	V(II) runs (King and Garner)
0.18	0.07	V(III) runs (King and Garner)
0.24	0.15	V(III) runs (Sugimoto[9])[a]

[a] 50.0°; ionic strength permitted to vary from 0.65 to 3.5.

Temperature Coefficient.—All experiments were performed at 49.9°. However, Furman and Garner[18] have observed that 0.1 f vanadium(III) perchlorate solutions develop amounts of chloride ion detectable by silver nitrate test in approximately one week at 0°.

Discussion

The mechanism proposed by Sugimoto[9] for the vanadium(III)–perchlorate reaction, equations 1, 5 and 6, assumes that there are two reaction paths, one dependent on hydrogen ion, the other independent. He gave for the acid-independent path

$$\mathrm{V}^{+++} + \mathrm{ClO_4}^- + \mathrm{H_2O} \xrightarrow{k_2'} \mathrm{VO_2}^+ + \mathrm{ClO_3}^- + 2\mathrm{H}^+ \quad \text{(rate determining)} \qquad (7)$$

$$\mathrm{V}^{+++} + \mathrm{ClO_3}^- \longrightarrow \text{products (rapid)} \qquad (8)$$

$$\mathrm{V}^{+++} + \mathrm{VO_2}^+ \longrightarrow 2\mathrm{VO}^{++} \text{ (rapid)} \qquad (9)$$

and for the reaction which is assumed to be first order in hydrogen ion

$$\mathrm{H}^+ + \mathrm{ClO_4}^- \rightleftarrows \mathrm{HClO_4} \text{ (rapid equilibrium)} \qquad (10)$$

$$\mathrm{V}^{+++} + \mathrm{HClO_4} + \mathrm{H_2O} \xrightarrow{k_2''} \mathrm{VO_2}^+ + \mathrm{ClO_3}^- + 3\mathrm{H}^+ \quad \text{(rate determining)} \qquad (11)$$

followed by equations 8 and 9. The uncertain nature of the hydrogen ion dependence of the reaction rate makes it difficult to formulate a satisfying detailed mechanism for the reaction.

Ignoring the possibility of a small hydrogen ion term in the rate expression, at least two satisfactory mechanisms may be formulated which are consistent with the rate expression for the vanadium(II)–perchlorate reaction: (1) an oxygen atom is transferred from $\mathrm{ClO_4}^-$ to (hydrated) V^{++} in the rate-determining step

$$\mathrm{V}^{++} + \mathrm{ClO_4}^- \xrightarrow{k_1} \mathrm{VO}^{++} + \mathrm{ClO_3}^- \text{ (rate determining)} \qquad (12)$$

$$3\mathrm{V}^{++} + \mathrm{ClO_3}^- \longrightarrow 3\mathrm{VO}^{++} + \mathrm{Cl}^- \text{ (rapid)} \qquad (13)$$

$$\mathrm{V}^{++} + \mathrm{VO}^{++} + 2\mathrm{H}^+ \longrightarrow 2\mathrm{V}^{+++} + \mathrm{H_2O} \text{ (rapid)} \qquad (14)$$

We found that $\mathrm{ClO_3}^-$ reacts rapidly with an excess of V^{++} in acid solution, and VO^{++} reacts rapidly with V^{++} as shown in equation 16. (2) An electron is transferred from V^{++} to $\mathrm{ClO_4}^-$ in the rate-determining step

$$\mathrm{V}^{++} + \mathrm{ClO_4}^- \xrightarrow{k_1} \mathrm{V}^{+++} + \mathrm{ClO_4}^{=} \text{ (rate determining)} \qquad (15)$$

---

[18] S. C. Furman and C. S. Garner, *J. Am. Chem. Soc.*, **74**, 2333 (1952).

$$7V^{++} + 3ClO_4^{=} + 16H_2O \longrightarrow 7V(OH)_4^+ + 3Cl^- + 4H^+ \quad \text{(rapid)} \quad (16)$$

$$2V^{++} + V(OH)_4^+ + 4H^+ \longrightarrow 3V^{+++} + 4H_2O \quad \text{(rapid)} \quad (17)$$

The unknown intermediate, $ClO_4^{=}$, was invoked by Bredig and Michel[3] in the mechanism they suggested for the weakly acid-dependent path of the titanium(III)-perchlorate reaction. In the absence of further data, the simpler oxygen atom transfer process seems more probable.

THE GALLIUM-INDIUM SYSTEM

By W. J. Svirbely and Sidney M. Selis[1]

Contribution from the Department of Chemistry, University of Maryland, College Park, Md.

Received August 22, 1952

The specific resistances of solid and liquid gallium and indium and their alloys have been determined. From the results of these resistance measurements, the phase diagram for the gallium-indium system has been redetermined. The diagram is not in close accord with others in the literature.

The phase diagram for the gallium-indium system has been studied previously.[2,3] The study of de Boisbaudran was limited to four alloys. He predicted a concave liquidus curve. French, Saunders and Ingle made a thorough study of this system. These investigators also found the liquidus curve to be concave over the whole concentration range. However, the liquidus curves of the two investigators are not compatible with one another as reference to Fig. 2 will show.

The purpose of this research was to reinvestigate the gallium-indium system. Accordingly, electrical resistance-temperature measurements of various alloys covering the complete concentration range have been made and from these data the gallium-indium phase diagram has been deduced.

Materials. Indium.—The indium was a grant from the Anaconda Mining Company of Great Falls, Montana. Their assay claimed a purity of 99.97%. Spectrographic analysis showed the presence of very small amounts of tin and copper. The indium was used without further purification.

Gallium.—The gallium was of the Eagle Picher brand and was purified, with slight modifications, by a method in the literature.[4] Spectrographic analysis indicated the complete absence of foreign elements. Since the supply of gallium was limited, it was necessary to reclaim and reuse the gallium from the gallium-indium alloys. After purification, spectrographic analysis indicated the same purity as before.

Mercury.—The mercury used for the calibration of test cells had been carefully distilled.

Apparatus.—A Leeds and Northrup high precision standard resistance was used in the experiments. This unit was certified by the National Bureau of Standards as having a resistance of 1.0004 ohms at 25° when carrying a current of 1 ampere. The unit had a pair of current carrying and potential measurement leads.

Three Everready Air Cells connected in parallel furnished the current for the measurements.

Potential drops were measured with a Type B Rubicon potentiometer using a Rubicon No. 3402 Spotlight galvanometer as the indicating instrument.

The test cells were of Pyrex tubing 40-cm. long and were sealed at one end. The current carrying and potential measurement leads sealed in the cell were of tungsten wire. The two end current carrying leads were placed 30 cm. apart. The potential measurement leads were each 2.5 cm. from the current carrying leads as suggested by Thomas.[5] The tubing used in the construction of the cells ranged from 4-mm. tubing with standard wall thickness to small bore, heavy walled capillary tubing with an inside diameter of 2 mm. and an outside diameter of 9 mm. The reason for using heavy-walled tubing was that the gallium-rich alloys expanded on freezing and in doing so, tended to break the test cells.

The control of temperature was maintained by the use of two baths, water and oil. The water-bath was used for temperatures up through 50°, and the oil-bath for temperatures over 50°. In the water-bath, resistance measurements could be made at temperatures known to within ±0.01°. The thermometer used in this bath was checked against a similar one calibrated at the National Bureau of Standards. In the oil-bath, the temperature could be controlled to within ±0.05°. The thermometer used in the oil-bath was checked against Anschütz thermometers calibrated at the National Bureau of Standards.

Experimental Method.—The measuring circuit consisted of a series arrangement of the current source, standard resistance, cell, rheostat and a d.c. ammeter. Measurements consisted of reading the potential drops across the standard and unknown resistances as the current passed through them. It is apparent that connections between resistances and potentiometer must be made at points *within* the leads linking the several series components; otherwise the resistances of these leads would give rise to errors in the measurement of potential differences. If the current passing through the main series circuit is about one ampere, then the small amount of current shunted through the potentiometer will result in a negligible error.

The current passing through the two resistances (*i.e.*, standard and unknown) in series must be the same, *i.e.*, $I_x = I_s$. By use of Ohm's law, one obtains

$$R_x = E_x(R_s/E_s) \qquad (1)$$

where E_s and E_x are the potential drops and R_s and R_x are the resistance values of the standard resistance and the unknown resistance, respectively.

A very convenient approach to studying alloy resistance is in terms of specific resistance. The cell constant, C, for converting measured resistance to specific resistance may be calculated by the use of equation 2

$$C = \rho/R \qquad (2)$$

where ρ is the specific resistance and R is the measured resistance.

One of the cells was calibrated using mercury[6] as a standard over the temperature range of 20 to 157° and the cell constant C was constant within 0.2%. The cell constants for the other seven cells used in this research were determined at one temperature only.

Alloys were prepared by melting weighed amounts of the

---

(1) Abstracted from the thesis of Sidney M. Selis presented to the Graduate School of the University of Maryland in partial fulfillment of the requirements for the Ph.D. degree.

(2) L. de Boisbaudran, *Compt. rend.*, **100**, 701 (1885).

(3) S. J. French, B. J. Saunders and G. W. Ingle, This Journal, **42**, 265 (1938).

(4) J. I. Hoffman, *Bur. Standards J. Research*, **13**, 665 (1934).

(5) We acknowledge our indebtedness to Dr. J. L. Thomas of the National Bureau of Standards for his advice on these electrical resistance studies.

(6) T. I. Edwards, *Phil. Mag.*, Series 7, **2**, 1 (1926).

metal components under mineral oil followed by thorough stirring of the molten alloy. The alloys were then drawn up into pieces of 3-mm. tubing which were later slipped off the sticks of solid alloy. These sticks were washed copiously with benzene and then dried. The sticks were then introduced into a resistance cell which was immersed in a bath whose temperature was above the melting point of the alloy. Care was taken to insure that the cell was completely filled. The alloy was allowed to solidify and it was then annealed for at least 15 hours. In the solid solution range, the annealing temperature was always a few degrees below the solidus temperature. For the remainder of the alloys the annealing temperature was 0 or 10°.

After the annealing process, the cell was immersed in a bath and electrical connections were made. A current of approximately one ampere was allowed to flow through the circuit for about one hour and the measurements of potential drop across the standard and unknown resistances were then begun. The thermometer was read, and the potential drop across the standard resistance was rechecked. The temperature of the bath was slowly increased to a new value and again potential drop measurements were made. Readings at small temperature intervals were made in the vicinity of those temperatures where discontinuities were expected on the basis of preliminary runs.

New alloys were frequently prepared by adding pure metal to an old alloy. Occasionally, check runs were made with alloys prepared from pure components. The check runs not only verified the use of old alloys to prepare new ones, but they also showed that, within the experimental error, one was dealing with equilibrium conditions.

Figure 1 shows the specific resistance–temperature plot for one of the alloys. Figure 2 shows typical critical portions of the temperature–specific resistance curve for some of the alloys. The existence of a discontinuity in such a plot indicates the appearance or disappearance of a phase. Similar plots of the data for pure indium and pure gallium gave discontinuities at 156.0 and 29.86°, respectively. The specific resistances for liquid indium and gallium at their melting points were 32.83×10^{-6} and 26.88×10^{-6} ohm-cm., respectively. Table I summarizes the temperatures of discontinuity for each alloy.

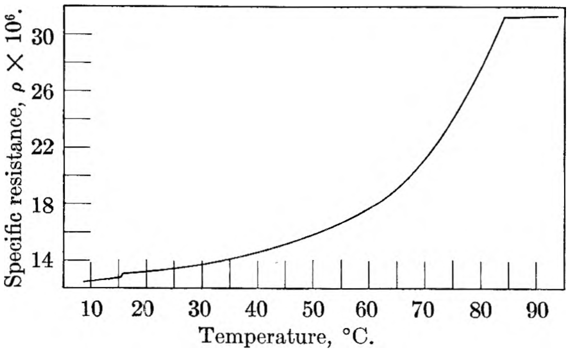

Fig. 1.—Specific resistance–temperature plot for 22.47% gallium with discontinuities at 15.72 and 84.3°.

Considering the fact that each of the alloys had a different history, the reproduction of the eutectic temperature to within ±0.03° can be considered as the evidence for equilibrium conditions existing at the eutectic temperature.

Discussion

In the past, sections of bimetallic phase diagrams have been determined by both thermal and electrical resistance methods. Among them are Li–Bi,[7] Mg–Tl,[8] Cd–Li,[9] Mg–Sn[10] and Li–Tl.[11]

Agreement between the two methods has been quite satisfactory. In some of these investigations the alloys were subjected to the heating technique only. Applying the criteria set up by Grube with respect to the discontinuities in resistance–temperature curves and their relation to a phase diagram to the data of Table I, one obtains the diagram for the Ga–In system shown in Fig. 3. The differences between our diagram and those of other investigators[2,3] are self evident. We are unable to

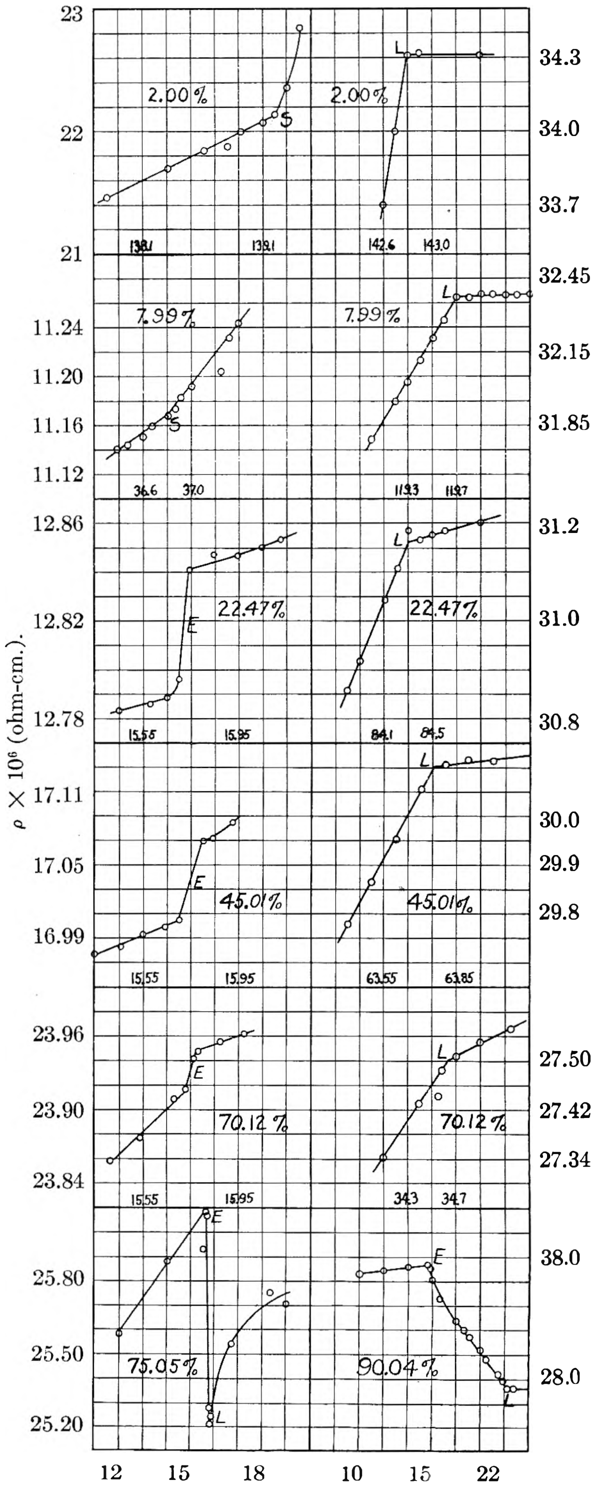

Fig. 2.—Specific resistance–temperature curves: S, Solidus; L, Liquidus; E, Eutectic. Percentages refer to gallium content.

---

[7] G. Grube, H. Vosskuhler and H. Schlect, *Z. Elektrochem.*, **40**, 270 (1934).

[8] G. Grube and J. Hille, *ibid.*, **40**, 101 (1934).

[9] G. Grube, H. Vosskuhler and H. Vogt, *ibid.*, **38**, 869 (1932).

[10] G. Grube and H. Vosskuhler, *ibid.*, **40**, 566 (1934).

[11] G. Grube and G. Schlaufer, *ibid.*, **40**, 593 (1934).

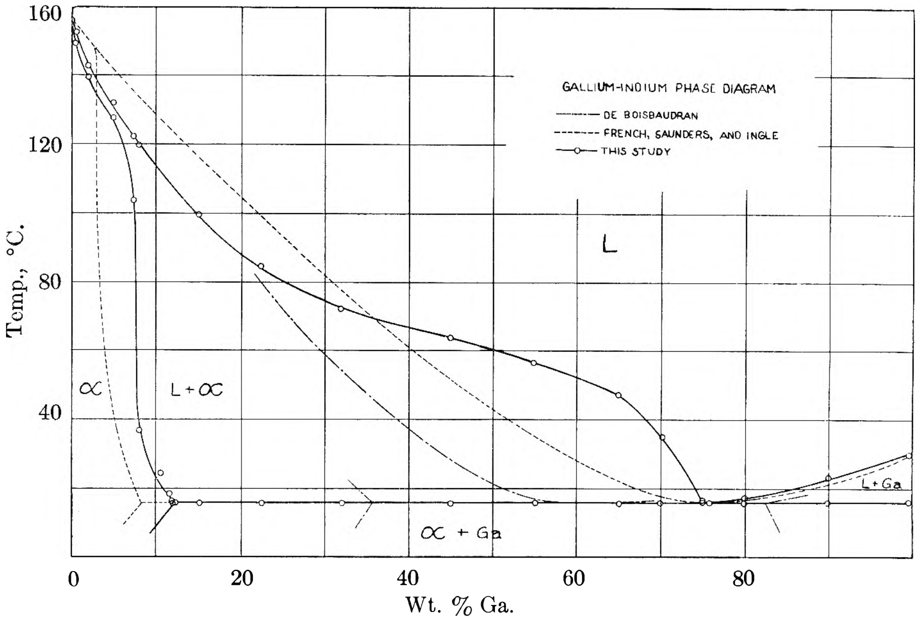

Fig. 3.—Gallium–indium phase diagram: —·—·—, de Boisbaudran; — — — — —, French, Saunders and Ingle; —o—, this study.

account for the large discrepancy between our results and those of French, *et al.*[3]

TABLE I

SUMMARY OF DATA

Wt. % Ga	Solidus temp., °C.	Liquidus temp., °C.	Eutectic temp., °C.
0	. .	156.0	. .
0.487[a]	149.3	152.8	. .
2.000	139.2	142.7	. .
2.01[a]	139.2	142.8	. .
5.00	127.7	131.8	. .
5.01[a]	127.5	131.8	. .
7.43	103.8	122.2	. .
7.99	36.8	119.7	. .
10.48	24.2	. .	. .
11.50[a]	18.29	. .	. .
11.87	16.42	. .	. .
12.03	. .	. .	15.71
12.21	. .	. .	15.75
15.09	. .	99.2	15.73
22.43[a]	. .	84.7	15.78
22.47	. .	84.3	15.72
31.95	. .	72.3	15.70
45.01	. .	63.8	15.74
54.89	. .	56.4	15.72
64.93	. .	47.0	15.70
70.12	. .	34.6	15.74
74.98	. .	16.3	15.73
75.05	. .	15.79	15.69
75.30[a]	. .	15.79	15.72
75.71	. .	15.84	15.78
79.96	. .	16.96	15.78
89.89[a]	. .	22.30	15.74
90.04	. .	22.70	15.69
99.53	. .	29.72	15.80
100.00	. .	29.86 ± 0.03	. .
		Ave. – 15.73 ± ADM 0.03	

[a] Pure metals were used in preparing these alloys; otherwise a new alloy was prepared by adding pure metal to another alloy.

Saldau,[12] in plotting isothermal curves for various physical properties *versus* composition in binary metal systems (Sn–Pb, Pb–Sb, Sn–Zn, Au–Zn, Au–Cd) found that either a maximum or a minimum was obtained in the plots at the composition corresponding to the eutectic or eutectoid composition. Using specific resistance data at 10°, a plot of specific resistance *versus* composition for the gallium–indium system gives a maximum in the curve at 80% Ga instead of at 75.2% Ga. The explanation of this anomaly may lie in the fact that gallium- and gallium-rich alloys expand on solidification.

Table II is a summary of physical properties obtained in this research in comparison with the results found in the literature.

TABLE II

SUMMARY OF SOME PHYSICAL PROPERTIES

	Gallium	Indium	Gallium–indium system
Specific resistance of solids at 20° in ohm-cm.	56.8×10^{-6}[c] 35.2×10^{-6}[b]	9.03×10^{-6}[a] 9.14×10^{-6}[b]	
Specific resistance of liquids at 30° in ohm-cm.	26.86×10^{-6}[b] 27.2×10^{-6}[c]		
Melting points in °C.	29.86[b] 29.92[d] 29.7[f]	156.0[b] 155[e] 157.2[b]	
Eutectic comp. in % Ga			75.2 ± 0.1[b] 76 ± 0.5[g]
Eutectic temp. in °C.			15.73 ± 0.03[b] 16[g]
Solubility limit of In in Ga in %			0 or <0.47[b] 0 or <1[g]
Solubility limit of Ga in In in %			11.95 ± 0.07[b] 9.5[g]

[a] S. Valentiner, *Z. Physik*, **115**, 11 (1940). [b] This study. [c] A. Guntz and W. Broniewski, *Compt. rend.*, **147**, 1474 (1908). [d] L. Riccobini, A. Foffani and T. Periotto, *Gazz. chim. ital.*, **79**, 344 (1949). [e] W. Guerther and M. Pirani, *Z. Metallkunde*, **11**, 1 (1919). [f] O. H. Henry and E. L. Badwick, *Am. Inst. Mining Met. Engrs., Inst. Metals Div., Metals Tech.*, **14**, Tech. Pub. 2159 (1947). [g] S. J. French, B. J. Saunders and G. W. Ingle, ref. 3.

---

[12] P. Saldau, *Z. anorg. allgem. Chem.*, **194**, 1 (1930).

HEAT OF WETTING OF COPPER, GRAPHITE AND SILICA GEL[1]

BY F. E. BARTELL AND R. MURRAY SUGGITT

Department of Chemistry, University of Michigan, Ann Arbor, Mich.

Received October 23, 1952

Determinations were made of the unit area heats of wetting and net heats of adsorption of ten liquids on graphite, and of five liquids each on silica gel and on copper powders. Evidence is presented to show that unit area heats of wetting values are reproducible if certain conditions are met. Comparison of the unit area heats of wetting of graphite and of copper showed that the heat of wetting of copper is much greater than the heat of wetting of graphite. This finding is opposite to that reported by others. Contrary to results reported in the literature the presence of moisture was found to have no appreciable effect on the heats of wetting of graphite by hydrocarbons. The effect of oxygen, dissolved in water, on the heat of wetting of copper was determined. Evidence is presented to show that the net heat of adsorption of water on graphite is negative and that negative net heats of adsorption are characteristic of liquid–solid systems that form contact angles. A description is given of the microcalorimeter used for the measurement of the heats of wetting of the low surface area powders. Various experimental aids used in the measurements are set forth, and two correction terms arising from the breaking of glass sample bulbs are shown to be necessary.

Introduction

When a solid surface is brought into contact with a non-reactive liquid, a thermal effect is noted. This phenomenon has been given several names; heat of wetting, heat of immersion and "Pouillet's effect." Boyd and Harkins[2] have used the term "heat of emersion" to refer to the reverse thermal process, namely, that of stripping the liquid off the solid to leave a clean surface.

Since heat of wetting is a surface phenomenon the heat effect is proportional to surface area. The heat of wetting per gram, H_i, is related to the heat of wetting per unit area, h_i, by the relation

$$H_i = Ah_i \qquad (1)$$

where A is the surface area of 1 g. of powder.

The heat of wetting is a measure of the enthalpy decrease of a surface upon wetting. If h_{S° and h_{SL} are the total surface energy contents per square centimeter of the surface when exposed to vacuum and when wetted by the liquid, respectively, then

$$h_i = H_i/A = h_{S^\circ} - h_{SL} \qquad (2)$$

The immersion of the clean solid in a liquid may be described in another way which may be real or may be imaginary, the total end effect being the same. For example let the following two processes be compared. (1) In the first consider that the solid surface which has been stripped of all adsorbed material is allowed to come to equilibrium with saturated vapor of the liquid, evolving Q_1 calories, the total or integral heat of adsorption, in the process. If Q_L calories are necessary for the vaporization of this saturating vapor, the net heat increase in forming the adsorbed layer is $Q_1 - Q_L$ calories. This quantity $Q_1 - Q_L$ is called the "net heat of adsorption." The solid with its adsorbed film is then immersed in the bulk liquid. If the solid is non-porous then the area of the adsorbed film is nearly equal to the area of the solid surface. Since the film disappears completely on immersion, a heat, h_{LV}, is evolved for each square centimeter of film surface. (2) In the second process consider that the evacuated solid is immersed directly into the wetting liquid releasing H_i calories. Since the initial and final states of the two processes are identical, the heat effects can be equated as shown in equations 3 and 4.

$$H_i = Q_1 - Q_L + Ah_{LV} \qquad (3)$$

$$h_i = q_1 - q_L + h_{LV} \qquad (4)$$

where $q_1 - q_L$ is the net heat of adsorption per unit area, and all other terms are as already defined. The net heat of adsorption per unit area can be calculated from equation 4 using heat of wetting data and surface tension data for the liquid.

Since it may be assumed that the outermost layers of an adsorbed film have the same properties as the bulk liquid,[3] the term h_{LV} can be obtained from surface tension data of the liquid according to the Gibbs–Helmholtz relation

$$h_{LV} = \gamma_{LV} - T\left(\frac{\delta\gamma_{LV}}{\delta t}\right)_p \qquad (5)$$

where γ_{LV} is the free surface energy or surface tension of the liquid.

For the measurement of heat of wetting in this research, copper, graphite and silica powders were selected since these materials have widely different surface properties. To check the reproducibility of the unit area heat of wetting values for different samples of the same material, two sources of each solid were used. The two graphites were of different degrees of fineness but were given similar pretreatments, as were the two silica powders. The two copper powders were prepared in distinctly different ways in order to determine the effect of preparation on the heat of wetting.

A twin or Joule microcalorimeter was constructed to measure the heat of wetting of the low surface area powders. This type of calorimeter can be made to give high sensitivity in differential thermal measurements and when the two calorimeter cans are stirred at identical rates the extraneous thermal effects produced in the two cans practically cancel each other. Some new techniques were developed in the measurement of the heat of wetting and studies were made of the effect of trace impurities and of the heat of sample bulb breaking. The results of the heat of wetting measurements showed several interesting relationships that might have been overlooked or misinterpreted if the new experimental methods and "correction" terms had not been used.

---

(1) The data in this paper were taken from a portion of a thesis by R. Murray Suggitt, submitted to the School of Graduate Studies of the University of Michigan in partial fulfillment of the requirements for the Ph.D. degree, August, 1952.

(2) G. E. Boyd and W. D. Harkins, *J. Am. Chem. Soc.*, **64**, 1190, 1195 (1942).

(3) W. D. Harkins and G. Jura, *ibid.*, **66**, 1362 (1944).

Experimental

Materials. Graphite.—Two graphites, A (high area), ash content 0.01%, and B (low area), ash content 0.09%, were obtained from the Acheson Colloids Company. Both graphites were purified by treatment with concentrated HCl and thorough washing. The powders were dried, screened and heated in a quartz tube to 1050° under a high vacuum for 60 hours. The graphites were cooled in an atmosphere of purified helium and stored under an atmosphere of nitrogen. The B.E.T. areas (nitrogen molecule assumed to be 16.2 Å.) were 86 $m.^2$ per g. for graphite A and 8.4 $m.^2$ per g. for graphite B.

Silica Powder.—Linde Silica powder #2669-95 B obtained from the Linde Air Products Corporation was used without further purification. The B.E.T. area of the dry powder was 328 $m.^2$ per g.

Silica Gel.—Commercial silica gel obtained from the Davison Chemical Company was purified by digestion in HNO_3. The gel was washed and dried at 300°. The B.E.T. area of the dry gel was 366 $m.^2$ per g.

Commercial Copper Powder.—Copper powder was obtained from the Mallinckrodt Chemical Works. Since the powder as received possessed a layer of oxide it was heated at 250° under a stream of purified hydrogen for 24 hours, then at 300° for 1 hour. The powder was cooled and stored under an atmosphere of hydrogen. Spectroscopic analysis showed a Pb content of the order of 0.01% and an Ag content of the order of 0.001%. The B.E.T. area was 0.23 $m.^2$ per g.

Synthetic Copper Powder.—Copper powder was formed by the thermal decomposition of cupric formate at 175°. The starting materials for the cupric formate were basic cupric carbonate and formic acid. The product obtained in the thermal decomposition was a soft spongy product that closely resembled red sponge rubber. After decomposition was complete as shown by constant weight, the copper was heated under a stream of hydrogen for 1 hour at 200°. The sponge was broken up and stored under an atmosphere of hydrogen. Spectroscopic analysis showed it to be free of Pb, Ag, As, Sb and Sn. The B.E.T. area was 0.76 $m.^2$ per g.

Apparatus. General Description.—A general idea of the apparatus can be obtained from the simplified section Fig. 1. Two similar calorimeters, C and C′ were suspended by thin walled (0.004″) inconel tubing, i and i′, from the lids of their respective vacuum tight copper submarine jackets, J and J′. Both submarine jackets were supported from a brass plate, R, by means of brass tubes, B and B′, and by D and D′ which accommodated the stirrer and the electrical leads, respectively. Both submarine jackets were completely submerged in a well-stirred water-bath regulated to 0.003°. The calorimeter stirrers were driven by identical sprockets, F and F′, fed by a ladder chain from a constant speed motor. A brass T-tube connection was made to the tubes, D and D′. This provided a means of obtaining a high vacuum around both calorimeters. Insulated electrical leads were brought out of each vacuum jacket at A and A′.

Calorimeter Cans.—The twin calorimeters, each having a capacity of approximately 133 ml., were spun from copper. The thickness of the can walls was about 0.025″. The lid (thickness 0.075″) contained a well which received the electrical heater, consisting of 73.5 ohms of manganin wire, and a second well receiving one end of the auxiliary control thermel, Th. A tube in the lid (not shown in figure) fitted with a cap, allowed the introduction of the wetting liquid. The stirrer, S, was attached to a long thin-walled (0.004″) monel shaft with a diameter of $^1/_8$″. Besides agitating the liquid the stirrer acted as bulb breaker. Sample bulbs, SB, were attached to the stirrer. A platform, P, consisting of sharp stainless steel points was placed under the bulb. To break the bulb the stirrer was forced downward causing the glass bulb to be smashed on the sharp points. A spring, Z′, restored the stirrer to its original portion after the breaking of the bulb.

By careful machining each lid was made to fit snugly to its calorimeter can. Heating the lid with a soldering iron caused it to expand and fit over the lip of the colder calorimeter can. To ensure complete sealing of the can to its lid the junction was soldered with Wood's metal. Following the addition of liquid to the calorimeter through the inlet provided, a cap was soldered on the inlet and the calorimeter was thus completely sealed from the interior of the vacuum jacket.

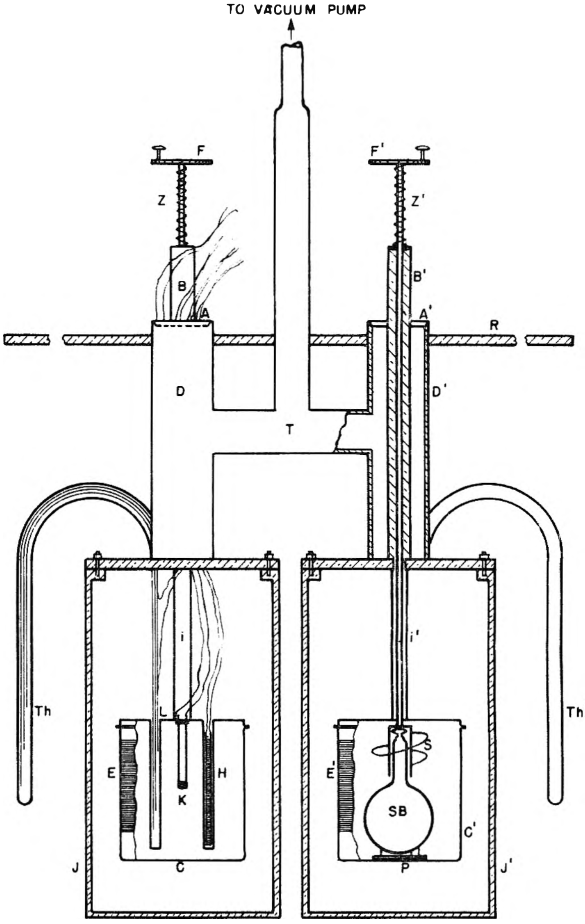

Fig. 1.

Temperature Measurement.—Two sets of resistance thermometers were used. One pair of thermometers consisted of 50 ohms of copper wire, E and E′, wrapped around each calorimeter can. The second pair of thermometers consisted of 100-ohm thermistors, K, immersed in the liquids of each calorimeter can. Thermistors, "thermally sensitive resistors," can be made of various semi-conducting materials. The temperature coefficient of resistivity of those used was approximately ten times that of copper. The electrical leads of the thermistors were connected to the outside through a small, two-lead connection, L, in each lid. The copper resistance thermometers were used mostly as a check on the performance of the thermistors though a number of results were obtained with them.

Either the two copper resistances or the two thermistors were incorporated into two arms of a Wheatstone bridge circuit. A White double potentiometer with a high sensitivity galvanometer was placed across the bridge. Thus the potential difference across the bridge rather than the current flow was observed.

The differences in temperature between the calorimeter cans and the bath were measured by two 6-junction thermels Th and Th′, constructed of #36 double silk wrapped copper wire and #24 glass insulated advance wire.

Thermal changes of less than a hundredth of a calorie were readily detectable. Electrical calibrations were reproducible to within 0.01 cal. or 0.2%, whichever was greater.

Preparation of Sample-filled Bulbs.—All sample bulbs used were blown from 10-mm. Pyrex tubing and were carefully selected according to rigorous standards governing size, shape and resiliency. Sample powder was weighed into the bulbs and the powders were evacuated at an elevated temperature to a vacuum of less than 10^{-5} mm. The temperature of evacuation for the graphite and for the

Silica powders was 300 to 350°, while the temperature of evacuation for the copper was 200°.

Sample bulbs containing copper, or other low surface area materials, were filled with purified helium to 500 mm. pressure after evacuation at an elevated temperature but prior to sealing. Helium filling was used to avoid temperature lags caused by slow heat transfer in powders in a high vacuum. It had been found that for small changes in temperature of the bulk liquid such temperature lags in the powder could cause serious errors in the measurements of the heat of wetting of low surface area powders. In one case a negative heat of wetting value was obtained after the solid sample had been stored in a vacuum at a few degrees below 25° until a half hour prior to measurement. Filling the sample bulbs with helium enabled thermal changes of the surroundings to be rapidly transmitted throughout the powder. Helium filling was not necessary, however, in the case of higher surface area powders such as Graphite A for which no difference in heat of wetting measurements was detected whether samples were sealed in a high vacuum or sealed in helium under 500 mm. pressure. The thermal effect of the heat of wetting of higher surface area powders greatly exceeds any thermal error due to the temperature lag in powder contained in a high vacuum.

Heat of Bulb Breaking.—Since the solid powders were introduced by breaking of glass sample bulbs, an investigation of the heat of bulb breaking was undertaken. Boyd and Harkins[2] reported a small correction but gave no numerical values. Others[4,5] found no detectable heat change. Measurements in this research showed that the heat produced in the breaking of a glass sample bulb constituted a factor in heat measurements when the bulbs were of appreciable size. This heat is the resultant of two counterbalancing effects: the heat of vaporization of liquid equivalent to that required to fill the space formerly occupied by the evacuated bulb, and the heat arising from the rupture of the bulb itself. Two sets of measurements were made to establish the need of considering these two effects. Typical results are reported in Table I. Measurements in series A gave the heats of breaking of highly evacuated bulbs. Measurements in series B gave the heats of breaking of bulbs containing a few drops of the liquid in which the bulbs were to be broken. In series A there was a heat of vaporization dependent on the volume of the bulb and the characteristics (vapor pressure, temperature, latent heat of vaporization) of the liquid, while in series B there was no heat of vaporization since the space occupied by the bulb was already saturated with vapor prior to the breaking. The average heat of bulb breaking of 14 bulbs (average volume 17.3 cc.), broken in various liquids, was +0.73 cal. The reproducibility was not very good, the average deviation being 0.07 cal. In most cases where reasonably volatile liquids were used the heat of vaporization nearly cancelled the heat of bulb breaking.

Table I

Heat of Bulb Breaking and Heat of Vaporization at 25°

	A. Evacuated bulbs	B. Bulbs containing a few drops of liquid
Liquid	Benzene	Water
Bulb vol., cc.	17.3	17.2
Obsd. heat, h_{obs}, cal.	+0.02	+0.74
Heat of vapor., h_{vap}, cal.	−0.71	0.00
Net heat of bulb breaking, $h_{obs} - h_{vap}$, cal.	+0.73	+0.74

The heat of bulb breaking probably arises from two sources; (1) the input of mechanical energy needed to break the bulb, and (2) the release of strain energy built up in the glass to resist the pressure differential between the interior and the exterior of the bulb. Experimentally it was found that for eight bulbs filled with helium at a pressure of 500 mm., thus lessening the pressure differential and the strain energy, the average heat of bulb breaking was reduced to 0.37 cal. Variations in bulb size in spite of careful selection, and variations in the input of mechanical energy needed to break the bulb were probably responsible for the poor reproducibility of the heat of bulb breaking.

Trace Impurities and Heat of Wetting.—Harkins and Dahlstrom[6] demonstrated the necessity of protecting nonpolar liquids from polar impurities (especially water) during the measurements of the heat of wetting of polar solids. In the present research every effort was made to use only purified liquids and to maintain anhydrous conditions, but an additional step was taken to guard against moisture or any other contamination of the wetting liquid. Powder, identical in preparation to the sample powder, was dispersed in the wetting liquid prior to the breaking of the sample bulb to adsorb any trace impurity that might be present in the wetting liquid and which might lead to incorrect values for the heat of wetting. This powder was called a "getter."

The measured heats of wetting of "wet" and of "dry" benzene on graphite A were identical, indicating that moisture in hyrocarbons did not alter their heats of wetting on Graphite A. Basford, Jura and Harkins[7] found that moisture did have an effect on the heat of wetting of benzene on graphite but their graphite contained 0.46% ash.

Measurements of the heat of wetting of copper powder by water showed that oxygen dissolved in the water used had a pronounced effect. The heat of wetting of water saturated with oxygen was found to be 1770 ergs per cm.^{2} on the synthetic copper at 25°, whereas, the heat of wetting of oxygen-free water supplemented with "getter" was found to be 725 ergs per cm.^{2}. Examination of the powder wetted by the oxygen-saturated water indicated that a portion of the surface had been oxidized. On the other hand, the presence of oxygen in very dry benzene did not affect the heat of wetting to within the limits of the experimental error (5%). As a result of these experiments all liquids were swept with purified nitrogen for a half hour before being placed in the calorimeter which had also been dried with a stream of purified nitrogen for six hours.

Results and Discussion

In Table II are listed the unit area heats of wetting at 25° of the graphites, silica powders and copper powders. Each value given is the average of three or more measurements. The probable error does not exceed 3% for the graphites and silica powders, 5% for the synthetic copper and 5 to 10% for the commercial copper. In every case except one, that of water on graphite, the unit area heats of wetting, h_i, were reproducible, within the limits of the experimental error, on different samples of graphite and on different samples of silica gel. The poor wettability of the graphite by water may have been responsible for the poor reproducibility of measurements of heat of wetting of water on a given graphite, but the difference of 18% between the two h_i values obtained for the two different graphites far exceeded the experimental error and constituted a significant difference. This significant difference was probably due to the slightly higher ash content of graphite B.

The reproducibility of h_i values is dependent on three factors; identity of chemical composition (*e.g.*, ash free condition in graphite), identity of physical composition (*e.g.*, crystal form, nonporosity) and identity in preparation such as in heat treatment (*e.g.*, identity of free surface energy in different samples). The necessity of meeting condition three is apparently not well known. Different heat treatments of graphite may give products with very different surface properties. Advancing contact angles formed by water against graphites

---

(4) F. LaPorte, *Ann. phys.*, [12] **5**, 5 (1950).

(5) E. F. Westrum, Jr., and L. Eyring, *J. Am. Chem. Soc.*, **74**, 2045 (1952).

(6) W. D. Harkins and R. Dahlstrom, *Ind. Eng. Chem.*, **22**, 897 (1930).

(7) P. R. Basford, G. Jura and W. D. Harkins, *J. Am. Chem. Soc.*, **70**, 1444 (1948).

subjected to different heat treatments may vary as much as 30 to 40°, as has been observed in this Laboratory. Unfortunately many of the investigators who have used graphite for adsorption and for heat of wetting studies have failed to give information concerning the details of the heat treatment of the graphite used. This fact alone may account for many of the apparent discrepancies in the data reported.

TABLE II

HEATS OF WETTING OF POWDERS AT 25° (ERGS PER CM.^{2})

Liquid	Graphite A	Graphite B	Synthetic copper	Commercial copper	Linde silica powder	Commercial silica gel
Benzene	114	117	880	250	97	100
Cyclohexane	101	101	740		68	
p-Xylene	124					
Tetralin	130					
Hexane	118					
n-Octane	120	123	660		54	
Carbon tetrachloride	115					
n-Butanol	106	102				
Methanol	119	115	950		185	
Water	47.5	56	725	235	261	263

Various investigators have noted the relation between particle size and heat of wetting[8–10] and between surface area and heat of wetting.[11] In this research the h_i values agreed for powders of like chemical composition and treatment even though there was a tenfold difference in surface area as in the case of the graphites.

The results of the heat of wetting measurements on the two copper powders demonstrate the pronounced effect that different methods of preparation can have on the heat of wetting of copper. The synthetic copper was prepared at a temperature sufficiently low that the "active" centers were not annealed off.[12]

The results obtained by us with copper and with graphite show that the heat of wetting per unit area of copper surface is from 2 to 7 times the corresponding heat of wetting of graphite. Bachmann and Brieger[13] reached a directly opposite conclusion from their data for these two solids. There is reason to suspect that their estimate of the surface area of their carbon was too low.

Net Heats of Adsorption.—Net heats of adsorption were calculated by equation 4 from the unit area heats of wetting values, h_i, and the total surface energy of the liquid, h_{LV}. Using the surface tension data of Vogel[14] and I.C.T.,[15] h_{LV} values were calculated by means of equation 5. The h_{LV} values used and the net heats of adsorption are reported in Table III.

TABLE III

NET HEATS OF ADSORPTION OF POWDERS AT 25° (ERGS PER CM.^{2})

Liquid	h_{LV} of liquid	$q_1 - q_L$ graphite A	$q_1 - q_L$ synthetic copper	$q_1 - q_L$ silica
Benzene	67.6	46	810	31
Cyclohexane	57	44	680	11
p-Xylene	74	50		
Tetralin	68	52		
Hexane	48	70		
n-Octane	49	71	615	5
Carbon tetrachloride	63	52		
n-Butanol	50	56		
Methanol	45	74	910	140
Water	118	−70	605	143

Of particular note is the value, a negative value, of the net heat of adsorption of water on graphite. Whether the net heat of adsorption of water on graphite be negative or positive has constituted a debatable subject for a number of years. A limited amount of data has been obtained calorimetrically but much of the evidence cited has been derived from the shape of adsorption isotherms.

Basford, Jura and Harkins[7] in their study of "The Heats of Emersion and Desorption of Water by Graphite at 25°" presented evidence which could be interpreted to indicate that under certain conditions negative net heats of adsorption were obtained. They stated "It is probable before a more complete understanding is possible, that, (1) other graphites and other solids which exhibit a similar behavior must be investigated, (2) the precision of the measurements, especially those of the heat involved, must be increased and (3) experimental procedures other than these used thus far must be used."

In adsorption studies with charcoal in 1927 Coolidge[16] concluded from a study of isotherms at different temperatures that the initial adsorption of water occurs with zero net heat at relatively low temperatures. At higher temperatures, however, the isotherms obtained indicate an initial negative heat of adsorption.

Pierce and associates as a result of adsorption studies with graphite in 1948[17,18] stated: "At all measured pressures the heat of adsorption exceeds the heat of liquefaction," but Pierce, Smith, Wiley and Cordes[19] as a result of their studies on adsorption of water by carbon in 1951 found that "The net heat appears to be zero for the initial adsorption of water, then as more molecules are adsorbed the heat becomes positive." At elevated temperatures they found a relatively large net heat of adsorption but this they concluded may be due to a chemical reaction between carbon and water.

From adsorption studies of water on carbons evacuated at 1200° Anderson and Emmett[20] had determined that the net heats of adsorption, ob-

---

(8) G. Gore, *Phil. Mag.*, **37**, 306 (1894).

(9) G. J. Parks, *ibid.*, **4**, 240 (1902).

(10) B. W. Iliin, A. A. Leontiew and S. V. Bragin, *ibid.*, **23**, 294 (1937).

(11) B. W. Iliin, A. V. Kiselev, V. F. Kiselev, O. A. Likhacheva and K. D. Shcherbakova, *Doklady Akad. Nauk S.S.S.R.*, **75**, 827 (1950).

(12) H. Schreiner, *Z. anorg. Chem.*, **262**, 113 (1950).

(13) W. Bachmann and C. Brieger, *Kolloid Z.*, Special No. 142 (1925); *ibid.*, **39**, 334 (1926).

(14) A. I. Vogel, *J. Chem. Soc.*, 1323 (1928); 133 (1940); 1814, 1833 (1948).

(15) "International Critical Tables," McGraw-Hill Book Co., Inc., New York, N. Y., 1926.

(16) A. S. Coolidge, *J. Am. Chem. Soc.*, **49**, 708 (1927).

(17) C. Pierce and R. N. Smith, THIS JOURNAL, **52**, 1111 (1948).

(18) R. N. Smith and C. Pierce, *ibid.*, **52**, 1115 (1948).

(19) C. Pierce, R. N. Smith, J. W. Wiley and H. Cordes, *J. Am. Chem. Soc.*, **73**, 4551 (1951).

(20) R. B. Anderson and P. H. Emmett, THIS JOURNAL, **56**, 753, 756 (1952).

tained from the C constant of the B.E.T. equation, were negative.

No calorimetric evidence prior to the present research clearly supported the conclusion that negative net heats of adsorption should be obtained in the case of water adsorbed on high temperature carbon. Previous evidence was based on the separate measurement of the two large, nearly equal, quantities q_1 and q_L (or their equivalents, E_1 and E_L calories per mole adsorbed). The difference, $q_1 - q_L$, was of the order of magnitude of the experimental error.[16,21]

The net heat of adsorption, obtained from heat of wetting data, is a measure of the entire interaction of the surface and its adsorbed film. Since water forms a contact angle on graphite, the adhesion of water to graphite is less than the cohesion of water. To cause the water to adhere to graphite rather than to itself, energy must be provided. This would result in an adsorption of energy, that is, a negative net heat of adsorption. The relation between the formation of a contact angle and negative net heats of adsorption can be shown.

Combining equations 2 and 4 one obtains

$$q_1 - q_L = h_{S^\circ} - h_{SL} - h_{LV} \qquad (6)$$

Then using the Gibbs–Helmholtz relation

$$h = \gamma - T(\delta\gamma/\delta t) \qquad (7)$$

where γ is the free surface energy, one can write the equation

$$q_1 - q_L = (\gamma_{S^\circ} - \gamma_{SL} - \gamma_{LV}) - T\left(\frac{\delta\gamma_{S^\circ}}{\delta t} - \frac{\delta\gamma_{SL}}{\delta t} - \frac{\delta\gamma_{LV}}{\delta t}\right) \qquad (8)$$

The quantity $(\gamma_{S^\circ} - \gamma_{SL} - \gamma_{LV})$, the spreading coefficient, is negative for liquids that form contact angles and positive for liquids that spread spontaneously. The second term on the right hand side of equation 8 cannot be neglected, yet if either the assumption that the temperature coefficient of the spreading coefficient is positive or that the second term is of lesser magnitude than the first, is valid, the formation of a contact angle (negative spreading coefficient) would result in a negative net heat of adsorption. Mercury forms a contact angle against carbon. It would then be expected that the net heat of adsorption of mercury on carbon would be negative. Coolidge[22] found that the net heat of adsorption of mercury on charcoal was −4000 cal. per mole.

The conclusion that negative net heats of adsorption can be predicted must be tempered with the reminder that for true predictions the free energy relations must be used rather than the total energy relations. Yet for qualitative predictions the enthalpy can often replace the free energy function.

---

[21] F. G. Keyes and M. J. Marshall, *J. Am. Chem. Soc.*, **49**, 156 (1927).

[22] A. S. Coolidge, *ibid.*, **49**, 1949 (1927).

A NEW METHOD FOR CALCULATING DISSOCIATION CONSTANTS FROM SPECTROPHOTOMETRIC DATA

BY DAVID H. ROSENBLATT

Chemical Corps Medical Laboratories, Army Chemical Center, Maryland

Received February 2, 1953

A new method has been developed for the calculation of the apparent dissociation constants of monobasic and (in many cases) dibasic acids from spectrophotometric data. It should prove of value in situations where it is inadvisable or impossible to determine extinction coefficients of the pure ionic or molecular forms. The method requires a small number of determinations.

It is often observed that the visible or ultraviolet spectral absorption peaks of an organic compound are shifted when the compound loses or gains a proton. Consider, for example, the monobasic acid equilibrium $HA \rightleftarrows H^+ + A$. (Charges are not attached to the symbols HA and A because the "acid" HA may be the conjugate acid of a base, an uncharged molecule or even a singly ionized dibasic acid.) When the two conjugate forms, HA and A, coexist in solution the observed molar extinction coefficient for the solute at any wave length is equal to the sum of the products of mole fraction and molar extinction coefficient of each form. This has provided a convenient means of determining the apparent dissociation constants of such compounds.

The most usual method for calculating dissociation constants from spectrophotometric data has been to make a series of determinations of molar extinction coefficients at a particular wave length and at various hydrogen ion concentrations. The hydrogen ion concentration corresponding to the point midway between the maximum and minimum values for the extinction coefficient is then equivalent to the dissociation constant.[1] This is true because the mean extinction coefficient represents a condition where the two forms are present in equal concentrations. Since

$$pK_A = pH + \log\frac{[HA]}{[A]} \qquad (a)$$

it follows that

$$pK_A = pH \text{ when } [HA] = [A] \qquad (b)$$

The above method requires the preparation and study of quite a number of solutions—with solutes ranging from pure HA to pure A—if any accuracy is to be obtained.

Another approach,[2] also applicable only when it is possible to measure the extinction coef-

---

[1] N. Bjerrum, *Samm. chem. chemische-tech. Vorträge*, **21**, 30 (1915).

[2] L. A. Flexser, L. P. Hammett and A. Dingwall, *J. Am. Chem. Soc.*, **57**, 2103 (1935)

ficients of the pure HA and A forms, uses the expression

$$\frac{[\mathrm{HA}]_n}{[\mathrm{A}]_n} = \frac{\epsilon_\gamma - \epsilon_n}{\epsilon_n - \epsilon_\beta} \qquad \text{(c)}$$

ϵ_β = molar extinction coefficient of HA
ϵ_γ = molar extinction coefficient of A
ϵ_n = molar extinction coefficient of a mixture at hydrogen ion activity a_n and containing solute concn. of $[\mathrm{HA}]_n$ and $[\mathrm{A}]_n$

The value of $[\mathrm{HA}]_n/[\mathrm{A}]_n$ may then be substituted in equation (a), together with the pH at which ϵ_n was determined, to give pK_A. This method involves only three determinations of extinction coefficients, but two of these must be made with the pure conjugate forms.

Neither the above treatments for a monobasic acid nor any other spectrophotometric methods within the purview of the present author makes any provision for cases where it is inconvenient or impossible to determine ϵ_β and/or ϵ_γ directly. Such a case, for example, might be that of a very weakly acidic substance, the A form of which would exist exclusively only in strongly basic solution, which condition might be impossible to attain in the medium used or might be achieved only at the cost of an inordinately high ionic strength.

The method presented here for the calculation of the dissociation constants of monobasic acids does not require pure conjugate forms. Any three solutions with sufficient differences in pH and apparent molar extinction coefficient can supply the required information. By combination of equation (c) with the common expression

$$K_\mathrm{A} = \frac{[\mathrm{A}]_n a_n}{[\mathrm{HA}]_n}$$

the following general equation is derived

$$a_n\epsilon_n\left(\frac{1}{K_\mathrm{A}}\right) - a_n\left(\frac{\epsilon_\beta}{K_n}\right) - (\epsilon_\gamma) = -\epsilon_n \qquad \text{(d)}$$

This is a linear equation in four terms and three unknowns (the latter in parentheses), since ϵ_n and α_n are measurable quantities. Solution for the unknown K_A requires three simultaneous equations which may be solved with determinants

$$K_\mathrm{A} = \frac{\begin{vmatrix} a_1\epsilon_1 & a_1 & 1 \\ a_2\epsilon_2 & a_2 & 1 \\ a_3\epsilon_3 & a_3 & 1 \end{vmatrix}}{\begin{vmatrix} a_1 & \epsilon_1 & 1 \\ a_2 & \epsilon_2 & 1 \\ a_3 & \epsilon_3 & 1 \end{vmatrix}} \qquad \text{(e)}$$

Optical density, D, which is the instrumentally measured quantity, is related to the molar extinction coefficient by the relationship $D = \epsilon cd$, where c is concentration of solute and d is the length of the light path of the spectrophotometric cell. If the light path and total concentration of absorbing solute are the same in each measurement, then c and d will cancel out, and D may then be substituted for ϵ in equation (e).

A convenient laboratory procedure consists of making a stock solution of the solute to be examined, and diluting equal portions of this solution with equal amounts of buffer. A precise knowledge of the solute concentration is then not necessary. Buffer concentrations should be kept low in order that the ionic strength may not change too much the degree of dissociation of the absorbing solute, or, alternatively, thermodynamic dissociation constants may be found by extrapolation to zero ionic strength.

The following example illustrates the use of the method. It was desired to determine whether the first apparent dissociation constant for 3-nitrocatechol (considered as a monobasic acid) in water, obtained in this Laboratory by potentiometric titration, was correct. This value had been found to differ appreciably from those of Gilbert, Laxton and Prideaux,[3] which had been arrived at by conductometric and color comparison methods. A 10^{-3} M solution of 3-nitrocatechol was added to each of three 0.005 M phosphate buffers at different pH's, so that the resulting solutions were 2×10^{-4} M in 3-nitrocatechol and 4×10^{-3} M in buffer. These solutions were examined in a Beckman Model DU spectrophotometer at wave lengths of 300 and 440 mμ. Data are shown in Table I. The values of K_A obtained by using these data in equation (e) are shown in Table II, along with values determined by potentiometric titration and the figures given by Gilbert, Laxton and Prideaux.

TABLE I

OPTICAL DENSITY OF EQUIMOLAR 3-NITROCATECHOL SOLUTIONS AT DIFFERENT HYDROGEN ION CONCENTRATIONS

Hydrogen ion activity, moles/l.	Optical density At 300 mμ	At 440 mμ
6.61×10^{-6}	1.276	0.122
1.07×10^{-7}	1.003	.499
1.86×10^{-8}	0.896	.670

TABLE II

VALUES OF K_1 FOR 3-NITROCATECHOL BY VARIOUS METHODS

Method	K_A
Conductometric[7]	1.9×10^{-6}
Color comparison[7]	1.1×10^{-5}
Potentiometric	2.0×10^{-7}
Spectrophotometric, at 300 mμ	2.2×10^{-7}
Spectrophotometric, at 440 mμ	1.9×10^{-7}

The close agreement of the present spectrophotometric values with the potentiometric value of K_A for 3-nitrocatechol suggests that the conflicting results obtained by Gilbert, Laxton and Prideaux may be due to impurities in their 3-nitrocatechol. The agreement of values of K_A in the present work demonstrates that the method of calculation is of practical value.

It has been borne in mind, in the present work, that 3-nitrocatechol is really a dibasic acid; but since K_1/K_2 (the ratio of the first to the second dissociation constant) was known to be greater than 10^3, the treatment as a monobasic acid[4] was considered justified. In the case of a dibasic acid for which $K_1/K_2 < 1000$, however, the validity of such treatment would be open to scrutiny, inasmuch as the intermediate form HA (of the dissociation $\mathrm{H_2A} \rightleftarrows \mathrm{H^+} + \mathrm{HA} \rightleftarrows 2\,\mathrm{H^+} + \mathrm{A}$) will always be accompanied by significant amounts of $\mathrm{H_2A}$ and/or A which prohibit the direct determination of its ex-

[3] F. L. Gilbert, F. C. Laxton and E. B. R. Prideaux, *J. Chem. Soc.*, 2299 (1927).

[4] B. J. Thamer and A. F. Voigt, THIS JOURNAL, **56**, 225 (1952).

tinction coefficient. The type of difficulty here encountered has been met in various ways. Vlès and Gex (as corrected by Thamer and Voigt[3]) elaborated a method in which, the extinction coefficients of H_2A and A being known, that of HA is found by successive approximations; it is necessary to use data at two different wave lengths. A second cumbersome procedure[5] also makes use of successive approximations and of the extinction coefficients of H_2A and A. The ingenious method of "indirect colorimetry"[6] necessitates the use of equipment not normally available in the laboratory. Finally, in the treatment by Thamer and Voigt,[4] individual experimental determinations of the extinction coefficients of pure H_2A and A must be made; also, the optical density at a suitable wave length must be graphed against pH and a maximum or minimum found on this curve in a region where HA is the predominant form of the solute. Because these approaches require considerable effort, it is worthwhile to inquire into the feasibility of extending the use of equation (e) into the region where $K_1/K_2 <$ 1000. The question cannot be given an absolute and all-encompassing answer, since several factors influence the accuracy with which K_1 (or K_2) can be estimated. There is one variable source of error, however, which the use of equation (e), rather than (b) or (c), may affect considerably; this is the relative error (E) in K_1, made by assuming that all ionized H_2A is in the form HA, and which is pH dependent, as shown in

$$E = \frac{a_n([\mathrm{HA}]_n + [\mathrm{A}]_n)/[\mathrm{H_2A}]_n - a_n[\mathrm{HA}]_n/[\mathrm{H_2A}]_n}{a_n[\mathrm{HA}]_n/[\mathrm{H_2A}]_n} = \frac{[\mathrm{A}]_n}{[\mathrm{HA}]_n} = \frac{K_2}{a_n}$$

Now the hydrogen ion activity (and hence E) at which [HA] is maximal is fixed, and best results with equation (c)—and in effect with (b)—are obtained when the extinction coefficient of HA is determined at maximal [HA]. With equation (e), however, the magnitude of E may be decreased to a considerable extent[7] by selecting appropriately large values of a_n, and this may lead to a smaller over-all error.

Another possible treatment for dibasic acids is to use the solution of five linear equations of the form

$$a_n\epsilon_n\left(\frac{1}{K_1}\right) + \frac{\epsilon_n}{a_n}(K_2) - a_n\left(\frac{\epsilon\alpha}{K_1}\right) - \frac{1}{a_n}(\epsilon_\gamma K_2) - (\epsilon_\beta) = -\epsilon_n$$

This form is derived in a manner analogous to that of equation (e) and may be solved for K_1 and K_2 with fifth order determinants. The symbols are the same as those used previously, except that ϵ_α is the molar extinction coefficient of H_2A. The difficulty of solving such equations is great, and the present author has made no effort to test their usefulness.

---

(5) E. S. Hughes, H. H. G. Jellinek and B. A. Ambrose, THIS JOURNAL, **53**, 414 (1949).

(6) L. Sacconi, *ibid.*, **54**, 829 (1950).

(7) Similarly, if the value of K_2 is sought, the error from assuming a monobasic acid HA would be $E = a_n/K_1$, and would be reduced by diminishing a_n.

THE MECHANISM OF GAS PHASE RADIATION-CHEMICAL REACTIONS

By HARRY ESSEX

Chemistry Department, Syracuse University, Syracuse, N. Y.

Received April 21, 1953

From the effect of electric fields on the ion yield, and other experimental data, the extent can be calculated to which a gaseous radiation-chemical reaction is initiated by each of four primary mechanisms. Both published and new data (the details of which will appear subsequently) are used to illustrate the methods for calculating the ion yield attributable to each mechanism. The effect of the nature of the irradiation on the ion yields and the maximum ion yields possible for each mode of initiation are discussed.

Introduction

Our studies of the last twenty years on gas phase radiation-reactions,[1-10] together with other evidence, indicate that such reactions are initiated by one or more of the following mechanisms.

1. Recombination of oppositely charged ions,[11] *e.g.*

$$\mathrm{AB^+ + e^- \longrightarrow A + B}$$
$$\mathrm{AB^+ + AB^- \longrightarrow 2A + 2B}, \text{ etc.}$$

2. Molecule splitting on electron collision with attachment of the electron to a fragment of the molecule and without ionization, *e.g.*

$$\mathrm{AB + e^- \longrightarrow A + B^-}$$

3. Molecule splitting on electron collision without attachment of the electron, and without ionization, *e.g.*

$$\mathrm{AB + e^- \longrightarrow A + B + e^-}$$

4. Molecule splitting on ionization, *e.g.*

$$\mathrm{AB} + \begin{matrix}\alpha\\ \text{or}\\ e^-\end{matrix} \longrightarrow \mathrm{A^+ + B^-} + \begin{matrix}\alpha\\ \text{or}\\ e^-\end{matrix} \qquad \text{(a)}$$

$$\mathrm{AB} + \begin{matrix}\alpha\\ \text{or}\\ e^-\end{matrix} \longrightarrow \mathrm{A^+ + B} + \begin{matrix}\alpha + e^-\\ \text{or}\\ e^- + e^-\end{matrix} \qquad \text{(b)}$$

As indicated above, these four primary mechanisms are different ways of effecting one and the

---

(1) H. Essex and D. Fitzgerald, *J. Am. Chem. Soc.*, **56**, 65 (1934).

(2) C. Smith and H. Essex, *J. Chem. Phys.*, **6**, 188 (1938).

(3) M. J. McGuinness, Jr., and H. Essex, *J. Am. Chem. Soc.*, **64**, 1908 (1942).

(4) A. D. Kolumban and H. Essex, *J. Chem. Phys.*, **8**, 450 (1940).

(5) N. T. Williams and H. Essex, *ibid.*, **16**, 1153 (1948).

(6) N. T. Williams and H. Essex, *ibid.*, **17**, 995 (1949).

(7) J. Efimenko, Thesis, Syracuse University, Syracuse, N. Y., 1949.

(8) P. S. Rudolph, Thesis, Syracuse University, Syracuse, N. Y., 1951.

(9) Philipp H. Klein, Thesis, Syracuse University, Syracuse, N. Y., 1951.

(10) Philipp H. Klein, Thesis, Syracuse University, Syracuse, N. Y., 1952.

(11) This mechanism was originally proposed by S. C. Lind, "The Chemical Effects of Alpha Particles and Electrons," 2nd Ed., Chemical Catalogue Co., New York, N. Y., 1928.

same chemical reaction, *i.e.*, $AB \rightarrow A + B$, (for neither addition of an electron to, nor removal of an electron from a molecule are chemical reactions).

It is possible to determine experimentally which of the four mechanisms initiates a reaction and to what extent each is involved. This listing appears to constitute almost complete coverage of initiation as in the one case for which the data are available the total ion yield is only slightly greater than the sum of the ion yields due to these four modes of initiation. Each mechanism, however, is probably the summation of several successive processes.

In mechanism 2, the first step is probably attachment of the electron to the molecule. Since negative ions of valence-saturated molecules are generally unstable, the negative ion thus formed may decompose into uncharged and negatively charged molecular fragments, *e.g.*

$$AB + e^- \longrightarrow AB^- \longrightarrow A + B^-$$

In mechanism 3, presumably the electron collision puts the molecule in an excited state, which is a repulsive state, and is followed immediately by decomposition; or, from the excited state a radiation-less transfer to a repulsive state may occur. In the first alternative, the process is analogous to photo-dissociation, and in the second to predissociation in photochemistry. It is generally recognized that what light can do, electrons can do, and the processes of mechanism 3 may therefore be identical with those involved in the photochemical decomposition of the same molecular species, except for the mode of excitation. However, although they are probably similar, they need not be identical for the selection rules which limit the transitions which can be caused by light do not apply strictly to the transitions caused by electrons.

If as seems theoretically probable, the foregoing analysis is correct, the fractions of the reaction initiated by mechanisms 2 or 3 may be described as the fraction initiated by negative ion formation or by excitation, respectively.

Likewise, intermediate states of the molecular complex are probably involved in mechanisms 1 and 4.

Other modes of initiation are possible, analogous to mechanism 3, experimental methods for the detection of which have not been discovered. It is to be expected that alpha particles can, like electrons, cause molecule splitting without ionization, *e.g.*

$$AB + \alpha \longrightarrow A + B + \alpha \qquad (5)$$

Also, it is conceivable that high energy molecules or molecular ions resulting, for example, from mechanisms 2, 3 and 4, may in turn on collision cause molecules to decompose. The resultant ion yields, however, from high energy molecules and molecular ions other than alpha particles, are probably small due to the rapid loss of kinetic energy in collisions between bodies of comparable magnitude and due to the rapid de-activation of activated molecules at the pressures generally used in this work. Our work shows that although the proportion of the various modes of initiation varies with the conditions, for instance pressure, under the conditions usually employed a reaction is initiated to a comparable extent by several of the four mechanisms acting simultaneously; contrasting with thermochemical and photochemical reactions in which the postulation of several simultaneous modes of initiation does not seem to be generally necessary.

Ion Yield by the Saturation Current Method.—For the elucidation of the mechanism of a radiation-chemical reaction, the types of initiation involved and the extent to which each contributes to the reaction must be determined. A method of obtaining information related directly to a primary reaction type was indicated by consideration of the possibilities of a new way of measuring ion yields. (The ion yield is defined as molecules decomposed per ion pair or per negative ion; negative ions are negative molecular ions plus electrons.) This new method consists in exposing the gas or gaseous mixture to ionizing radiation in a vessel (Fig. 1) provided with large platinum or graphite electrodes at either end. The number of ions produced per second was determined by the saturation current. The number of molecules reacting in unit time was determined by pressure changes—generally by freezing out the reacting gas with liquid air after a known time lapse, and measuring the pressure of any produced but uncondensed gas with a McLeod gage. For example, in the NH_3 decomposition, the NH_3 was frozen out and the residual pressure of the N_2 plus H_2 which are produced in the ratio of 1 to 3 was measured.

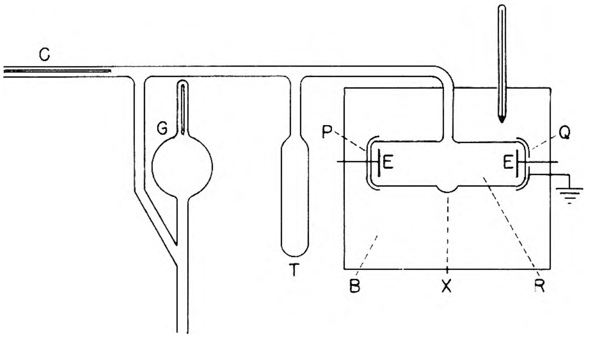

Fig. 1.—B, constant temperature air bath; R, reaction vessel; G, McLeod gage; X, radium; T, trap for condensing out gases by liquid air; P-Q, thin metal shields.

The success of this method plainly depended, in most cases, on measuring the rate of the reaction when proceeding extremely slowly, as it is impossible to get saturation currents with an intense source of radiation. Probably because of the difficulty in measuring the rate of very slow reactions this method had not been previously used. It was found, however, that with field strengths of the order of 10^3 volts per cm., saturation can be obtained with radiation intensities which produce a build-up in pressure on the McLeod gage of several microns per day. With runs of several days to a week's duration, pressure changes could be measured with a reproducibility of a few per cent. In the case of one reaction, namely, that between hydrogen and chlorine,[7] the ion yield is so extraordinarily high, about 30,000, that even at the low radiation intensities necessitated by the saturation current method, the reaction could be followed by the decrease in pressure of the hydrogen on an ordinary manometer, after Cl_2 and HCl had been frozen out with liquid air.

Ion yields previously reported in the literature were determined by the classical, indirect method in which the number of ions produced was calculated from the known strength of the radioactive material, the geometry of the apparatus, and specific data of the system studied. The intensities of radiation were greater, often hundreds of times greater, than those used with the new method. When this difference in intensity of radiation, which effects the ion yield, is taken into account the ion yield values determined by the two methods compare favorably.[2,4] The values obtained by the new method are, percentage-wise, probably less accurate, due to the greater difficulty of measuring the extremely slow reaction rates. But any measurements made by the classical method at low intensities of radiation would be subject to the same error. Ion yield measurements at low intensities of radiation are desirable since systems under these conditions present simpler pictures for the study of what are plainly complicated mechanisms. But independent of accuracy considerations it is the relative value of the ion yield as a function of field strength which is significant for the elucidation of mechanism and the new method is the only technique, so far, by which it is possible to determine ion yields both in the absence and presence of electric fields. Also as the technique is continuously improved, more confidence can be placed in the absolute values obtained by the new method. Some of the earlier results are cited here primarily to illustrate methods of attacking the problems.

Ion Yield Due to Recombination of Oppositely Charged Ions.—With the new method it is possible to measure the ion yield while an electric field is applied across the gas which removes a definite fraction of the ions produced per second. This fraction is the ratio of the ion current to the saturation current, which is measured at the beginning and end of and at intervals during a run. To give an accurate value of the ion yield such a run would normally last several days. Insofar as the reaction is initiated by recombination of ions, the ion yield should decrease as the field is increased. If the reaction is entirely so effected, the ion yield should be zero when the field is sufficiently strong to cause saturation, *i.e.*, at fields corresponding to the horizontal portion of the current-potential curve, Fig. 2; if the reaction is 80% initiated by ion recombination, the ion yield should be 20% of that at no field.

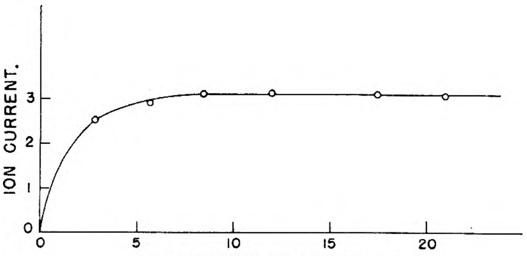

Fig. 2.

Such a calculation is valid if the only effect of a field sufficiently strong for saturation is to remove ions before mutual neutralization. However, at such fields electrons are often sufficiently accelerated to cause molecule decomposition on collision. This phenomenon is indicated by a sudden increase in the ion yield on our ion yield–field strength curves, and the field strengths necessary for its onset are known from the work of Bradbury[12,13] and others on negative ions. But even in cases in which molecular splitting on electron collision occurs at a field insufficient for saturation, the fraction of the reaction (in the absence of a field) contributed by ion recombination may be determined with considerable exactness. This is possible because as shown by the current potential curves *e.g.*, Fig. 2, a large fraction of the ions are removed at a small fraction of the field strength necessary for (practically) complete saturation. For example, $^9/_{10}$ths of the ions might be removed at $^1/_2$ of the field strength necessary for saturation and well below that required for the onset of the electron reaction due to the field. Then, if y is the fraction of the reaction due to ion recombination, the ion yield at this high field should be $(1.00 - 0.90y)$ of the ion yield at no field; the ion yield due to this mechanism (in the absence of a field) is

$$\left(\frac{M}{N}\right)_1 = \frac{(M/N) - (M/N)_H}{f_s} \qquad (6)$$

in which (M/N) is the total ion yield at no field, $(M/N)_H$, the total ion yield at the high field strength and f_s the ratio of the ion current at the high field strength to the saturation current. However, for accuracy the calculation should be made at a high fraction, f_s, of the saturation current. If made at a small fraction of the saturation current the calculation is unreliable since it assumes that when the fraction, f_s, of the ions are removed this same fraction of each kind of ion will be removed. Of the negative ions, the electrons will be most easily removed. Fortunately, the problem presents no difficulty, when as is generally the case at low pressure, the ion yield is independent of field strength to considerable values of f_s.

This method of obtaining ion yields due to "ion recombination" depends on the assumption that no reaction accompanies neutralization of ions at the electrodes, an assumption originally based on the rapid dissipation of energy among the degrees of freedom of vibration of the surface atoms. Considerable experimental evidence supports this hypothesis. If decomposition does accompany such electrode neutralization the ion yield due to ion recombination $(M/N)_1$ is the difference between the ion yield at no field and at saturation, plus the ion yield due to electrode neutralization. In that case, figures obtained for ion yields due to ion recombination as above are minima. Specifically, this means (the hypothesis of electrode decomposition) that in the many cases observed by us particularly at low pressure, *e.g.*, NH_3,[3] N_2O[5] and H_2S[14] in which the ion yield remains independent of field strength up to half saturation or further, the ion

---

(12) N. E. Bradbury, *J. Chem. Phys.*, **2**, 827 (1934).

(13) N. E. Bradbury and W. Tatel, *ibid.*, **2**, 835 (1934).

(14) Unpublished work.

yield due to ion recombination $(M/N)_1$ is positive and exactly balanced by the decomposition on neutralization of ions at the electrodes, a very improbable explanation. Still more experimental evidence pointing in the direction of no decomposition on electrode neutralization is discussed under the hydrogen–chlorine reaction.

A decrease in pressure then, or the application of an electric field, tends to stop initiation due to ion recombination as both changes result in the rapid removal of ions before reaction, to the walls or to the electrodes, respectively, and should experimentally have the same effect. In the alpha ray decomposition of ammonia[2,3] the total ion yield is 1.37 at 62 cm. and 1.03 at 20 cm.; at the lower pressure none of the reaction is initiated by ion recombination. The difference 0.34 is, within the experimental error, equal to the value 0.40 calculated for the ion yield due to ion recombination at the higher pressure. Similar agreement between the ion yield due to ion recombination and the effect of pressure has been found in other cases.

Effect of Higher Electric Fields.—In most of the cases studied, the ion yield at first decreased with increasing field strength or was independent of the field, but sooner or later the curves turned upward, or at least became convex to the field strength axis. Eventual increase in ion yield with field strength is to be expected if part of the negative ions are electrons, as electrons dissociate molecules on sufficiently severe collision. At the pressures of these experiments ($^1/_{10}$ to 1 atmosphere), the terminal energy of electrons is continuously increased with field strength. But the energy of the molecular ions is practically independent of the field and not appreciably different from the thermal energy at no field, a fact originally established by Townsend.[15]

Figure 3 is the curve for ammonia[2] at 62 cm. pressure and Fig. 4 for N_2O[5,16] at 10 cm. pressure. The second experimental point on each curve corresponds to one-half saturation current. The curve for NH_3 at 62 cm. (Fig. 3) drops off first at a rate which fixes the fraction of the reaction initiated by ion recombination at 30%. But at 20 cm. none of the reaction is initiated by ion recombination, the curve being horizontal at first[3] though rising finally to ion yields twice the value at no field.

The curve in Fig. 4 and the very similar curve for N_2O at 20 cm.[5] can be explained as follows: (1) None of the reaction is initiated by ion recombination; the ion yield at half saturation (second point on each curve) being identical with the ion yield at $X/p = 0$. (Here half of the ions are removed.) (2) At a particular value of the field strength, the curve starts to rise due to decomposition of molecules on electron collision. That this rise is not due to ionization is apparent from the appearance of the current–potential curve shown as a dotted line in the same diagram; the onset of ionization by electron collision is indicated on a current–potential curve by a very sharp rise generally following the horizontal portion which denotes saturation. Such field strengths were not reached. The increase in ion yield occurs at a field strength not very different from that at which Bradbury and Tatel[13] found the reaction

$$N_2O + e^- \longrightarrow N_2 + O^-$$

to take place. But if this were the sole reaction of the electrons at these fields the maximum increase in ion yield would be 1.0.[19] To explain the rise

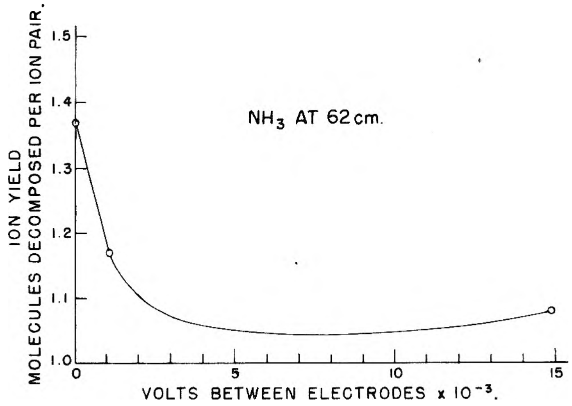

Fig. 3.

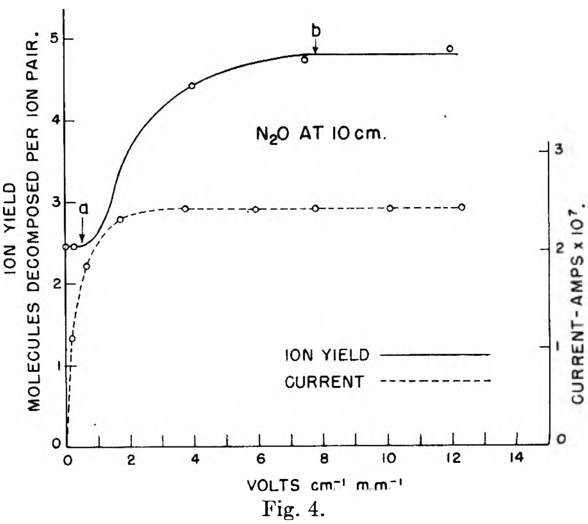

Fig. 4.

---

(15) J. S. Townsend, "Electricity in Gases," Clarendon Press, Oxford, 1915, p. 183.

(16) In the N_2O decomposition[5] the ion yields were measured in terms of molecules of products uncondensed by liquid air per ion pair. These figures were converted to molecules of reactant decomposed per ion pair, to conform to the convention used in this paper using the ratio 1.58 molecules of uncondensed gas produced per molecule of N_2O decomposed.[4,17,18]

(17) W. Mund, THIS JOURNAL, **30**, 890 (1926).

(18) G. R. Gedye, *J. Chem. Soc.*, 3016 (1931).

(19) As pointed out by A. O. Allen (private communication) the maximum ion yield due to "splitting with attachment" may be greater than 1 if a fragment formed in the split attacks another molecule. A possibility in the present case is: $O^- + N_2O \rightarrow N_2 + O_2^-$ (a), or after neutralization of O^-, $O + N_2O \rightarrow 2NO$ or $N_2 + O_2$ (b). This latter reaction was considered by W. A. Noyes[20] as a possibility following an initial split to N_2 and O in the photolysis of N_2O. Noyes[21] later suggested the reaction: $N + N_2O \rightarrow N_2 + NO$ (c), following an initial split into N and NO. However, it is not necessary to assume any of these possibilities, all known facts being satisfactorily explained by N_2O splits into $N_2 + O$ and $N + NO$ in the proper proportions, followed by established reactions. At the low pressure (10 cm.) and high surface–volume ratio of the experiments under discussion, the reactions (a), (b) or (c) would necessarily have high probabilities to occur to an appreciable extent before the active ion or atom becomes the stable wall compound, wall-O or wall-N.

(20) W. A. Noyes, Jr., *J. Chem. Phys.*, **5**, 807 (1937).

(21) W. A. Noyes, Jr., and P. A. Leighton, "Photochemistry of Gases," Reinhold Publ. Corp., New York, N. Y., 1941, p. 398.

in ion yield of 2.4 "splitting without attachment," *i.e.*

$$N_2O + e^- \longrightarrow N_2 + O + e^-$$

must be also assumed.

If both splitting "with" and "without attachment" occur the curve should finally level off, as observed, since with increasing field strength all electrons will finally become attached. Once an electron is captured by a molecular fragment the probability of further reaction is low as molecular ions are not accelerated by these fields.

This explanation has been supported by work with the Loeb Electron Filter,[22] a grid of fine parallel wires which may be placed before the positive plate. A high frequency alternating potential is applied across adjacent wires which removes electrons but not the heavier molecular ions from the negative ion stream. With such a grid, it was shown[10] in the α-ray decomposition of N_2O (Fig. 4), that the electron content of the negative ion stream starts to decrease where the curve turns upward, point "a" (Fig. 4) and that the electrons are all removed where the curve becomes horizontal, point "b."

If this is the correct explanation of the curve, "splitting with" and "without attachment" must be primary processes in the reaction in the absence of a field, as the initial energy of a large proportion of the electrons ejected from molecules by alpha particles and secondarily by electrons, exceeds the value at which these reactions occur.

For N_2O, splitting "without attachment" is evidently an important primary process. The relative contributions of these two processes can be roughly estimated from the increase in ion yield observed of 2.4 when a field is applied, compared with an increase of 1.0[19] for splitting with attachment alone. These figures indicate a ratio of 1.4:1 for "splitting without attachment" to "splitting with attachment," but this ratio is a minimum as it depends upon the assumption that all the negative ions are electrons. The actual electron content of the negative ion stream and a more accurate estimate of the relative frequency of these processes can be calculated from data obtained with the Loeb Electron Filter placed before the anode and work with the Filter for this purpose was in progress in the Syracuse laboratory by 1948.[5] However, further consideration of the possibilities of this filter led the author to the conclusion that it is not only possible as predicted to find the ratio of ion yields due to "splitting without" and "splitting with" attachment but that the information furnished by the filter goes much further and actually enables the calculation, except in rare cases, of the ion yields due to each of these processes.

Ion Yield Due to "Splitting with Attachment" (Negative Ion Formation).—At sufficiently low pressure, the electron current which can be measured with the filter reaches saturation below those fields which cause reaction (*i.e.*, below point "a," Fig. 4) and below those fields necessary for saturation in the total ion current. The saturation electron current evidently measures the number of electrons produced in the gas, at no field, after all processes except neutralization. The ratio of the saturation electron current I_{se^-} to the total saturation current I_s, is the number of electrons produced per negative ion or the ion yield of electrons, and $(I_s - I_{se^-})/I_s$ is the fraction of the negative ions which are negative molecular ions or the ion yield of negative molecular ions. Insofar as negative molecular ions are only produced by mechanism 2, a condition which is generally met, this is the ion yield due to mechanism 2.[23]

$$\left(\frac{M}{N}\right)_2 = \frac{I_s - I_{se^-}}{I_s} \tag{7}$$

However, the possibility of negative molecular ion formation by other processes should not be ignored. Mass spectrograph data show that negative molecular ions are formed abundantly in CCl_4 and $SiCl_4$[24] (by mechanism 4a) and to a considerable extent with other polyhalides[25]; with other molecules, ionization in this way occurs to only a slight extent. The formation of negative molecular ions by direct electron addition to molecules of reactant ($AB + e^- \rightarrow AB^-$) is impossible where the electron affinity is negative as is usually the case with valance saturated molecules. The formation by direct addition of an electron to a molecular fragment is impossible in the initial stages of the reaction where the saturation electron current I_{se^-}, should be measured. It will be observed that the ion yield due to initiation by mechanism 2 is calculable, simply from two electric current measurements without the use of any other data.

Ion Yield Due to "Splitting without Attachment" (Excitation).—If in addition to these two currents the total ion yield is known at no field and at a field so high that all electrons have become attached, then if this high field is also a saturation field, the ion yield due to "splitting without attachment" may be calculated. If $\Delta(M/N)$ is the increase in the ion yield from no field to the high field, then as any reaction due to mechanism 1 is stopped by the field, the increase in ion yield attributable to mechanisms 2 plus 3 is

$$\Delta'\left(\frac{M}{N}\right) = \Delta\left(\frac{M}{N}\right) + \left(\frac{M}{N}\right)_1$$

$(M/N)_1$ may be 0 as in the N_2O decomposition at low pressure in which case $\Delta'(M/N) = \Delta(M/N)$. The ratio of "splitting without" to "splitting with" attachment is

$$\frac{\Delta'(M/N) - I_{se^-}/I_s}{I_{se^-}/I_s} \tag{8}$$

and the ion yield due to mechanism 3 is

$$\left(\frac{M}{N}\right)_3 = \frac{I_s - I_{se^-}}{I_s}\left(\frac{\Delta'(M/N) - I_{se^-}/I_s}{I_{se^-}/I_s}\right) \tag{9}$$

Equations 8 and 9 hold because I_{se^-}/I_s is necessarily the electrons per ion pair which react accord-

---

[22] L. B. Loeb, "Fundamental Processes of Electrical Discharge in Gases," John Wiley and Sons, Inc., New York, N. Y., 1939, p. 272.

[23] Exceptions occur when a fragment formed from the splitting of one molecule attacks another molecule, *e.g.*, $HBr + e^- \rightarrow H + Br^-$; $H + HBr \rightarrow H_2 + Br$ (A. O. Allen, private communication, see note 19).

[24] R. F. Baker and J. T. Tate, *Phys. Rev.*, **53**, 683 (1938); R. H. Vought, *ibid.*, **71**, 93 (1947); H. S. W. Massey and E. H. S. Burhop, "Electronic and Ionic Impact Phenomena," Oxford Univ. Press., 1952, pp. 272–274.

[25] A. O. Allen, private communication.

ing to mechanism 2 on increasing the field from zero to the high value. In the calculation of the ion yield due to mechanism 3 in the absence of a field by equation 9, it is assumed that the ratio, equation 8, is independent of electron energy, an assumption which may not be accurate; it is meagerly supported by the fact that, in the few cases where any sort of plateau[5] is finally reached, the ion yield–field strength curve is horizontal within the error of the measurements. Although it is theoretically highly improbable that the ratio of occurrence of these two processes remain indefinitely independent of electron energy, it seems not unlikely that in the reactions under consideration practically all splits by mechanisms 2 and 3, in the absence of a field, occur at low electron energies; with electron energies sufficient for ionization, ionization is much more probable.

For the decomposition of N_2O at 105.7 mm.,[10] $I_s = 79.00$ mmμa., $I_{se^-} = 44.82$ mmμa., so

$$(M/N)_2 = \frac{79.00 - 44.82}{79.00} = 0.433$$

At approximately the same pressure (see Fig. 4), the increase in ion yield due to the field $\Delta(M/N) = \Delta'(M/N) = 2.40$ from which

$$\left(\frac{M}{N}\right)_3 = 0.433 \left\{\frac{2.40 - (44.82/79.00)}{44.82/79.00}\right\} = 1.39$$

The ion yield due to decomposition on ionization (mechanism 4) calculated from positive ion mass spectrographic abundance data for N_2O,[26] as described below is 0.41. The ion yield due to mechanism 1 is 0 as shown by the initially horizontal ion yield–field strength curve. The difference therefore between the total ion yield 2.47 and the sum of the ion yields due to mechanisms 1, 2, 3 and 4 is 0.24. This value then is the ion yield due to those processes (*e.g.*, reaction 5) which account for part of a radiation—chemical decomposition, but for the detection of which experimental methods are lacking. As this is the first such calculation the figures are tabulated below, in spite of inaccuracies and uncertainties, for easy inspection.

Total ion yield	2.47
Increase in ion yield from 0 field to saturation	2.40
Ion yield due to mechanism 1	0.00
Ion yield due to mechanism 2	0.43
Ion yield due to mechanism 3	1.39
Ion yield due to mechanism 4	0.41
Ion yield due to other mechanisms	0.24

It has been assumed that in addition to causing ionization an electron has a certain probability of "splitting a molecule with attachment" and in general a different probability of "splitting the molecule without attachment." The possibility that all splits are "without attachment" and that the negative ions are produced by the direct attachment of electrons to products of the reaction is ruled out by finding that the ion yield following an induction period, if any, is the same in successive runs in which the products are not removed and, in the absence of an induction period, in short and long runs starting from zero decomposition. On the basis of the latter hypothesis the molecules of reactant and product are competing for the electron in its normal path in the absence of a field and in its path toward the anode in the presence of a field. Such competition would result in decreased ion yield as the products accumulate, because more and more electrons would be fixed by addition to a product, $B + e^- \rightarrow B^-$, before causing decomposition of the reactant either with or without electron attachment.

Ion Yield Due to Ionization.—The ion yield due to mechanism 4, "decomposition on ionization" may be estimated from mass spectrograph abundance data for positive ions produced by electron bombardment. With alpha rays, 80% of the ionization is secondary and the average energy of these electrons is comparable with that of the electrons responsible for the positive ions analyzed with the mass spectrograph. Let N = the total number of positive ions analyzed by the mass spectrograph and N_D = the number of these with formulas different from the parent molecule. The ratio N_D/N is the number of positive ions with formulas different from the parent molecule produced per positive ion, or the number of molecules decomposed in ionization by electrons per positive ion or per ion pair. This ratio is then approximately the molecules decomposed per ion pair in alpha irradiation or the ion yield due to mechanism 4.

For N_2O, $N_D/N = 0.412$,[26] the ion yield approximately, $(M/N)_4$ due to the decomposition on ionization in the α-ray disintegration of nitrous oxide. The value has already been cited in connection with the ion yields consequent on other primary mechanisms in this reaction. For most molecules the above ratio is less than 0.5, *i.e.*, the most abundant ion on electron bombardment is the one formed by simple electron removal from the parent molecule. C_2H_6, one of the gases whose α-ray decomposition has been studied, presents an exception. With C_2H_6 the total ion yield is 1.75 and N_D/N[27] $= (M/N)_4 = 0.87$ from which it follows that in this case the α-ray reaction is about 50% initiated by decomposition on ionization.

Results in General.—The ion-yield curve in Fig. 4 is typical of the many radiation–chemical reactions which have been studied by the saturation current method with these modifications.

(a) Particularly at high pressure (one atmosphere), the initial portion of the ion-yield curve may slope downward, indicating partial initiation by ion recombination.

(b) Frequently the ion-yield field strength curve does not finally level off, indicating that it was not possible to reach field strengths at which all of the electrons became attached before reaching the electrode. In none of the experimental work have the electric fields been raised to the point of ionization by electron collision.

(c) In one case, the decomposition of ethane[6] (Fig. 5), the ion yield increases with field strength at both pressures as the field is increased from zero to saturation. This suggests that a reaction involving ions, which decreases the amount of noncondensable gas produced, is stopped by the field.

---

[26] R. C. Taylor, R. A. Brown, W. S. Young and C. E. Headington, *Anal. Chem.*, **20**, 396 (1948).

[27] J. A. Hipple, Jr., *Phys. Rev.*, **53**, 530 (1938).

The ions $C_2H_5^+$ and H^- have been shown in the mass-spectrograph[27] studies to be produced by electron bombardment of ethane. In a field, the $C_2H_5^+$ ions would be neutralized at the negative electrode yielding C_4H_{10} and the H^- ions at the positive electrode yielding H_2, whereas in the absence of a field the $C_2H_5^+$ and H^- would be neutralized at the wall and some of them would react with each other to give ethane. Finally with increase in field strength, the curves rise steeply indicating the onset of molecule decomposition on electron collision.

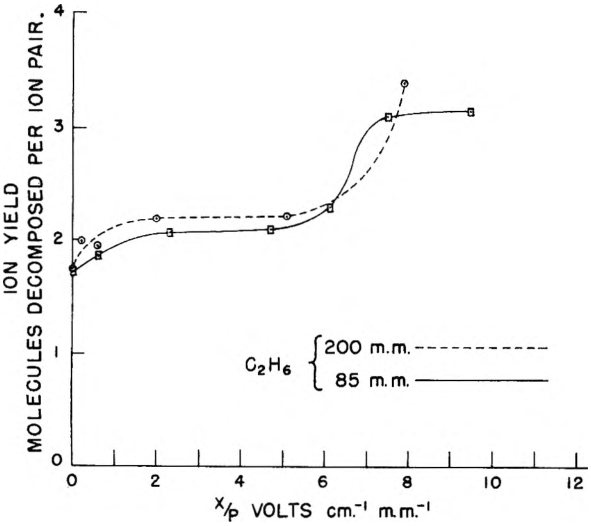

Fig. 5.

Occasionally a radiation-chemical reaction is found which, under certain conditions, is initiated almost entirely by a single mechanism.

The Hydrogen–Chlorine Reaction.—The hydrogen–chlorine reaction[7] is an example of initiation almost entirely by ion recombination, although mechanisms 2 and 4 are probably involved to a minor extent. Its study involved the use of new techniques.

Since Lind and Livingston[28] found near identity of ion and quantum yields and of temperature coefficients for the radiation-chemical and the photochemical HCl synthesis, the reaction in all probability proceeds by Nernst chains.

$$Cl + H_2 \longrightarrow HCl + H$$
$$H + Cl_2 \longrightarrow HCl + Cl, \text{ etc.}$$

If all chains were started by

$$Cl_2^+ + e^- \longrightarrow 2Cl \qquad (11)$$

and/or

$$H_2^+ + e^- \longrightarrow 2H$$

and this were the sole mechanism, the ion yield at half saturation should be 0.50 of that at no field. But at these low intensities of ionization the probability of the reaction

$$Cl_2 + e^- \longrightarrow Cl + Cl^- \qquad (12)$$

occurring on collision is high, 10^{-3} according to both Wahlin[29] and Bradbury.[12] Cl atoms produced in (12) can start Nernst chains, but not the Cl^- ions, the reaction of Cl^- ions with H_2 being highly endoergic. But the Cl^- could neutralize the Cl_2^+ or H_2^+ ions to start chains, possibly in the manner

$$Cl_2^+ + Cl^- \longrightarrow 3Cl \qquad (13)$$

In so far as reaction 12 (mechanism 2) successfully competes with reaction 11 for electrons, the ratio of the ion yield at half saturation and at no field should exceed 0.50, because reaction 12 is not appreciably affected by the electric field. Furthermore, any splitting of H_2 or Cl_2 on ionization (mechanism 4b) would result in a ratio in excess of 0.50, as the number of chains started by Cl or H atoms so produced would be independent of an applied electric field.

For the study of this reaction graphite electrodes were used because of the reactivity and possible catalytic effect of platinum. Due to the tremendous ion yield (*ca.* 30,000) the reaction was followed by the pressure change of the hydrogen on an ordinary sulfuric acid–mercury manometer after freezing out Cl_2 and HCl with liquid nitrogen. In agreement with the findings of previous investigators,[28,30] the ion yield was found to vary greatly, by several hundred per cent, and apparently fortuitously in separate experiments under conditions which appeared identical. Also in any single run the ion yield was found to drop rapidly in successive measurements as the HCl accumulated. Therefore, the method previously described for the determination of the fraction initiated by ion recombination, from the ratio of the ion yield in the presence and absence of electric fields, could not be applied without modification. The first procedure for solving the difficulty consisted in making with a particular mixture three successive measurements of ion yield at no field at 24-hour intervals, then continuing with the same mixture but making ion yield measurements in a half-saturation field at 24-hour intervals. The ion yield–time curve at no field, for which three points were known was extrapolated to extend over the ion yield curve at half-saturation. The ratio of ordinates at any time is the ratio desired. The second procedure consisted in making from the first, alternative measurements at 24-hour intervals, of the ion yield at no field and at half-saturation. The average H_2 or HCl partial pressure during each 24-hour interval was available from the manometric data. A smooth curve was run through the points giving the ion yield at no field as a function of HCl partial pressure and a similar curve was run through the points at half-saturation. The ratio of the ordinates on these two curves is the ratio of the ion yields at any HCl partial pressure. Both methods gave values for the ratio close to 0.50 and the best value 0.57 is in agreement with the hypotheses that (a) most of the reaction is initiated by ion recombination, (b) that at these low ionization intensities a smaller fraction is initiated by mechanisms 2 and/or 4, and (c) that the ions, *e.g.*, Cl_2^+ and H_2^+, do not decompose on neutralization at the electrodes, supporting again the kinetically probable postulate that no decomposition occurs on ion neutralization at an electrode or wall.

---

(28) S. C. Lind and R. Livingston, *J. Am. Chem. Soc.*, **52**, 593 (1930).

(29) H. B. Wahlin, *Phys. Rev.*, **19**, 173 (1922).

(30) F. Porter, D. C. Bardwell and S. C. Lind, *J. Am. Chem. Soc.*, **48**, 2603 (1926).

Azomethane.—A reaction which appears to be largely initiated by mechanism 3 including possibly some of the analogous splitting "without attachment," by alpha particles (equation 5) is the radiation-chemical decomposition of azomethane at 55 mm.[8] The ion yield[31] is 5.5 at no field, remains constant to an X/p value of 0.43 ($^1/_4$ saturation) and then rises to a value of 23 at the highest field strength attained ($X/p = 4.9$) with no indication of a final plateau.

Effect of Type of Irradiation on Mechanism.—The effect of the nature of the irradiation on the ion yield, and on the relative importance of the various modes of initiation, is under investigation. Already some data are available on the N_2O decomposition by high energy electrons[32] (Lenard rays) and by X-rays. The measurements with Lenard rays were made at a pressure of 54 mm. at (X/p)'s from 0 to 6. The length of each run was approximately three hours. The ion yield–field strength curve is very similar in appearance to that obtained for the alpha irradiated reaction at 100 mm. (Fig. 4), in which the length of each run was about five days, which means that under the condition of the Lenard ray experiments the reaction is initiated not at all by mechanism 1 but by mechanisms 2 and 3 and also, as the ionization is by electrons, necessarily by mechanism 4. But with Lenard irradiation the numerical value of the ion yield at no field is less and the rise in ion yield with field strength is markedly less than with alpha rays but it is difficult to draw quantitative conclusions from the available data as the experiments are not strictly comparable, the ion yields in this reaction being pressure dependent,[4,5] probably surface volume-ratio dependent and exhibiting a marked induction period[4] lasting more than 24 hours.

Some measurements on N_2O decomposition by X-rays[33] have been completed under similar conditions of pressure and time. The results suggest that differences in mechanism of initiation between the α-ray and X-ray reactions, if any, occur in the ratio $(M/N)_2:(M/N)_3:(M/N)_4$.

Maximum Ion Yields.—The measured ion yield of a radiation-chemical reaction must be the sum of the ion yields due to each of the several types of initiation involved. Limiting values can be given for the ion yield possible from each of the mechanisms which have been discussed. If only endoergic dissociations are considered, thermal chain reactions are ruled out, and the ion yields from each mode of initiation (1), (2), (3) and (4) are limited as follows.

(1) Due to ion recombination: as pointed out by Lind,[11] if the neutralization is assumed to be $AB^+ + e^- \rightarrow$ products, the maximum ion yield is 1; if the neutralization is assumed to be $AB^+ + AB^- \rightarrow$ products, the maximum value is 2; and if ion clusters are assumed, the maximum value may be larger. In each case the ion yield will be less than the value indicated insofar as neutralization occurs without decomposition, a condition which occurs frequently according to our measurements.

(2) Due to molecule decomposition on electron collision with attachment of the electron to a molecular fragment: the maximum ion yield is 1 except in those reactions in which the fragment attacks another molecule of the reactant.[19,23] It will be less than 1 insofar as electrons reach thermal energies unattached. The almost universal and often considerable rise in ion yield–field strength curves with field strength indicates the presence of considerable concentrations of electrons at near thermal energies. Loeb electron filter data enable the calculation of the fraction of the electrons which reached thermal energies unattached. This fraction is the ratio of the saturation electron current to the total saturation current and has the value 0.57 for the one case, the α-ray decomposition of N_2O for which electron filter data are available.

(3) Due to molecule decomposition on electron collision without attachment of the electron: the ion yield due to this mechanism may be considerable. Much of the initial electron energy is consumed in ionization, but an electron which has insufficient energy for ionization may still have several times the energy necessary for molecule decomposition.

(4) Due to molecule splitting on ionization: the maximum ion yield is 1. The ion yield will be less than 1 insofar as ionization takes place without decomposition, *i.e.*

$$AB + \begin{matrix}\alpha \\ \text{or} \\ e^-\end{matrix} \longrightarrow AB^+ + \begin{matrix}\alpha + e^- \\ \text{or} \\ e^- + e^-\end{matrix}$$

From positive ray analyses it is known that in the majority of cases more than 50% of the ionization by electrons is without decomposition; this is almost certainly true for many other types of radiation including α-rays.

The restrictions to the ion yields from mechanisms 2 and 4 mean that non-chain reactions with ion yields greater than 1 and not initiated by ion recombination, as shown by initially horizontal ion yield field strength curves, probably involve initiation by mechanism 3 (molecular excitation) and the greater the difference between the ion yield and 1 the greater the involvement of initiation by this mechanism.

---

(31) Measured in molecules of gas uncondensed by liquid nitrogen per ion pair.

(32) M. Carncrcse, Thesis, Syracuse University, Syracuse, N. Y., 1953.

(33) B. P. Burtt and J. Kircher, forthcoming publication.

MEMBRANE POTENTIALS FOR KERATIN AND CELLOPHANE AND THE MEYER–TEORELL THEORY

By M. L. Wright

Wool Industries Research Association,
Headingley, Leeds, England

Received April 23, 1953

It is emphasized that membrane potential measurements are merely ionic transport number determinations for diffusion in the polymer, and that from the membrane potential data alone, no further quantitative information concerning the system can be deduced. The use of the Meyer–Teorell theory for analyzing membrane potential measurements to obtain the ionic mobility ratio is criticized on the grounds that it does not take into account the internal diffusion potential which can arise from a difference in ionic concentration gradients inside the membrane, and this potential difference may exist even when the mobilities are equal. Calculations of the boundary and internal diffusion potential components have been made using sorption data, which agree with experiment, and show that the second potential can often account for a large proportion of the total potential. Therefore any data deduced using the original Meyer–Teorell analysis are of doubtful value. It is suggested that to characterize a membrane, sorption data are also required: the ratio of the ionic mobilities can then be calculated; and from this, the individual mobilities can be obtained using membrane conductivity data.

As a result of the direct measurements of ionic mobilities in polymers which have recently been described[1,2] it is now possible to check the validity of the Meyer-Teorell theory. This theory states that the ionic mobility ratio (*not* merely the transport number) can be obtained directly from membrane potential measurements. Meyer[3] and Teorell[4] assumed that the concentration of immobile ions present in the membrane, is the same at all points and this leads to the anomaly that no internal diffusion potential can exist if the positive and negative ionic mobilities are equal; in fact it is possible for the concentration gradients of the two ion species to be unequal in the membrane phase. Clearly for liquid junction potentials in aqueous salt solutions of two components, this cannot arise because of the requirement of electro-neutrality; in the membrane this condition is satisfied by means of the immobile charged groups.

Theory

Consider the electrical potential ΔE developed across a membrane separating two electrolyte solutions containing the same ionic species at different concentrations c_1, c_2. At any point in the membrane consider an element AB parallel to the membrane faces (Fig. 1). Let $t_i^{\pm}$ be the transport numbers of the i^{th} positive and negative ion species in AB. Let $\mu_i^{\pm}$ and $\mu_i^{\pm} + \mathrm{d}\mu_i^{\pm}$ be the chemical potentials of the positive and negative ion species in solutions which would be in equilibrium with AB on either side.

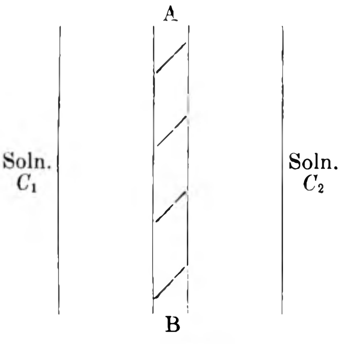

Fig. 1.

$$F\mathrm{d}E = \Sigma t_i^{+}\mathrm{d}\mu_i^{+} - \Sigma t_i^{-}\mathrm{d}\mu_i^{-} \qquad (1)$$

For a uni-univalent solution, concentration c, then $\mu = RT \ln c$, and therefore

$$F\mathrm{d}E/RT = (t^{+} - t^{-})\mathrm{d}(\ln c) \qquad (2)$$

(This derivation is only strictly true for ideal solutions but Meyer and Teorell made a similar assumption. The rigorous treatment for membrane potentials is given in an appendix.) If $t^{\pm}$ is independent of concentration in the range c_1 to c_2 this may be integrated at once to give

$$F\Delta E/RT = (t^{+} - t^{-}) \ln (c_1/c_2) \qquad (3)$$

When the transport number is expressed in terms of the cationic and anionic concentrations (c_K, c_A) and mobilities (u_K, u_A) of the total internal electrolyte in the membrane, eq. 3 may be rewritten in the familiar Nernst form

$$F\Delta E/RT = [(c_K u_K - c_A u_A)/(c_K u_K + c_A u_A)] \ln (c_1/c_2) \qquad (4)$$

For each concentration range the membrane potential ΔE gives the transport number for diffusion in the membrane in that range. This simple theory cannot give any information about the actual ratio of mobilities unless the ionic concentrations (or their ratio) in the polymer are known. To overcome this difficulty Meyer and Teorell introduced two ideas: (i) the concept of immobile sites in the membrane and (ii) the substitution, before integration, of a sorption equation to relate ionic concentrations in the membrane to those in solution. For the distribution of ions between solution and membrane the general equation[5] is

$$f_K f_A c_K c_A = c^2 \exp (\Delta\mu_K + \Delta\mu_A)/RT \qquad (5)$$

This was used by Meyer and Teorell in its simplest form after equating the ionic activity coefficients (f_K, f_A) in the membrane phase to unity and the affinity terms ($\Delta\mu_K$, $\Delta\mu_A$) to zero to obtain the simple Donnan relation

$$c_K c_A = c^2 \qquad (6)$$

Using the same assumptions the Donnan boundary potentials are given by

$$E_1 = (RT/F) \ln (c_{K_1}/c_1)$$

and

$$E_2 = (RT/F) \ln (c_{K_2}/c_2)$$

---

(1) M. L. Wright, *Trans. Faraday Soc.*, **49**, 95 (1953).

(2) M. L. Wright, *ibid.*, in press.

(3) K. H. Meyer and J. F. Sievers, *Helv. Chim. Acta*, **19**, 649 (1936).

(4) T. Teorell, *Proc. Soc. Exptl. Biol.*, **33**, 282 (1935).

(5) S. M. Neale and J. Farrer, *J. Colloid Sci.*, **7**, 186 (1952).

Equation 6 is now used to substitute in 2 giving

$$FdE/RT = t^{+}d(\ln c_K) - t^{-}d(\ln c_A) + d[\ln (c/c_K)] \qquad (7)$$

Therefore

$$\frac{F\Delta E}{RT} = \int_{c_1}^{c_2}\left[\frac{u_K\, dc_K}{u_K c_K + u_A c_A} - \frac{u_A\, dc_A}{u_K c_K + u_A c_A}\right] + \ln\left[\frac{c_1}{c_2} \times \frac{c_{K_2}}{c_{K_1}}\right] \qquad (8)$$

The first term on the right-hand side represents an internal diffusion potential ΔE_D and the second may be identified with the net Donnan boundary potential $E_1 - E_2$. The integration has been performed by Meyer, putting

$$(c_K - c_A) = X$$

where X is the concentration of non-diffusible ions in the membrane, and assuming that X is constant throughout the membrane. This leads to the well-known Meyer–Teorell relation for the internal diffusion potential

$$F\Delta E_D/RT = u \ln \{(X^2 + 4c_1^2)^{1/2} + Xu\}/\{(X^2 - 4c_2^2)^{1/2} + Xu\} \qquad (9)$$

where

$$u = (u_K - u_A)/u_K + u_A)$$

which becomes zero when $u_K = u_A$.

If we now consider the case when $u_K = u_A$, the expression for ΔE_D derived fom eq. 8 becomes

$$\frac{F}{RT}\Delta E_D = \int_{c_1}^{c_2}\frac{dc_K}{c_K + c_A} - \int_{c_1}^{c_2}\frac{dc_K}{c_K + c_A} = \int_{c_1}^{c_2}\frac{1}{c_K + c_A}\, d(c_K - c_A) \qquad (10)$$

For any given boundary conditions the diffusion potential can be obtained by graphical integration from sorption data. As shown by Henderson[6] the equation can be integrated directly if any linear relationship is assumed between c_K and c_A, *i.e.*, it is not necessary to assume either $c_K = c_A$ or $c_K + c_A$ = constant. Such a relationship is not necessarily true although it may be a sufficient approximation for small concentration differences. The solution under these conditions is

$$\frac{F}{RT}\Delta E_D = \frac{(c_{K_2} - c_{K_1}) - (c_{A_2} - c_{A_1})}{(c_{K_2} - c_{K_1}) + (c_{A_2} - c_{A_1})} \ln \left(\frac{c_{K_2} + c_{A_2}}{c_{K_1} + c_{A_1}}\right) \qquad (11)$$

It can be seen from eq. 11 that even if $u_K = u_A$ the diffusion potential ΔE_D will only be zero when $(c_{K_2} - c_{K_1}) = (c_{A_2} - c_{A_1})$, which is equivalent to $(c_{K_2} - c_{A_2}) = (c_{K_1} - c_{A_1})$ or $X_2 = X_1$, unless $\ln (c_{K_2} + c_{A_2})/(c_{K_1} + c_{A_1})$ is zero. Neither of these assumptions is likely to be true. The former assumption, which is that made by Meyer and Teorell, implies that the slopes of the sorption isotherms of the two ions of a salt in a polar polymer membrane are equal and this is very rarely the case. The second assumption requires that the absorption of one ion decreases as the concentration of the salt solution is increased.

Equations 9 and 11 show that a diffusion potential can arise from either a difference in mobilities of the two ions or a difference in the slope of the sorption isotherms or any combination of these effects. It is therefore only when the latter effect is non-existent that the Meyer–Teorell relation can be used to determine the mobility ratio. It will be shown later that the diffusion potential due to the variation in $(c_K - c_A)$ when there is no difference in mobilities may be considerable (at least as great as the net Donnan boundary potential). The importance of this contribution to the total potential will be most pronounced in dilute solutions because it is then that the sorption isotherms for the two ion species differ most. The diffusion potential arising from any inequality in the ionic mobilities has very little influence until the solution concentrations are quite large; this may be deduced from the theoretical curves given by Meyer.[3] It is to be noted that the expressions used by Meyer and Teorell for the boundary potentials are also incorrect unless appropriate values of X for the two sides of the membrane are used, but this will not produce a very serious error.

Once it has been established within the limits of experimental error, that the Nernst eq. 4 is valid for a particular system, any further interpretation of the membrane potential results depends on the correctness of the assumption involved in using the Donnan substitution or in the conditions imposed during the subsequent integration. If $(c_K - c_A)$ is known to be constant then the membrane potential results can be used to test the sorption equation. If X is not constant, then the system is too complicated to be analyzed by the method proposed by Meyer and hence the membrane potential results can give no further quantitative information about the system. Furthermore if X is constant, then the Meyer analysis still cannot be used unless it can be proved that u_K/u_A is independent of concentration.

Discussion

Keratin.—Using membranes of horn keratin two types of system have previously been investigated and in both cases the membrane potential measurements have been shown to be in agreement with transport number determinations, *i.e.*, the Nernst eq. 4 is obeyed. In solutions of mineral acid (HBr) it has been shown[1] that the membrane potential arises from the dissimilar mobilities of hydrogen and bromide ions which are present in equal numbers in the membrane. In the second system using a simple salt (NaBr) it has been shown[2] that the ionic mobilities are approximately equal and that the membrane potential is due to unequal concentrations of sodium and bromide ions in the membrane.

As the mobilities are equal for the salt, the internal diffusion potential due to unequal ionic concentration gradients can be discussed without the complication of the presence of a "normal" diffusion potential, *i.e.*, one arising from dissimilar mobilities. Also it is possible to calculate the components of the membrane potential using only the sorption data; the results (in mv.) are given in Table I, the potential of the weaker solution being negative. (The effect of the hydrogen ions in the membrane is negligible in this case because of their very low "over-all" mobility.) It is seen that the net boundary potentials $E_1 - E_2$ are much smaller

---

(6) P. Henderson, *Z. physik. Chem.*, **59**, 118 (1907).

TABLE I

MEMBRANE POTENTIAL CALCULATION FOR NaBr + KERATIN SYSTEM

Soln. concn., moles/l.	c_{Br} mmoles/g.	c_{Na} mmoles/g.	$E_1 - E_2$ (from c_{Br})	$E_1 - E_2$ (from c_{Na})	ΔE_D	ΔE (from c_{Br})	ΔE (from c_{Na})	ΔE (expt.)
0.001/0.002	0.01 .014	0.000054 .00014	9.4	7.0	8.0	17.4	15.1	17.2
0.004/0.008	.019 .027	.0004 .0012	8.6	8.8	8.6	17.2	17.4	17.0
0.016/0.032	.038 .055	.003 .007	7.9	5.6	5.1	13.0	10.7	15.5
0.064/0.128	.078 .118	.0168 .038	6.6	4.1	2.2	8.8	6.4	10.7
0.256/0.512	.175 .280	.076 .17	4.8	2.9	...	4.8	2.9	3.2

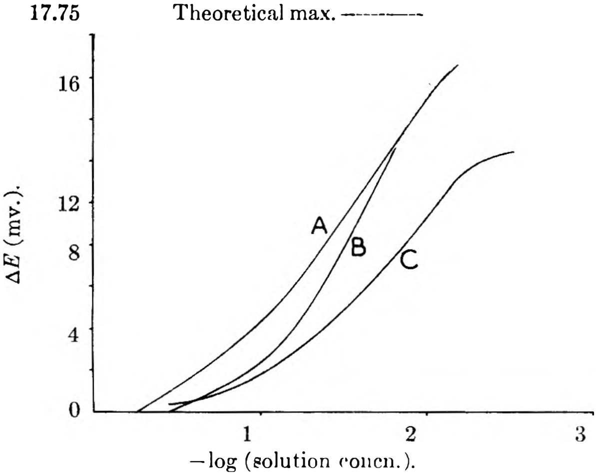

Fig. 2.—Membrane potentials for KCl–Cellophane system: A, calcd. from sorption data; B, calcd. from transport number; C, expt. (after Neale).

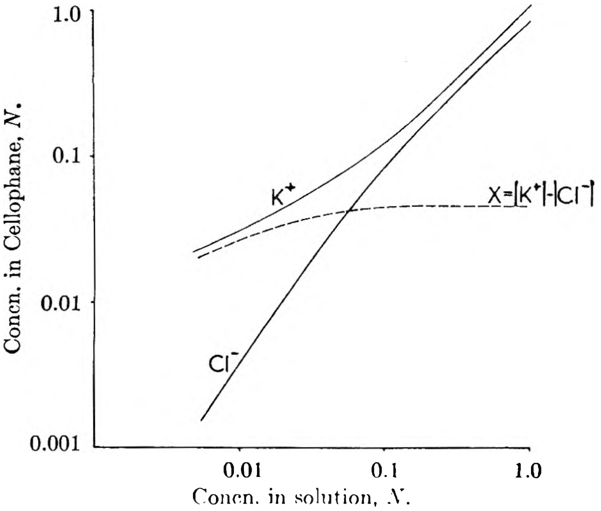

Fig. 3.—Ionic sorption in Cellophane (after Neale).

than the experimentally measured potentials. The discrepancy cannot be explained in terms of a diffusion potential arising from different ionic mobilities since $u_{Na} \approx u_{Br}$. The results can be brought into line with the measured values by the addition of the diffusion potential due to the unequal concentration gradients calculated using eq. 10 or 11. (The Meyer–Teorell eq. 9 gives zero diffusion potential when $u_{Na} = u_{Br}$.) The calculated values are in fair agreement with the experimental results when it is considered that the Donnan eq. 6 does not strictly hold[2] for the NaBr + keratin system since $\Delta\mu_{Na} + \Delta\mu_{Br} \neq 0$, and that the sodium and bromide mobilities are not exactly equal. If the Donnan equation was valid for this system, the boundary potentials calculated for either the sodium or bromide sorption data should be equal whereas it is seen that the values using the sodium data are consistently smaller.

Cellophane.—The membrane potential measurements obtained by Neale and Standring[7] for Cellophane in KCl solutions may be compared in Fig. 2 with direct transport determinations made in the same system. These were also measured by Neale and Standring[7] by analyzing the change in strength of KCl solutions at either side of a membrane, after the passage of a quantity of electricity. The membrane potential results are plotted against the mean of the concentrations of the two solutions. The results from the two different types of experiment are in fair agreement, especially as it is well known that for very permeable membranes it is difficult to obtain accurate measurements of the potentials: the results always tend to be low in magnitude. Neale and Farrer[5] have shown for simple uni-univalent electrolytes in Cellophane that the concentration of cations does not in general equal that of chloride ions (see Fig. 3). The values for the ionic sorption when taken in conjunction with the transport number permit the ionic mobility ratio to be calculated for that solution concentration. Although sorption data for KCl are not available the results for NH_4Cl and KCl should be similar according to the Donnan theory and therefore sorption values[5] for NH_4Cl have been taken in conjunction with transport values[7] for KCl to obtain u_K/u_{Cl}. These results are given in Table II and it is seen that the ionic mobility ratio for the diffusion of KCl in Cellophane is approximately equal to unity and is independent of concentration. (The ratio is about 0.96 in aqueous solution at 25°.) Because the membrane potential tends to be zero in concentrated solutions, it often has been assumed that $u_K = u_A$ at all concentrations, for the diffusion of simple salts in Cellophane and similar substances which swell greatly in aqueous solution. These results are the first to show that this is true for Cellophane; similar substances probably behave in a like manner.

---

[7] S. M. Neale and P. T. Standring, *Proc. Roy. Soc. (London)*, **A213**, 530 (1952).

Since $u_K/u_{Cl} \approx 1$, the variation of permeability for each ion species at various concentrations follows the sorption isotherms (Fig. 3). It is now possible to affirm that the selective permeability of Cellophane is due to unequal concentrations of ions although the mobilities are similar.

TABLE II

IONIC MOBILITY RATIO FOR KCl DIFFUSION IN CELLOPHANE

Soln. concn., moles/l.	Cation transport no.	c_K	c_A	u_K/u_A
0.0135	0.88	0.039	0.0051	0.96
.0207	.803	.045	.0092	.83
.0315	.736	.059	.0176	.83
.0629	.617	.087	.046	.86
.1256	.55	.148	.109	.90
.5021	.493	.52	.48	.89

It has been shown[7] that the sorption results for Cellophane in simple uni-univalent salt solution are in general agreement with the Donnan equation 6 and therefore in this case it is permissible to calculate the boundary potentials using the Donnan formula and similar results are obtained using either the cation or the anion sorption data. The results calculated for E_1, E_2 and ΔE_D are shown (in mv.) in Table III, the potential of the weaker solution being positive. It is again seen that the net boundary potentials $E_1 - E_2$ are much smaller in magnitude than the experimental membrane potentials, despite the fact that the measured potentials are themselves somewhat low in magnitude. Figure 2 clearly shows that the ionic sorption isotherms are dissimilar and the value of $c_K - c_A$ is not constant but falls in dilute solutions, which indicates that the use of eq. 10 or 11 is appropriate rather than eq. 9. When the values for ΔE_D are added to the net boundary potentials, previously calculated, the results are in approximate agreement with the measured potentials and in good agreement, especially at low concentrations, with the membrane potentials calculated from the directly measured transport numbers (see Fig. 2). The contribution to the diffusion potentials of hydrogen ions inside the membrane phase has been calculated and found to be negligible. The deductions made by Neale and Standring,[7] which are based on the assumption that the membrane potential in the KCl + Cellophane system is entirely composed of the boundary potential components, are therefore clearly invalid.

TABLE III

MEMBRANE POTENTIAL CALCULATION FOR KCl + CELLOPHANE SYSTEM

Soln. concn., moles/l.	E_1	E_2	$E_1 - E_2$	ΔE_D	Total (ΔE)
0.01/0.005	36.0	29.8	6.2	9.9	16.1
0.02/0.01	29.8	22.6	7.2	5.6	12.7
0.10/0.05	10.4	5.3	5.1	0.1	5.2
1.0 /0.5	1.08	1.025	0.025	.03	0.06

Since it has been shown that the original Meyer–Teorell theory requires modification even when used with membranes of a polymer as relatively simple as Cellophane, it can now be stated that it is dangerous to apply their analysis to systems in which no other data are available. It is preferable to measure the membrane conductivity K as well as the membrane potential in order to characterize the system fully by obtaining the individual values of the mobilities using

$$K/F = c_K u_K + c_A u_A \tag{12}$$

This has been done for a sample of Cellophane similar to that used by Neale and it has been found that the mobilities are smaller in magnitude than in water by a factor of 10. For keratin, a substance which does not swell so much when in aqueous solution, the values are about 1000th smaller than the corresponding values in water.

Acknowledgment.—I wish to thank Dr. A. B. D. Cassie, Director of Research, for encouragement in this work and the Council of the Wool Industries Research Association for permission to publish this account.

Appendix

Consider the potential ΔE_1 of the liquid-junction cell

$$\mathrm{Ag}\,|\,\mathrm{AgCl}\,|\,a_1\,|\,\text{transition layer}\,|\,a_2\,|\,\mathrm{AgCl}\,|\,\mathrm{Ag}$$

Then

$$\Delta E_1 = (\Delta E_{El} + \Delta E_J) = 2t_s^+(RT/F)\ln(a_1/a_2) \tag{13}$$

where t_s^+ the cation transport number in solution is assumed constant in the range a_1 to a_2. (For convenience ΔE_1 has been arbitrarily split up into the sum of the electrode potentials ΔE_{El} and the liquid-junction potential ΔE_J.) Consider the potential ΔE_2 of a similar cell but with a membrane instead of the liquid-junction transition layer, then by analogy

$$\Delta E_2 = (\Delta E_{El} + \Delta E) = 2t_m^+(RT/F)\ln(a_1/a_2) \tag{14}$$

where ΔE is the membrane potential and t_m^+ is the cation transport number for diffusion in the membrane. Elimination of the electrode potential between 13 and 14 gives

$$(\Delta E_2 - \Delta E_1) = (\Delta E - \Delta E_J) = (2t_m^+ - 2t_s^+)(RT/F)\ln(a_1/a_2) \tag{15}$$

Although it is impossible, using thermodynamic argument to evaluate ΔE using either 14 or 15 since ΔE_{El} and ΔE_J are indeterminate, it has often been assumed (for example, Neale[7,8]) either that

$$\Delta E_J = (2t_s^+ - 1)(RT/F)\ln(a_1/a_2)$$

or

$$\Delta E_{El} = (RT/F)\ln(a_1/a_2)$$

and therefore

$$\Delta E = (2t_m^+ - 1)(RT/F)\ln(a_1/a_2) = (t_m^+ - t_m^-)(RT/F)\ln(a_1/a_2) \tag{16}$$

Eq. 16 may be compared with eq. 3 which was derived in terms of concentration; clearly in the limit for ideal solutions eq. 16 should give eq. 3. Further justification of these approximations is obtained from the fact that similar values for t_m^+ are obtained either from 14 or 16. The important point to note is that the quantity t_m^+ can be obtained by the use of eq. 14 and in fact membrane potential measurements should always be made in this type of cell and eq. 14 used to obtain t_m^+.

---

(8) S. M. Neale, *Trans. Faraday Soc.*, **43**, 325 (1947).

THE ADSORPTION AND THE MAGNETIC ORTHO–PARA CONVERSION OF HYDROGEN ON DIAMAGNETIC SOLIDS. I. SOME EXPERIMENTS IN SURFACE PARAMAGNETISM[1]

By Y. L. Sandler[2]

Division of Chemistry, National Research Laboratories, Ottawa, Canada

Received May 7, 1953

The rates of the magnetic ortho–para conversion of hydrogen adsorbed on some diamagnetic solids are determined and the true half lives are found by means of adsorption measurements. True half lives of 1 to 6 minutes are found with $BaSO_4$ and 2 samples of TiO_2 at 90° K. The appearance of a strong blue color in a sample of TiO_2 due to loss of oxygen on heating *in vacuo* and disappearance of the color on contact with oxygen at room temperature is accompanied by changes in surface paramagnetism, as determined by the parahydrogen conversion. A method for estimating the number of extra-electrons due to surface defects is indicated; for this, the found true conversion rate is compared with the true conversion rate in presence of measured amounts of molecular oxygen adsorbed on diamagnetic surfaces. The true half life on a solid D_2O surface is found to be about 10 hours; this is shown to be the expected order of magnitude if compared with conversion rates of hydrogen, dissolved in diamagnetic liquids.

Charcoal at liquid air temperatures is a good catalyst for the ortho-para conversion of hydrogen.[3] A short review of the work done on this type of reaction up to 1934 is found in Farkas' book.[4] The "low temperature mechanism" in this case involves a nuclear spin inversion in the hydrogen molecule due to inhomogenous magnetic fields in the surface of the catalyst; the conversion is of the same type as found with paramagnetic solids.[4–7] The magnetic fields have been assumed to be due to "unsaturated valences" in the surface of the charcoal. The true half-lives of the conversion,[8] as measured in a static system, were between a few seconds and about 40 minutes for different charcoals. Conversions of a similar nature were also observed on other diamagnetic solids.[4] However, in most cases no quantitative conclusions can be drawn as adsorption data were not always given, and in some cases a chemical mechanism, analogous to the $H_2 + D_2$ reaction, may have been involved. In other cases again in which no conversion was found,[9] the magnetic centers may have been poisoned by chemisorbed hydrogen. In these cases apparently no precaution was taken to cool the catalyst to a sufficiently low temperature before contacting with hydrogen (for example, by using helium as a heat exchanger). One might also suspect that some sort of a residual conversion may exist with solids, analogous to the conversion of hydrogen, dissolved in diamagnetic liquids.[10,11]

The experiments described below were performed to obtain more quantitative information on the magnetic type of conversion on diamagnetic solids and about the nature of the magnetic fields causing the conversion.

Experimental

The Volumetric Gage.—A simple gage was used which in various slight modifications has been used previously by the author and has proved useful in quantitative work involving gases. The gage resembles a McLeod gage in which, however, the capillary of the high pressure arm is closed by tap T, instead of being sealed. The capillary tube above tap T leads to a central capillary system. This system on the one hand was connected to a series of gas storage bulbs, on the other hand to the reaction vessel. The gage can thus be used as a Toepler pump for transferring and mixing gases, as a McLeod gage, and for volumetric work such as the calibration of volumes or adsorption measurements. The connection between the central capillary system and the reaction vessel contained a small U-shaped liquid air trap, a micro-Pirani gage and a three-way tap, closing the reaction vessel and containing a doser for withdrawing small amounts of gas from the vessel for analysis. The total volume between tap T of the gage and the 3-way tap of the reaction vessel was about 15 cc. The meniscus heights of the mercury were read off to the nearest millimeter on a calibrated scale, placed behind the gage, by means of a vertically mounted sliding telescope. The distance between the meniscus and the nearest millimeter line was determined by means of a micrometer screw mounted on the telescope and controlling its vertical travel.[12]

Corrections due to varying capillary depression[13] were applied where the accuracy required it.

Materials.—TiO_2 (rutile) was supplied by the National Lead Company. It contained about 0.5% impurities, mainly SiO_2 and P_2O_5. The surface area of the powder was 81 m.²/g.; it had been previously determined[14] on a sample taken from the same stock by the BET method[15] using nitrogen. The material had a light cream color.

Sample "TiO_2 I" was outgassed *in vacuo* for 3 days. The temperature was gradually raised to a maximum of about 520°, at which temperature it was kept for about 10 hours. After this treatment the color of the powder was intensely blue; 3.42 g. was used, leaving a void space of 7.55 cc. in the reaction vessel.

Sample "TiO_2 II" was outgassed in the course of 5 days, with the sample at a maximum temperature of 350° for 24 hours. The heating was twice interrupted for about 5 hours. In the intermediate stage of the heating process faint blue and brown colors were observed which, however,

---

[1] Presented at the 122nd National Meeting of the American Chemical Society, Atlantic City, N. J., September 1952.

[2] Laboratory for Insulation Research, Massachusetts Institute of Technology, Cambridge 39, Mass.

[3] K. F. Bonhoeffer and P. Harteck, *Z. physik. Chem.*, **B4**, 113 (1929).

[4] A. Farkas, "Orthohydrogen, Parahydrogen and Heavy Hydrogen," Cambridge University Press, 1935.

[5] L. Farkas and Y. L. Sandler, *J. Chem. Phys.* **8**, 248 (1940).

[6] D. D. Eley, *Trans. Faraday Soc.*, **36**, 500 (1940).

[7] Y. L. Sandler, *Can. J. Chem.*, in press.

[8] We define the "true" half-life as the measured half-life times the fraction of gas adsorbed. In case of charcoal in a static system generally the fraction adsorbed was practically equal to one, due to the large surface area of the coals.

[9] H. S. Taylor and A. Sherman, *J. Am. Chem. Soc.*, **53**, 1614 (1931).

[10] L. Farkas and H. Sachsse, *Z. physik. Chem.*, **B23**, 1 and 19 (1933).

[11] L. Farkas and Y. L. Sandler, *Trans. Faraday Soc.*, **35**, 337 (1939).

[12] The advantage in accuracy of this system compared with the usual cathetometer carrying the scale on its stem was kindly pointed out to me by Dr. J. A. Morrison.

[13] J. Kistemaker, *Physica*, **11**, 277 (1945).

[14] J. A. Morrison, J. M. Los and L. E. Drain, *Trans. Faraday Soc.*, **47**, 1023 (1951).

[15] S. Brunauer, P. H. Emmett and E. Teller, *J. Am. Chem. Soc.*, **60**, 309 (1938).

TABLE I

1 Catalyst	2 Temp., °K.	3 Pressure, mm.	4 Fraction H_2 adsorbed	5 Reacn. time, min.	6 u_t/u_0	7 τ, min.	8 τ_s, min.
$BaSO_4$	194	20 pH_2		760	0.810	2500	
	90	29.5 pH_2		69	.750	167	
				108	.630	162	
	90	18 pH_2	0.038	149	.480	137	5.2
				170	.423	137	
	90	20 oD_2		178	.700	345	
				257	.585	332	
TiO_2 I (blue)	193	18.5 pH_2		27.1	.317	16	
		32 pH_2		33.6	.280	18	
	195	26 $H_2 + D_2$		63		⩾700	
	90	7 pH_2	.88	1.67	.400	1.27	1.12
		9	.87	2.08	.387	1.53	1.33
		13	.86	2.00	.49	1.96	1.68
		23	.85	2.08	.603	2.87	2.43
	90	12 oD_2		2.08	.38	1.50	
		20		2.00	.55	2.33	
		25		2.00	.58	2.50	
TiO_2 II	90	6 pH_2	.93	4.4	.482	4.2	3.9
		20.5	.93	5.0	.593	6.7	6.2
O_2–TiO_2							
0.109 cc. O_2 (per 290 m.^{2})	90	6 pH_2	.93	2.17	.552	2.53	2.36
				4.13	.241	2.00	1.86
0.272 cc. O_2	90	6 pH_2	.93	1.56	.508	1.67	1.55
				2.60	.281	1.42	1.32
TiO_2 II (oxygen-poisoned)	90	5.5 pH_2	.93	9.50	.50	19	18
D_2O–TiO_2	90	40 pH_2		3.0	1.00		
		40	.085	855	0.922	~7300	~620
		40 oD_2		459	.946	~6800	
		13 pH_2	.085	740	.914	~6000	~510
O_2–D_2O–TiO_2							
0.150 cc. O_2 (0.24 mm.)	90	17.5 pH_2	.085	20.5	.572	25.6	2.13
				31.55	.402	24.1	
0.050 cc. O_2 (0.088 mm.)		19 pH_2	.085	33.5	.713	69	6.0
				45.7	.637	70	

had practically disappeared at the end of the heat treatment. The amount used was 3.42 g., the void space in the vessel was 8.84 cc.

$BaSO_4$ was obtained by precipitation in aqueous solution from $Ba(CH_3COO)_2$ and Na_2SO_4. Both substances contained 0.0002% Fe as the largest paramagnetic impurity. The powder was outgassed in the same manner as "TiO_2 I." 11.36 grams was used, leaving 5.19 cc. void space in the vessel.

"D_2O-TiO_2" was a coating of heavy ice on TiO_2. It was produced by distilling 0.56 cc. of D_2O onto the 3.42 g. of "TiO_2 I." This amount of water should produce a coverage of 7 to 10 layers. A small vessel containing the water was connected to the doser on the 3-way tap of the reaction vessel and the water was very carefully outgassed under repeated freezing and melting. Turning the 3-way tap, the D_2O was then distilled onto the powder, keeping the powder about 5° below the temperature of the water. Then, after admitting about 10 mm. helium to the vessel, the vessel was gradually cooled down to $-80°$ in the course of 8 hours. Twice in the course of this cooling process the bath temperature was slightly raised again to reverse the temperature gradient in the vessel; an ice film was so removed which had collected on the walls of the vessel. No visible ice film was found on the glass at $-80°$. The powder was then cooled to $-183°$ in a single step. The color of the powder remained blue.

The hydrogen contacted with the powders for rate measurements was 68% parahydrogen or 84% orthodeuterium. Analysis of the ortho–para composition was carried out by the Farkas micromethod.[4] Equilibrium hydrogen for calibrating the measuring cell was produced by allowing hydrogen to come to equilibrium over charcoal at the temperature of the experiment.

In the experiment in which the surface contained adsorbed oxygen, small amounts of oxygen must have been in the analyzed hydrogen. Separate tests showed that the possible concentration of oxygen in the hydrogen cannot have an effect on the determined hydrogen composition, nor can they cause an appreciable conversion in the gas phase during the time of an experiment.

Results

The results obtained with various types of surfaces are summarized in Table I. In column 3 the pressure and type of hydrogen contacted is given. In column 4 the fraction of adsorbed hydrogen is given (amount of hydrogen adsorbed N_s/total amount in the reaction vessel N). Column 5 gives the reaction time t after which the analysis of the hydrogen was made. The half-life τ of the conversion was evaluated assuming a perfect first order decay law

$$u_t = u_0 \exp\,[-kt]; \qquad \tau = \ln 2/k \tag{1}$$

Here u_t is the measured excess over the equilibrium concentration in the gas phase at the time t, and u_0 was taken to be the excess concentration of the gas before contact with the catalyst. The values of u_t/u_0 and τ are listed in columns 6 and 7 of the table. Column 8 gives the "true" half-life of the surface reaction $\tau_s = \tau N_s/N$.

No appreciable hydrogen–deuterium interchange took place in an H_2–D_2 mixture contacted with TiO_2I at 195°K. (see Table I, "TiO_2I," third row). This shows that no chemical mechanism is involved in the observed conversion at, and below, this temperature. The same is also indicated by the negative temperature coefficient[4] of the observed conversion rates with TiO_2 I and $BaSO_4$.

The conversion rates of orthodeuterium at 90°K. were found to be of the same order as the conversion rates of parahydrogen under the same conditions. A discussion of the relative conversion rates of hydrogen and deuterium for magnetic surface reactions will be given elsewhere.[7]

It was noticed in the course of the experiments with parahydrogen on TiO_2 at 90°K. that the assumptions made in equation 1 are not quite justified. The measurements taken after a relatively short contact time (larger values of u_t/u_0) yielded higher half-lives than the measurements taken after a longer time at the same pressure and temperature. The observed apparent deviations from a first-order decay law in this case are due to an increase of the para-concentration in the gas phase on contacting the gas with the surface, owing to a preferential adsorption of orthohydrogen. u_0 in equation 1 therefore should be larger than the admitted excess concentration. This effect is discussed in greater detail in the following paper.[16] As a consequence of a relatively large ortho–para separation effect with TiO_2, the observed pressure dependence of the half-life is the result of differences in u_t/u_0 as well as of the real reaction order. In all the other cases the separation effect should have little influence on τ as the fraction of adsorbed hydrogen (Table I, column 4) is small.

The true half-life τ_s for all measured powders at 90°K. is seen to be between 1 and 6 minutes. This is within the range of values also found with charcoals.[4] It thus seems reasonable to expect a similar mechanism in all these cases, *viz.*, a conversion through the existence of unpaired electrons in the surface.

In order to obtain information on the conversion rate to be expected from a certain concentration of paramagnetic particles on a surface, measured amounts of oxygen were adsorbed on TiO_2 II at 90°K. The results are given in Table I under "O_2–TiO_2." The rates are seen to be increased by the adsorbed oxygen. The same has been previously demonstrated with other surfaces.[4,17] It shows that the oxygen is adsorbed in molecular form. The observed increase in the rates of conversion remained practically unchanged after 10 hours, showing that dissociative adsorption at 90°K. is negligible. Deducting from the observed rates the conversion on the bare surface, we find from the given data that 1 cc. (STP) of O_2 per 290 square meter total surface ($= 1 \times 10^{17}$ molecules/m.^{2}) cause a true conversion half-life of about 30 seconds.[18]

On warming up the catalyst to room temperature most of the gas could be recovered. The same catalyst was then contacted with oxygen of 30 cm. pressure at room temperature for 10 minutes. After about 20 hours pumping the conversion half-life was again determined (see "TiO_2 II, oxygen poisoned," Table I). The true half life τ_s = 18 minutes is 4.5 times longer than the half-life prior to the oxygen adsorption. This poisoning effect of oxygen adsorbed at room temperature, in contrast to low temperature adsorbed oxygen, is again in agreement with previous results with charcoal and other surfaces. A few days' pumping at room temperature produced no measurable change in activity. It cannot be said on the basis of the present experiments whether the residual conversion found has any physical significance or whether it is due to impurities.

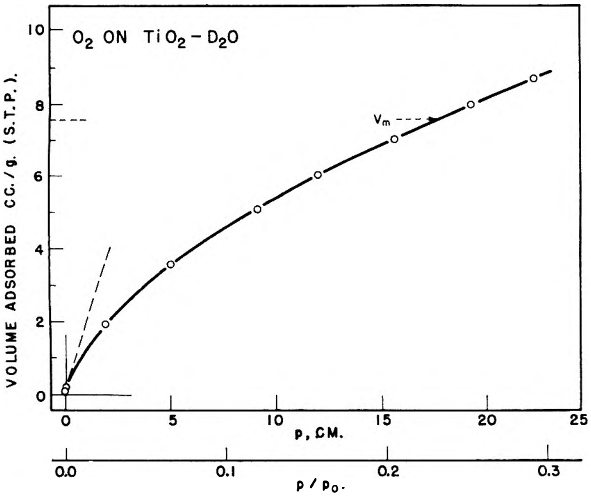

Fig. 1.—Adsorption isotherm of oxygen on the surface "D_2O–TiO_2" at 90.2°K.

In order to obtain some information on the conversion rate to be expected with a surface having no electronic paramagnetism, a coating of heavy ice[19] was deposited on the TiO_2 I (see Experimental section). In this way a very pure and large surface could be obtained requiring no heating. The results are given in Table I under "D_2O–TiO_2." The observed half-life was approximately 100 hours; this is about 300 times greater than with the poisoned TiO_2 surface. The adsorption isotherm for hydrogen on the surface "D_2O–TiO_2" was also measured; it was found to be linear up to 20 cm. pressure. The amount of hydrogen adsorbed at 2 cm. pressure was only 0.02 cc./g. (S.T.P.), which is 55 times less than the amount adsorbed on the bare TiO_2 I surface at the same temperature and pressure. The fraction of gas adsorbed, however, is smaller by only a factor 10. The true half life τ_s on the water surface then is between 500 and 600 minutes; this is still 30 times larger than the true half life with the poisoned TiO_2 surface.

On the same composite surface "D_2O-TiO_2" small measured amounts of oxygen were adsorbed at 90°K. to create once more a synthetic paramagnetic surface. The results are given in Table I under "O_2–D_2O–TiO_2." Neglecting a possible small change in surface area by the coating with D_2O, the true half life τ_s for 1 cc. O_2 on 290 m.^{2}, *i.e.*, for 10^{17} molecules O_2/m.^{2}, is 18 seconds. This is very near to the corresponding value of 30 seconds, previously found with TiO_2 II.

In order to make sure that the surface area of the powder was not considerably changed by distilling the D_2O onto the TiO_2, the adsorption isotherm was measured with oxygen at 90°K. The isotherm is shown in Fig. 1. A B.E.T. plot[15] of $p/v(p_0 - p)$ against the relative pressure p/p_0 (not shown here) gave a straight line between p/p_0 = 0.05 and 0.03. The oxygen volume corresponding to a monolayer V_m was found to be 25.49 cc. (7.45 cc./g.), as indicated in Fig. 1. With an assumed area per oxygen molecule of 14 Å.^{2}, this corresponds to a total area of 140 m.^{2}, which is one-half as large as the total area of the bare TiO_2 I. The constant "*c*"[15] found in this case was only 11. In such a case the B.E.T. method easily yields values too low by a factor 2 or 3. It appears that in any case there was no essential change of surface area by the distillation process.

When the powder vessel, still containing oxygen from the adsorption experiment, was allowed to warm up to room temperature a practically instantaneous change of color from blue to the original cream color took place. It should be noted that this is under practically the same conditions under which (with TiO_2 II) the decrease in the conversion rate was observed. The blue color of TiO_2 I had been stable at room temperature under vacuum.

Discussion

The experiments indicate that there is a common primary cause for both color and surface paramagnetism. This is indicated by the fast conversion obtained with blue TiO_2, as well as the disappearance of color and the decrease of the conversion rate on contact with oxygen at room temperature. The formation of color centers indicates the formation of lattice defects[20] which in the present case

---

(16) Y. L. Sandler, This Journal, **58**, 58 (1954).

(17) P. H. Emmett and R. W. Harkness, *J. Am. Chem. Soc.*, **57**, 1624 (1935).

(18) Here the half-lives found near $t = \tau/2(u_t/u_0 = 0.5)$ were used. It was taken into account that these values must then consistently be too high by a factor 1.37 due to the separation effect (ref. 16).

(19) D_2O was chosen instead of H_2O because of its smaller nuclear magnetic moment. The conversion rate due to this moment alone should be 1/16 as large as for H_2O as the rate is proportional to the square of the resultant magnetic moment. However, if other factors also influence the conversion, as discussed further below, the difference may not be large.

(20) *Cf.* Report of Conference on Conduction of Electricity in Solids, *Proc. Phys. Soc.* (*London*), **49**, 3 (1937).

should be due to a stoichiometric deficiency in oxygen produced by the heat treatment. The extra electrons left on the surface through removal of oxygen atoms are the source of the paramagnetism causing the increased conversion rate. The exact conditions for the appearance or non-appearance of the color are not clear. With TiO_2 I the blue color was obtained, with TiO_2 II (taken from the same stock) it was not. The difference is apparently not only connected with the difference in the maximum outgassing temperature but also with the difference in the whole heating history; this is indicated by the slight appearance and disappearance of colors during the heating of TiO_2 II.[21]

On the basis of the conversion rates found with adsorbed O_2 we may attempt to make an estimate of the concentration of paramagnetic centers. On TiO_2 II 1×10^{17} molecules O_2/m.^{2} caused a conversion half-life of $\tau_s = 30$ seconds (at 6 mm. H_2 pressure). Then $\tau_s = 3.9$ minutes, as found for the bare TiO_2 II surface at the same H_2 pressure, corresponds to 1.3×10^{16} O_2 molecules/m.^{2}; or to 3.5×10^{16} unpaired electrons/m.^{2} if a factor 8/3 is applied to allow for the difference in the square of the magnetic moment between O_2 and an electron. With an estimated 1×10^{19} Ti^{4+} ions per m.^{2} surface this represents about 0.3% paramagnetic defects. Magnetic susceptibility measurements[22] show that the extra-electrons in a slightly reduced TiO_2 are uncoupled. The paramagnetism can therefore be used as a measure for the number of extra-electrons. With TiO_2 I (blue) the percentage of defects would be about 3 times larger.

An uncertainty in this type of estimate with solid surfaces arises from a possible activation energy required for the diffusion of hydrogen in the surface to less approachable paramagnetic sites. The good agreement found for the two synthetic paramagnetic surfaces "O_2–TiO_2" and "O_2–D_2O–TiO_2" might be due to a relatively free approach of adsorbed hydrogen to the adsorbed oxygen. However, the presence of an activation energy does not necessarily lead to a decrease in the conversion rate. As pointed out elsewhere,[7] the effect on the observed rate of a decreased chance of approaching a site in the presence of a high energy barrier may be largely compensated and possibly even overcompensated by the effect of a longer time of contact with such a site.[23] It is difficult at present to give an estimate of the possible error involved until comparisons with other methods have been carried out. There are inherent difficulties in any method of estimating surface sites because what is to be considered as "surface" largely depends on the method of measurement and its purpose.

The "Residual Conversion" on "D_2O–TiO_2."—We may obtain information as to the possible nature of the conversion on the D_2O surface by a numerical comparison with the conversion obtained with adsorbed oxygen. A concentration of 1×10^{17} molecules/m.^{2} of O_2 was found to lead to a conversion half-life of 18 seconds. Roughly 2×10^{19} D_2O molecules should be exposed on 1 m.^{2} D_2O-surface; these cause a conversion half-life of 510 minutes (at the same H_2 pressure of 6 mm.). From this it follows that the conversion on the D_2O surface is about $1/(3 \times 10^5)$ as fast as the conversion by adsorbed oxygen, if reduced to the same concentration. On the other hand, for O_2 in aqueous solution[10] the conversion rate constant is 10.5 l. mole^{-1} min.$^{-1}$, while for liquid D_2O[11] the rate constant is 3.0×10^{-5}. This again gives a ratio of 3.5×10^5. The agreement once more indicates the possibility of using the parahydrogen conversion for estimating paramagnetic concentrations in surfaces, at least as far as their order of magnitude is concerned.

The conversion in liquid D_2O is only in part due to the nuclear magnetic moment of the deuterons. It has been shown[11] that there must be some other factor in diamagnetic liquids causing a conversion of similar order of magnitude. This factor may be the magnetic moment due to the rotation of the molecules of the liquid, or perhaps a moment induced in the collision process. Free rotation of the D_2O molecules on a surface at 90°K. is practically out of the question. Whether an induced moment could have caused part of the observed conversion on the solid surface, cannot be decided on the basis of the present experiments.

In this connection it would be interesting to extend the present measurements to other pure diamagnetic surfaces using the same technique of coating a powder of large surface with diamagnetic liquids. By measuring, for example, the conversion on a SO_2 surface, it should be possible to decide whether a measurable conversion due to induced moments may exist or not, because this surface would have no magnetic moments due to the nuclei or due to rotation. In the case that no appreciable conversion of hydrogen occurs due to induced moments, one would expect a much faster conversion of deuterium due to the electric dipole of SO_2,[24] because this electric type of conversion cannot exist with light hydrogen.

Acknowledgment.—The author is much indebted to the National Research Council of Canada for a postdoctorate fellowship.

---

[21] A very pure sample of titania of different origin gave no color when heated to about 800° *in vacuo*. The presence of foreign ions probably is a necessary condition for obtaining the blue color in titania by heating *in vacuo*.

[22] P. Ehrlich, *Z. Elektrochem.*, **45**, 362 (1939).

[23] An indication of this effect is found in the conversion in presence of paramagnetic gases in aqueous solution (L. Farkas and U. Garbatski, *Trans. Faraday Soc.*, **35**, 263 (1939)), where a similar "cage" effect is assumed to be operative. The conversion rate is almost the same as in the gas phase although slightly faster (*cf.* also ref. 7).

[24] Y. L. Sandler, *J. Chem. Phys.*, **20**, 1050 (1952).

THE ADSORPTION AND ORTHO-PARA CONVERSION OF HYDROGEN ON DIAMAGNETIC SOLIDS. II. THE RELATIVE ADSORBABILITIES OF ORTHOHYDROGEN AND PARAHYDROGEN

BY Y. L. SANDLER[1]

Division of Chemistry, National Research Laboratories, Ottawa, Canada

Received May 7, 1953

It is shown that orthohydrogen is more strongly adsorbed than parahydrogen when physically adsorbed on TiO_2 or charcoals. A separation factor of about 1.6 is observed with TiO_2 at −183°. The effect of the preferential adsorption on the kinetics of the ortho–para conversion is demonstrated. It may be obscured by a lag in the establishment of the adsorption equilibrium. The separation effect is explained as being principally due to hindered rotation.

In liquid and solid hydrogen the para-modification has a higher vapor pressure than the ortho-modification.[2] Ubbelohde[3] inferred from his experiments on the composition of hydrogen desorbed from charcoal at 90°K. that a similar effect may exist in case of adsorbed hydrogen. However, no reproducible results could be obtained by his technique. The ortho–para separation effect has so far generally been assumed to be too small to have an appreciable effect on the kinetics of the ortho–para conversion on solids or on the adsorption equilibrium. In the following some experiments are described which establish the existence and magnitude of the preferential adsorption of orthohydrogen in some cases.

The adsorption and conversion of ortho–para mixtures at low temperatures was studied with TiO_2 (rutile) and charcoals of high surface area. In these cases the observed conversion appears to be of the magnetic type[2b,4] involving adsorbed hydrogen molecules. Mainly two kinds of experiments were performed: (1) Kinetic experiments: if the establishment of the adsorption–desorption equilibrium is fast enough, a change of the gas phase composition is to be expected immediately after contacting the gas with the surface. (2) Equilibrium experiments: the gas was allowed to come to a complete ortho–para equilibrium in presence of the catalytic surfaces. It was then very rapidly desorbed and its composition determined.

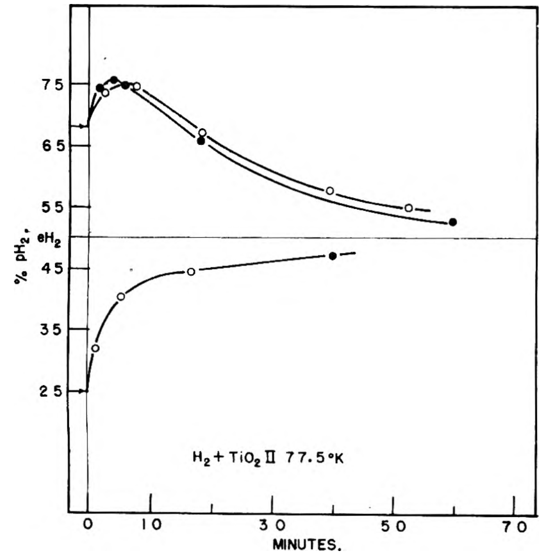

Fig. 1.—The conversion of 68% parahydrogen (upper curves) and normal hydrogen (lower curve) to equilibrium hydrogen on TiO_2 II at 77.5°K.

Experiments and Results

The ortho–para analysis was carried out by means of the Farkas micromethod.[2b] The stability of the cell was carefully checked before and during each experiment by alternate measurement of hydrogens of known concentration. The error of measurement of a given para concentration (in %) is less than 0.4. The experimental set-up for measuring the conversion and for the volumetric determinations was the same as described in the preceding paper.[4]

Materials.—3.42 grams of titanium dioxide (rutile) was used in a reaction vessel, leaving a void space of 8.84 cc. It was the same sample as used in the previous investigation ("TiO_2 II").[4] It had been carefully outgassed at 350°, and then had been contacted with oxygen at room temperature. By this latter treatment the conversion half-life at 90°K. increased by a factor 4.5. The adsorption isotherms at 77.5 and 90.2°K. were measured. These were taken with equilibrium hydrogen prepared by desorption from charcoal at the corresponding temperature. The isotherms were not linear; the isosteric heats decreased with coverage. At 5.0 cc. coverage (1.46 cc./g.; about 5×10^{-3} monolayers) the isosteric heat is about 2.1 kcal.

Maple wood charcoals and a sugar charcoal were carefully outgassed at 200°. With sugar charcoal a coverage of 6 cc. per gram of coal was used giving an equilibrium pressure of 1.3 mm. at 77.7°K. The heat of adsorption at this coverage was about 1.1 kcal./mole.

Kinetic Experiments.—In the lower section of Fig. 1 a typical conversion curve is shown obtained at 77.5°K. when contacting normal hydrogen (25% parahydrogen) with TiO_2. About 6.5 cc. (STP) was adsorbed, giving an equilibrium pressure of about 3.5 mm. The system was allowed to come to an approximate pressure equilibrium by leaving the tap of the reaction vessel open for about 20 seconds. After closing the tap, any subsequent changes in the adsorption equilibrium may have somewhat changed the equilibrium pressure in the vessel, but not the coverage, because practically all the gas in the reaction vessel was in the adsorbed phase (98% at equilibrium). In the present case, there seems to be no immediate change of the gas phase composition on contacting the gas with the surface. However, the relative rate of change of the gas composition appears greatly increased during the initial period of the conversion. The equilibrium concentration at the given temperature is 50.0% parahydrogen.[2b] The excess over this concentration sinks to one-half of its original value within the first 3.5 minutes; then it decreases again to half within about 8 minutes.

The effect of the ortho–para separation becomes much more striking when one observes the conversion in the reverse direction. Conversion and separation then act in opposite directions. In the upper part of Fig. 1 the results of two runs are plotted in which 68% parahydrogen was contacted with the surface, again for 6.5 cc. gas and 77.5°K.

---

(1) Laboratory for Insulation Research, Massachusetts Institute of Technology, Cambridge 39, Mass.

(2) (a) K. F. Bonhoeffer and P. Hartek, *Z. physik. Chem.*, **B4**, 113 (1929); (b) *cf.* A. Farkas, "Orthohydrogen, Parahydrogen and Heavy Hydrogen," Cambridge University Press, 1935.

(3) A. R. Ubbelohde, *Trans. Faraday Soc.*, **28**, 291 (1932).

(4) Y. L. Sandler, THIS JOURNAL, **58**, 54 (1954).

As the desorption of the gas at this temperature was rather slow, the previously adsorbed hydrogen was pumped off at a higher temperature and the reaction vessel was then cooled *in vacuo* to 77.5°K. This method of cooling probably was not quite effective. After admission of the parahydrogen from the measuring buret, the tap of the reaction vessel was left open for about 12 seconds to allow the pressure equilibrium to be approximately established. The curve marked by open circles was so obtained. Before the second run was made (full circles), the gas was pumped off as previously, but the powder was cooled in 1-2 mm. helium for 1 hour. The tap was left open for 20 seconds when contacting with the parahydrogen. The total depletion of the adsorbed gas through the successive amounts of gas withdrawn for analysis, was less than 1%. The curves are seen to rise to a maximum para concentration of about 75% (due to the separation effect), before falling off (due to the ortho-para conversion). There is a time lag of 4 to 6 minutes before the maximum separation is reached.

Similar experiments were performed at 90.2°K. To attain the temperature equilibrium of the powder, in this case the powder was first contacted with hydrogen which was then removed by pumping for half an hour. 2.7 cc. of 68% parahydrogen was adsorbed giving an equilibrium pressure of 5.5 mm. The results of two runs are shown in Fig. 2. Here log u_t/u_0 is plotted against time; u_t is the excess para concentration over the equilibrium para concentration in the gas phase at the time t, and u_0 is the excess concentration before contacting the gas with the powder. The points are seen to lie on a good straight line. There is no evidence for the existence of an initial lag, as observed at the lower temperature. In absence of a separation effect and a lag period for the establishment of the adsorption equilibrium, one would expect a straight line starting from log $u_t/u_0 = 0$ at $t = 0$. The equation of the found conversion curve is log $u_t/u_0 = -kt + 0.138$ with $k = \ln 2/\tau$ and half life $\tau = 13$ minutes. The initial concentration was 68%, the equilibrium concentration at 90.2°K. is 42.6%[2b]; from this the intercept at $t = 0$ is found to correspond to 77.5% parahydrogen.

The results are conveniently expressed in terms of a separation coefficient

$$s = (N_p/N_0)_{gas}/(N_p/N_0)_{ads} \quad (1)$$

where N_p and N_0 are the nunber of para and ortho molecules, respectively. s is a constant at constant temperature, if Henry's law is valid. In case of a non-linear isotherm, however, as found in the present case, s may be expected to vary somewhat with composition and coverage.

The para concentration of the adsorbed phase after contact was somewhat below the admitted para concentration of 68% due to the fact that in the present case only 93% of the gas was adsorbed. Allowing for this, we obtain from equation 1

$$s = (77.5/22.5)/(67.4/32.6) = 1.67$$

This value may be slightly too high, if any initial lag exists also in the present case. The lag must be shorter than 1.45 minutes, the time after which the first point on the curve was taken. From this point we find that s must be greater than 1.42.

In Fig. 3 is given a logarithmic plot of a conversion curve obtained with sugar charcoal when contacting normal hydrogen at 77.7°K. and 1.3 mm. pressure. There is no clear indication of a separation effect at zero time. However, the relative rate of change of the para concentration in the first two minutes is faster than later. It seems that we have here again a case similar to that described for TiO_2 (Fig. 1, lower curve), though less distinct. There appears to be a lag in the establishment of equilibrium which masks the separation effect.

Equilibrium Experiments.—In Table I the results of some experiments are summarized in which the equilibrium concentrations in the adsorbed phase at 90.2°K. were determined. A known amount of hydrogen in these experiments was first allowed to come to a complete ortho-para equilibrium. The adsorbed gas was then desorbed as rapidly as possible by connecting the powder vessel for a short measured time to an evacuated volume of 1 liter and by heating the vessel to room temperature. In some cases a pressure reading was taken by means of a gage[4] connected to the large volume; it was later compared with a second reading after desorbing the remaining gas completely. The relative amount desorbed during the experiment was so determined (last column, Table I). In column 8 of Table I the para concentration of the adsorbed gas is given; it is assumed to be equal to the composition of the collected gas, a small correction only being applied for the gas coming from the gas phase in the reaction vessel.

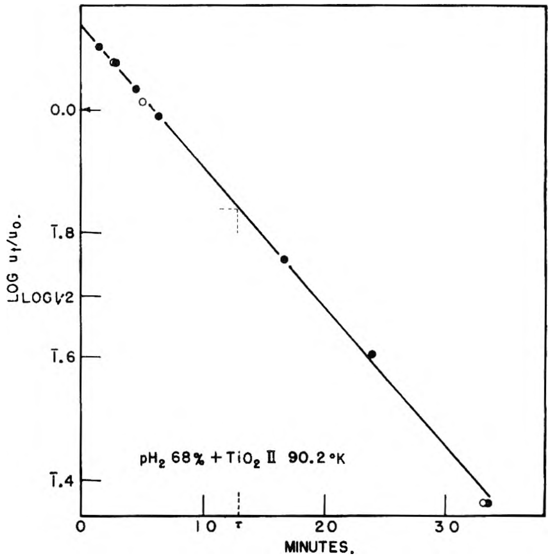

Fig. 2.—The conversion of 68% parahydrogen on TiO_2 II at 90.2°K.

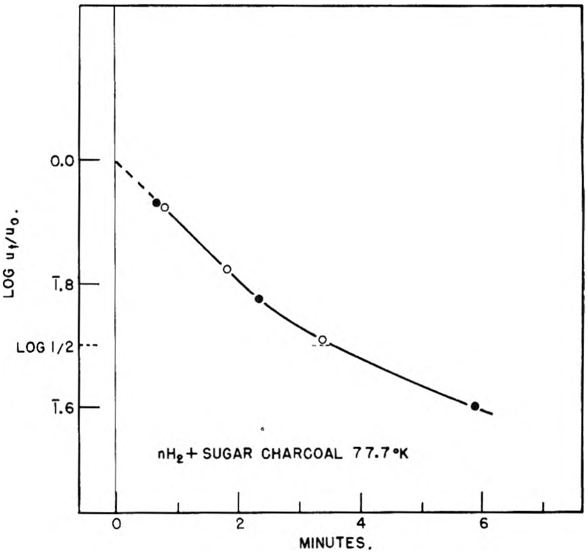

Fig. 3.—The conversion of normal hydrogen on sugar charcoal at 77.7°K.

The value $s = 1.30$ found for TiO_2 (Table I, row 1) is lower than the value 1.67 found in the corresponding kinetic experiment. This should be largely due to the incompleteness of the desorption. As the free energy of desorption for parahydrogen is smaller than for orthohydrogen, it might be expected that the former desorbs faster than the latter.

The following qualitative experiment showed that this actually is the case. The admitted gas was first allowed to equilibrate on the powder at 90°K. Then part of the adsorbed gas was withdrawn by connecting the reaction vessel (this time remaining at the low temperature) to evacuated volumes of varying size for a short time. A sample of the gas in contact with the powder was then rapidly withdrawn for analysis. It was found that the larger the amount of gas rejected before taking the sample for measurement, the lower was the para concentration in the measured hydrogen. This proves the faster desorption of parahydrogen. The lower value of s found on incomplete desorption is thus explained.

TABLE I

Catalyst	Temp., °K.	Equilibr. pressure, mm.	H_2 adsorbed, %	Conversion half-life, min.	Desorption time, sec.	Para concentration, % Gas phase	Para concentration, % Adsorbed phase	Separation factor, s	Remarks
TiO_2	90.2	5.5	93	13	15	42.6	36.4	1.30	Only 76% desorbed
Maple wood charcoal	77.5	~50	~100	14	~15	50.0	47.3	1.1	Desorption incomplete
	77.5	1.5	~100	6	~15	50.0	47.7	1.1	
Sugar charcoal	77.7	1.35	~100	>3	3	50.0	47.0	1.13	
	77.7	1.35	~100	>3	6	50.0	46.4	1.16	99.4% desorbed

In rows 2 and 3 of Table I the results of equilibrium experiments with a maple wood charcoal are given. This charcoal had been previously used for producing parahydrogen by the static method.[2b] It had been noticed with this and other charcoals that the gas obtained after rapid desorption always had a para concentration somewhat lower than the corresponding equilibrium concentration in the gas phase, even if the conversion half-life was as long as in the present case. The separation factor is seen to be of the order of 1.1 at 77°K. for the charcoals investigated here.

The experiments with the sugar charcoal were carried out under better controlled conditions. 0.273 gram of coal was placed in a very thin-walled vessel of only 3.5 mm. diameter thus ensuring a rapid heat transfer on desorption. Desorption was carried out by dipping the vessel into an alcohol-bath at room temperature. 1.63 cc. (S.T.P.) of hydrogen was adsorbed at 77.7°K. giving an equilibrium pressure of 1.35 mm. As seen from the data in Table I, desorption was practically complete after 6 seconds. The error of measurement in the para percentage was less than 0.2.

The time of desorption was small compared with the conversion half life; also the major part of the gas was desorbed in an even shorter time. It therefore is improbable that the reconversion due to the warming up of the catalyst had an appreciable effect on the observed para concentration. However, the possibility of a certain influence of this effect on the obtained value of s cannot be completely excluded.

The results obtained with charcoal are much less striking then the results with TiO_2, and the conclusions are less certain. In view of the similarity of the observed phenomena the interpretation of the measurements with charcoal is probably correct.

Discussion

The observed initial time lag in some of the kinetic experiments cannot be due to slowness of the diffusion in the gas phase. This is seen when comparing the conversion curves for TiO_2 at 77.5°K. and 90.2°K. (Figs. 1 and 2). The time required for the establishment of the equilibrium is much shorter at 90° although the pressure is higher. The observed lag indicates that the rate of ad- and desorption is fast at 90°K. but becomes comparable with the conversion rate at 77°K. The rapid change of the lag period with temperature indicates the existence of high barriers to migration of the gas in the surface. The values $s = 1.67$ found for TiO_2 at 90°K. may still be assumed to be roughly equal to the true equilibrium value.

We would suggest that the observed preferential adsorption of orthohydrogen is largely due to hindered rotation of the adsorbed hydrogen. However, there may be other contributing factors[3,5] such as a greater polarizability of a rotating molecule as compared with a non-rotating one (parahydrogen in the lowest rotational state).

We shall estimate the order of magnitude of the influence of hindered rotation on s by assuming that the hydrogen in the surface can be approximated by a plane rotator.

Then solely on the basis of a change in the rotational states, *i.e.*, neglecting the interaction with vibrations and the influence of configurational effects—we expect a separation factor given by

$$s = (f_p/f_0)_{gas}/(f_p/f_0)_{ads}$$

where f_p and f_0 are the rotational partitional functions of parahydrogen and orthohydrogen, respectively.

We consider here the ground states only. At 90°K. this leads to a value for s only 3% different from the value found when taking the complete functions.

Then $(f_p/f_0)_{gas} = 1/(9 \exp [-\epsilon_1/kT])$,[2b] where $\epsilon_1 = 338$ cal./mole is the energy difference between the rotational states in the gas phase with $j = 0$ and $j = 1$. In the adsorbed phase $(f_p/f_0)_{ads} = 1/(6 \exp [-\epsilon_1/2kT])$.[6]

Therefore $s = {}^2/_3 \exp [\epsilon_1/2kT]$. At 90°K. this leads to $s = 1.7$, which is of the correct order of magnitude.

Similarly, assuming that the partition function of the resulting oscillation is = 1, a completely hindered rotation in the surface would lead to $s = {}^1/_3 \exp [\epsilon_1/kT] = 2.2$ at 90°K.

In view of the difference in adsorbability of the two modifications, the adsorption isotherm of hydrogen will somewhat depend on its composition. The difference in adsorption found for orthohydrogen and parahydrogen on charcoal seems to be of the same order as the difference found for hydrogen and deuterium[7]; it may be greater in other cases. In order to avoid a change in composition by conversion in the course of an adsorption experiment, it may be the simplest procedure to use hydrogen previously equilibrated at the same temperature.[8]

The present experiments suggest the use of the

---

(5) K. Cohen and H. C. Urey, *J. Chem. Phys.*, **7**, 157 (1939).

(6) The partition function of a "2-dimensional parahydrogen" according to the plane rotator model would be (*cf.* H. Eyring, J. Walter and G. E. Kimball, "Quantum Chemistry," John Wiley and Sons, New York, N. Y., 1944, p. 75)

$$f_p = 1 + 2 \sum^{m} \exp [-m^2\epsilon'/kT] \text{ with } m = 2, 4, 6 \ldots$$

similarly, including a factor 3 for the nuclear spin degeneracy of orthohydrogen

$$f_0 = 6 \sum^{m} \exp [-m^2\epsilon'/kT] \text{ with } m = 1, 3, 5 \ldots$$

$\epsilon' = \epsilon_1/2$.

(7) W. v. Dingenen and A. v. Itterbeck, *Physica*, **6**, 49 (1939).

(8) This procedure is not quite correct as the equilibrium composition required depends on the value of s of the adsorbent and the fraction of gas adsorbed. In most cases, however, this will cause errors beyond the usual accuracy of adsorption experiments.

separation effect for preparing orthohydrogen or paradeuterium. The method should be considerably simpler and more efficient than the fractional distillation of liquid hydrogen. These modifications are at equilibrium at no temperature in the gas phase in concentrations greater than 75% (orthohydrogen) and $33^{1}/_{3}\%$ (paradeuterium), and they have so far not been prepared in pure form.

Acknowledgment.—The author is much indebted to the National Research Council of Canada for a postdoctorate fellowship.

INFRARED SPECTRA OF ALUMINUM SOAPS AND SOAP–HYDROCARBON GELS[1]

BY FREDERICK A. SCOTT, JEROME GOLDENSON, STEPHEN E. WIBERLEY AND WALTER H. BAUER

Contribution from the Walker Laboratory of Rensselaer Polytechnic Institute and Chemical Corps Chemical and Radiological Laboratory

Received May 14, 1953

Comparison of the infrared spectra of aluminum hydroxylaurate and aluminum deuteroxylaurate, and the spectra of aluminum hydroxy-2-ethyl-hexanoate and aluminum deuteroxy-2-ethyl-hexanoate showed that absorption at 2.7 μ in aluminum hydroxy soaps, ascribed to free OH, is replaced by absorption at 3.67 μ in aluminum deuteroxy soaps, the spectra of soaps of the corresponding acid being otherwise similar. Absorption at 10.14μ in aluminum soaps was shifted to 10.24μ for gallium laurate and to 10.31μ for indium laurate. The spectra were otherwise similar, except for small shifts in the 6.33μ absorption band of aluminum soaps. Absorption at 10.14μ in aluminum soaps was ascribed to the aluminum–oxygen linkage. When infrared absorption at 2.7μ is shown by aluminum soaps, it occurs also in the aluminum soap–cyclohexane gels, indicating that gelation is independent of bonded hydroxyl. Intensity of absorption at 10.14μ for a series of gels of constant concentration of aluminum dilaurate in benzene was found to decrease with the amount of added *m*-cresol, showing that modification of the bond in aluminum soaps causing absorption at 10.14μ is associated with loss in viscosity of gels caused by cresols.

Introduction

It has been suggested by Alexander and Gray[2,3] that aluminum soaps are made up of linked aluminum–oxygen octahedra with fatty acid chains extended from the main chain, two carbonyl groups occupying four of the coördinating positions while the two remaining positions contain hydroxyl ions, shared to form a chain. McGee[4] has pointed out that such a structure yields polymer chains which must end in charged groups. He has proposed that the adjacent disoap chains are held together by both van der Waals forces between the hydrocarbon chains and by hydrogen bonds between the hydrogen of the shared hydroxyl ions and the oxygen atoms of the carboxyl groups. In contradiction with this proposal, infrared absorption measurements[5] have shown that aluminum disoaps have a free hydroxyl group. McRoberts and Shulman[6] proposed a structure of aluminum disoaps similar to that of Gray and Alexander, and assumed that aluminum soap–hydrocarbon gels are made up of a dispersion of large soap molecules held together by hydroxyl bonds and van der Waals attraction of long hydrocarbon chains.

In view of the theories outlined, it appeared important to investigate further the assignment of absorption at 2.7 μ in aluminum disoaps to free hydroxyl,[5] and to compare the infrared absorption of aluminum disoaps and their corresponding spectra in soap–hydrocarbon gels. Since infrared absorption at 3.67 μ has been ascribed to the presence of the free deuteroxy group,[7] the preparation of aluminum deuteroxy soaps was undertaken for comparison with aluminum hydroxy soaps of corresponding fatty acids. Gallium and indium soaps were prepared from lauric acid with the expectation that a study of their infrared spectra, together with that of aluminum laurate, would aid in identifying the group contributing to the absorption at 10.14 μ, which has been shown to be characteristic of aluminum soaps. A study of the viscosities of a series of aluminum soap gels of fixed soap concentration in toluene containing *m*-cresol showed progressive weakening of the gel structure as the amount of *m*-cresol present increased.[8] An investigation of the infrared absorption spectra of such a series was made, in an attempt to identify the aluminum soap bonds causing gelation from the changes in the infrared absorption as the gel structure was modified.

Experimental

Fatty Acids.—Stearic and palmitic acids were purified by repeated recrystallizations. Lauric and myristic acids were Eastman Kodak, White Label grade. The 2-ethylhexanoic acid was Eastman Kodak, Yellow Label grade. It was treated by saponification, benzene extraction of non-saponifiable matter, conversion to the acid, and fractional distillation at 5 mm. pressure. Purity of the acids was checked by determination of the melting point, neutralization equivalent, long spacings found from pinhole X-ray diffraction measurements, analysis of the silver salts and the long spacings found by X-ray diffraction measurements on the silver salts. The results are shown in Table I. The powder X-ray diffraction patterns were obtained with a General Electric XRD-3 instrument using copper K_α radiation.

Preparation and Analyses of Soaps.—Aluminum hydroxy soaps were prepared by addition of aluminum sulfate solu-

---

[1] Study conducted under contract between the Chemical Corps, U. S. Army and Rensselaer Polytechnic Institute.

[2] A. E. Alexander and V. R. Gray, *Proc. Roy. Soc.* (*London*), **200**, 165 (1950).

[3] V. R. Gray, *Trans. Faraday Soc.*, **42B**, 197 (1946).

[4] C. G. McGee, *J. Am. Chem. Soc.*, **71**, 278 (1949).

[5] W. W. Harple, S. E. Wiberley and W. H. Bauer, *Anal. Chem.*, **24**, 635 (1952).

[6] T. S. McRoberts and J. H. Shulman, *Nature*, **162**, 101 (1948).

[7] Herzberg, "Infrared and Raman Spectra of Polyatomic Molecules," D. Van Nostrand Co., Inc., New York, N. Y., 1947, p. 335.

[8] H. Jackson, Ph.D. Dissertation, Rensselaer Polytechnic Institute, 1951.

TABLE I

PHYSICAL CONSTANTS OF FATTY ACIDS AND SILVER SALTS

							Silver salt			
	M.p., °C.		Neut. equiv.		Long spacing, Å.		Silver, %		Long spacing, Å.	
Acid	Found	Lit.	Found	Theory	Found	Lit.	Found	Theory	Found	Lit.
Stearic	69.8	69.6[b]	283.2	284.5	39.3	39.7[c]	27.67	27.51	49.0	48.8[a]
Palmitic	63.2	63.1[b]	256.5	256.4	36.1	35.6[c]	29.63	29.70	44.7	42.2[a]
Myristic	54.6	53.9[b]	226.5	228.4	31.5	31.6[c]	32.35	32.18	39.2	39.0[a]
Lauric	43.8	44.2[b]	201.7	200.3	28.1	27.4	35.15	35.15	34.2	34.1[a]
2-Ethylhexanoic (α-ethylcaproic)			144.3	144.2	..	..	...	...	..	..

[a] Matthews, Warren and Michell, *Anal. Chem.*, **22**, 514 (1950).
[b] Markley, "Fatty Acids," Interscience Publishing Co., New York, N. Y., 1947, p. 114.
[c] Frances and Piper, *J. Am. Chem. Soc.*, **61**, 577 (1939).

tion to a solution of the sodium soap of the appropriate fatty acid. The soaps were washed with water until the filtrate was free from sulfate, after which they were dried for 24 hours in a forced draft oven at 65°. Soaps were dried over phosphorus pentoxide at 20° for a minimum of seven days before measurement. The dried soaps were analyzed for aluminum by ignition to the oxide. To determine the extractable free fatty acid content, samples of the aluminum soaps were extracted with anhydrous isoöctane at 0°. Characteristics of the aluminum hydroxy soaps prepared are shown in Table II.

TABLE II

PREPARATION AND ANALYSIS OF ALUMINUM DISOAPS

Acid	NaOH in excess in sodium soap soln., mole %	Al, wt. %	Mole acid per mole Al calcd. from Al analyses	Mole acid per mole Al extractable
Stearic	45	4.42	2.01	0.0
Palmitic	45	4.87	2.00	.1
Myristic	45	5.33	2.03	.0
Lauric	45	6.05	2.03	.05
2-Ethylhexanoic	35	8.03	2.04	..

In the preparation of aluminum deuteroxylaurate, sodium was allowed to react with an excess of 99.8% D$_2$O. The solution was used to react with dry lauric acid to form a sodium laurate solution in D$_2$O. Aluminum deuteroxy laurate was precipitated from the sodium laurate solution upon addition of a solution of aluminum sulfate in D$_2$O. The aluminum soap was washed with D$_2$O and dried over phosphorus pentoxide.

Aluminum deuteroxylaurate and aluminum deuteroxy-2-ethylhexanoate also were prepared by a non-aqueous method similar to that described by Alexander and Gray.[2] Aluminum s-butoxide was allowed to react with lauric acid to form *s*-butyl alcohol and an intermediate. To prevent isotope exchange during deuterolysis, the alcohol was removed by distillation at 0.005 mm. pressure. The intermediate was allowed to react with an excess of D$_2$O. After the reaction was complete, the alcohol and D$_2$O present were removed by distillation at 0.005 mm. Aluminum deuteroxy-2-ethylhexanoate was prepared by a similar method.

Gallium and indium sulfates were prepared by the method of Frechi and Blenchi[9] from the metal. Solutions of the gallium and indium sulfates were used to prepare laurate soaps by the aqueous method described for aluminum soaps. Analyses for gallium and indium were made by direct ignition.

The compositions of the deuteroxy and gallium and indium soaps are shown in Table III.

Preparation of Gels.—Gels were prepared from soap and anhydrous solvent by agitation in a sealed container until settling of the soap no longer occurred. The gels were then transferred to aluminum aging tubes, sealed, aged for 24 hours at 55° and stored at 20°.

Determination of Infrared Spectra.—Infrared absorption spectra were determined with a Perkin–Elmer, Model 12-B, recording spectrometer at a temperature of 20° and a relative humidity of 25%. A rock salt prism was used except in the 2 to 6 μ region where a lithium fluoride prism was used to obtain greater dispersion. The soaps were studied dispersed as mulls in Nujol or in perfluorokerosene. In some cases the spectrum of the pure soap in sheeted form was compared with the spectrum of the soap in Nujol mull, and agreement was found. The gels were made with cyclohexane as a solvent because of the relative simplicity of its absorption spectrum. For the quantitative measurements, cells of 0.010 mm. fixed thickness were filled with gel from a glass syringe. The total absorbance[10] reading (0% transmittance) was set with a lithium fluoride shutter in the optical path. The zero absorbance reading (100% transmittance) was set with cyclohexane in the optical path by adjusting the slit width to give full scale deflection on the logarithmic recorder paper.

TABLE III

COMPOSITION OF SOAPS

Soaps	Metal, wt. %	Calcd. moles acid per mole of metal
Aluminum deuteroxylaurate (aqueous)	6.39	1.96
Aluminum deuteroxylaurate (non-aqueous)	4.92	2.59
Aluminum deuteroxy-2-ethylhexanoate (non-aqueous)	6.29	2.19
Gallium laurate	24.9	1.42
Indium laurate	25.7	1.56

Results and Discussion

The infrared absorption spectra of the aluminum disoaps listed in Table I were determined. Typical of the spectra are strong absorption bands at 2.7, 6.3 and 10.14 μ. The band at 2.7 μ has been assigned to a free OH group, the band at 6.3 μ to the —C=O stretching vibration in the carboxylate group, and the band at 10.14 μ to an Al–O linkage.[5] Spectra were also obtained for gels containing one mole per cent. of the same soaps in cyclohexane. It was found that the spectrum of each gel showed no marked difference from that of the corresponding soap and the solvent. In particular, it was found that the absorption band at 2.7 μ, characteristic of a free OH group, appeared unchanged in the spectra of the gels. This indicates that the formation of aluminum soap–hydrocarbon gels is not dependent upon hydrogen bonding involving the free OH group.

The infrared spectra of the aluminum deuteroxy soaps prepared from lauric acid and from 2-ethylhexanoic acid are shown in Figs. 1 and 2. For comparison, the absorption spectra of the corresponding aluminum hydroxy disoaps have been included. A new absorption band at 3.67 μ is present in the spectra of the aluminum deuteroxy soaps (in which the hydrogen in the hydroxyl of aluminum hydroxy soaps has been replaced by deuterium) and absorption at 2.7 μ has been greatly re-

---

(9) R. Frechi and W. Blenchi, *Z. anorg. Chem.*, **143**, 183 (1925).

(10) Nomenclature recommended by Hughes, *et al.*, *Anal. Chem.*, **24**, 1349 (1952).

duced in intensity. The absorption at 3.67 μ occurs at nearly the wave length as does the free OD absorption in heavy methanol vapor, listed by Herzberg,[7] 3.67 μ.

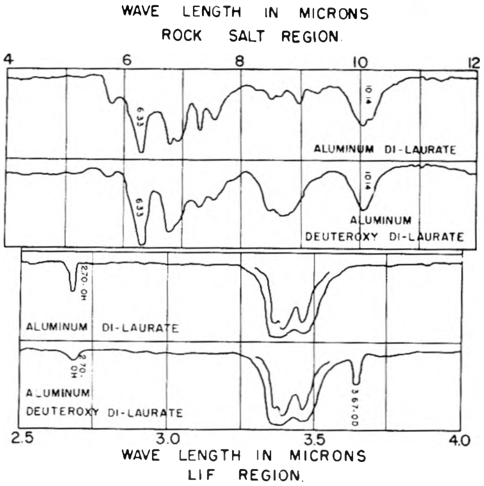

Fig. 1.—Comparison of spectra of aluminum dilaurate and aluminum deuteroxy dilaurate.

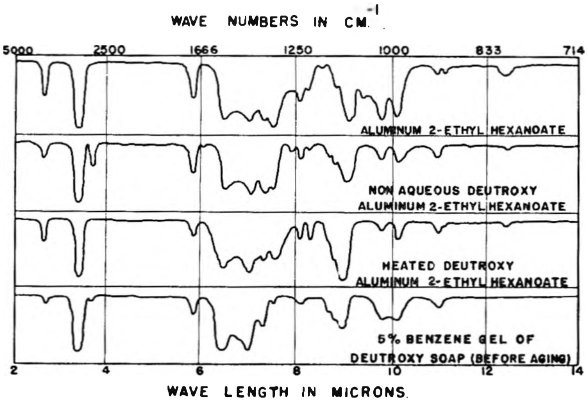

Fig. 2.—Comparison of spectra of aluminum hydroxy 2-ethylhexanoate and aluminum deuteroxy 2-ethylhexanoate. Effect of heating and gelation on spectra of deuteroxy soaps.

Since isotope exchange should be possible between the deuterium of the OD group and the adjacent hydrogens of the fatty acid chain, a sample of aluminum deuteroxy-2-ethylhexanoate was heated, and the infrared absorption spectrum was determined. It was found, as shown in Fig. 1, that the absorption at 3.67 μ had disappeared and that absorption at 2.7 μ was enhanced in the spectrum of the heated soap, indicating that exchange had taken place. Similar results were found when the spectrum of a sample of heated aluminum deuteroxy laurate was examined. The assignment of absorption at 2.7 μ in the aluminum hydroxy soaps to free hydroxyl is thus further confirmed.

Because the strong band at 10.14 μ shown in the spectrum of aluminum hydroxy soaps occurs unshifted in the spectrum of the deuteroxy soaps, it is concluded that this band is not associated with the presence of OH or OD groups. If the 10.14 μ band is to be ascribed to the metal–oxygen linkage in the soaps, a shift to lower frequencies would be expected if gallium and indium were substituted for aluminum. The infrared absorption spectra found for gallium and indium laurates are shown in Fig. 3, with the spectrum of aluminum laurate for comparison.

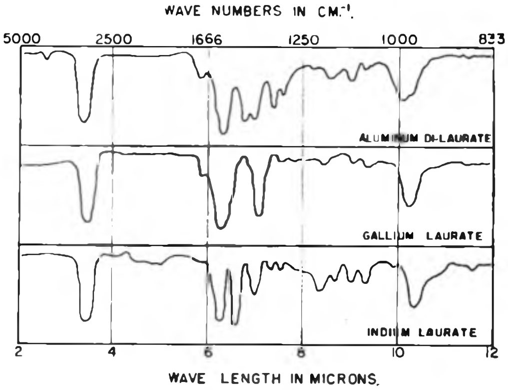

Fig. 3.—Comparison of spectra of aluminum, gallium and indium soaps.

Absorption at 10.14 μ is not shown by the gallium and indium laurates, but a band is found at 10.24 μ for gallium laurate and at 10.31 μ for indium laurate. The shift in the 10.14 μ band is in the direction to be expected if the absorption is due to the metal–oxygen linkage, and the band is accordingly ascribed to that group.

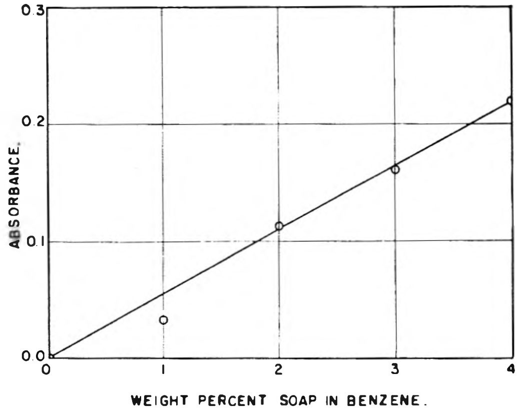

Fig. 4.—Plot of weight per cent. aluminum dilaurate soap in benzene *versus* absorbance at 10.14 μ.

A study was made of the intensity of absorption at 10.14 μ for aluminum dilaurate–benzene gels of various concentrations. The absorbance of 0.01 mm. section of each of the gels was measured at

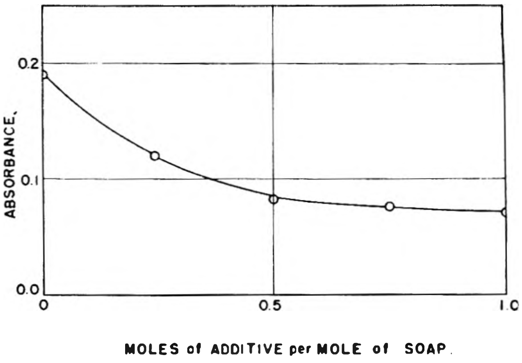

Fig. 5.—Plot of moles of cresol per mole of aluminum dilaurate in benzene *versus* absorbance at 10.14 μ. Concentration of soap was 5% by weight (approximately 0.01 mole fraction in each case.

10.14 μ. The results are shown in Fig. 4, in which are plotted absorbancies at various concentrations of soap in benzene. The absorbance furnishes a sensitive test for concentration of the aluminum soap, and would be useful in testing for uniformity in a gel.

The highly viscous character of gels of aluminum soaps in hydrocarbons has been attributed to the presence of large molecules, which are formed by bonding occurring between the aluminum carboxyl groups in the soap molecules. It has been found[8] that the viscosity of aluminum soap–hydrocarbon gels of fixed soap concentration is lowered progressively when small amounts of *m*-cresol are added to the solvent, reaching a limiting value at a *m*-cresol to soap mole ratio of two. A series of gels, each containing 5% by weight (approximately 0.01 mole per cent.) of aluminum dilaurate, was prepared by dissolving the soap in benzene solutions containing varying amounts of *m*-cresol. After aging for 24 hours at 60° and cooling to 20°, the absorbance of each gel at 10.14 μ was measured. The absorbance was found to decrease rapidly as the ratio of *m*-cresol to soap increased, approaching a limiting value, as shown in Fig. 5. It thus appears that the bond in aluminum laurate associated with absorption at 10.14 μ is directly connected with the gelling power of the soap for benzene.

SOME PHYSICAL PROPERTIES OF THE POLYMORPHIC FORMS OF 1,2-DIACETO-3-STEARIN AND 1-ACETO-3-STEARIN[1]

By E. J. Vicknair, W. S. Singleton and R. O. Feuge

Southern Regional Research Laboratory,[2] New Orleans, Louisiana

Received June 1, 1953

Fatty products containing the triglyceride 1,2-diaceto-3-stearin and the diglyceride 1-aceto-3-stearin are unusual in that they are quite plastic and stretchable. In the present investigation each of the two glycerides was prepared, purified and examined dilatometrically over the temperature range of −17 to 60°. Expansibilities, melting dilations and temperatures at which polymorphic transitions occurred were determined from the dilatometric curves obtained. X-Ray data for all polymorphic forms of each glyceride were obtained and crystal spacings were calculated. Photomicrographs of two forms of each glyceride were made.

A review of the chemical literature reveals a dearth of information on the physical properties of di- and triglycerides containing one *n*-saturated fatty acid radical having 14 to 18 carbon atoms and either one or two *n*-saturated fatty acid radicals having two to six carbon atoms. The optical activity and refractive index of several compounds falling into this class have been reported[3-5] and Jones, *et al.*,[6] reported the melting point of 1,2-diaceto-3-palmitin. With the exception of information released recently by this Laboratory[7,8] these few data comprise the only published information on compounds of this type.

It was discovered in this Laboratory that fatty products containing the triglyceride, 1,2-diaceto-3-stearin and the diglyceride 1-aceto-3-stearin are unusual in that they are non-greasy solids possessing a relatively large amount of plasticity and stretchability. Because these fatty products appear to have practical use, additional information concerning the physical properties of the two acetoglycerides was deemed desirable.

In the present investigation 1,2-diaceto-3-stearin and 1-aceto-3-stearin were prepared, purified and examined dilatometrically over the temperature range of −17 to 60°. Expansibilities, melting dilations and temperatures at which polymorphic transitions occurred were determined from the dilatometric curves obtained. By means of X-ray data, the interplanar spacings of three polymorphic forms for each glyceride were calculated.

Experimental

Preparation of Materials.—Both 1,2-diaceto-3-stearin and 1-aceto-3-stearin were prepared by the direct esterification of 1-monostearin with acetyl chloride, using a modification of the procedure of Malkin, *et al.*[9] The 1-monostearin employed was prepared as described in a previous publication.[10] Its purity analyzed 99.4% by the periodic acid oxidation method.[11]

The 1,2-diaceto-3-stearin was prepared by the dropwise addition with stirring of 30.3 g. (0.39 mole) of acetyl chloride in 50 g. of chloroform to a solution of 53.8 g. (0.15 mole) of 1-monostearin in a mixture of 34.0 g. (0.43 mole) of pyridine and 200 g. of chloroform at room temperature. An excess of acetyl chloride was used to ensure complete esterification. The mixture was allowed to stand at room temperature (26°) for two days and then was taken up in 250 ml. of ethyl ether and washed successively with cold 0.25 *N* hydrochloric acid, 5% potassium bicarbonate solution and water. The solvents were removed by stripping with dry nitrogen under reduced pressure, and the product then was crystallized 7 times from acetone (1:8) at −18° and dried over phosphorus pentoxide.

Anal. Calcd. for $C_{25}H_{46}O_6$: C, 67.84; H, 10.48. Found: C, 67.99; H, 10.61; m.p. 48.6°.

The 1-aceto-3-stearin was prepared by the slow addition of 16.3 g. (0.21 mole) of acetyl chloride in 125 g. of chloro-

---

(1) Presented at the 8th Southwest Regional Meeting of the American Chemical Society, Little Rock, Arkansas, December 4-6, 1952.

(2) One of the laboratories of the Bureau of Agricultural and Industrial Chemistry, Agricultural Research Administration, U. S. Department of Agriculture.

(3) Emil Abderhalden and Egon Eichwald, *Ber.*, **48**, 1862 (1915).

(4) Emil Abderhalden and Arthur Weil, *Fermentforschung*, **4**, 76 (1920), through *Chem. Zentr.*, **91**, III, 643 (1920).

(5) George Stafford Whitby, *J. Chem. Soc.*, 1458 (1926).

(6) Mary Ellen Jones, F. C. Koch, Arthur E. Heath and Paul L. Munsen, *J. Biol. Chem.*, **181**, 755 (1949).

(7) R. O. Feuge, E. J. Vicknair and N. V. Lovegren, *J. Am. Oil Chemists' Soc.*, **29**, 11 (1952).

(8) R. O. Feuge, E. J. Vicknair and N. V. Lovegren, "Modification of Vegetable Oils. XIII. Some Additional Properties of Acetostearins," paper presented at the 43rd Annual Meeting of the Am. Oil Chemists' Soc., Houston, Texas, April 28-30, 1952.

(9) T. Malkin, M. R. el Shurbagy and M. L. Meara, *J. Chem. Soc.*, 1409 (1937).

(10) W. S. Singleton and E. J. Vicknair, *J. Am. Oil Chemists' Soc.*, **28**, 342 (1951).

(11) E. Handschumaker and L. Linteris, *ibid.*, **24**, 143 (1947).

form to a solution of 79.5 g. (0.22 mole) of 1-monostearin in a mixture of 49.2 g. (0.62 mole) of pyridine and 537 g. of chloroform. The mixture was refluxed on a steam-cone for 3 hours under anhydrous conditions, then was taken up in 1500 ml. of ethyl ether and washed successively with cold 0.5 *N* sulfuric acid, 5% solution of sodium bicarbonate, and water. The solvents were removed by stripping with dry nitrogen under reduced pressure. A solution of the product in 1500 ml. of hexane was cooled to room temperature and filtered. The filtrate was further cooled to −15°, and the crystallized 1-aceto-3-stearin was recovered and purified by recrystallization from hexane and from acetone.

Anal. Calcd. for $C_{23}H_{44}O_5$: C, 68.96; H, 11.20; hydroxyl value, 140. Found: C, 69.04; H, 11.19; hydroxyl value, 142; m.p. 50.3°.

Heating and cooling curves obtained by Smit's procedure[12] indicated that both of the final products were of high purity.

Expansibility.—The expansibilities of the solid and liquid states of 1,2-diaceto-3-stearin and 1-aceto-3-stearin were determined with gravimetric-type dilatometers. Melting dilations of the various polymorphic forms were calculated by the method reported in previous publications.[13] Dilation measurements on all samples were begun at −17°, at which temperature only the solid state existed, and were continued until the samples were completely melted.

Densities of the acetostearins were determined by the pycnometer method.

X-Ray Diffraction.—X-Ray diffraction patterns of the lower-melting polymorphic forms of the two glycerides were obtained by photographing the samples after solidification in capillary tubes. In each case the freshly prepared form was aligned on the camera mount while it was in a large cooler maintained at −10°, and the mounted sample was kept in an insulated box cooled to −10° with Dry Ice. This precaution was necessary to avoid exceeding the transition temperature of the lower-melting forms during the time they were exposed to radiation. For the higher-melting form of each glyceride the crystals were packed in a capillary tube and photographed at room temperature. The photographs were made with a General Electric X-Ray Diffraction Unit, Model XRD, using CuKα radiation with a nickel filter (0.0007 inch thick).

Photomicrographs.—A photomicrograph of the high-melting form of each of the glycerides was obtained by evaporating the solvent from a solution of the appropriate sample on a glass slide and photographing the crystals through a petrographic microscope with crossed nicol prisms. The sample then was warmed to melt the crystals, and after solidification in the alpha form, another photograph was made.

Results and Discussion

1,2-Diaceto-3-stearin.—The calculated "d" spacings of the various forms of 1,2-diaceto-3-stearin are recorded in Table I. Three forms were distinguished, which have been designated as beta, alpha and subalpha, respectively, in accordance to their correspondence with the short spacings of 1-monostearin, a similar compound.[14]

The stable or high-melting form, beta, which was obtained by crystallization of the glyceride from solvent, or by tempering a previously melted sample, had a dilatometric melting point of 49.5°, and a capillary tube melting point of 48.6^c. The transparency of the material makes it difficult to visually ascertain the exact melting point by the capillary tube method. Cooling the melted glyceride at a moderate rate produced the alpha or lower-melting polymorphic form. On slow heating this lower-melting form began melting at approximately 35°, but transformed to the beta form before the point of complete melting was reached. When held at a temperature just below 35°, the alpha form transformed into the beta form without melting. This transformation occurred slowly if the sample was allowed to stand at room temperature. The melting dilation of the alpha form had to be determined at a rapid rate in order to avoid transformation to the beta form. Therefore the exact melting point of the alpha form could not be determined dilatometrically. The capillary tube melting point of the alpha form was 36.4°.

Table I

Interplanar Spacings of 1,2-Diaceto-3-stearin and 1-Aceto-3-stearin[a]

1,2-Diaceto-3-stearin			1-Aceto-3-stearin		
Beta	Alpha	Sub-alpha	Beta prime	Alpha	Sub-alpha
6.25 W	4.12 VS	4.11 VS	4.38 M	4.18 S	4.12 VS
5.68 W		3.68 S	4.14 S	3.93 W	3.68 S
4.82 W		2.95 W	3.84 M		2.96 M
4.58 S		2.48 W	3.55 M		2.49 M
4.07 W		2.19 W	2.92 W		2.20 M
			2.54 W		
3.76 VS			2.26 W		
2.17 W			2.17 W		
			2.10 W		

[a] Spacings reported in ångströms and relative intensity; W, weak; M, medium; S, strong; VS, very strong.

The third polymorphic form of 1,2-diaceto-3-stearin, the subalpha form, was found to exist only below −4°. It did not melt on being heated but gave evidence of transformation to the alpha form between −4 and −2°.

Expansibilities of the solid state were determined to be 0.000301 ml./g./deg. for the beta form (up to 14.7°) and 0.00115 ml./g./deg. for the alpha form (0 to 25°). Expansibility of the liquid state was 0.000960 ml./g./deg. The melting dilation of the beta form was 0.1118 ml./g., and of the alpha form, calculated at 36.4°, 0.0649 ml./g. The volume change accompanying the transformation of the subalpha form into the alpha form was 0.0048 ml./g.

1-Aceto-3-stearin.—Three polymorphic forms of this compound have been distinguished on the basis of X-ray and dilatometric data. The calculated short spacings of these forms are included in Table I, the forms being designated beta prime, alpha and subalpha.

The dilatometric melting point of the beta prime form, obtained by crystallization from solvent, was 49.1°. The capillary tube melting point was 50.3°. The latter was difficult to observe accurately owing to the transparency of the material at temperatures near its melting point.

On being melted and resolidified, the 1-aceto-3-stearin was found to have a capillary tube melting point of 47.5°. The melting point of this alpha form could not be determined dilatometrically because of an apparent transformation at some temperature below 47.5°. A very rapid determination of the expansibility of the alpha form gave evidence of its transformation to the beta prime form at about 36°.

The third polymorphic form, subalpha, occurred

---

(12) W. M. Smit, "A Tentative Investigation Concerning Fatty Acids and Fatty Acid Methyl Esters," Hilversum, Drukkerig "De Mercuser," 1946.

(13) A. E. Bailey and W. S. Singleton, *Oil & Soap*, **21**, 251 (1945); **22**, 265 (1945).

(14) E. S. Lutton and F. L. Jackson, *J. Am. Chem. Soc.*, **70**, 2445 (1948).

upon cooling the melted acetostearin to below 0°. So cooled, an apparently irreversible transformation occurred between 0 and 4°, with a decrease in volume of 0.01 ml./g.

The expansibility of the beta prime form of 1-aceto-3-stearin in the solid state (up to 15°) was 0.000352 ml./g./deg., and in the liquid state 0.000945 ml./g./deg. Melting dilation was 0.1185 ml./g.

Comparison of Density.—The densities of 1,2-diaceto-3-stearin and 1-aceto-3-stearin at 50°, at which temperature both were liquid, were found to be 0.9423 and 0.9373 g./ml., respectively. The densities of these two glycerides in both the solid and liquid states were found to differ from the densities of ordinary fats such as lard, shortening and triglycerides of stearic through lauric acids[13] by from 0.04 to 0.07 g./ml., a significant difference. Also, the densities of the glyceride series consisting of a monostearin,[9] 1-aceto-3-stearin and 1,2-diaceto-3-stearin at comparative temperatures in the liquid state were found to increase as the number of acetyl radicals increased. With respect to melting dilation of this series, an increase in the number of acetyl radicals decreased the dilation.

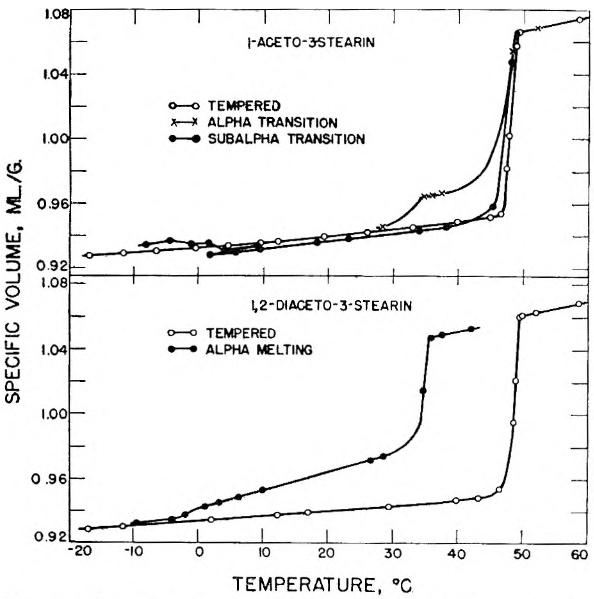

Fig. 1.—Specific volumes of the polymorphic forms of the acetostearins as functions of temperature.

From the density and expansibility data the absolute specific volume of each compound at various temperatures over its melting range was calculated. These results were plotted as functions of temperature and are reproduced in Fig. 1.

Effect of Polymorphic Form on Plasticity.—Photomicrographs were made of 1-aceto-3-stearin, 1,2-diaceto-3-stearin, and, for comparison, 1-monostearin. Crystals of the acetostearins obtained by crystallization from acetone are shaped quite differently from those of 1-monostearin obtained in a corresponding manner. The acetostearin crystals are long and narrow and seem to form a chain-like structure while the 1-monostearin crystals are block-like. Upon melting and resolidification, the 1-monostearin crystals merge into a pattern of rosettes, with distinct boundaries of the individual crystals being maintained. The acetostearins, however, form an unordered network of interlocked ribbon-like crystals.

The alpha forms of the acetostearin compounds exhibit the property of stretchability, which is unique among fatty materials. Ordinary fats can be stretched only about 2% of their original length, whereas the alpha forms of 1-aceto-3-stearin and 1,2-diaceto-3-stearin can be stretched 200 and 300 times as much, respectively, when tested under conditions described in a previous publication.[7] The high melting forms of the acetostearins, obtained by tempering the alpha form, can be stretched only as much as an ordinary fat.

A photograph of a stretched sample of the alpha form of 1,2-diaceto-3-stearin gives the appearance of the crystalline network having become more ordered and aligned, possibly by the phenomenon of plastic flow. This phenomenon probably contributes to the stretching and flexing properties possessed by these compounds.

Acknowledgment.—The authors wish to express their appreciation to Robert T. O'Connor, Inez DeGruy and Mildred Murray for obtaining the X-ray photographs and calculating the crystal spacings, and also for making the photomicrographs.

ION-EXCHANGE MEMBRANES. I. EQUATIONS FOR THE MULTI-IONIC POTENTIAL

By M. R. J. Wyllie

Gulf Research & Development Company, Pittsburgh, Penna.

Received June 1, 1953

Equations have been derived for the potentials which are set up when perfectly selective ion-exchange membranes separate mixtures of critical ions. It is shown that the equations are relatively simple when the ions separated are all of like valence, complex when the valences are dissimilar. It is shown also that for ions of the same valence, transference number ratios derived from potential measurements may be related to the selectivity coefficients and electrical conductivities of the membranes.

1. Introduction

Recent discoveries of methods of making heterogeneous[1] and homogeneous[2-4] membranes of ion-exchange materials have stimulated interest in the electrochemistry of such membranes. Perfectly selective ion-exchange membranes, when used to separate two solutions containing different concentrations of an identical critical ion, give rise to identical membrane potentials. Here the critical ion is a cation if the selective membrane has cation-exchange properties, an anion if it has anion-exchange properties. If, however, perfectly selective ion-exchange membranes are used to separate two solutions each of which contains a different critical ion, it is found that the potentials developed across the membranes are not all identical. The potentials are now functions not only of the concentrations and nature of the critical ions in the two solutions but of the nature of the membranes themselves. An extensive review of the phenomenological and historical aspects of potentials of this type, which have been called bi-ionic potentials (B.I.P.'s), has been given by Sollner.[5,6]

The problem of formulating equations quantitatively descriptive of observed B.I.P. phenomena was undertaken by Marshall[7] and by Sollner.[5,6] Marshall also considered multi-ionic potentials, (M.I.P.'s), *i.e.*, potentials which arise when mixtures of different ions are separated by a selective membrane. The treatment used by Marshall is essentially that employed earlier by Michaelis.[8] In this treatment it is assumed that a membrane gives rise to a potential by reducing to zero the mobility of the non-critical ion. The potential is treated as a limiting case of a liquid junction potential. The Henderson equation[9] is employed in straight-forward fashion, *i.e.*, in the case of a cation-exchange membrane anion mobilities are set equal to zero and *vice versa* in the case of an anion-exchange membrane.

It is clear from the discussion of Marshall and his collaborators[10] that this procedure is reasonably satisfactory in the event a membrane is used to separate solutions in which all the critical ions have the same valence. In particular, intramembrane mobility ratios appear to be largely constant and independent of the concentrations of the ions in the solutions separated by the membrane. For solutions in which the critical ions are not of identical valence, the experimental data, when treated in terms of the modified Henderson equation, give rise to intramembrane mobility ratios which are markedly concentration dependent.

Sollner,[5,6] unlike Marshall, has concerned himself with the probable mechanism of the B.I.P. Sollner assumes that the B.I.P. arises from a combination of factors. These factors are primarily the existence of fixed charges within the pores of a membrane,[11,12] competitive ion-exchange adsorption of the critical ions and the heteroporosity of membranes.

In essence, Sollner assumes that the intramembrane mobility ratio (transference number ratio[13]) of a pair of critical ions is a function of the relative numbers of each of the ions adsorbed within the membrane and their individual intramembrane diffusion velocities. Although Sollner's discussion is limited to the case of monovalent ions, it is apparent that in the general case the valence of the two ions should be considered also. The valence together with the total number of ions diffusing would control the magnitude of the charge transferred across a membrane and hence the B.I.P. developed.

The differential adsorption and diffusion mechanism which Sollner describes is considered by him to be liable to critical modification in the event that a membrane is not functionally homoporous. Real membranes are likely to be heteroporous. With such membranes certain pores may be too small to be permeable to the larger of two critical ions. The barring of the larger ion would result in the diffusion of a relatively greater number of smaller ions and, assuming the smaller ion to have the higher intramembrane diffusion constant, an increase in the B.I.P. observed.

Sollner's theory appears to encompass almost all the major considerations which are likely to bear on the origin of the B.I.P. Any new theory is unlikely to modify any of his basic concepts. The chief weakness of the theory seems to lie in the as-

---

[1] M. R. J. Wyllie and H. W. Patnode, THIS JOURNAL, **54**, 204 (1950).

[2] W. Juda and W. A. McRae, *J. Am. Chem. Soc.*, **72**, 1044 (1950).

[3] T. R. E. Kressman, *Nature*, **165**, 568 (1950).

[4] T. Westermark, *Acta Chem. Scand.*, **6**, 1194 (1952).

[5] K. Sollner, THIS JOURNAL, **53**, 1211 (1949).

[6] K. Sollner, *ibid.*, **53**, 1226 (1949).

[7] C. E. Marshall, *ibid.*, **52**, 1284 (1948).

[8] L. Michaelis, *Bull. Natl. Research Council (U. S.)*, **69**, 119 (1929).

[9] P. Henderson, *Z. physik. Chem.*, **59**, 118 (1907); **63**, 325 (1908).

[10] E. O. McLean, S. A. Barber and C. E. Marshall, *Soil Sci.*, **72**, 315 (1951).

[11] T. Teorell, *Proc. Natl. Acad. Sci. U. S.*, **21**, 152 (1935).

[12] K. H. Meyer and J. F. Sievers, *Helv. Chim. Acta*, **19**, 649, 665, 963 (1936).

[13] H. P. Gregor and K. Sollner, THIS JOURNAL, **50**, 53 (1946).

sumption that the distribution within the membrane pores of the critical ions which give rise to a B.I.P. is uniform or that, if non-uniform, this non-uniformity is of little significance.[5] On the contrary, the concept of a non-uniform ionic distribution within the membrane appears to reconcile the basic postulates of Sollner with the liquid junction treatment of Michaelis and Marshall and the essentials of the fixed-charge membrane theory of Meyer and Sievers and Teorell.

It may be noted also that Marshall[7] has suggested that B.I.P. data may be used to compute the differential heat of adsorption of the two critical ions on the membrane material. Recently Coleman[14] has claimed that Marshall's calculations lead to an evaluation not of the differential heat of adsorption but of the free energy change of the ion-exchange reaction between the two critical ions on the membrane material.

2. Derivation of a Multi-ionic Potential Equation

The following simplifying assumptions are made: that the membranes considered are porous and possess ion-exchange properties; that they are almost perfectly ion selective, *i.e.*, their permeability to non-critical ion species is so small that it may be ignored; that swelling effects are negligible. It is assumed also that both the B.I.P.'s and M.I.P.'s considered are the maximum stable values that can be measured. Maximum stable potentials may be defined as the potentials observed when the solutions separated by a membrane are continuously flowed past the faces of the membrane or are so frequently renewed that they are not significantly contaminated by transmembrane diffusion of critical ions. As noted by Sollner,[5] M.I.P.'s arise by definition in systems which undergo continual degradation; nevertheless, if fresh solutions are maintained on each side of a membrane, it is entirely possible to sustain and measure a stable and reproducible potential. It is also implicit in the discussion given that none of the critical ions considered is so large that it is incapable of penetrating into any pores of the membrane.

Although B.I.P.'s have received more attention, it would seem that they merely represent a special case of a M.I.P. Accordingly, it is appropriate to derive an equation for a typical M.I.P.

Consider the system

$$\begin{array}{c|c|c} \mathrm{M}^{n_\mathrm{M}+} & \text{Cation-exchange} & \mathrm{O}^{n_\mathrm{O}+} \\ \mathrm{N}^{n_\mathrm{N}+} & \text{membrane} & \mathrm{P}^{n_\mathrm{P}+} \end{array}$$

Here a cation-exchange membrane separates a solution containing the cations M and N of valences n_M and n_N from a solution containing the cations O and P of valences n_O and n_P. The individual ionic activities of the ions will be written a_M, a_N, a_O and a_P when in solution and $\bar{a}_\mathrm{M}$, $\bar{a}_\mathrm{N}$, $\bar{a}_\mathrm{O}$ and $\bar{a}_\mathrm{P}$ when in the membrane. In both the solution and the membrane, activities will be defined in terms of molalities, m and activity coefficients γ, such that $a = m\gamma$ and $\gamma \rightarrow 1.0$ as $m \rightarrow 0$. The activity coefficients are necessarily those of individual ions as the discussion will show. Molalities $\bar{m}$ refer to moles per 1000 g. of pore water in the membranes.

The fundamental assumption is made that the distribution of the ions within the membrane under the steady state conditions postulated above will not be uniform. It is assumed that the ion-exchange sites in the pores of the membrane face in contact with the solution containing the ions M and N will be occupied wholly by those ions. At the membrane face in contact with the other solution the exchange sites in the pores will be wholly occupied by the ions O and P. Between these two extremes, within the body of the membrane, the exchange sites will be occupied by varying proportions of all four species of ions. Hence, the membrane interior may be considered a zone of transition between two facial "solutions" of constant activities $\bar{a}_\mathrm{M}$, $\bar{a}_\mathrm{N}$ and $\bar{a}_\mathrm{O}$, $\bar{a}_\mathrm{P}$, respectively. In turn, the activities of the two facial solutions will depend upon the relative activities a_M, a_N and a_O, a_P in the two solutions in contact with the faces, the ionic strength of these solutions and the affinity of the ion-exchange material constituting the membrane for the ions considered.

The distribution of ions within the membrane may be regarded as a continuous series of mixtures of the four ions in which the effects of diffusion are relatively minor. To a good approximation such a mixture of ions constitutes a boundary of the type postulated by Henderson[9] with, of course, the exception that the anion concentration within the membrane is assumed to be vanishingly small.

The potential across the membrane then has three components. These are the phase-boundary or Donnan potentials at each membrane face and a liquid junction potential within the membrane itself.[11,12]

From the Donnan concept, it follows that at the interfaces between the solutions containing the ions M and N and O and P and the membrane the following relationships hold

$$a_\mathrm{M}{}^{n_\mathrm{N}}/\bar{a}_\mathrm{M}{}^{n_\mathrm{N}} = a_\mathrm{N}{}^{n_\mathrm{M}}/\bar{a}_\mathrm{N}{}^{n_\mathrm{M}}$$

$$a_\mathrm{O}{}^{n_\mathrm{P}}/\bar{a}_\mathrm{O}{}^{n_\mathrm{P}} = a_\mathrm{P}{}^{n_\mathrm{O}}/\bar{a}_\mathrm{P}{}^{n_\mathrm{O}}$$

Thus, the Donnan potential between the membrane face and the solution containing the ions M and N is

$$E_1 = \frac{RT}{n_\mathrm{M}F} \ln \frac{a_\mathrm{M}}{\bar{a}_\mathrm{M}} = \frac{RT}{n_\mathrm{N}F} \ln \frac{a_\mathrm{N}}{\bar{a}_\mathrm{N}}$$

where R is the gas constant, T the absolute temperature and F the Faraday constant. The Donnan potential at the other membrane face is

$$E_3 = \frac{RT}{n_\mathrm{O}F} \ln \frac{a_\mathrm{O}}{\bar{a}_\mathrm{O}} = \frac{RT}{n_\mathrm{P}F} \ln \frac{a_\mathrm{P}}{\bar{a}_\mathrm{P}} = \frac{RT}{n_\mathrm{M}F} \ln (a_\mathrm{O}/\bar{a}_\mathrm{O})^{n_\mathrm{M}/n_\mathrm{O}}$$

The liquid junction potential within the membrane appears to be of a type which is most compatible with the assumptions made by Henderson when integrating the liquid junction potential equation. Hence, the liquid junction potential may be written as

$$E_2 = \frac{RT}{F}\left[\frac{\bar{a}_\mathrm{M}\bar{U}_\mathrm{M} + \bar{a}_\mathrm{N}\bar{U}_\mathrm{N} - \bar{a}_\mathrm{O}\bar{U}_\mathrm{O} - \bar{a}_\mathrm{P}\bar{U}_\mathrm{P}}{n_\mathrm{M}\bar{a}_\mathrm{M}\bar{U}_\mathrm{M} + n_\mathrm{N}\bar{a}_\mathrm{N}\bar{U}_\mathrm{N} - n_\mathrm{O}\bar{a}_\mathrm{O}\bar{U}_\mathrm{O} - n_\mathrm{P}\bar{a}_\mathrm{P}\bar{U}_\mathrm{P}}\right] \ln \frac{n_\mathrm{M}\bar{a}_\mathrm{M}\bar{U}_\mathrm{M} + n_\mathrm{N}\bar{a}_\mathrm{N}\bar{U}_\mathrm{N}}{n_\mathrm{O}\bar{a}_\mathrm{O}\bar{U}_\mathrm{O} + n_\mathrm{P}\bar{a}_\mathrm{P}\bar{U}_\mathrm{P}}$$

---

(14) N. T. Coleman, *Soil Sci.*, **74**, 115 (1952).

Here $\bar{U}_\mathrm{M}$, $\bar{U}_\mathrm{N}$, $\bar{U}_\mathrm{O}$, $\bar{U}_\mathrm{P}$ are the apparent intramembrane mobilities of the ions M, N, O, P.

The total membrane potential is the algebraic sum of E_1, E_2 and E_3. The summation may be expressed in a number of ways, but it is convenient to write the intramembrane mobilities as ratios in terms of a particular ion as reference standard. If such ratios are multiplied by the ratio of the valence of each ion to that of the reference ion, convenient transference number ratios are obtained. The summation may be written

$$E = E_1 + E_2 + E_3$$

$$= \frac{RT}{n_\mathrm{M}F}\left[\ln\frac{a_\mathrm{M}}{a_\mathrm{O}{}^{n_\mathrm{M}/n_\mathrm{O}}} + \ln\frac{\bar{a}_\mathrm{O}{}^{n_\mathrm{M}/n_\mathrm{O}}}{\bar{a}_\mathrm{M}} + \left(\frac{\bar{a}_\mathrm{M} + \bar{a}_\mathrm{N}\dfrac{\bar{U}_\mathrm{N}}{\bar{U}_\mathrm{M}} - \bar{a}_\mathrm{O}\dfrac{\bar{U}_\mathrm{O}}{\bar{U}_\mathrm{M}} - \bar{a}_\mathrm{P}\dfrac{\bar{U}_\mathrm{P}}{\bar{U}_\mathrm{M}}}{\bar{a}_\mathrm{M} + \bar{a}_\mathrm{N}\dfrac{\bar{U}_\mathrm{N}n_\mathrm{N}}{\bar{U}_\mathrm{M}n_\mathrm{M}} - \bar{a}_\mathrm{O}\dfrac{\bar{U}_\mathrm{O}n_\mathrm{O}}{\bar{U}_\mathrm{M}n_\mathrm{M}} - \bar{a}_\mathrm{P}\dfrac{\bar{U}_\mathrm{P}n_\mathrm{P}}{\bar{U}_\mathrm{M}n_\mathrm{M}}}\right) \ln\frac{\bar{a}_\mathrm{M} + \bar{a}_\mathrm{N}\dfrac{n_\mathrm{N}\bar{U}_\mathrm{N}}{n_\mathrm{M}\bar{U}_\mathrm{M}}}{\bar{a}_\mathrm{O}\dfrac{n_\mathrm{O}\bar{U}_\mathrm{O}}{n_\mathrm{M}\bar{U}_\mathrm{M}} + \bar{a}_\mathrm{P}\dfrac{n_\mathrm{P}\bar{U}_\mathrm{P}}{n_\mathrm{M}\bar{U}_\mathrm{M}}}\right] \quad (2.1)$$

Equation 2.1 may be used to derive equations for the B.I.P. in two cases which have received attention from Marshall.

For the B.I.P. between two ions, M and P, of the same valence, n

$$E = \frac{RT}{nF}\ln\frac{a_\mathrm{M}(\bar{U}_\mathrm{M}/\bar{U}_\mathrm{P})}{a_\mathrm{P}} \quad (2.2)$$

For the B.I.P. between a monovalent ion and a divalent ion ($n_\mathrm{M} = 1$, $n_\mathrm{O} = 2$)

$$E = \frac{RT}{2F}\ln\frac{a_\mathrm{M}{}^2}{a_\mathrm{O}} \times \frac{\bar{a}_\mathrm{O}}{\bar{a}_\mathrm{M}{}^2} + \frac{RT}{2F}\left[\frac{2\bar{a}_\mathrm{M} - \bar{a}_\mathrm{O}\dfrac{2\bar{U}_\mathrm{O}}{\bar{U}_\mathrm{M}}}{\bar{a}_\mathrm{M} - \bar{a}_\mathrm{O}\dfrac{2\bar{U}_\mathrm{O}}{\bar{U}_\mathrm{M}}}\right]\ln\frac{\bar{a}_\mathrm{M}}{\bar{a}_\mathrm{O}\dfrac{2\bar{U}_\mathrm{O}}{\bar{U}_\mathrm{M}}} \quad (2.3)$$

Two further cases which have been considered by Marshall also may be noted. The M.I.P. between a mixture of two ions, a_M and a_N, of the same valence, n, and a third ion, a_O, also of valence n is

$$E = \frac{RT}{nF}\ln\frac{a_\mathrm{M} + (a_\mathrm{N}\bar{U}_\mathrm{N}/\bar{U}_\mathrm{M})}{a_\mathrm{O}\ (\bar{U}_\mathrm{O}/\bar{U}_\mathrm{M})} \quad (2.4)$$

The M.I.P. between a mixture of two ions, which differ in valence, and a third ion is complex. Thus, the M.I.P. between a solution containing both a monovalent ion, M, and a divalent ion, N, and a solution containing a monovalent ion, O, only is given by

$$E = \frac{RT}{F}\ln\frac{a_\mathrm{M}}{a_\mathrm{O}} \times \frac{\bar{a}_\mathrm{O}}{\bar{a}_\mathrm{M}} + \frac{RT}{F}\left[\frac{\bar{a}_\mathrm{M} + \bar{a}_\mathrm{N}\dfrac{\bar{U}_\mathrm{N}}{\bar{U}_\mathrm{M}} - a_\mathrm{O}\dfrac{\bar{U}_\mathrm{O}}{\bar{U}_\mathrm{M}}}{\bar{a}_\mathrm{M} + \bar{a}_\mathrm{N}\dfrac{2\bar{U}_\mathrm{N}}{\bar{U}_\mathrm{M}} - a_\mathrm{O}\dfrac{\bar{U}_\mathrm{O}}{\bar{U}_\mathrm{M}}}\right]\ln\frac{\bar{a}_\mathrm{M} + \bar{a}_\mathrm{N}\dfrac{2\bar{U}_\mathrm{N}}{\bar{U}_\mathrm{M}}}{\bar{a}_\mathrm{O}\dfrac{\bar{U}_\mathrm{O}}{\bar{U}_\mathrm{M}}} \quad (2.5)$$

One further case is of practical interest. In the electric logging of deep boreholes, potentials are measured which appear to indicate that shale strata act as cation selective membrane electrodes.[1,15] It is important to know how the observed potentials are affected by varying concentrations of monovalent and divalent ions in the interstitial waters of porous sedimentary rocks and in the mud fluid which fills a borehole. Since the principal ions in both interstitial waters and muds are primarily sodium and calcium, the case where M = Na, N = Ca, O = Na, P = Ca may be considered. If superscripts are used to identify the two solutions, equation 2.1 may be written in the form

$$E = \frac{RT}{F}\ln\frac{a'_\mathrm{Na}}{a''_\mathrm{Na}} \times \frac{\bar{a}''_\mathrm{Na}}{\bar{a}'_\mathrm{Na}} + \frac{RT}{F}\left[\frac{\bar{a}'_\mathrm{Na}\dfrac{\bar{U}_\mathrm{Na}}{\bar{U}_\mathrm{Ca}} + \bar{a}'_\mathrm{Ca} - \bar{a}''_\mathrm{Na}\dfrac{\bar{U}_\mathrm{Na}}{\bar{U}_\mathrm{Ca}} - \bar{a}''_\mathrm{Ca}}{\bar{a}'_\mathrm{Na}\dfrac{\bar{U}_\mathrm{Na}}{\bar{U}_\mathrm{Ca}} + 2\bar{a}'_\mathrm{Ca} - \bar{a}''_\mathrm{Na}\dfrac{\bar{U}_\mathrm{Na}}{\bar{U}_\mathrm{Ca}} - 2\bar{a}''_\mathrm{Ca}}\right]\ln\frac{\bar{a}'_\mathrm{Na}\dfrac{\bar{U}_\mathrm{Na}}{\bar{U}_\mathrm{Ca}} + 2\bar{a}'_\mathrm{Ca}}{\bar{a}''_\mathrm{Na}\dfrac{\bar{U}_\mathrm{Na}}{\bar{U}_\mathrm{Ca}} + 2\bar{a}''_\mathrm{Ca}}$$

In order to simplify this expression and to make its practical implications clearer, the activities of the ions on the shale membrane (*i.e.*, on the clays in the shale) will be assumed proportional to their equivalent fractions on the exchange sites of the clay. That this is a reasonable approximation in the case of the sodium–calcium system has been demonstrated by Ericksson.[16] Then

$$\bar{a}'_\mathrm{Na} = \frac{\bar{m}'_\mathrm{Na}}{\bar{m}'_\mathrm{Na} + 2\bar{m}'_\mathrm{Ca}} \qquad \bar{a}'_\mathrm{Ca} = \frac{2\bar{m}'_\mathrm{Ca}}{\bar{m}'_\mathrm{Na} + 2\bar{m}'_\mathrm{Ca}}$$

$$\bar{a}''_\mathrm{Na} = \frac{\bar{m}''_\mathrm{Na}}{\bar{m}''_\mathrm{Na} + 2\bar{m}''_\mathrm{Ca}} \qquad \bar{a}''_\mathrm{Ca} = \frac{2\bar{m}''_\mathrm{Ca}}{\bar{m}''_\mathrm{Na} + 2\bar{m}''_\mathrm{Ca}}$$

The symbol $\bar{m}$ has been defined as the molality of the exchange ion expressed in moles per 1000 grams of pore water for an ion-exchange resin membrane. In the case of shale where the pore water is less well defined, $\bar{m}$ is the number of moles per unit weight of dry clay. For a constant exchange capacity it follows that

$$\bar{m}'_\mathrm{Na} + 2\bar{m}'_\mathrm{Ca} = \bar{m}''_\mathrm{Na} + 2\bar{m}''_\mathrm{Ca} = \bar{x}$$

Thus, $\bar{a}'_\mathrm{Na}$ may be written $\bar{x}'_\mathrm{Na}$, *i.e.*, the fraction of exchange sites occupied by Na′ on the face of the shale in contact with the solution containing the ions Na′ and Ca′. Accordingly, $\bar{a}'_\mathrm{Ca} = 1 - \bar{x}'_\mathrm{Na}$, $\bar{a}''_\mathrm{Na} = \bar{x}''_\mathrm{Na}$ and $\bar{a}''_\mathrm{Ca} = 1 - \bar{x}''_\mathrm{Na}$.

Substituting these values for activities in the expression for the potential across the shale gives

$$E = \frac{RT}{F}\ln\frac{a'_\mathrm{Na}}{a''_\mathrm{Na}} + \frac{RT}{F}\ln\frac{\bar{x}''_\mathrm{Na}}{\bar{x}'_\mathrm{Na}} + \frac{RT}{F}\left[\frac{\dfrac{\bar{U}_\mathrm{Na}}{2\bar{U}_\mathrm{Ca}} - \dfrac{1}{2}}{\dfrac{\bar{U}_\mathrm{Na}}{2\bar{U}_\mathrm{Ca}} - 1}\right]\ln\frac{\bar{x}'_\mathrm{Na}\left[\dfrac{\bar{U}_\mathrm{Na}}{2\bar{U}_\mathrm{Ca}} - 1\right] + 1}{\bar{x}''_\mathrm{Na}\left[\dfrac{\bar{U}_\mathrm{Na}}{2\bar{U}_\mathrm{Ca}} - 1\right] + 1} \quad (2.6)$$

From equation 2.6 it appears that for any shale for which the transference number ratio $\bar{U}_\mathrm{Na}/2\bar{U}_\mathrm{Ca}$ is constant, the potential depends upon two factors. These factors are the activity ratio of the sodium ions and the ratio of the fractions of exchange sites on the clays in the shale faces occupied by sodium ions when these clays are in equilibrium with the solutions in contact with them. The fraction of exchange sites occupied by a monovalent ion in a mon-

---

(15) M. R. J. Wyllie, "Proceedings of First National Conference on Clays and Clay Technology," in press.

(16) E. Ericksson, *Soil Sci.*, **74**, 103 (1952).

ovalent–divalent exchange system is dependent not only on the ratio of the activities of the monovalent and divalent ions in the solution, but also on the ionic strength of the solution. It follows that if the ratios $a'_{\mathrm{Na}}/a'_{\mathrm{Ca}}$ and $a''_{\mathrm{Na}}/a''_{\mathrm{Ca}}$ are, respectively, small and large, x'_{Na} may still be approximately equal to x''_{Na} if the ionic strength of the first solution is large and the second small. This condition often appears to be satisfied in practice.[15]

Equations 2.2 and 2.4 are identical with the corresponding equations derived by Marshall. Equations 2.3 and 2.5 are dissimilar.

The dissimilarity between equations 2.3 and 2.5 and equations derived by Marshall by direct application of the Henderson equation and the similarity of equations 2.2 and 2.4 to those he derived stems directly from the tripartite nature of the potential distribution assumed in the derivation of equation 2.1. In equations 2.2 and 2.4 the activities in the membrane phase, which occur both in the Donnan and liquid junction potential equations, cancel, and the final result therefore agrees with Marshall's equation. When all ions involved are not of the same valence, cancellation no longer occurs and both equation 2.3 and 2.5 involve terms which are descriptive of activities in the membrane. It is implicit in Marshall's derivation that the activities of the critical ions within the membrane and in the solution are identical. This seems inherently improbable. Indeed, Marshall himself[7] has noted this fact.

Equations 2.2 and 2.4 contain only one membrane parameter. This parameter is the intramembrane transference number of the ions involved. In equation 2.2, if the conditions postulated in the derivation of equation 2.1 obtain, it is to be anticipated that the intramembrane transference number should be a constant which is independent of the activities of the two solutions separated by the membrane. This follows because the liquid junction within the membrane is between two facial "solutions" of constant cation activities $\bar{a}_{\mathrm{M}}$ and $\bar{a}_{\mathrm{P}}$, respectively, and negligible anion activities. The data of Marshall and Bergman[17] and those of Wyllie and Kanaan[18] confirm this view.

In the case of equation 2.4, it may be expected that the intramembrane transference number ratios will be only approximately constant. This conclusion is based on the work of Spiegler and Coryell[19] who show that the ionic mobilities of two ions within a cation-exchange resin are dependent on the concentration of each. This in turn means that they will be dependent upon the activities of the cations on the exchange sites of the membrane faces and, in consequence, on the relative activities of the cations and the ionic strengths of the mixed ion solutions in contact with the faces. However, if approximate values of transference number ratios are derived from equation 2.2, it is anticipated that, to a good approximation, these values may be used in equation 2.4. The data of Marshall and Krinbill[20] are in general accord with this anticipation.

Equations 2.3 and 2.5, unlike 2.2 and 2.4, contain terms which reflect ionic activities in the membrane phase. These terms cannot as yet be evaluated with any precision. The equations, therefore, do not appear to lend themselves to the applications envisaged by Marshall and his co-workers,[10] *i.e.*, to the determination of individual ionic activities in solutions containing ions of different valences. Marshall and his co-workers[10] note that equations based on the simple Henderson equation give rise, in the case of mixed monovalent and divalent ion solutions, to transference number ratios which are markedly concentration dependent. This observation probably reflects the fact, already noted, that direct application of the Henderson equation gives rise to equations for the B.I.P. and M.I.P. in such systems which are over-simplified. The apparent variations in transference number ratios with concentration changes are not, therefore, necessarily real phenomena.[21]

3. Limitations of the Equation

The M.I.P. equation derived was for an extremely idealized case. It may be noted particularly that the application of the Henderson liquid junction equation to the conditions prevailing within the membrane assumes that this equation is applicable at the ionic concentrations which prevail within the pores of ion-exchange membranes. These concentrations may be as high as 7.5 molal in terms of pore water and represent concentrations for which the accuracy of the Henderson equation may be considered problematical at best.

The assumption that the anion activities within the membrane are negligible is less serious than might be supposed. Heterogeneous ion-exchange membranes may be shown to give potentials which approximate those satisfying the Nernst equation when the concentrations of the solutions separated by the membrane exceed one molal.[1] The concentration range over which a membrane, when separating solutions having identical critical ions, gives potentials that follow the Nernst equation may be considered, to a first approximation, as the concentration range over which the idealized M.I.P. equation may be expected to hold. Several factors influence the validity of this approximation. The concentration range over which the Nernst equation holds is itself an inverse function of the valence of the critical ions separated by the membrane and, for any valence, of the activity of those ions in the membrane phase. Thus, a cation exchange membrane obeys the Nernst equations to a much higher concentration when separating potassium ions than when separating silver ions, since the activity of the silver ions in the membrane is generally only about one-third that of potassium ions.[22] In terms of the Meyer–Sievers and Teorell equation,[11,12] the selectivity constant, A, of the membrane in the silver form is only one-third the selectivity constant of

---

[17] C. E. Marshall and W. E. Bergman, This Journal, **46**, 325 (1942).

[18] M. R. J. Wyllie and S. L. Kanaan, *ibid.*, **58**, 73 (1953).

[19] K. S. Spiegler and C. D. Coryell, *ibid.*, **56**, 106 (1952).

[20] C. E. Marshall and C. A. Krinbill, *J. Am. Chem. Soc.*, **64**, 1814 (1942).

[21] The fact that Marshall believes his membranes to be nonporous,[1] *i.e.*, without any internal liquid junction potential does not affect this view. Nevertheless, the fact that ionic transference across his membranes must take place makes it probable that junction potentials analogous to those in ion-exchange resin membranes must also be set up within them.

[22] M. R. J. Wyllie, "Gordon Research Conference on Ion Exchange," July, 1952.

the same membrane in the potassium form. If the plotting technique used by Wyllie and Kanaan[18] is followed, it is generally possible to estimate the range of applicability of the M.I.P. equations derived.

It was implicit in the derivation of the equations that the activities of the solvent in two solutions separated by a membrane could be ignored. In cases where the concentrations of the two solutions separated by the membrane are very similar this approximation is reasonable. In many cases, however, the concentrations of the two solutions differ markedly and a significant potential error may be expected to arise because of the probability that the ions transferred across the membrane are solvated. The number of moles of water transferred across the membrane per mole of critical ion transferred will reflect the solvation of the ion within the membrane. Thus, calculation of water transferred across membranes made of ion-exchange resins may further knowledge concerning the state of solvation of ions within ion-exchange resins.

The potential across a membrane which results in the case of the aqueous system

$$\begin{array}{c|c|c} a'_{\mathrm{M}} & \text{Cation-exchange} & a''_{\mathrm{M}} \\ a'_{\mathrm{H_2O}} & \text{membrane} & a''_{\mathrm{H_2O}} \end{array}$$

$$a'_{\mathrm{M}} + a'_{\mathrm{H_2O}} \xrightarrow{\mathrm{M}\cdot S\mathrm{H_2O}} a''_{\mathrm{M}} + a''_{\mathrm{H_2O}}$$

Here $a'_{\mathrm{M}} > a''_{\mathrm{M}}$ and it is assumed that S moles of water are transferred per mole of the cation M. The potential is thus[23]

$$E = \frac{RT}{nF} \ln \frac{a'_{\mathrm{M}}}{a''_{\mathrm{M}}} + \frac{SRT}{F} \ln \frac{a'_{\mathrm{H_2O}}}{a''_{\mathrm{H_2O}}} \qquad (3.1)$$

But, if $a'_{\mathrm{M}} > a''_{\mathrm{M}}$ it follows that for the water activities, $a'_{\mathrm{H_2O}} < a''_{\mathrm{H_2O}}$. In consequence, the transfer of water gives rise to a potential which serves to diminish the observed membrane potential. The effect of variations in water activity on the membrane potential is qualitatively identical with the effects of membrane imperfections or a low selectivity constant. A further complication is the necessity for substituting in equation 3.1 single ion activities for a'_{M} and a''_{M}. Since there is no thermodynamic method for computing single ion activity coefficients, it is necessary to make non-thermodynamic assumptions. In special cases the latter difficulty may be overcome. If chloride solutions, molalities m' and m'', of the monovalent cation M are used, the system

$$\begin{array}{c|c|c|c|c} \mathrm{Ag} & (\mathrm{AgCl})\cdot\mathrm{MCl} & \text{Cation-exchange} & \mathrm{MCl}\cdot(\mathrm{AgCl}) & \mathrm{Ag} \\ & m' & \text{membrane} & m'' & \end{array}$$

may be set up. The potential measured is in this case

$$E = \frac{2RT}{F} \ln \frac{a'_{\mathrm{MCl}}}{a''_{\mathrm{MCl}}} + \frac{SRT}{F} \ln \frac{a'_{\mathrm{H_2O}}}{a''_{\mathrm{H_2O}}} \qquad (3.2)$$

Here a'_{MCl} and a''_{MCl} are mean ionic activities and readily obtainable. Equation 3.2 is better suited to a determination of S than equation 3.1. The fact that potential changes resulting from membrane imperfections may be confused with those resulting from solvent activity effects remains a stumbling block.

4. The Significance of Intramembrane Mobility Ratios

All M.I.P. equations derived contain a term which, by analogy with the electrochemistry of free solutions, has been called intramembrane mobility ratio. In equations which pertain to ions of a common valence, the intramembrane mobility ratio is the only term which reflects membrane properties.

The significance of the intramembrane mobility ratio has been considered by Sollner.[5] Sollner noted that where the non-critical ion played no part in current transfer, the intramembrane mobility ratio was related to the transference number ratio of the critical ions. The intramembrane mobility ratio of two monovalent ions was shown to be identical with their transference number ratio. The general relationship between intramembrane mobility ratio and transference number ratio may readily be shown to depend upon valence. Thus, if $\bar{U}_1/\bar{U}_2$ is the intramembrane mobility ratio of two ions, their transference number ratio is equal to $\bar{U}_1 n_1/\bar{U}_2 n_2$ where n_1, n_2 are the valences of the ions.

In deriving equation 2.1, intramembrane mobilities were substituted in the Henderson equation. It might appear that these mobilities are identical with the mobilities of the same ions in free solution or, more precisely, with their mobilities in an uncharged porous medium possessing pores identical to those in the ion-exchange membrane. This view ignores the fact that the critical ions are subject to at least one constraint on their mobilities which is not applicable in an uncharged membrane. This constraint stems from the attraction of the exchange sites in the pores of the ion-exchange membrane for the critical ions. Were this attraction to be identical for both ions, the absolute mobilities of the two ions in the membrane *vis-a-vis* their mobilities in free solution might be diminished but their relative mobilities would be left unchanged. In general, however, an ion-exchange resin adsorbs one ion preferentially. Thus, the distribution of ions in the liquid junction formed within the membrane pores may be very different from that assumed in the derivation of the Henderson equation. The mobility ratio computed by application of the Henderson equation can only be an apparent value. This apparent value is compounded of the actual relative mobilities and relative numbers of the two ions in the boundary. The actual relative mobilities will be related, ideally, to the self-diffusion constants of the ions in the membrane or to the conductivities possessed by the membrane when its exchange sites are wholly occupied by each of the ions. The relative numbers of the two ions in the junction zone will depend on the selectivity constant of the ion-exchange material for these ions.[24] Similar considerations apply when a junction is formed between more than two ions.

If the specific case of two ions, M and P, of identical valence is considered, it follows that

$$\frac{\bar{U}_{\mathrm{M}}}{\bar{U}_{\mathrm{P}}} = \frac{\bar{T}_{\mathrm{M}}}{\bar{T}_{\mathrm{P}}} = \frac{\bar{m}_{\mathrm{M}}}{\bar{m}_{\mathrm{P}}} \times \frac{\bar{k}_{\mathrm{M}}}{\bar{k}_{\mathrm{P}}} \qquad (4.1)$$

---

[23] P. B. Taylor, THIS JOURNAL, **31**, 1478 (1927).

[24] The selectivity constant, if actually determined for the membrane, automatically takes account of any steric effects of the kind postulated by Sollner.[6]

In equation 4.1, $\bar{T}_M/\bar{T}_P$ is the intramembrane transference number ratio, $\bar{m}_M$ the steady state equilibrium concentration of the ion M in the junction zone, $\bar{k}_M$ the conductivity of the membrane when wholly in the form M and $\bar{k}_P$ the conductivity of the membrane when wholly in the form P. It may be noted that the ratio $\bar{k}_M/\bar{k}_P$ is properly the ratio of the mobilities of the two ions when simultaneously present in the membrane. Spiegler and Coryell[19] have shown that the ratio of the mobilities of two ions, if these are based on the conductivities of an exchange resin when wholly converted to each of the two ionic forms, is not identical with the same ratio when the ions are simultaneously present in the resin. This effect, which is probably a consequence of the failure of the Kohlrausch principle of independent ionic mobilities at high ionic concentrations, is sufficiently small that it may, for present purposes, be neglected.

The ratio $\bar{m}_M/\bar{m}_P$ is related to the selectivity constant of the ion-exchange material from which a membrane is made. The equilibrium concentrations $\bar{m}_M$ and $\bar{m}_P$ in the junction zone may be viewed as those which obtain in a thin film of ion-exchange material in simultaneous contact with two facial membrane "solutions" which are continuously maintained at activities $\bar{a}_M$ and $\bar{a}_P$, respectively.

For this equilibrium

$$K = (\bar{\gamma}_P\bar{M})(\bar{\gamma}_M\bar{m}_M)/(\bar{\gamma}_M\bar{M})(\bar{\gamma}_P\bar{m}_P) \tag{4.2}$$

In equation 4.2, $\bar{M}$ is the exchange capacity of the ion-exchange membrane in moles per 1000 g. of pore water, $\bar{\gamma}_P$ and $\bar{\gamma}_M$ are the activity coefficients of ions P and M in the membrane phase. If these activity coefficients are assumed, as an approximation, to be for each ion independent of the presence of the other ion in the membrane, equation 4.2 reduces to

$$K \simeq \bar{m}_M/\bar{m}_P \tag{4.3}$$

The selectivity constant K_P^M, where M is the reference ion, refers conventionally to the exchange between ion P on the exchange material and ion M in the solution. It is generally written

$$K_P^M = \frac{\bar{m}_M}{\bar{m}_P} \times \frac{a_{PA}}{a_{MA}} \tag{4.4}$$

In equation 4.4 the mean activities a_{PA}, a_{MA} refer to a solution phase in which A is a common anion. From equation 4.4 it is apparent that K_P^M values, as customarily reported, may be substituted for K values in equation 4.3. Thus, as an approximation

$$\frac{\bar{U}_M}{\bar{U}_P} \simeq K_P^M \times \frac{\bar{k}_M}{\bar{k}_P} \tag{4.5}$$

Implicit in the derivation of equation 4.5 is the assumption that variations in the activities a_M and a_P in the external solutions separated by the membrane have no effect on conditions within the membrane itself. That is, the activities $\bar{a}_M$, $\bar{a}_P$ and the internal liquid junction potential are not dependent upon the activities a_M, a_P. Variations in a_M and a_P will effect changes in the Donnan potentials across the interfaces, $(RT/F) \ln a_M/\bar{a}_M$ and $-(RT/F) \ln a_P/\bar{a}_P$, respectively, and thus of the over-all membrane potential. In these respects, the derivation of equation 4.5 differs from the simpler treatment of Sollner.[5,6] Sollner assumed the ionic distribution within the membrane to be constant throughout its thickness and, for the particular case of $a_M = a_P$, was able to derive an equation which is substantially the same as equation 4.1.

Marshall[7] has attempted a thermodynamical interpretation of intramembrane mobility ratio. He assumed an ionic distribution in the membrane identical to that used in the derivation of equation 4.5. For this distribution he assumed that the passage of one faraday of electricity through a membrane separating two ions, M and P, of the same valence served to migrate one gram equivalent of ion M on to the membrane face in contact with the solution containing the ion M and one gram equivalent of ion P off the membrane face into the solution containing the ion P. The over-all effect of the passage of one faraday was to replace one equivalent of ion P on the membrane by one equivalent of ion M. A reversal of the direction of current flow was shown similarly to effect the exchange of one equivalent of ion M by one equivalent of ion P. Marshall initially interpreted the B.I.P. in terms of the electrical work done in effecting the ionic interchange and equated the electrical work with the differential heat of adsorption of the two ions. Coleman[14] has recently pointed out that Marshall's later view is that the electrical work should properly be equated against the free energy change involved in the exchange of the two ions on the membrane.

If, following Marshall, E, the B.I.P., is assumed equal to $-\Delta F_0/F$, where ΔF_0 is the standard free energy change and F is the faraday, and $\Delta F^0 = -RT \ln K_P^M$, where K_P^M is the equilibrium constant or selectivity constant of the exchange of ion M for ion P, it follows that

$$E = \frac{RT}{F} \ln K_P^M \tag{4.6}$$

It may be noted that the formal equality $\Delta F^0 = -RT \ln K_P^M$ has been used by Boyd, *et al.*,[25] and Kressman and Kitchener[26] for ion-exchange reactions.

Equation 4.6 may be compared with equation 4.5. Evidently equation 4.6 takes no account of the relative mobilities of the ions in the membrane.

The derivation of equation 4.6 appears to be erroneous. It would seem that the error resides principally in Marshall's implicit assumption that a B.I.P. represents a true equilibrium; more properly, as conventionally defined, it is a steady state phenomenon. The assumption that the exchange sites on each membrane face are occupied wholly by the ions M and P is only an approximation. This approximation is reasonable only if the purity of the two solutions is continuously maintained either by changing these solutions frequently or flowing them past the membrane faces. In actuality, ions P are continually entering the external solution containing M ions and *vice versa*. Only if the ex-

---

[25] G. E. Boyd, J. Shubert and A. W. Adamson, *J. Am. Chem. Soc.*, **69**, 2818 (1947).

[26] T. R. E. Kressman and J. A. Kitchener, *J. Chem. Soc.*, 1190 (1949).

ternal solutions are constantly changed, so that their contamination is reduced to a negligible level, is the equilibrium between membrane faces and solutions maintained at such a level as to justify the assumption that the exchange sites on each face are wholly occupied by one ion. Marshall's derivation ignores the work done in maintaining these equilibria and thus gives rise to an equation appropriate only to B.I.P. systems which do not continuously degrade. As Sollner has observed,[5] such a system has no physical meaning.

Acknowledgment.—This discussion is based on material presented at the A.A.A.S. Gordon Research Conference on Ion Exchange held at New Hampton, New Hampshire, July, 1952. The writer is indebted to Dr. Paul D. Foote, Executive Vice President, Gulf Research & Development Company, for permission to publish the material.

ION-EXCHANGE MEMBRANES. II. MEMBRANE PROPERTIES IN RELATION TO BI-IONIC POTENTIALS IN MONOVALENT ION SYSTEMS

BY M. R. J. WYLLIE AND SHIRLEY L. KANAAN

Gulf Research and Development Company, Pittsburgh, Penna.

Received June 1, 1953

Measurements of bi-ionic potentials (B.I.P.'s) have been made across cation selective ion-exchange membranes. The monovalent ions H, Li, K, Na and Ag have been utilized. Heterogeneous membranes have been made from the ion-exchange resins Amberlite IR-100 and IR-120 and two sulfonated polystyrene cation exchangers of 4 and 17% nominal divinylbenzene cross linking. In addition, measurements have been made utilizing two proprietary homogeneous and one proprietary heterogeneous cation-selective membranes. The results obtained have been compared where possible with the known properties of the ion-exchange materials in the membranes, utilizing a theory of the B.I.P. enunciated previously. Satisfactory agreement between theory and experiment has been observed. It has been noted that for membranes made from IR-100 the nature of the bonding material appears to affect the properties of the membrane. It has been suggested that B.I.P. measurements may be utilized in some cases for rapid approximate measurements of the selectivity constants of ion-exchange materials.

Introduction

In a previous publication[1] equations were derived for multi-ionic potentials across selective ion-exchange membranes. For the particular case of a membrane separating solutions of two different monovalent ions, it was shown that the membrane potential or bi-ionic potential (B.I.P.) reduced to the following form

$$E = \frac{RT}{F} \ln (a_{\mathrm{M}}\bar{U}_{\mathrm{M}}/a_{\mathrm{P}}\bar{U}_{\mathrm{P}}) \qquad (1)$$

In equation 1, R is the gas constant, T the absolute temperature, F the Faraday constant, a_{M} and a_{P} the activities of the critical monovalent ions M and P in the solutions separated by an ideally selective ion-exchange membrane and $\bar{U}_{\mathrm{M}}/\bar{U}_{\mathrm{P}}$ is the apparent intramembrane mobility ratio of the two ions. It was further shown that the ratio $\bar{U}_{\mathrm{M}}/\bar{U}_{\mathrm{P}}$ could be related to the chemical and electrical properties of a membrane by the approximate relationship

$$\bar{U}_{\mathrm{M}}/\bar{U}_{\mathrm{P}} \simeq K_{\mathrm{P}}^{\mathrm{M}}(\bar{k}_{\mathrm{M}}/\bar{k}_{\mathrm{P}}) \qquad (2)$$

In equation 2, $K_{\mathrm{P}}^{\mathrm{M}}$ is the conventional selectivity constant of the ion-exchange material in the membrane for the exchange reaction between ion P on the membrane and ion M in the solution. The ratio $\bar{k}_{\mathrm{M}}/\bar{k}_{\mathrm{P}}$ is the ratio of the electrical conductivities of the membrane when wholly in the ionic forms M and P, respectively

The object of this paper is to examine the validity of equations 1 and 2.

Experimental

Membranes.—Heterogeneous membranes selective to cations were made from two commercial cation-exchange resins, Amberlites IR-100 and IR-120,[2] and two sulfonated polystyrene resins of 4 and 17% nominal divinylbenzene (D.V.B.) cross linking.[3] The methods of membrane manufacture used followed lines outlined previously by Wyllie and Patnode.[4] Certain modifications were made to these methods in order to investigate relationships that might exist between methods of manufacture and B.I.P.'s observed. All membranes used were of one inch diameter.

Amberlite IR-100/Polystyrene Membranes.—These were molded in a hydraulic press. An intimate mixture of < 325 mesh U. S. Standard Screen series IR-100 and polystyrene powders was compressed to 1000 p.s.i. and heated to 120° and then compressed to 5200 p.s.i. and heated to 205°. Other membranes were molded similarly except that a final pressure of 10,000 p.s.i. was utilized. In all cases, bone-dry exchange resin in the hydrogen form was used in the proportions by weight of 70% IR-100 and 30% polystyrene.

Amberlite IR-100/Lucite Membranes.—<325 mesh U. S. Standard Screen series IR-100 and Lucite powders in the proportions by weight of 25% bone-dry IR-100 in the hydrogen form and 75% Lucite were molded utilizing a pressure of 3000 p.s.i. and a maximum temperature of 150°.

Amberlite IR-100/Paraffin Wax Membranes.—IR-100 granules of 20 to 50 mesh U. S. Standard Screen series were mixed with a quantity of molten paraffin wax just sufficient to fill the voids between them. The temperature of the molten wax was 80°. The resulting slurry was allowed to cool and set in a one-inch diameter mold. The upper and lower faces of the button of resin and wax formed were trimmed flat with a sharp knife.

Amberlite IR-120/Polystyrene Membranes.—Molding conditions identical with those for IR-100/polystyrene membranes were used except that the proportions of the two powders were 60% by weight of the hydrogen form of bone-dry IR-120 and 40% by weight of polystyrene. Maximum molding pressure was 5200 p.s.i.

Amberlite IR-120/Selectron Membranes.—Air-dried <325 mesh U. S. Standard Screen series IR-120 powder in

---

(1) M. R. J. Wyllie, THIS JOURNAL, 58, 67 (1954).

(2) Amberlite exchange resins are a proprietary product of the Rohm and Haas Company, Philadelphia, Penna.

(3) Kindly supplied by Dr. H. E. Weaver of the Rohm and Haas Company.

(4) M. R. J. Wyllie and H. W. Patnode, THIS JOURNAL, 54, 204 (1950).

the hydrogen form was briquetted under a pressure of 5000 p.s.i.[5] The briquette was then evacuated and, while under vacuum, was flooded with Selectron 5001[6] containing 1% methyl ethyl ketone peroxide as catalyst and 0.05% cobalt naphthenate as accelerator. Restoration of atmospheric pressure served to force the Selectron binding plastic into the pores of the briquette. After the plastic had set, the membrane was ground to size. This procedure is convenient if membranes of relatively high conductivity are required.

Amberlite IR-120/Paraffin Wax Membranes.—Air-dried 16–50 mesh U. S. Standard Screen series IR-120 spheres were used. Otherwise conditions were identical to those used for making IR-100/paraffin wax membranes.

Sulfonated Polystyrene 17% D.V.B./Polystyrene Membranes.—Molding conditions were similar to those used for making IR-100 polystyrene membranes except that a mixture of 50% by weight of bone-dry exchange resin in the hydrogen form and 50% by weight of polystyrene was utilized. Maximum molding pressure was 5200 p.s.i. and maximum temperature 170°.

Sulfonated Polystyrene 17% D.V.B./Paraffin Wax Membranes.—Air-dried <325 mesh U. S. Standard Screen series ion-exchange resin powder was stirred into molten paraffin wax (80°) until a thick slurry was formed. The slurry was cast into a membrane in the manner used for IR/100 paraffin wax membranes.

In addition to the membranes that were made, the following commercially available cation-exchange membranes were also employed.

Amberplex C-1 Membranes.—A heterogeneous cation-exchange membrane made by the Rohm and Haas Company of Philadelphia, Pennsylvania.[7]

Permionic CR-51 Membranes.—This is a homogeneous cation-exchange membrane made by Ionics, Inc., of Cambridge, Massachusetts.[8]

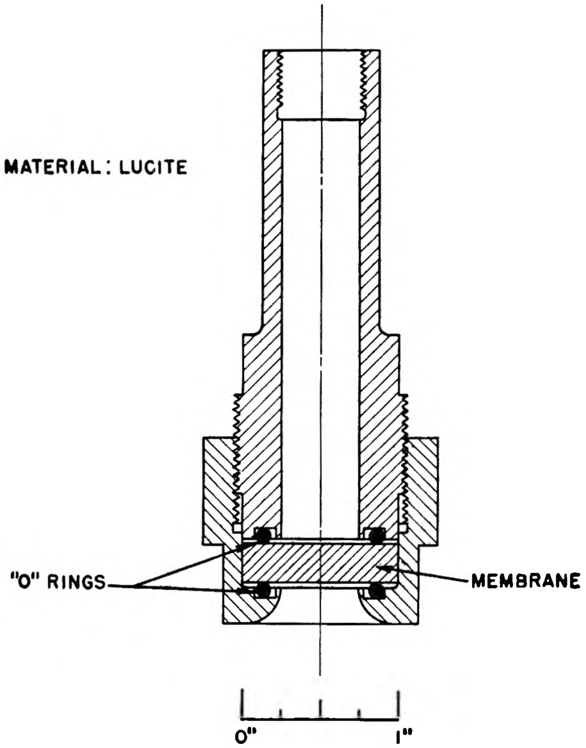

Fig. 1.—Membrane holder.

Permutit Membranes.—This is a homogeneous cation-exchange membrane made by the Permutit Company of London, England.[9]

Membrane Potential Measurements.—The membranes, which varied in thickness from 25 mils in the case of the Amberplex C-1 membranes to 4 mm. in the case of the membranes bonded with paraffin wax, were mounted in simple Lucite cells. These cells were designed to accommodate membranes of one inch diameter. Sealing and quick interchange of membranes was achieved satisfactorily by utilizing rubber "O" ring seals. A cross-section of the holder is shown in Fig. 1. The measurements reported were all made with calomel electrodes and saturated KCl bridges when chloride solutions were used, and calomel electrodes and saturated NH_4NO_3 bridges when nitrate solutions were used. Care was taken to reduce to a minimum contamination of test solutions with salts from the bridges. Potential measurements were made with a Leeds and Northrup Type K-2 potentiometer and thermionic amplifier. The latter is not essential except during the short period when a membrane made from dry resin is hydrating on first use. Measurements were recorded when three changes in the test solutions, after an apparently constant potential had been attained, did not lead to a potential variation exceeding ±0.2 mv. At least two membranes were utilized in each experiment. It was found unnecessary to flow solutions past the membranes. All potentials were corrected to 25°.

Conductivity Measurements.—In order to make measurements of their conductivity after equilibration in various solutions, a number of membranes were made in the form of right cylinders of one inch diameter and one-half inch length. The resistances of these cylinders, after wiping dry, were measured between faces utilizing a 1000 cycle a.c. bridge with capacitance correction and a cathode ray oscilloscope as null-point indicator. The electrodes used were platinized-platinum gauze backed by felt saturated with a solution identical to that in which a cylinder had been equilibrated. The reproducibility of measurements was about ±5%. The method used is convenient if the highest accuracy is not required. Its disadvantage is the length of time required to bring a cylinder to equilibrium with a solution of a particular nature and concentration. This is most noticeably the case when cylinders composed of compact heterogeneous membrane materials are converted from one ionic form to another. Periods of a week or more, with frequent changes of the equilibrating solutions, appear necessary before a constant conductivity is attained.

Solutions.—The following solutions were used: HCl, HNO_3, NaCl, KCl, LiCl and $AgNO_3$. All were made from C.P. reagents and distilled water.

Results

If $\bar{U}_M/\bar{U}_P$ is truly a membrane property, *i.e.*, is independent of changes made in the activities a_M and a_P of the external solutions, it is apparent from equation 1 that a plot of E on a linear scale against a_M on a logarithmic scale, for a_P constant, should give a straight line. Similarly a straight line should be obtained for the analogous case in which a_M is maintained constant and a_P varied. Both straight lines should show potential changes of RT/F, or 59.16 mv. at 25°, for each tenfold change in activity.

Figure 2 shows typical examples of such plots for membranes made with different binding materials and different ion-exchange resins. In all cases, the B.I.P.'s plotted on Fig. 2 were determined in turn between a 0.01 m KCl solution and solutions of LiCl varying in molality from 0.01 to 4.0 m, and then between a 0.01 m LiCl solution and KCl solutions ranging from 0.01 to 4.0 m. The potentials were plotted as shown against mean molal activi-

---

(5) This pressure is suitable if a one-inch diameter mold is used for the briquetting process and leads to an interstitial porosity in the briquette of about 20%. For molds of other sizes, the pressure required to produce a porosity of 20% should first be determined.

(6) Made by Pittsburgh Plate Glass Company.

(7) A. G. Winger, G. W. Bodamer and R. Kunin, *J. Electrochem. Soc.*, **100**, 178 (1953).

(8) W. Juda, N. W. Rosenberg, J. A. Marinsky and A. A. Kasper, *J. Am. Chem. Soc.*, **74**, 3736 (1952).

(9) T. R. E. Kressman, *Nature*, **165**, 568 (1950).

TABLE I

Membrane, $\bar{U}_M/\bar{U}_P$	Permutit	Permionic CR-51	Amberplex C-1	IR-100/ wax	IR-100/ lucite	IR-100/ poly-styrene 5200 p.s.i.	IR-120/ polystyrene	Sulfonated polystyrene 4% D.V.B./ wax	Sulfonated polystyrene 17% D.V.B./ polystyrene
$\bar{U}_K/\bar{U}_{Li}$	1.8	1.7	2.1	2.6	4.3	5.7	3.1	1.4	3.0[a]
$\bar{U}_K/\bar{U}_{Na}$	1.4	1.4	1.6	1.7	1.9	2.4	1.6	1.4	1.8
$\bar{U}_H/\bar{U}_K$	...	3.1	4.0	3.2	3.9	3.3	2.2	3.6	1.4
$\bar{U}_H/\bar{U}_{Na}$	...	5.3	4.6	5.5	5.9	6.3	3.5	4.8	2.0
$\bar{U}_{Na}/\bar{U}_{Li}$	1.3	1.2	1.6	1.7	1.8	2.7	1.8	1.9	2.3
$\bar{U}_H/\bar{U}_{Ag}$	...	1.8	2.0	2.2	1.5	1.4	1.8	2.0	2.2
$\bar{U}_H/\bar{U}_{Li}$	...	7.1	6.7	8.9	12.8	9.8	5.9	6.2	6.0

[a] From 0.0089 *m* activity LiCl *versus* KCl only.

ties. Mean activity coefficients were taken from Harned and Owen[10] or Conway.[11]

Figure 2 shows graphically a number of the general observations made in this work. Among these are the fact that excellent straight-line plots in accordance with the expectations of equation 1 are obtained if mean activities form the basis for plotting the lines. It appears that mean activities are a good approximation to the single ion activities theoretically required in equation 1. A similar inference has been drawn by Kressman.[12] The concentration range over which the plot of log activity against potential is a straight line has been found to depend upon the method used to manufacture a membrane and the nature of the ion-exchange material in the membrane. Since certain membranes, for example those made from IR-100/polystyrene, generally maintain linearity to the highest concentrations used, it seems probable that with these membranes the effect of water transfer[1] in reducing the observed potential is either negligible or compensated by the error involved in using mean activity data. The falling-off in potential with increase in concentration, observed in the case of IR-100/wax and homogeneous membranes, is probably in large measure the consequence of the lower selectivity constants of these membranes. A low selectivity constant implies also a high Donnan uptake of anion.[8] The relatively flat conductivity–concentration curves of IR-100/polystyrene membranes, shown in Fig. 3, confirm that these membranes have a relatively low Donnan uptake of anion and, accordingly, a high selectivity constant. From plots of the form of Fig. 2, it is possible to establish two pairs of corresponding a_M and a_P values for which E in equation 1 is zero. The ratio of a_M/a_P for $E = 0$ is then equal to $\bar{U}_P/\bar{U}_M$. Accordingly, two values of $\bar{U}_P/\bar{U}_M$ may be obtained from each plot by reading off the activities at which the straight lines cut the activity axis at zero potential. The apparent intramembrane mobility ratios listed in Table I were obtained using this technique. In certain cases the ratios calculated from the two different sets of a_M/a_P values were not identical; in such cases the arithmetic average of the two ratios is recorded.

A difficulty which was noted when checks were being made of the reproducibility of the ratios re-

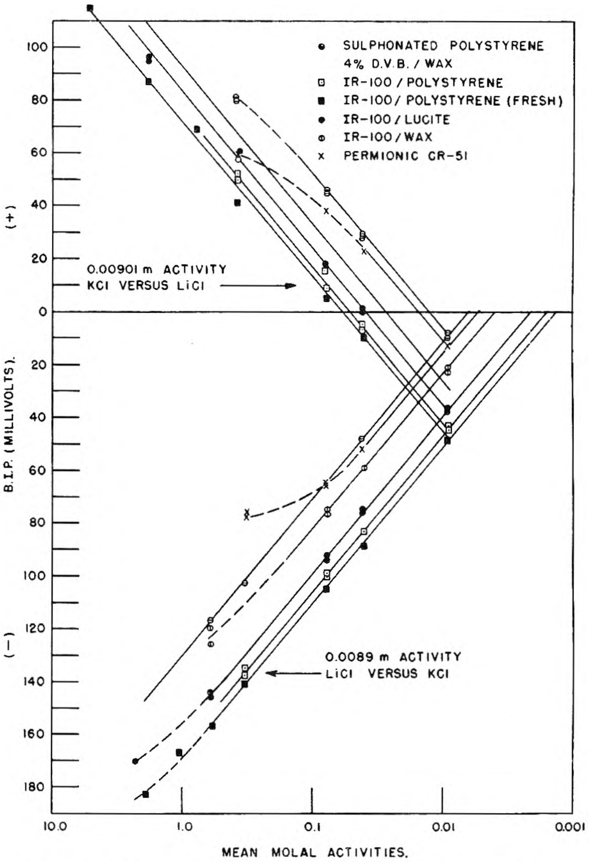

Fig. 2.—Typical plots of bi-ionic potentials against logarithms of mean molal activities for the system KCl–LiCl.

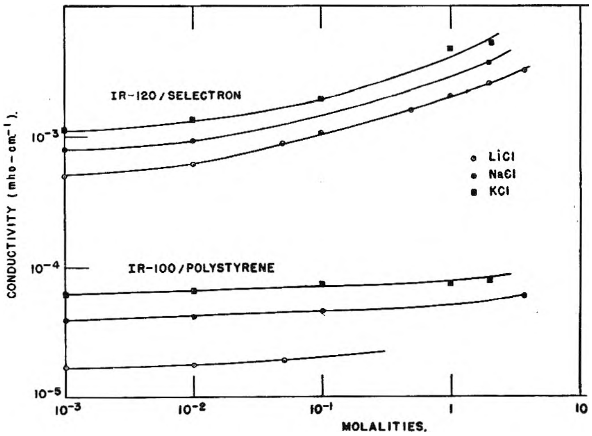

Fig. 3.—Conductivity of IR-120 and IR-100 membranes as a function of molality of equilibrating solution.

---

(10) H. S. Harned and B. B. Owen, "The Physical Chemistry of Electrolytic Solutions," 2nd Ed., Reinhold Publ. Corp., New York, N. Y., 1950.

(11) B. E. Conway, "Electrochemical Data," 1st Ed., Elsevier Publishing Co., Houston, Texas, 1952.

(12) Reported by J. F. Duncan, *Nature*, **169**, 22 (1952).

corded in Table I is exemplified in Fig. 2 by the data plotted for a fresh IR-100/polystyrene membrane. By a fresh membrane is meant one used for the first time in the LiCl/KCl system. Two good straight lines, as demanded by equation 1, result when the potentials given by the fresh membrane are plotted, but the ratio $\bar{U}_K/\bar{U}_{Li}$ is about 7.0, whereas that determined for similar membranes after extensive use and soaking in the solutions is 5.7. This phenomenon is tentatively ascribed to the fact that a fresh membrane has not had time to imbibe an equilibrium water content. It is customary when measurements are made of the physical properties of granular ion-exchange resins to work the resin before a series of experiments are commenced; an analogous procedure appears to be desirable when utilizing ion-exchange membranes.

The plotting method used to determine $\bar{U}_M/\bar{U}_P$ ratios has been found to have advantages over one based on measurements of potential at known ratios a_M/a_P in equation 1. The ratio of a_M/a_P generally selected is unity. While the latter method was used in a few cases in order to establish the fact that results in agreement with those obtained by plotting could be obtained, it appears to be considerably less accurate than the plotting method. The inaccuracy stems from the fact that the plotting method enables a much better average value to be obtained for $\bar{U}_M/\bar{U}_P$, since all data obtained are utilized in the plotting and, in addition, the slope of the line through these data is known. The major theoretical disadvantage of the plotting method, the relatively large difference in the activities of the solvents in the two solutions separated when a_M is large by comparison with a_P, or *vice versa*, does not appear in practice to overshadow errors inherent in the measurement of B.I.P.'s.

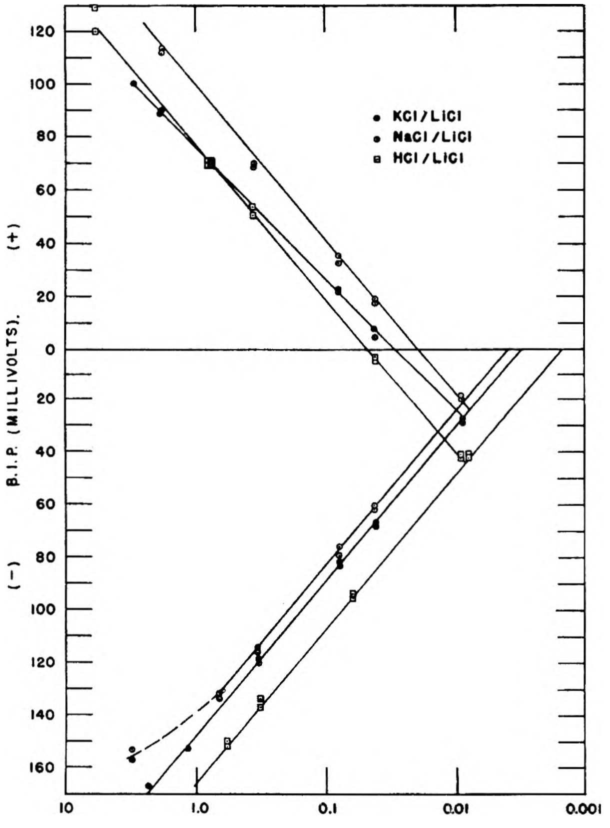

Fig. 4.—B.I.P. data for sulfonated polystyrene 17% D.V.B. resin membranes with paraffin wax or polystyrene bonding material in LiCl systems.

An anomaly encountered when membranes made from sulfonated polystyrene of 17% nominal D.V.-B. cross linking were used is shown in Fig. 4. For the systems HCl/LiCl and NaCl/LiCl the potential data are in accord with the requirements of equation 1. For the system KCl/LiCl the potentials between solutions of KCl of increasing mean molal activity and a LiCl solution of constant mean molal activity (0.0089 *m*) increased by 59 mv. for each tenfold change in the mean molal activity of the KCl solutions. When the mean molal activities of the LiCl solutions were increased and the mean molal activity of the KCl solution maintained constant (0.00901 *m*), the potential increased by only about 50 mv. for each tenfold change in LiCl activity. The anomalous slope of this plot was reproducible and was obtained using membranes made both with polystyrene and paraffin wax as bonding material. Membranes made from IR-100/polystyrene and molded at 10,000 p.s.i. in some cases gave rise to similar anomalous slopes in KCl/LiCl systems if measurements were made before the membranes were fully equilibrated. Only membranes made from sulfonated polystyrene of 17% nominal D.V.B. cross linking invariably gave the anomalous slope. The age or previous history of these membranes did not appear to affect the phenomenon.

If the anomalous slope is attributed to the effects of water transfer, calculations based on an equation given previously[1] indicate a transfer of about 14.5 moles of water per mole of lithium ion transferred. While the quantity of water so calculated is not an unreasonable amount, the explanation does not seem acceptable in view of the fact that the systems HCl/LiCl and NaCl/LiCl give normal slopes. It seems more probable that the anomalous slope reflects the approximate nature of equations 1 and 2 and the fact that these equations ignore B.I.P. effects resulting from volume changes in the membrane.

In Fig. 5 the effects of working at molalities less than 0.01 *m* are shown. The B.I.P. data refer to the system LiCl/HCl. Figure 5 reveals that when the molalities of both the HCl and LiCl used fell below about 0.005 *m* the potentials recorded were less than those theoretically anticipated. The apparent breakdown in theoretical membrane properties at very low concentrations of one or both solutions separated by the membranes appears to be quite general. It has been observed also by Scatchard[13] and McLean, *et al.*[14] The fact that the breakdown occurs with HCl as well as alkali salt solutions tends to discredit the theory[14] that it is a result of membrane hydrolysis. Preliminary investigations suggest that the breakdown is a form of membrane polarization and that it occurs when the rate-determining step in the movement of

---

[13] G. Scatchard, paper presented to N.E. Section, A.C.S., November 13, 1952.

[14] E. O. McLean, S. A. Barber and C. E. Marshall, *Soil Sci.*, **72**, 315 (1951).

ions through an ion-exchange material changes from particle diffusion to film diffusion.[15] For present purposes the phenomenon is not significant. All measurements of apparent intramembrane mobility ratios recorded in Table I are based on straight lines of theoretical slope resulting from measurements made against 0.01 *m* solutions.

Although potentials reproducible within ±0.2 m.v. can be obtained for any one membrane if care is exercised, it is rare to obtain exact agreement between the potentials given by two nominally identical membranes under the same conditions. For this reason an accuracy better than about ±10% cannot be ascribed to the mobility ratios given in Table I.

In Table I, separate mobility ratios are not given for IR-120/wax, IR-120/Selection or sulfonated polystyrene 17% D.V.B./wax membranes since these membranes were found to give B.I.P. data identical, within the error of measurement, to the data given by membranes utilizing polystyrene as bonding material. Similarly, there appeared to be no significant difference between mobility ratios found when IR-100/polystyrene membranes molded at 5200 and 10,000 p.s.i. were used.

Attempts were made to establish whether the potentials given by the sulfonated polystyrene 4% D.V.B. resin membranes were affected by changing the bonding material from paraffin wax to polystyrene, Lucite or other relatively rigid plastic. Owing to the low cross linking of the exchange resin and its consequent large change in volume on hydration[16] it was not found possible to bond the resin into consistently satisfactory membranes with any available rigid plastic.[17] Membranes made by molding the 4% D.V.B. exchange resin with polystyrene disintegrated rapidly. It may be noted, however, that in the few cases in which significant data could be recorded before disintegration took place, the mobility ratios of membranes molded with polystyrene were substantially identical to the ratios given by membranes bonded with paraffin wax.

The data of Table I may be compared with mobility ratios computed from the B.I.P. data reported by Coleman.[18] Coleman's data refer to membranes molded from 60% powdered ion-exchanger in the sodium form and 40% powdered polystyrene. The molding pressure was 5000 p.s.i. and the molding temperature 205°. The ion-exchange resins employed were Amberlites IR-100 and IR-120. For IR-100 membranes Coleman found $\bar{U}_K/\bar{U}_{Li} = 3.7$ and $\bar{U}_K/\bar{U}_{Na} = 2.2$; for IR-120 $\bar{U}_K/\bar{U}_{Li} = 4.4$ and $\bar{U}_K/\bar{U}_{Na} = 2.5$. These ratios differ significantly from the same ratios reported in Table I for membranes almost identical to those used by Coleman. Unless the discrepancy between the two sets of figures results from considerable batch-to-batch variations in the properties of commercial IR-100 resins, its cause is not obvious.

Discussion

From equation 2 it follows that

$$\frac{\bar{k}_M}{\bar{k}_P} \simeq \frac{(\bar{U}_M/\bar{U}_P)}{K_P^M} \qquad (3)$$

In Table II the consequences of equation 3 are examined for the membranes made from IR-100, IR-120 and the sulfonated polystyrene exchange resins of 4 and 17% nominal D.V.B. cross linking. The K_P^M data for each of the four exchange resins have been taken from the literature. It may be noted that the K_P^M figures used can be considered to be only approximate. Apart from the lack of agreement in the literature between values of K_P^M reported by different workers for identical exchange reactions and nominally identical ion-exchange materials,[19] it is now accepted that the value of K_P^M is a function of the extent to which ion M has been replaced by ion P. The values of K_P^M chosen for use in Table II are, as far as possible, those which have been reported by more than one worker. The effect of the extent of replacement of one ion by another has been largely neglected as an error small by comparison with the others involved in equation 3. Where possible, however, K_P^M values corresponding to 50% replacement of ion M by ion P were chosen.

In Table II the ratios $\bar{k}_M/\bar{k}_P$ calculated from equation 3 are compared where possible with ratios

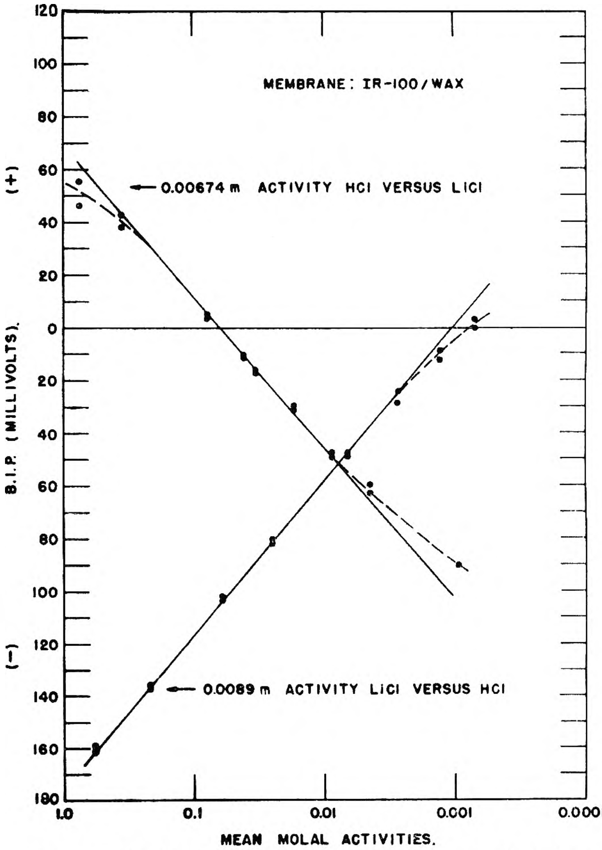

Fig. 5.—Typical departure of measured potentials from theoretical potentials at both high and low solution activities is shown by broken lines.

---

[15] D. Reichenberg, *J. Am. Chem. Soc.*, **75**, 589 (1953)

[16] H. P. Gregor and J. I. Bregman, *J. Colloid Sci.*, **6**, 323 (1951).

[17] Success has been obtained utilizing urea-formaldehyde as bonding plastic.

[18] N. T. Coleman, *Soil Sci.*, **74**, 115 (1952).

[19] For comments on this point see, for example, W. C. Bauman, R. E. Anderson and R. M. Wheaton in the chapter "Ion Exchange," "Annual Review of Physical Chemistry," Vol. 3, Annual Reviews, Inc., Stanford, Calif., 1952.

Table II

System M-P	Membrane	K_P^M	Source of K_P^M val.	$\bar{U}_M/\bar{U}_P$	$\bar{k}_M/\bar{k}_P$ Calcd.	$\bar{k}_M/\bar{k}_P$ Measd.	Source of $\bar{k}_M/\bar{k}_P$ val.	$l_{\infty M}/l_{\infty P}$
K–Li	IR-100/wax	2.63	20	2.6	1.0	1.36	21	1.90
K–Li	IR-100/polystyrene 5200 p.s.i.	2.63	20	5.7	2.2	3.6	This work	1.90
K–Li	IR-100/Lucite	2.63	20	4.3	1.6			1.90
K–Li	IR-120/polystyrene	2.66	16	3.1	1.2	2.3	This work	1.90
K–Li	Sulfonated polystyrene 4% D.V.B./wax	2.1	16	1.4	0.7			1.90
K–Li	Sulfonated polystyrene 17% D.V.B./polystyrene	2.46	16	3.0	1.2			1.90
K–Na	IR-100/wax	1.95	20	1.7	0.9	1.3	21	1.47
K–Na	IR-100/polystyrene 5200 p.s.i.	1.95	20	2.4	1.2	1.6	This work	1.47
K–Na	IR-100/Lucite	1.95	20	1.9	1.0			1.47
K–Na	IR-120/polystyrene	1.60	16	1.6	1.0	1.5	This work	1.47
K–Na	Sulfonated polystyrene 4% D.V.B./wax	1.20	16	1.4	1.2			1.47
K–Na	Sulfonated polystyrene 17% D.V.B./polystyrene	2.1	16	1.8	0.9			1.47
H–K	IR-100/wax	0.48	22	3.2	6.7	6.9	21	4.75
H–K	IR-100/polystyrene 5200 p.s.i.	.48	22	3.3	6.9			4.75
H–K	IR-100/Lucite	.48	22	3.8	7.9			4.75
H–K	IR-120/polystyrene	.52	16	2.2	4.2			4.75
H–K	Sulfonated polystyrene 4% D.V.B./wax	.64	16	3.6	5.6			4.75
H–K	Sulfonated polystyrene 17% D.V.B./polystyrene	.41	16	1.4	3.4			4.75
Na–Li	IR-100/wax	1.77	20	1.7	1.0	1.36	21	1.30
Na–Li	IR-100/polystyrene 5200 p.s.i.	1.77	20	2.7	1.5	2.3	This work	1.30
Na–Li	IR-100/Lucite	1.77	20	1.8	1.0			1.30
Na–Li	IR-120/polystyrene	1.85	16	1.8	1.0	1.6	This work	1.30
Na–Li	Sulfonated polystyrene 4% D.V.B./wax	1.75	23	1.9	1.1			1.30
Na–Li	Sulfonated polystyrene 17% D.V.B./polystyrene	1.2	23	2.3	1.9			1.30
H–Ag	IR-100/wax	0.15	24	2.2	15	43.0	21	5.65
H–Ag	IR-100/polystyrene 5200 p.s.i.	.15	24	1.4	9.3			5.65
H–Ag	IR-100/Lucite	.15	24	1.5	10			5.65
H–Ag	IR-120/polystyrene	.059	25	1.8	31			5.65
H–Ag	Sulfonated polystyrene 17% D.V.B./polystyrene	.062	26	2.2	36			5.65
H–Li	IR-100/wax	1.54	22	8.9	14	12.5	21	9.03
H–Li	IR-100/polystyrene 5200 p.s.i.	1.54	22	9.8	15			9.03
H–Li	IR-100/Lucite	1.54	22	12.8	20			9.03
H–Li	IR-120/polystyrene	1.3	16	5.9	7.7			9.03
H–Li	Sulfonated polystyrene 4% D.V.B./wax	1.34	27	6.2	8.3			9.03
H–Li	Sulfonated polystyrene 17% D.V.B./polystyrene	1.02	27	6.0	6.1			9.03
H–Na	IR-100/wax	0.8	22	5.5	6.9	9.2	21	6.97
H–Na	IR-100/polystyrene 5200 p.s.i.	.8	22	6.3	7.9			6.97
H–Na	IR-100/Lucite	.8	22	5.9	7.4			6.97
H–Na	IR-120/polystyrene	.6	29	3.5	6.0	7.95	28	6.97
H–Na	Sulfonated polystyrene 4% D.V.B./wax	.8	29	4.8	6.0			6.97
H–Na	Sulfonated polystyrene 17% D.V.B./polystyrene	.39	29	2.0	5.1			6.97

$\bar{k}_M/\bar{k}_P$ directly measured and ratios of the limiting ionic conductances in water at 25° ($l_{\infty(M)}/l_{\infty(P)}$) of the ions M and P. The latter data were taken from Conway.[11]

A comparison of the calculated and measured $\bar{k}_M/\bar{k}_P$ ratios reveals that the numerical agreement between the two ratios is reasonably good; in the worst case, the $\bar{k}_H/\bar{k}_{Ag}$ ratio for IR-100/wax membranes, the measured ratio is only about threefold greater than the computed ratio. The data of Spiegler and Coryell[26] for ion-exchange resins suggest that the ratio $\bar{k}_M/\bar{k}_P$ in a resin containing a mixture of the ions M and P will be smaller than the same ratio for two pure ionic forms of the same resin if $\bar{k}_M > \bar{k}_P$. Hence the calculated $\bar{k}_M/\bar{k}_P$ ratios in Table II would be expected to be smaller than the computed ratios. The effect is apart from other approximations involved in the method used to derive the computed ratios. Table II shows that where such comparisons are possible, only the computed ratio $\bar{k}_H/\bar{k}_{Li}$ for IR-100/wax membranes exceeds the measured ratio. In all other cases the ratios computed are, as would be expected, smaller than those measured.

In general the agreement between the computed and measured $\bar{k}_M/\bar{k}_P$ ratios must be deemed satisfactory. The data for the silver–hydrogen system are particularly noteworthy. In this system the ratio $\bar{U}_H/\bar{U}_{Ag}$ has the relatively small value of 2.2 although the hydrogen ion is able to move very much more freely through the IR-100 resin than the silver ion.[17] The wide difference in the mobilities of the two ions appears to be offset, as forecast by equation 3, by the much higher adsorbability of silver ion on IR-100 by comparison with hydrogen ion.

A comparison of the calculated $\bar{k}_M/\bar{k}_P$ ratios with the ratios $l_{\infty(M)}/l_{\infty(P)}$ shows, for IR-100/wax and IR-120/polystyrene membranes, good agreement for all the systems considered except hydrogen–silver. Similar comparisons may be made from the data of Table II for the other membranes tabulated. In the case of the sulfonated polystyrene membranes of both 4 and 17% nominal D.V.B. cross linking, the agreement between calculated $\bar{k}_M/\bar{k}_P$ ratios and $l_{\infty(M)}/l_{\infty(P)}$ ratios is also satisfactory. Again, however, the hydrogen–silver systems are an exception. The data suggest that for hydrogen and the alkali cations considered, the effect of the internal structure of all the membranes on cation mobilities is very largely geometric in nature. That is, the hydrogen and alkali ions are all subjected to substantially similar restraints. Silver ions are apparently held much more tightly in all the ion-exchange materials used. In this respect, it is apparent that the behavior of sulfonated polystyrene cation-exchanger materials[30] is similar to that noted by Heymann and O'Donnell[21] for IR-100.

Paraffin wax was selected as a bonding agent in the fabrication of certain heterogeneous ion-exchange membranes because this material does not require the imposition of pressure or high temperature to produce a membrane. In addition it was hoped that the negligible tensile strength of paraffin wax would obviate any tendency for the bonding material to constrain the ion-exchange resin particles. Such constraint might prevent the particles from imbibing an equilibrium water saturation when the membranes were used.[4]

A comparison of the $\bar{U}_M/\bar{U}_P$ and $\bar{k}_M/\bar{k}_P$ ratios in Table II for membranes made from IR-100/wax, IR-100/polystyrene and IR-100/Lucite shows what are believed to be significant differences. The differences are particularly marked for the systems potassium–lithium and hydrogen–lithium. The fact that molding pressures of 5200 and 10,000 p.s.i., when polystyrene was utilized as bonding plastic, produced no significant changes in $\bar{U}_M/\bar{U}_P$ ratios suggests that the differences observed in the ratios depend upon the nature of the bonding plastic rather than the pressure of molding. For all systems except hydrogen–silver, the ratios $\bar{U}_M/\bar{U}_P$ are lower for the IR-100/wax membranes than for the IR-100/polystyrene or IR-100/Lucite membranes. Differences between the $\bar{U}_M/\bar{U}_P$ ratios given by the IR-100/polystyrene and IR-100/Lucite membranes are less unequivocal. However, with the notable exception of the hydrogen–lithium system, it would appear that the apparent intramembrane mobility ratios for polystyrene-bonded IR-100 membranes exceed those for membranes bonded with Lucite.

Two possibilities suggest themselves as an explanation for the apparent influence of the nature of the bonding material on the $\bar{U}_M/\bar{U}_P$ ratios of IR-100 membranes. These are steric effects and effects dependent on the internal concentration of the ions in the pores of the membranes. Both effects stem from the probability that the equilibrium expansion of the particles of ion-exchange resins in a heterogeneous membrane, when the membrane is immersed in a solution, will be controlled by the osmotic swelling pressure of the resin particles and a constraining force, opposing expansion, set up by the bonding plastic. The latter force would be related to the physical properties of the material used to bond the ion-exchange resin particles.

Assume that the pores of a fully hydrated ion-exchange resin are not all of identical size. This does not appear to be an unreasonable assumption. Then the effect of a bonding material able to prevent full hydration of the resin will be to cause a decrease in the size of all the pores. Certain of the pores may then become too small to permit passage of ions which exceed a certain size. The hydrated lithium ion, being the largest of those considered in this study, will be most affected. In

---

(20) C. Krishnamoorthy and R. Overstreet, *Soil Sci.*, **64**, 41 (1950).

(21) E. Heymann and I. J. O'Donnell, *J. Colloid Sci.*, **4**, 405 (1949).

(22) R. K. Cannan, *Ann. N. Y. Acad. Sci.*, **47**, 135 (1946).

(23) Calculated from K^K_{Li} and K^K_{Na} data of Gregor and Bregman.[18]

(24) T. R. E. Kressman and J. A. Kitchener, *J. Chem. Soc.*, 1190 (1949).

(25) W. K. Lowen, R. W. Stoenner, W. J. Argersinger, A. W. Davidson and D. N. Hume, *J. Am. Chem. Soc.*, **73**, 2666 (1951).

(26) O. D. Bonner and V. Rhett, THIS JOURNAL, **57**, 254 (1953) (Data for 16% D.V.B. exchange resin).

(27) Calculated from K^K_{Li} and K^K_H data of Gregor and Bregman.[18]

(28) K. S. Spiegler and C. D. Coryell, THIS JOURNAL, **56**, 106 (1952).

(29) D. Reichenberg, K. W. Pepper and D. J. McCauley, *J. Chem. Soc.*, 493 (1951).

(30) IR-120 is a sulfonated polystyrene with about 8% nominal D.V.B. cross linking.

consequence the distribution of ions in very small pores will be abnormal in systems involving lithium ions since these pores will not be able to accommodate lithium ions. The consequence will be an apparent increase in the intramembrane mobility ratio of ions smaller than lithium by comparison with lithium ions, since, on the average, fewer lithium ions will be available to carry current. The increase in the ratios $\bar{U}_K/\bar{U}_{Li}$, $\bar{U}_H/\bar{U}_{Li}$ and $\bar{U}_{Na}/\bar{U}_{Li}$ for IR-100 membranes bonded with polystyrene and Lucite by comparison with those bonded with wax, shown in Table I, conforms to this view. The possibility of effects of this type has been forecast by Sollner.[31]

If the resin is prevented by the bonding material from swelling fully, less water will be contained in the pores and an increase in the internal concentration of the exchangeable ions in the pores of the membranes will result. In this regard the effect of the bonding material may be regarded as analogous to an increase in cross linking. According to Glueckauf's[32] recent quantitative theory of the selectivity of ion-exchangers, an increase in the internal concentration of an ion-exchange material will generally lead to an increase in its selectivity constant K_P^M. On this basis, assuming $\bar{k}_M/\bar{k}_P$ to be unaffected by the concentration increase, the ratios $\bar{U}_K/\bar{U}_{Li}$, $\bar{U}_K/\bar{U}_{Na}$, $\bar{U}_{Na}/\bar{U}_{Li}$, $\bar{U}_H/\bar{U}_{Li}$ would be expected to increase for membranes bonded with polystyrene and Lucite while the ratios $\bar{U}_H/\bar{U}_K$, $\bar{U}_H/\bar{U}_{Ag}$ and $\bar{U}_H/\bar{U}_{Na}$ would be expected to decrease. As shown in Table I the increases are noted but of the expected decreases only that of $\bar{U}_H/\bar{U}_{Ag}$ is observed.

In its simplest form Glueckauf's theory will not account for the observed data. A possible key to the failure of the theory may be the neglect, in Glueckauf's work, of the external pressure acting on the ion-exchange system. The external pressure term serves to diminish the increase in K_P^M resulting from an increase in internal concentration. While the external pressure term is negligible in the ion-exchange resins considered by Glueckauf, in bonded membranes the term is probably significant. No easy method for its measurement is evident. The effect of the nature of the bonding material used in heterogeneous membranes clearly requires further study, since it appears to offer a method of altering intramembrane mobility ratios.

In membranes made from sulfonated polystyrene the nature of the bonding materials utilized did not appear to have any significant effect on the intramembrane mobility ratios observed. The results are not conclusive since the number of bonding materials used was small. It seems possible that the generally higher osmotic pressures produced by sulfonated polystyrene resins by comparison with IR-100 resins are sufficient to overcome entirely the tendency of the bonding material to prevent full hydration of the resin particles. It may be observed that a quantitative investigation of the extent of hydration of resin particles in bonded membranes could not be carried out because of the impossibility of determining whether all the particles bonded were free to hydrate, *i.e.*, were not particles, like flies in amber, completely isolated by bonding material.

The data of Table II suggest that where membranes may be made from ion-exchange material by bonding in paraffin wax, approximate values of K_P^M may be determined from measurements of $\bar{U}_M/\bar{U}_P$ and $\bar{k}_M/\bar{k}_P$. This technique may be of value in certain clay systems which are of practical importance but for which the measurement of K_P^M by conventional methods is tedious or difficult.

Acknowledgment.—The writers wish to thank Dr. Paul D. Foote, Executive Vice President, Gulf Research and Development Company, for permission to publish this work.

---

(31) K. Sollner, This Journal, **53**, 1226 (1949).

(32) E. Glueckauf, *Proc. Roy. Soc.* (*London*), **A214**, 207 (1952).

POLAROGRAPHIC STUDIES IN NON-AQUEOUS MEDIA.
II. FORMAMIDE-ACETAMIDE MIXTURES[1-3]

By John H. Hook,[4] Harry Letaw, Jr.,[5] and Armin H. Gropp

Chemistry Department, University of Florida, Gainesville, Florida

Received June 2, 1952

A polarographic study of several inorganic and organic substances was carried out in formamide–acetamide mixtures. It was found that the $E_{1/2}$ values obtained in these mixtures are in good agreement with those obtained in pure formamide. Exceptional behavior is described in which extreme departure of $(i_d/C)\cdot\eta^{1/2}$ values from their predicted linearity was observed

Introduction

Virtually ideal polarographic behavior of a number of inorganic ions and organic compounds in formamide solutions has been reported.[6] A further extension of polarographic investigations of non-aqueous media was carried out by studies of solutions in formamide–acetamide mixtures.

The question of the effect of viscosity on the polarographic wave has been experimentally investigated several times in recent years.[7] In all the papers cited, save that of Vavruch, it has been reported that i_d is inversely proportional to the square root of the viscosity of the solvent. Vavruch, in studies of saccharose solutions with viscosities as high as 16.0 cp., found that as the viscosities of solutions containing inorganic ions were increased, the i_d values became systematically greater than those predicted by the relationship mentioned above. Although Brasher and Jones[7] had studied NaOH and H_2SO_4 solutions whose viscosities were in the neighborhood of 5.5 cp., they encountered no such anomalous behavior. It is believed that the increase in viscosity provided by the addition of acetamide to its next lowest homolog, formamide, yields a more nearly ideal system than those previously mentioned.

Heyrovsky,[8] in the classical derivation of the expression for $E_{1/2}$, related this quantity to the viscosity of the solution in which it is determined. Although differences in $E_{1/2}$ values have been reported for materials investigated polarographically in various solvent systems, there has been no systematic study of this problem. In view of the fact that no such differences have been mentioned in previous discussions of the effects of changing viscosity, it must be presumed that the functional relationship between $E_{1/2}$ and viscosity predicted by Heyrovsky has not been observed. The choice of systems available in the present research lead us to believe that this functionality, if demonstrable by conventional polarographic instrumentation, could be determined.

Experimental

Materials.—Baker reagent grade $Zn(C_2H_3O_2)_2\cdot 2H_2O$ and Baker and Adamson reagent grade $Pb(NO_3)_2$ were dried and used without further purification. Dr. F. H. Heath of this Laboratory prepared and recrystallized Tl_2SO_4 for this research. Recrystallized fluorenone was provided by Dr. F. E. Ray, Director of the Cancer Research Laboratories of the University of Florida. Recrystallized benzalacetone and benzophenone were given to us by Dr. C. B. Pollard of this Laboratory. Dried reagent grade KCl and KNO_3 were used as supporting electrolytes. Metal Salts Corporation triple-distilled mercury was used without further purification. Eimer and Amend chemically pure grade formamide, after being placed under a pressure of less than 1 mm. for two hours, was found to be polarographically pure in the range studied. Eimer and Amend chemically pure grade acetamide was found to be polarographically pure.

All solutions except those of Tl_2SO_4 were prepared in stock solution of 0.1 *M* KCl in the formamide–acetamide mixture of desired composition. A 0.1 *M* KNO_3 supporting electrolyte was used for the Tl_2SO_4 solutions.

The solvent system studied consisted of formamide–acetamide mixtures which were 20.3, 30.9 and 43.2 mole per cent. acetamide. Mixtures of higher concentrations were solids at 25°.

Apparatus.—Polarograms were obtained using a Sargent–Heyrovsky Model XII Polarograph. Potentials were measured on a Gray "Queen" Potentiometer calibrated with a Weston Standard Cell. A 0.1 *N* calomel reference electrode equipped with an agar–KCl bridge was used in order that transference effects across the interface be minimized. All potentials are referred to the saturated calomel electrode.

The mercury reservoir was 45 cm. above the level of the solutions. It was attached by neoprene tubing to a glass capillary of Corning "marine barometer" tubing 8 cm. long with an internal diameter of 0.08 mm. The capillary constant was 2.98 $\text{mg.}^{2/3}/\text{sec.}^{-1/2}$ at −0.40, and 2.94 $\text{mg.}^{2/3}$ $\text{sec.}^{-1/2}$ at −0.80 applied volt in 0.1 *M* KCl in the 30.9 mole per cent. acetamide mixture.

Tank nitrogen was bubbled through a tower of alkaline pyrogallol and then through a tower of formamide–acetamide mixture of the proper composition before being introduced into the Heyrovsky-type electrolysis cell for the purpose of sweeping out atmospheric oxygen. The solvent tower eliminated errors in concentrations caused by the removal of solvent from the cell by the sweeping gas. During all determinations, the polarographic cell was immersed in a water-bath thermostatically controlled at 25 ± 0.1°.

Results

In Table I, the densities, viscosities and molar volumes of the formamide–acetamide mixtures used are given. The viscosities and the molar volume of the solutions are found to be linearly related to the mole per cent. acetamide.

Table I

Properties of Formamide–Acetamide Mixtures

Acetamide, mole per cent.	d^{25}_4, g./cm.^{3}	η, mp.	*MV*, cm.^{3}/mole
20.3	1.103	46.43	44.0
30.9	1.091	54.93	45.9
43.2	1.090	65.19	47.7

---

(1) Adapted in part from a thesis presented by John H. Hook to the Graduate Council of the University of Florida in partial fulfillment of the requirements for the M.S. degree, February, 1951.

(2) Supported in part by a grant from the Research Corporation.

(3) Presented in part at the Meeting-In-Miniature of the Florida Section of the American Chemical Society, May 5, 1951, at Orlando, Florida.

(4) Research Corporation Fellow.

(5) A.E.C. Predoctoral Fellow, 1950–1952.

(6) H. Letaw, Jr., and A. H. Gropp, This Journal, **57**, 964 (1953).

(7) E. S. Peracchio and V. W. Meloche, *J. Am. Chem. Soc.*, **60**, 1770 (1938); D. M. Brasher and F. R. Jones, *Trans. Faraday Soc.*, **42**, 775 (1946); C. H. R. Gentry, *Nature*, **157**, 479 (1946); O. Collenberg and A. Scholander, *ibid.*, **158**, 449 (1946); I. Vavruch, *Collection Czechoslov. Chem. Communs.*, **12**, 429 (1947); H. A. McKenzie, *J. Council Sci. Ind. Research*, **21**, 210 (1948); P. Rutherford and L. A. Cha, *Anal. Chem.*, **23**, 1714 (1951).

(8) J. Heyrovsky, "Polarographie," Springer-Verlag, Vienna, 1941, p. 151 ff.

Table II

Half-Wave Potentials

Compound or ion	Formamide (ref. ( )	Half-wave potential referred to SCE (volts) Formamide-acetamide mixtures, mole per cent. acetamide 20.3	30.9	43.2
Benzalacetone	−1.08 ± 0.00	−1.13 ± 0.01	−1.12 ± 0.01	−1.08 ± 0.01
	−1.28 ± .03	−1.27 ± .03	−1.26 ± .01	−1.29 ± .03
Benzophenone	−1.26 ± .01	−1.22 ± .01	−1.22 ± .01	−1.21 ± .01
Fluorenone	−0.87 ± .02	−0.86 ± .01	−0.89 ± .01	−0.89 ± .02
Lead(II)	− .38 ± .02	− .35 ± .01	− .36 ± .01	− .40 ± .01
Thallium(I)	− .35 ± .01	− .35 ± .01	− .34 ± .01	− .35 ± .01
Zinc(II)	− .97 ± .01	− .99 ± .01	− .99 ± .91	− .97 ± .01

The half-wave potentials previously reported in formamide[6] and those determined in the formamide-acetamide mixtures are found in Table II.

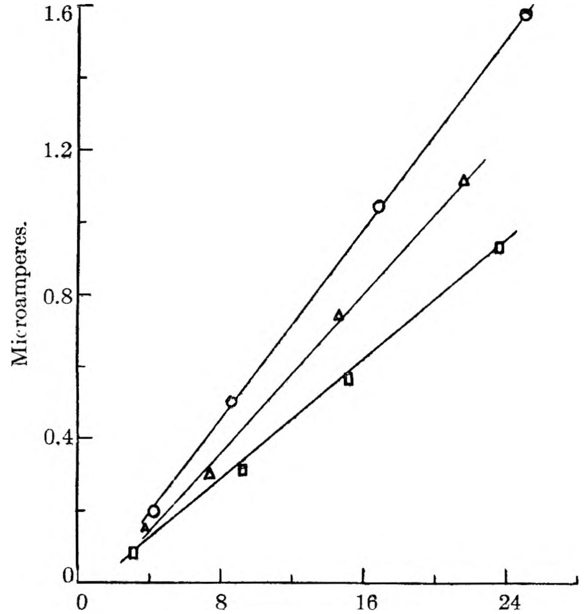

Fig. 1.—i_d *vs.* c curves for Tl^+: ○, 20.3; △, 30.9; □, 43.2 mole per cent. acetamide.

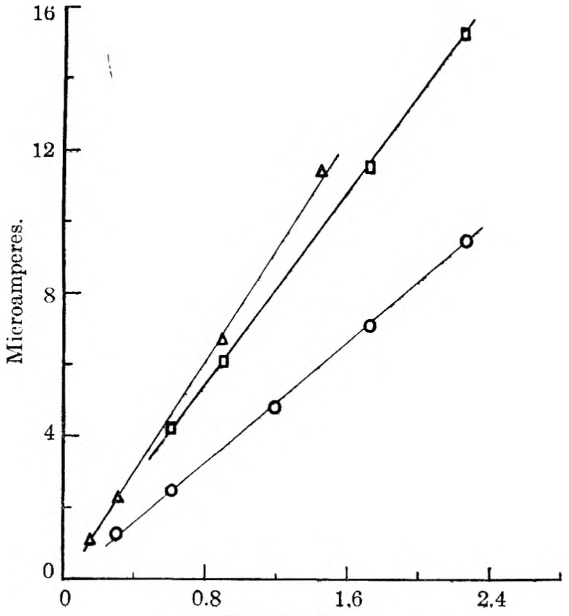

Fig. 2.—i_d *vs.* c curves for Pb^{++}: ○, 20.3; △, 30.9; □, 43.2 mole per cent. acetamide.

Average $(i_d/c)\cdot\eta^{1/2}$ values for each of the compounds investigated are tabulated for each solvent system in Table III. Graphs of i_d *vs.* c curves are plotted for Tl^+, Pb^{++} and fluorenone in Figs. 1, 2 and 3, respectively.

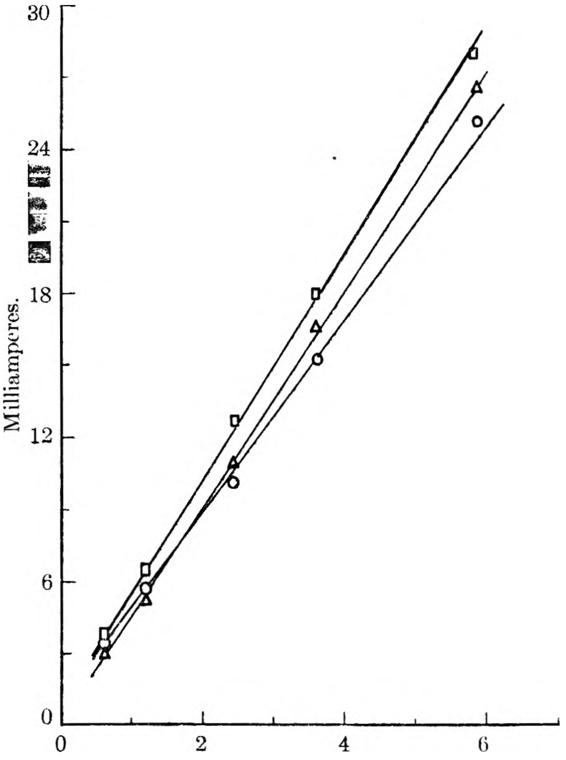

Fig. 3.—i_d *vs.* c curves for fluorenone: ○, 20.3; △, 30.9; □, 43.2 mole per cent. acetamide.

Discussion

It can be seen from the data in Table I that the solutions dealt with were virtually ideal in the range studied. The linear nature of the increase in viscosity with increasing mole per cent. of acetamide would seem to indicate that the information obtained relative to the effects of viscosity is valid.

The data collected in Table II indicate that the $E_{1/2}$ values are not functionally related to the viscosity of the solvent in which they are determined. It must be remembered, however, that a functional relationship of this type may be so subtle as to be undetectable by the instrumental methods used. Because the potential measurements involve an unknown and variable junction e.m.f. between acetamide-formamide solutions and water extruded from an agar-KCl bridge, it is not possible to extend the precision of these determinations. Good agreement of the $E_{1/2}$ values determined in formamide with those evaluated in formamide–acetamide mixtures was obtained.

The data presented in Figs. 1, 2 and 3 are apparently anomalous. It is evident that i_d/c is not, in general, inversely proportional to the square root of the viscosity. The data in Table III indicate that Zn^{++} is the only ion studied which behaved approximately according to this relationship.

TABLE III

AVERAGE $(i_d/C)\cdot\eta^{1/2}$ VALUES, MA. MP.$^{1/2}$ MOLE^{-1}

Compound or ion	Formamide–acetamide mixtures, mole per cent. acetamide 20.3	30.9	43.2
Benzalacetone	34.0	32.2	38.0
Benzophenone	25.5	28.5	31.2
Fluorenone	27.2	34.2	38.4
Lead(II)	27.2	57.4	54.0
Thallium(I)	44.3	40.8	33.1
Zinc(II)	30.2	30.7	31.6

The results of Vavruch[7] have shown that exalted i_d values result when Tl^+, Pb^{++} and Zn^{++} are studied in saccharose solutions of viscosity higher than 20 mp. In contrast to these results, we have found that $(i_d/C)\cdot\eta^{1/2}$ is not necessarily a monotonically increasing function with increasing viscosity.

There seems to be no clear-cut pattern in the data. The i_d *vs.* C curves for the organic compounds investigated show complete inversion, with respect to behavior predicted on increase in viscosity, for fluorenone and benzophenone, but inversion only of the 30.9 mole per cent. acetamide solution of benzalacetone. Virtually ideal behavior was found for Zn^{++}, but Pb^{++} was completely inverted with the 30.9 and 43.2 mole per cent. acetamide solutions reinverted. Tl^+ presents no inversion, but it is seen from Table III that i_d/C decreases at a greater rate with increasing viscosity than is predicted by the formula stated.

It is reasonable to assume that the inversions found for fluorenone and benzophenone are attributable to a greater solvation tendency exerted by formamide than by acetamide with respect to these two compounds. A reverse explanation would seem to pertain in the case of Tl^+. Though this ion ordinarily is not solvated or complexed in aqueous solutions, it is entirely possible that it is solvated by acetamide.

The description of the phenomena observed on the basis of solvation becomes somewhat tenuous in the light of the data obtained for Pb^{++} and benzalacetone. It would be necessary to state that a minimum and a maximum, respectively, occur in selective solvation of these materials. This is not unreasonable, but the absence of data concerning solvation and complex formation prevents the unambiguous resolution of this question.

Mixtures of formamide and acetamide are suitable solvents for polarographic determinations. Although extensive solubility work has not been carried out in this system, it offers advantages in that a wider choice of supporting electrolytes is available for use than is offered by the commonly used alcohols. It has been shown that the $E_{1/2}$ values of several organic compounds and inorganic ions remain constant over a rather wide range of viscosities. Anomalous behavior of the diffusion currents of benzalacetone, benzophenone, fluorenone, Pb^{++} and Tl^+ has been observed. These latter phenomena indicate that the viscosity relationship cited above must be applied with caution to other than aqueous systems.

ELECTRICAL POTENTIAL OF NYLON FIBERS IN AQUEOUS MEDIA

BY FREDERICK T. WALL AND PATRICIA M. SAXTON

Noyes Chemical Laboratory, University of Illinois, Urbana, Illinois

Received May 25, 1953

The electrical potential of a nylon fiber interacting with solutions of bases is calculated from theoretical considerations and previously obtained experimental data. It is shown that the fiber potential, which is in the neighborhood of −0.3 volt, is relatively insensitive to temperature changes. The number of end groups on the fiber that must be charged to produce this potential is shown to be negligibly small compared to the number of end groups interacting with the basic solutions. This calculation verifies the assumption, usually made for the theoretical development of the absorption equations, that equivalent numbers of cations and anions are absorbed by the fiber.

Introduction

Several investigators[1-6] have studied the interactions of polymeric fibers such as wool or nylon with acids and bases. Gilbert and Rideal[7] developed the first theoretical equations for the special case of absorption of acids on materials having equal numbers of carboxyl and amine groups. Wall and Swoboda[8] subsequently extended these equations to cover the more general problem of absorption of acids or bases on fibers having either equal or unequal numbers of those groups. The latter theory was experimentally confirmed by measurements of the absorption of sodium hydroxide on commercial nylon fibers, and extension of this experimental work to different temperatures has enabled the present authors[9] to calculate the heats of reaction associated with the absorption processes.

---

[1] G. A. Gilbert, *Proc. Roy. Soc. (London)*, **183A**, 167 (1944).

[2] R. H. Peters, *J. Soc. Dyers Colourists*, **61**, 95 (1945).

[3] O. R. Lemin and T. Vickerstaff, *ibid.*, **63**, 405 (1947).

[4] F. C. McGrew and A. K. Schneider, *J. Am. Chem. Soc.*, **72**, 2547 (1950).

[5] W. R. Remington and E. K. Gladding, *ibid.*, **72**, 2553 (1950).

[6] B. Oloffssen, *J. Soc. Dyers Colourists*, **67**, 57 (1951).

[7] G. A. Gilbert and E. K. Rideal, *Proc. Roy. Soc. (London)*, **182A**, 335 (1944).

[8] F. T. Wall and T. J. Swoboda, THIS JOURNAL, **56**, 50 (1952).

[9] F. T. Wall and P. M. Saxton, *ibid.*, **57**, 370 (1953).

Implicit in these theories and calculations is the assumption that the electrical potential of the fiber is very small, not only for all degrees of absorption but also at different temperatures, implying that essentially equivalent amounts of cations and anions are absorbed by the fiber. At this time we shall investigate this assumption further and determine more precisely its validity.

Calculations

When nylon fibers are suspended in an aqueous solution of a monovalent base such as sodium hydroxide, the following reactions can occur

$$\mathrm{COOH} \rightleftarrows \mathrm{COO^-} + \mathrm{H^+} \qquad (1)$$

$$\mathrm{NH_3^+} \rightleftarrows \mathrm{NH_2} + \mathrm{H^+} \qquad (2)$$

$$\mathrm{COONa} \rightleftarrows \mathrm{COO^-} + \mathrm{Na^+} \qquad (3)$$

$$\mathrm{H_2O} \rightleftarrows \mathrm{H^+} + \mathrm{OH^-} \qquad (4)$$

The free energy changes accompanying reactions 1 and 2 will be

$$\Delta\mu_1 = \Delta\mu_1{}^\circ + RT\ln\frac{(\mathrm{COO^-})}{(\mathrm{COOH})} + RT\ln(\mathrm{H^+}) - \psi F \qquad (5)$$

$$\Delta\mu_2 = \Delta\mu_2{}^\circ + RT\ln\frac{(\mathrm{NH_2})}{(\mathrm{NH_3^+})} + RT\ln(\mathrm{H^+}) - \psi F \qquad (6)$$

$\Delta\mu_1$ is the free energy change per unit of reaction, and $\Delta\mu_1{}^\circ$ is the corresponding standard free energy change. The last term in each equation represents the influence of the electrostatic potential of the fiber, where ψ equals that potential and F is the value of the faraday. (H^+) represents the concentration of hydrogen ions in solution, whereas (COOH), (COO^-), etc., represent the concentrations of the indicated species within the fiber. Similar free energy equations can be written for reactions 3 and 4.

Let us now ask what the effect of the electrical potential will be on these ionic reactions. Taking reaction 1 for example, we see from equation 5 that at equilibrium

$$\frac{(\mathrm{H^+})(\mathrm{COO^-})}{(\mathrm{COOH})} = K_a = K_a{}^\circ \exp(F\psi/RT) \qquad (7)$$

where $K_a{}^\circ$ is the ionization constant at zero potential. Evidently, if the apparent ionization constant $K_a{}^\circ \exp(F\psi/RT)$ can be determined, an estimate of ψ can be obtained by assuming a reasonable value for $K_a{}^\circ$. A similar procedure can be employed with respect to reaction 2, which involves ionization of the alkyl ammonium ions.

The apparent ionization constant, which we denote by K_a, can be obtained in two different ways as follows. Consider a nylon fiber containing A_0 carboxyl groups and B_0 amino groups per gram of fiber, with $A_0 > B_0$. If this fiber is titrated with sodium hydroxide, the first stage of the reaction will be represented by

$$\mathrm{COOH} + \mathrm{Na^+} + \mathrm{OH^-} \rightleftarrows \mathrm{COONa} + \mathrm{H_2O} \qquad (8)$$

with an equilibrium constant K_1. This stage of the reaction will be complete when (COONa) = $A_0 - B_0$, a state which we shall call the "mid-point" of the titration. The second stage, with an equilibrium constant K_2, will then follow

$$\mathrm{COO^-} + \mathrm{NH_3^+} + \mathrm{Na^+} + \mathrm{OH^-} \rightleftarrows \mathrm{COONa} + \mathrm{NH_2} + \mathrm{H_2O} \qquad (9)$$

Since (COONa) + (COOH) + (COO^-) = A_0 and (NH_3^+) + (NH_2) = B_0, it follows that at the "mid-point," (NH_3^+) = (COO^-) and (NH_2) = (COOH), assuming the fiber potential to be small. But under any circumstances

$$\frac{K_1}{K_2} = \frac{(\mathrm{COO^-})(\mathrm{NH_3^+})}{(\mathrm{COOH})(\mathrm{NH_2})} \qquad (10)$$

Substituting equation 10 into equation 7 and using the midpoint relationships, we obtain

$$K_a = \frac{K_w}{(\mathrm{OH^-})_m}\sqrt{\frac{K_1}{K_2}} \qquad (11)$$

where $(\mathrm{OH^-})_m$ is the hydroxide ion concentration at the "mid-point." We can similarly write for the apparent equilibrium constant of reaction (2)

$$K_c = \frac{K_w}{(\mathrm{OH^-})_m}\sqrt{\frac{K_2}{K_1}} \qquad (12)$$

The necessary data for three temperatures, taken from the work of Wall and Saxton,[9] and the values of K_a and K_c calculated in this manner are given in Table I.

Table I

Values of K_a and K_c Calculated from "Mid-point" Data

T, °C.	$K_1 \times 10^{-6}$	$K_2 \times 10^{-4}$	$(\mathrm{OH^-})_m \times 10^3$	$K_w \times 10^{14}$	$K_a \times 10^{11}$	$K_c \times 10^{13}$
25.0	1.96	0.70	2.69	1.008	6.28	2.24
36.4	0.80	0.43	3.80	2.28	8.14	4.43
49.7	0.40	0.19	5.50	5.45	14.2	6.90

The values for the apparent equilibrium constants of reactions 1 and 2 at other points along the titration curve can be obtained by the following procedure. We can express the concentrations of end groups within the fiber at any point of the titration as

$$(\mathrm{COONa}) = y \qquad (13)$$

$$(\mathrm{NH_2}) = x \qquad (14)$$

$$(\mathrm{NH_3^+}) = B_0 - x \qquad (15)$$

$$(\mathrm{COO^-}) = B_0 - x \qquad (16)$$

$$(\mathrm{COOH}) = (A_0 - B_0) + x - y \qquad (17)$$

Substituting these quantities into equation 10 we obtain

$$\frac{K_1}{K_2} = \frac{(B_0 - x)^2}{x[(A_0 - B_0) + x - y]} \qquad (18)$$

For each experimental value of y, this equation can be solved for x. Knowing the value of x, we can then calculate K_a, which can be written as

$$K_a = \frac{(B_0 - x)K_w}{[(A_0 - B_0) + x - y](\mathrm{OH^-})} \qquad (19)$$

Table II gives the values for K_a at 25° calculated from the experimental values of x, y and (OH^-) previously measured.[9]

To calculate the electrical potential, we still need to determine values for the intrinsic dissociation constants, $K_a{}^\circ$ or $K_c{}^\circ$, because ψ is given by

$$\psi = \frac{RT}{F}\ln\frac{K_a}{K_a{}^\circ} \qquad (20)$$

or

$$\psi = \frac{RT}{F}\ln\frac{K_c}{K_c{}^\circ} \qquad (21)$$

Equating equations 20 and 21 we obtain a restriction on the values of $K_a°$ and $K_c°$, namely

$$\frac{K_a°}{K_c°} = \frac{K_a}{K_c} = 2.8 \times 10^2 \text{ at } 25° \qquad (22)$$

By choosing values of $K_a°$ and $K_c°$ subject to the constraint imposed by equation 22, yet reasonable in relation to the corresponding values for organic acids and amines, we can then complete the calculation of ψ. Let us assume that $K_c^0 = 10^{-7}$ (compared to glycine ethyl ester, for which $K_c = 2 \times 10^{-8}$) and that $K_a^0 = 2.8 \times 10^{-5}$ (compared to butyric acid[10] with $K_a = 1.5 \times 10^{-5}$). Using these values, ψ is calculated from the data of Table I to be -0.33 volt at the mid-point at 25°. In addition, the potentials for other points along the 25° titration curve are given in Table II. It will be observed that the potential is quite constant but that it appears to begin to fall off more rapidly near the end of the complete titration. The negative sign of the potential can be readily explained by the excess acidic character of the fiber.

TABLE II

ELECTRICAL POTENTIAL OF NYLON FIBERS DURING TITRATION AT 25°

$B_0 = 43 \times 10^{-6}$ moles/g. fiber; $(A_0 - B_0) = 33.9 \times 10^{-6}$ moles/g. fiber; $K_1/K_2 = 280$.

(COONa) $\times 10^6$	(OH⁻) $\times 10^8$	(NH$_2$) $\times 10^6$	K_a $\times 10^{11}$	ψ (volts)
7.62	0.393	0.25	4.16	−0.342
10.3	.472	.29	4.03	− .343
16.5	.653	.37	3.72	− .345
17.7	.715	.38	3.49	− .347
22.9	1.02	.56	3.63	− .346
23.65	1.11	.60	3.57	− .346
24.7	1.19	.64	3.41	− .347
30.0	1.78	1.18	4.45	− .341
31.5	2.00	1.51	5.08	− .338
33.1	2.34	2.08	6.10	− .332
34.1	2.63	2.52	6.65	− .330
36.6	3.80	4.04	7.66	− .326
38.2	4.20	5.25	9.27	− .322
38.8	4.61	5.75	9.38	− .322
44.8	6.92	11.2	14.25	− .311
45.4	7.24	11.8	14.6	− .310
47.0	7.90	13.3	15.9	− .308
47.4	8.30	13.7	15.9	− .308
62.5	19.1	28.6	29.1	− .293
64.4	22.38	30.6	31.2	− .291

We can now compare this calculated value for the electrical potential on nylon fibers with experimental values that have been measured in the past few years. Neale and Peters[11] measured the streaming potential on nylon and found it to be approximately -0.025 volt in the basic region. However, the authors state that the experimental streaming potential may be only a fraction of the actual potential existing between the fiber and the solution. More recently Neale and Strandring[12] have been able to measure the actual Donnan potential on cellophane containing 5 milliequivalents of acid groups per 100 grams of cellophane. At low concentrations of electrolytes they found potentials as high as 0.1 volt and further state that "materials having very low carboxyl contents might be expected to exhibit quite large Donnan potentials in dilute aqueous solution." The nylon fibers used by the present authors contained approximately 3 milliequivalents of acid groups per 100 grams of fiber so that the calculated potential for nylon is not unreasonably high in comparison with the measured potential for cellophane.

By a rough approximation we can calculate an upper limit to the order of magnitude of the net concentration of negative groups on the fiber. If we assume the fiber to be made up of spheres, each with a radius equal to the radius of the fiber, and the charged groups uniformly distributed over the surface, then the potential will be given by the formula

$$\psi = 4\pi\rho r^2/3D \qquad (23)$$

where

r = radius of the fiber = 6.3×10^{-3} cm.
D = dielectric constant of water = 80
ρ = av. vol. density of charges

If we assume for ψ the value calculated for the fiber potential, -0.33 volt, then $\rho = 10^{12}$ electronic charges per gram of fiber. The numbers of end groups on the fiber interacting with the base are of the order of 10^{-5} mole per gram of fiber, or approximately 6×10^{18} groups per gram of fiber. Thus the number of these groups which must be ionized to produce the observed potential of the fiber is so small that for most practical purposes it is proper to assume that equal numbers of anions and cations are absorbed by the fiber. Assuming rod-like particles of nylon instead of spheres, the calculated density of charges would be even less. An infinite rod, of course, would require only a vanishingly small density of charges to build up the potential observed; accordingly the calculation based on spheres gives an upper limit to the charge density.

From the value of ψ at 25° we can also calculate the temperature coefficient of the fiber potential by differentiating equation 20

$$\frac{d\psi}{dT} = \frac{\psi}{T} + \frac{RT}{F}\frac{d \ln K_a}{dT} - \frac{RT}{F}\frac{d \ln K_a°}{dT} \qquad (24)$$

The temperature coefficients of the equilibrium constants will be related to the heats of reaction by the van't Hoff equation, so that

$$FT\frac{d\psi}{dT} = F\psi + \Delta H_a - \Delta H_a° \qquad (25)$$

The corresponding equation from the equilibrium constant of reaction 2 is

$$FT\frac{d\psi}{dT} = F\psi + \Delta H_c - \Delta H_c° \qquad (26)$$

The apparent heats of reaction, ΔH_a and ΔH_c, have been calculated,[9] using the van't Hoff equation and the values of K_a and K_c at various temperatures given in Table I. The values so obtained are $\Delta H_a = 5{,}660$ cal. and $\Delta H_c = 9{,}200$ cal.

To calculate the temperature coefficient of ψ we must now assume a value for $\Delta H_a°$ for $\Delta H_c°$. Subtracting equation 25 from 26 we obtain

$$\Delta H_a° - \Delta H_c° = \Delta H_a - \Delta H_c = -3{,}540 \text{ cal.} \qquad (27)$$

---

[10] H. S. Harned and B. B. Owen, "The Physical Chemistry of Electrolytic Solutions," Reinhold Publ. Corp., New York, N. Y., 1940.

[11] S. M. Neale and R. H. Peters, *Trans. Faraday Soc.*, **42**, 478 (1946).

[12] S. M. Neale and P. T. Strandring, *Proc. Roy. Soc.* (*London*), **213A**, 530 (1952).

Here again we can adjust the values of ΔH_c° and ΔH_a° so as to satisfy equation 27 and at the same time be reasonably similar to the corresponding heats of reaction for organic amines and acids. We shall let $\Delta H_c^\circ = 2{,}800$ cal., which is close to the value for the amine group of glycine (2,713 cal.),[10] and $\Delta H_a^\circ = -740$ cal., which can be compared with the corresponding value for butyric acid (-693 cal.).[10] From the assumed values of K_a° and ΔH_a°, and the resulting potential ψ at 25°, we find approximately that

$$\frac{d\psi}{dT} = -2 \times 10^{-4} \text{ volts/deg.} \qquad (28)$$

This means that in going from a temperature of 25 to 50°, ψ will change from about -0.330 to -0.335 volt. Therefore, within the accuracy of the experimental measurements, ψ can be considered to be constant with temperature.

To obtain some idea of the validity of this approximate value for ψ and its temperature coefficient, we have made further calculations assuming other values of K_c° and ΔH_c°. It is found that changing K_c° by a factor of ten changes ψ by only 0.05 volt. Thus the potential corresponding to $K_c^\circ = 10^{-8}$ is -0.28 volt, while that associated with a $K_c^\circ = 10^{-4}$ is -0.48 volt. As these are well beyond reasonable limits for possible values of K_c°, we can safely assert that the fiber potential must be in the neighborhood of -0.35 ± 0.05 volt at 25°. The approximate value obtained for the temperature coefficient of the potential, $d\psi/dT$, is equally certain, for ΔH_c° can be varied from $-5{,}000$ cal. to $+5{,}000$ cal. without making the change in ψ more than 0.02 volt in going from 25 to 50°. Thus we can also say that the fiber potential must be approximately -0.35 volt over a moderate range of temperatures. The approximate calculation of the number of charged groups corresponding to this potential also validates the assumption, essential for the theoretical development of the absorption equations, that substantially equal numbers of cations and anions are absorbed by the fiber.

THE ABSORPTION OF DIVALENT BASES ON NYLON FIBERS

BY FREDERICK T. WALL AND PATRICIA M. SAXTON

Noyes Chemical Laboratory, University of Illinois, Urbana, Illinois

Received June 15, 1953

The absorption of strontium hydroxide on nylon fibers has been experimentally investigated over the range 0 to 45×10^{-6} mole of base per gram of fiber. The results suggest that the divalent cations are absorbed by the carboxyl ions in predominantly two forms, $COOSr^+$ and COOSrOH. Because several different reactions can occur more or less simultaneously, it was difficult to analyze the results graphically. However, the equilibrium constants for the reactions of strontium hydroxide with the fiber were found by suitable mathematical calculations. The constancy of the results so obtained for the range of reliable experimental data provides good evidence in support of the theoretical analysis.

Introduction

The absorption of monovalent acids and bases on nylon or wool fibers has been quantitatively studied by several workers,[1-7] but the absorption of divalent substances has received much less attention. Peters[8] and McGrew and Schneider[7] have measured the absorption of certain dibasic acid dyes on fibers, but the complexity of the dye molecules makes an analysis of the absorption processes difficult. Peters and Speakman,[9] Donovan and Larose,[10] and Olofsson[4] have studied the combination of wool with sulfuric acid. They found the titration curve for the dibasic acid to be parallel to that for a monobasic acid such as hydrochloric, but displaced to a higher pH. In other words, the divalent anions showed greater affinity for the fibers than univalent anions. The presence on the fiber of the monovalent ion, HSO_4^-, was considered by each of these authors to be insignificant during the course of the titrations.

The present study is concerned with the absorption of a divalent base, $Sr(OH)_2$, on nylon fibers having an excess number of carboxyl end groups. Wall and Swoboda[2] have previously analyzed the absorption of a monovalent base, NaOH, on such a fiber. Since the absorption of the divalent base, though much more complex, is nevertheless similar to that for a monovalent base, we shall briefly summarize the description of the absorption process.

Before reacting with electrolytes in solution, the carboxyl and amine groups of a nylon fiber will interact with each other, so that a fiber originally containing an excess number of carboxyl groups will have equal numbers of carboxyl and alkyl ammonium ions and some additional uncharged carboxyl groups. The first reaction between the nylon fibers and added base is the titration of the excess carboxyl groups according to a reaction of the type

$$\text{COOH} + \text{B}^+ + \text{OH}^- \rightleftarrows \text{COOB} + \text{H}_2\text{O} \qquad (1)$$

This reaction proceeds until there are essentially no free carboxyl groups left on the fiber. The absorption then continues by reaction with the carboxyl and alkyl ammonium ions

$$\text{COO}^- + \text{NH}_3^+ + \text{B}^+ + \text{OH}^- \rightleftarrows \text{COOB} + \text{NH}_2 + \text{H}_2\text{O} \qquad (2)$$

---

[1] W. R. Remington and E. K. Gladding, *J. Am. Chem. Soc.*, **72**, 2553 (1950).

[2] F. T. Wall and T. J. Swoboda, THIS JOURNAL, **56**, 50 (1952).

[3] F. T. Wall and P. M. Saxton, *ibid.*, **57**, 370 (1953).

[4] B. Olofsson, *J. Soc. Dyers Colourists*, **67**, 57 (1951).

[5] G. A. Gilbert and E. K. Rideal, *Proc. Roy. Soc.* (*London*), **182A**, 335 (1944).

[6] D. R. Lemin and T. Vickerstaff, *J. Soc. Dyers Colourists*, **63**, 405 (1947).

[7] F. C. McGrew and A. K. Schneider, *J. Am. Chem. Soc.*, **72**, 2547 (1950).

[8] L. Peters, *J. Soc. Dyers Colourists*, **61**, 95 (1945).

[9] L. Peters and J. B. Speakman, *ibid.*, **65**, 63 (1949).

[10] R. Donovan and P. Larose, *Can. J. Research*, **27B**, 870 (1949).

The total amount of absorbed B^+ at completion of the titration will thus be equal to the original number of carboxyl groups on the fiber. Graphical analyses of experimental data for the absorption of sodium hydroxide verify this description of the absorption process.[2,3]

The initial reaction of a divalent base with nylon fibers having an excess number of carboxyl groups should likewise be a titration of the free carboxyl groups, since these are more acidic than the alkyl ammonium ions. Assuming that a divalent ion will occupy only one end group site at a time, and that only divalent Sr^{++} and OH^- are absorbed, we can write the reaction representing the initial absorption of $Sr(OH)_2$ by the fiber as

$$2COOH + Sr^{++} + 2OH^- \leftrightarrows COOSr^+ + COO^- + 2H_2O \quad (3)$$

To avoid the formation of a prohibitively large electrostatic potential on the fiber, the same number of equivalents of Sr^{++} and of OH^- must be absorbed.

Unlike the situation arising during the titration with a monovalent base, there is a second reaction possible involving the free carboxyl groups as well as the alkyl ammonium ions, namely

$$NH_3^+ + COOH + Sr^{++} + 2OH^- \leftrightarrows COOSr^+ + NH_2 + 2H_2O \quad (4)$$

When the free carboxyl groups are virtually gone, the absorption will continue by a titration of the alkyl ammonium ions in a manner analogous to equation 2

$$2NH_3^+ + COO^- + Sr^{++} + 2OH^- \leftrightarrows COOSr^+ + 2NH_2 + 2H_2O \quad (5)$$

We can obtain an estimate of the relative order and importance of reactions 3, 4 and 5 from the equilibrium constants previously found in the work with NaOH. Subtracting equation 4 from 3 we obtain

$$COOH + NH_2 \leftrightarrows COO^- + NH_3^+ \quad (6)$$

From previous work of the present authors,[3] the equilibrium constant for this reaction is 280, so we can write $K_1 = 280K_2$, where K_1 is the equilibrium constant for equation 3 and K_2 that for equation 4. If we subtract equation 5 from 4 we also obtain equation 6, so that $K_2 = 280K_3$, where K_3 is the equilibrium constant for equation 5.

From these relative values of the equilibrium constants, the initial interaction of a divalent base with the fiber should proceed according to equation 3 until the free carboxyl groups are almost gone. At this point, which we shall call the "midpoint" of the titration curve, $(COOSr^+) = (A_0 - B_0)/2$. In the immediate vicinity of the midpoint, reaction 4 will occur simultaneously with reactions 3 and 5, but removal of the remainder of the free carboxyl groups will leave reaction 5 proceeding alone to the point of maximum absorption corresponding to $(COOSr^+) = A_0/2$. Therefore, the titration curve for the absorption of a divalent base should show two distinct stages with a break at $(COOSr^+) = (A_0 - B_0)/2$, and a limiting absorption of $(COOSr^+) = A_0/2$.

Experimental Results and Discussion

The absorption of the divalent base, $Sr(OH)_2$, on nylon fibers has been experimentally measured over a wide range of base concentrations. The nylon fiber used was the same kind of polyhexamethylene adipamide previously used in the study by Wall and Swoboda[2] for the absorption of sodium hydroxide on nylon fibers. The end group constants of this fiber were found both from the experimental absorption studies and from the analytical methods of Waltz and Taylor[11] to be $A_0 = 82 \times 10^{-6}$ and $B_0 = 42 \times 10^{-6}$, where A_0 is the concentration of carboxyl end groups and B_0 that of the amine end groups in moles per gram of fiber.

The procedure used in the measurements was the static method described in detail for the absorption of sodium hydroxide.[2] To summarize briefly, the change in concentration was found for a known volume of a basic solution that had been allowed to come to equilibrium with a known weight of nylon placed in a constant temperature bath. The normalities of the dilute solutions of base (0.0003 to 0.01 N) were determined with the use of a radiotracer, Sr^{98}, obtained from the Atomic Energy Commission at Oak Ridge, Tennessee. Since the half-life of this isotope is only 54 days, corrections had to be made in the calculations for the decay of the tracer over the five to six day period necessary for the absorption.

The normalities of the more concentrated solutions were determined titrimetrically with standard solutions of potassium biphthalate. Although an atmosphere of nitrogen was maintained above the solutions it was found difficult to avoid the formation of $SrCO_3$ in these titrations. This may be the reason why reproducible data were obtained only up to a pH of approximately 12.3, corresponding to an absorption of 40×10^{-6} moles $Sr(OH)_2$ per gram of nylon. Absorption measurements were also made at higher concentrations of $Sr(OH)_2$, but these were so erratic that they were of little use in developing a theoretical interpretation of the data.

The experimental data obtained from six runs, each with samples at several concentrations, are given in Table I, together with pH and (OH^-) of the equilibrium solutions. At higher concentrations of base, the second dissociation constant for $Sr(OH)_2$, as obtained from the literature

$$K_2 = \frac{(Sr^{++})(OH^-)}{(SrOH^+)} = 0.15 \pm 0.01 \quad (7)$$

was used to calculate (OH^-), (Sr^{++}) and $(SrOH^+)$ from the normalities obtained by titration. The experimental data are shown in Fig. 1, in which moles $Sr(OH)_2 \times 10^6$ absorbed per gram of fiber is plotted against the pH of the solution.

The titration curve given in Fig. 1 shows two distinct stages with a "midpoint" at approximately $(COOSr^+) = 21 \times 10^{-6}$. This corresponds well to the value of $A_0 - B_0 = 40 \times 10^{-6}$ found from the sodium hydroxide absorption studies. This agreement with experiment leads us to a further analysis of the data, for by simple mass action law considerations, we can derive from equation 3 the following equation

$$K_1 = \frac{(COOSr^+)(COO^-)}{(COOH)^2(Sr^{++})(OH^-)^2} \quad (8)$$

---

[11] T. E. Waltz and G. B. Taylor, *Anal. Chem.*, 19, 448 (1947).

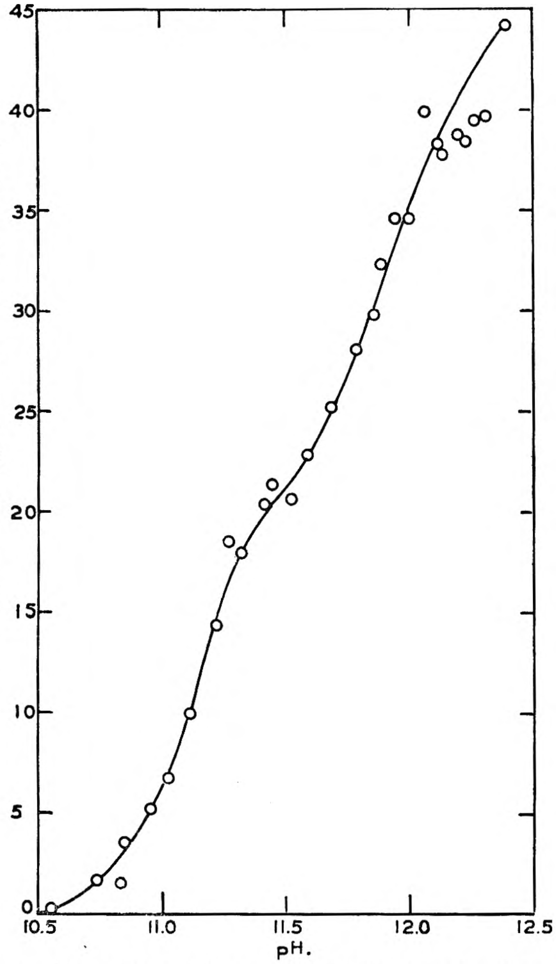

Fig. 1.—Absorption of strontium hydroxide by nylon fibers.

If this is the only reaction proceeding in the initial stages of the absorption we can assume the further restrictions

$$(\mathrm{COOH}) = (A_0 - B_0) - 2(\mathrm{COOSr}^+) \qquad (9a)$$

and

$$(\mathrm{COO}^-) = B_0 + (\mathrm{COOSr}^+) \qquad (9b)$$

In these dilute solutions we can also assume that

$$(\mathrm{Sr}^{++}) = (\mathrm{OH}^-)/2 \qquad (10)$$

Substituting these restrictions into equation 8 we obtain

$$K_1 = \frac{2(\mathrm{COOSr}^+)[B_0 + (\mathrm{COOSr}^+)]}{[(A_0 - B_0) - 2(\mathrm{COOSr}^+)]^2(\mathrm{OH}^-)^3} \qquad (11)$$

Equation 11 can be rearranged as

$$\alpha = \frac{2(\mathrm{COOSr}^+)[B_0 + (\mathrm{COOSr}^+)]}{(\mathrm{OH}^-)^3} = (A_0 - B_0)\sqrt{K_1} - 2\sqrt{K_1}(\mathrm{COOSr}^+) \qquad (12)$$

By plotting α against (COOSr^+), we should obtain a straight line with an intercept of $(A_0 - B_0)/2$ and a slope of $-2\sqrt{K_1}$. Table II gives the calculated values for α using the end group constant $B_0 = 42 \times 10^{-6}$, obtained from the sodium hydroxide absorption studies. The values of K_1 were calculated from equation 11. A plot of α *versus* (COOSr^+) shows that a straight line with the proper intercept is obtained only from values of (COOSr^+) less than 10×10^{-6} mole per gram of fiber. Since this corresponds to less than half of the first stage of the absorption, either reaction 4 must occur to an appreciable extent much earlier than we assumed, or there must be some other absorption process taking place in addition to those represented by equations 3 to 5.

TABLE I

ABSORPTION OF $Sr(OH)_2$ BY NYLON FIBER

$Sr(OH)_2$ × 10^6	pH	(OH^-) × 10^3	(Sr^{++}) × 10^3	$(SrOH^+)$ × 10^3
0.21	10.55	0.3577		
1.6	10.73	.533		
3.55	10.85	.714		
5.2	10.95	.896		
6.8	11.02	1.04		
9.9	11.11	1.302		
14.35	11.22	1.645		
18.4	11.27	1.88		
17.95	11.32	2.10		
20.35	11.405	2.52	1.25	0.020
21.45	11.44	2.725	1.35	.025
20.65	11.52	3.32		
22.8	11.59	3.83	1.89	.050
25.15	11.69	4.79	2.364	.0635
28.1	11.79	5.99	2.94	.1175
29.75	11.86	7.04	3.44	.163
32.3	11.89	7.60	3.71	.189
34.5	12.00	9.635	4.67	.2955
39.9	12.07	11.52		
37.7	12.14	13.306	6.37	.5635
38.7	12.20	15.178	7.22	.7325
39.5	12.31	19.44	9.13	1.183
44.2	12.395	22.765	10.575	1.615

TABLE II

ANALYSIS OF THE FIRST STAGE OF THE ABSORPTION

$(COOSr^+)$ × 10^6	(OH^-) × 10^3	α	K_1 × 10^{-8}	K_1^* × 10^{-8}
0.21	0.3577	0.625	2.5	2.31
1.6	.533	.96	6.82	6.75
3.55	.714	.942	8.2	8.09
5.2	.896	.824	7.73	7.61
6.8	1.04	.769	8.47	8.20
9.9	1.302	.68	11.35	10.7
14.35	1.645	.603	28.5	25.6
18.4	1.88	.578	32.5	...
17.95	2.10	.482	138	70.9

The extent to which reaction 4 occurs can be determined quite readily. Using the known equilibrium constants for reaction 6 and the known values for the end group constants, the values of the other end groups at any point on the titration curve can be calculated. The equilibrium constant, K_1, can then be directly calculated from equation 8. These revised values of K_1 are given in Table II as K_1^*. Comparison of K_1 and K_1^* shows that the latter increases more slowly than the former, but still to a very appreciable extent. We must therefore conclude that absorption reactions other than those already suggested are taking place.

There is an alternative conclusion, namely, that the assumed values of the end group constants are inaccurate, although they were found both by a direct quantitative analysis and from previous titration studies. The extent of the change which would be necessary in the end group constants to keep K_1 relatively constant was determined. It was found necessary to alter the end group figures from $B_0 = 42 \times 10^{-6}$ to 50×10^{-6} and from $A_0 = 82 \times 10^{-6}$ to 120×10^{-6}. Such a large error in the previously found value of A_0 seems so unlikely that we shall dismiss this possibility altogether.

Equations 3 to 5 are the only possible reactions by which Sr^{++} can be absorbed on the fiber as $COOSr^+$, so we must consider the other forms in which Sr^{++} may be absorbed on the fiber, namely, $(COO)_2Sr$ and COOSrOH. The amount of $(COO)_2Sr$ on the fiber was calculated for the first stage of the titration, assuming the initial value for the equilibrium constant, $K_1 = 7.8 \times 10^8$. The amounts of $(COO)_2Sr$ necessary to maintain this constant value of K_1 were found to be quite large, even greater than the amounts of $COOSr^+$ at the same points of the titration curve. The probability of this many carboxyl groups occurring close enough together to allow the formation of the species $(COO)_2Sr$ would seem quite small. Furthermore, the calculated values of the equilibrium constant for the absorption of Sr^{++} in this form were found to be far from constant, since they increased by several orders of magnitude during even the first stage of the titration.

The occurrence of the species —COOSrOH would seem more likely, especially in the concentrated basic solutions where $SrOH^+$ ions exist in appreciable concentrations. The calculation of the amount of this species which must be present at any given total absorption to keep K_1 constant is carried out as follows. Let us denote the experimentally measured amount of $Sr(OH)_2$ absorbed on the fiber by c, so that

$$c = (COOSr^+) + (COOSrOH) \tag{13}$$

Other restrictions on the fiber are

$$A_0 = (COO^-) + (COOH) + c \tag{14}$$

$$B_0 = (NH_3^+) + (NH_2) \tag{15}$$

$$(NH_3^+) + (COOSr^+) = (COO^-) \tag{16}$$

Applying these restrictions, equation 8 becomes

$$K_1 = \frac{(COOSr^+)[A_0 - (COOH) - c]}{(COOH)^2(Sr^{++})(OH^-)^2} = 7.8 \times 10^8 \tag{17}$$

We can also write the known equilibrium constant for equation 6

$$\frac{(COO^-)(NH_3^+)}{(COOH)(NH_2)} = 280 \tag{18}$$

Substituting from equations 15 and 16 into equation 18, we obtain

$$\frac{(COO^-)[(COO^-) - (COOSr^+)]}{(COOH)[B_0 - (COO^-) + (COOSr^+)]} = 280 \tag{19}$$

For a given experimental value of c and (OH^-), assuming a value of $(COOSr^+)$, equation 17 can be solved for (COOH). Then (COO^-) can be calculated from equation 14, and equation 19 solved for $(COOSr^+)$ using these calculated values of (COOH) and (COO^-). Repeating this calculation, values of $(COOSr^+)$ and (COOH) can be found satisfying both equations 17 and 19 for each experimental point. From these two end groups the values of all the other end groups can be easily calculated. Table III gives the values of $(COOSr^+)$ and (COOSrOH) determined from this calculation at each experimental point. The species (COOSrOH) might be produced in the first stage of the titration in either one of two ways

$$COOH + Sr^{++} + 2OH^- \rightleftarrows COOSrOH + H_2O \tag{20}$$

with

$$K_4 = \frac{(COOSrOH)}{(COOH)(Sr^{++})(OH^-)^2} \tag{21}$$

or

$$COOH + SrOH^+ + OH^- \rightleftarrows COOSrOH + H_2O \tag{22}$$

with

$$K_5 = \frac{(COOSrOH)}{(COOSr^+)(OH')} \tag{23}$$

In either case there must exist an equilibrium between the $(COOSr^+)$ and the (COOSrOH) if both these groups are present

$$COOSr^+ + OH^- \rightleftarrows COOSrOH \tag{24}$$

with

$$K_6 = \frac{(COOSrOH)}{(COOSr^+)(OH^-)} \tag{25}$$

TABLE III

CALCULATION OF (COOSrOH)

c $\times 10^6$	(COOH) $\times 10^6$	(COO^-) $\times 10^6$	$(COOSr^+)$ $\times 10^6$	(COOSrOH) $\times 10^6$
0.21	39.58	42.21	0.21	
1.6	36.8	43.6	1.6	
3.55	32.9	45.55	3.55	
5.2	29.6	47.2	5.2	
6.8	26.85	48.35	6.6	0.2
9.9	22.1	50.0	8.35	1.55
14.35	16.7	50.95	9.4	4.95
17.95	12.3	51.75	10.45	7.5
20.35	9.55	52.1	10.9	9.45
21.45	8.54	52.0	10.9	10.55
22.8	5.66	53.5	12.9	9.9
25.15	3.99	52.9	12.7	12.45
28.1	2.72	51.2	11.8	16.3
29.75	2.08	50.17	11.5	18.25
32.3	1.7	48.0	9.9	22.4
34.5	1.15	46.35	9.6	24.9
37.7	0.7	43.6	9.5	28.2
38.7	.57	42.7	9.6	29.1
39.5	.42	42.08	11.2	28.3
44.2	.28	37.52	9.1	35.1

These three equilibrium constants K_4, K_5 and K_6 have been calculated for each of the experimental points from the data of Table III and are given in Table IV. The approximate constancy of K_6 over the whole range of the reliable experimental data is surprisingly good. Both K_4 and K_5 are also relatively constant when we consider the fact that they involve the cube or square of the experimental (OH^-), which cannot be very accurately determined. Since the calculation of these equilibrium constants is completely independent of the assumptions and equations used to calculate the end group values of Table III, the approximate constancy seems a very good indication of the actual existence of COOSrOH on the fiber.

Table IV

Calculation of Equilibrium Constants Based on $K_1 = 7.8 \times 10^8$

$c \times 10^6$	$K_4 \times 10^{-7}$	$K_5 \times 10^{-7}$	K_6
6.8	1.32		29.1
9.9	6.37		143
14.35	13.3		319
17.95	13.2		342
20.35	12.5	1.96	343
21.45	12.4	1.82	356
22.8	6.32	0.91	200
25.15	5.78	1.03	205
28.1	5.68	0.85	230
29.75	5.16	.77	226
32.3	6.15	.92	298
34.5	5.00	.76	269
37.7	3.58	.54	223
38.7	3.07	.46	200
39.5	1.96	.29	130
44.1	2.3	.34	155

Thus, the first stage of the absorption process, the titration of the free carboxyl groups, will be a combination of three principal reactions. Equation 3, with an equilibrium constant equal to 7.8×10^8, will predominate up to an absorption of approximately 8×10^{-6} mole per gram of fiber. At this point COOSrOH will begin to form on the fiber according to equations 20 and 22. Since the equilibrium constants for these reactions are 7.6×10^7 and 1.0×10^7, respectively, the formation of COOSrOH will be due to their simultaneous occurrence. Shortly before the free carboxyl groups are gone, reaction 4 with an equilibrium constant equal to 2.6×10^6 will become prominent.

In the second stage of the absorption, the alkyl ammonium ions may be titrated by any combination of the following reactions

$$NH_3^+ + COO^- + Sr^{++} + 2OH^- \rightleftarrows COOSrOH + NH_2 + H_2O \quad (26)$$

$$NH_3^+ + COO^- + SrOH^- + OH^- \rightleftarrows COOSrOH + NH_2 + H_2O \quad (27)$$

$$2NH_3 + COO^- + Sr^{++} + 2OH^- \rightleftarrows COOSr^+ + 2NH_2 + 2H_2O \quad (28)$$

The equilibrium constants for these three reactions are 2.7×10^5, 3.6×10^4 and 9.3×10^3, respectively. Hence, the second stage of the absorption probably consists of these three reactions proceeding simultaneously, with no single one predominating in any portion of the titration curve.

This description of the absorption process is the only one of the several analyses tried that seems plausible in view of previous studies of the absorption of a monovalent base on this same nylon.

THE SOLUBILITY OF *cis*- AND *trans*-DINITROTETRAMMINECOBALT(III) SULFATES IN WATER-DIOXANE MIXTURES

By Stuart A. Mayper, H. Lawrence Clever[1] and Frank H. Verhoek

Contribution from the Chemical Laboratory of The Ohio State University, Columbus, Ohio

Received June 8, 1953

The solubilities of *cis*- and *trans*-dinitrotetramminecobalt(III) sulfates in mixtures of water and dioxane in the dielectric constant range to 18 have been determined at 25 and 15°. The results have been compared with theoretical and empirical expressions relating change of solubility to change in dielectric constant. Values of $\Delta H°$, $\Delta F°$ and $\Delta S°$ for the solution process have been calculated.

This paper represents a contribution to the problem of determining the factors which affect the solubility of electrolytes in solvents of different dielectric constant. It reports the results of a study of the solubility of the sulfates of two cobaltammine ions which are geometrical isomers, using as solvents mixtures of water and dioxane. The dinitrotetramminecobalt ions are among the most stable ions of the type $Co(NH_3)_4X_2^+$. They are easily determined quantitatively by titration of the ammonia formed by their decomposition, and, possessing *cis* and *trans* isomers, they are adapted for comparison with each other. The sulfates of these ions were chosen for study, since the solubility of the sulfates of both isomers lies in an accessible dilute range in the solvents used.

Croceo sulfate (*trans*-dinitrotetramminecobalt(III) sulfate) was prepared by the method of Jorgensen.[2] Sample I was prepared by an oxidation of cobaltous ion in the presence of sulfuric acid, ammonium chloride and sodium nitrite. The precipitate was washed free of xantho salts and recrystallized by dissolving in water at 60–65° and cooling the solution. Analysis by heating with sulfuric acid and weighing as cobalt sulfate gave 21.96 ± 0.10% Co (theoretical 22.07%). For sample II croceo chloride was first prepared, following Jorgensen[3] and recrystallized from 0.1 *m* acetic acid by adding ethanol. Analysis gave 23.37 ± 0.08% Co and 26.78 ± 0.04% NH_3 (theoretical 23.16, 26.76%). Croceo sulfate was precipitated from a solution of the chloride by adding ammonium sulfate, and shaken with successive portions of water until a constant solubility was obtained. Analysis showed 22.13 ± 0.13% Co and 25.37 ± 0.02% NH_3 (theoretical 22.07%, 25.50%).

Flavo sulfate (*cis*-dinitrotetrammine cobalt(III) sulfate) was prepared from carbonatotetramminecobalt(III) sulfate by dissolving the latter in sodium nitrite solution containing sulfuric acid, heating on the steam-bath, and causing the desired sulfate to crystallize out by cooling and adding more sulfuric acid. The crystals were washed with 3 *N* sulfuric acid, warm water and alcohol. The product obtained by this method was much better than that obtained by the method of Jorgensen[2] which requires the preparation of an acid flavo nitrate as an intermediate. It is necessary, however, that only well-defined crystals of the carbonato salt be used; the latter was prepared according to Jorgensen's directions,[2] observing the precautions of Lamb and Damon.[4]

---

[1] Holder of a fellowship provided from funds granted by The Ohio State University Research Foundation to the University for aid in fundamental research, 1950–1951.

[2] S. M. Jorgensen, *Z. anorg. allgem. Chem.*, **5**, 159 (1894); **7**, 306 (1894); **17**, 455 (1898).

[3] S. M. Jorgensen, *ibid.*, **17**, 468 (1898).

[4] A. B. Lamb and E. B. Damon, *J. Am. Chem. Soc.*, **59**, 383 (1937).

Sample I of the flavo sulfate (22.11 ± 0.03% Co) was used without further purification samples II and III (22.20 ± 0.11% Co and 22.16 ± 0.03% Co, respectively) were recrystallized by dissolving in warm dilute sulfuric acid, cooling to 0° and slowly adding ethanol, filtering, and washing with 70% ethanol.

Dioxane was refluxed 20 hours over metallic sodium and distilled in a stream of dry nitrogen, collecting the fraction boiling over a 0.3° range.

For the solubility measurements the solid salt was placed in a Pyrex sample tube which had a standard taper stopper. Tubes for samples II and III were coated with black paint; for sample I they were uncoated. Dioxane and water were weighed in, the stopper was sealed with paraffin and the tube revolved end over end in a thermostat for a measured period. At the end of this time the solution was allowed to settle in the thermostat for half an hour or more and the supernatant liquid drawn up into a pipet through a filtering tip. Analysis of samples I of both salts was carried out by adding 6 N NaOH and boiling down to half the volume, catching the ammonia evolved in standard 0.01 N H_2SO_4 and back-titrating with 0.01 N NaOH to pH 5 using methyl red–brom cresol green indicator. For samples II and III the analytical method and apparatus used was similar to that of Rieman, Neuss and Naiman.[5]

The densities of the solutions of sample I were determined for possible conversion to a mole fraction basis; the measured densities agreed with the literature values for the solvent mixture.[6]

Special experiments were carried out to ensure that saturation equilibrium had been obtained. In the water solutions samples were rotated for periods up to 40 hours; the solubility became constant after 8–9 hours, indicating that equilibrium was reached in that time. Similar experiments in 38.2% dioxane showed that equilibrium was reached in 8–9 hours. In the other solvent mixtures, samples were rotated 20 hours or more. Another test of saturation was carried out at 38.3% dioxane by rotating 6 hours at 28°, then 18 hours at 25° in order to approach equilibrium from supersaturation. The results were in agreement with the other experiments.

The experiments at 15° were carried out by rotating 25 hours at that temperature.

The results of the solubility determinations are given in Table I. The values at even 10% intervals of weight per cent. dioxane are those interpolated from large-scale plots of the data.

Discussion

The change of solubility of a binary electrolyte with change in dielectric constant at infinite dilution, assuming that only electrostatic forces are important, is given by the Born equation.[7]

$$\ln s = \ln s_0 + \frac{|z_+z_-|\epsilon^2}{2kTr}\left(\frac{1}{D_0} - \frac{1}{D}\right) \qquad (1)$$

Here z_+ and z_- are the charges on the ions of the electrolyte, r is an averaged value of the radii of the two ions, assumed spherical, and s and s_0 represent the solubilities in the solvents of dielectric constant D and D_0. This equation has been examined, for the two salts studied, in Fig. 1. The solubility values plotted are the interpolated values at even 10% intervals, corrected to zero ionic strength by the Debye–Hückel limiting law. For this correction, the values 0.5091 and 0.5002 were used for the constant term in water at 25 and 15°,[8] and the dielectric constants of the solvent mixtures were obtained from the data recorded by Harned and Owen.[9]

TABLE I

SOLUBILITY OF *cis*- AND *trans*-DINITROTETRAMMINECOBALT(III) SULFATES IN DIOXANE–WATER MIXTURES

Wt. % dioxane	Solubility in moles/l. × 10^3			
	cis		*trans*	
	15°	25°	15°	25°
0	2.405[b,i]	3.67[a,d]	1.705[b,j]	2.43[a,f]
0	...	3.63[b,e]	...	2.44[b,g]
0	...	3.62[c]	...	...
0	2.41	3.65	1.71	2.44[h]
2.6	2.17[b]	...	1.52[b]	...
7.7	1.75[b]	...	1.16[b]	...
8.2	...	...	...	1.58[a]
8.9	...	2.52[a]	...	...
10	1.58	2.39	1.015	1.43
11.5	...	...	...	1.31[a]
15.4	1.23[b]	...	...	...
16.7	...	1.76[a]	...	...
19.6	...	1.49[a]	...	...
20	0.967	1.47	0.566	0.848
20.5	...	...	...	.854[a]
23.4	...	...	...	.685[a]
24.9	...	1.18[a]	...	...
25.6	...	...	.406[b]	...
30	.547	0.863	.300	.449
30.6	.522[b]	...	...	...
34.6	...	...	...	.332[a]
36.5	...	.604[a]	...	...
37.0	...	...	...	.240[a]
38.2	...	.470[b,k]	...	.225[b,m]
38.3	...	.485[b,n]	...	.212[b,n]
38.4	...	...	...	.236[a]
39.7	...	...	...	.226[b,p]
40	.260	.456	.123	.198
40.7	...	...	.113[b]	...
47.0	...	.294[a]	...	...
47.1	...	...	...	.108[a]
50	.112	.218	.045	.079
51.0	...	...	...	.088[c]
53.3	...	...	.034[b]	...
57.0	...	.130[a]	...	...
59.8	...	...	...	.017[b]
60	.040	.072	...	.017
60.7	.038[b]	...	...	...
64.7	...	.025[b]	...	...
67.9	...	...	...	.005[b]
71.5	...	.009[b]	...	...

[a] Samples I. [b] Samples II. [c] Sample III; average of 4 determinations; av. deviation 0.022. [d] Average of 7 determinations; av. deviation 0.037. [e] Average of 4 determinations; av. deviation 0.030. [f] Average of 9 determinations; av. deviation 0.025. [g] Average of 4 determinations; av. deviation 0.005. [h] L. A. Hansen and J. W. Williams, *J. Am. Chem. Soc.*, **52**, 2759 (1930), obtained 2.447 × 10^{-3} moles/l. as the average of 14 determinations. [i] Average of 3 determinations; av. deviation 0.005. [j] Average of 3 determinations; av. deviation 0.002. [k] Average of 4 determinations; av. deviation 0.016. [m] Average of 3 determinations; av. deviation 0.0006. [n] From supersaturation. [p] Average of 6 determinations; av. deviation 0.007.

It is evident that, as not uncommonly found,[10] the Born equation does not satisfactorily reproduce the results, since a curve is obtained and not a

---

[5] W. Rieman, J. O. Neuss and B. Naiman, "Quantitative Analysis," McGraw-Hill Book Co., Inc., New York, N. Y., 1942, p. 162.

[6] F. Hovorka, R. A. Schaefer and D. Dreisbach, *J. Am. Chem. Soc.*, **58**, 2264 (1936).

[7] M. Born, *Z. Physik*, **1**, 45 (1920).

[8] H. S. Harned and B. B. Owen, "The Physical Chemistry of Electrolytic Solutions," Reinhold Publ. Corp., New York, N. Y., 1950, p. 587.

[9] H. S. Harned and B. B. Owen, ref. 8, p. 118.

[10] See, for example, T. W. Davis, J. E. Ricci and C. G. Sauter, *J. Am. Chem. Soc.*, **61**, 3274 (1939).

straight line. No significantly better agreement is obtained if the solubility is expressed in mole fractions rather than in volume concentrations, nor if, in place of the limiting law, the activity coefficients for correcting to zero ionic strength are calculated allowing for the finite size of the ions by means of reasonable estimates of the parameter *a* in the Debye–Hückel equation.

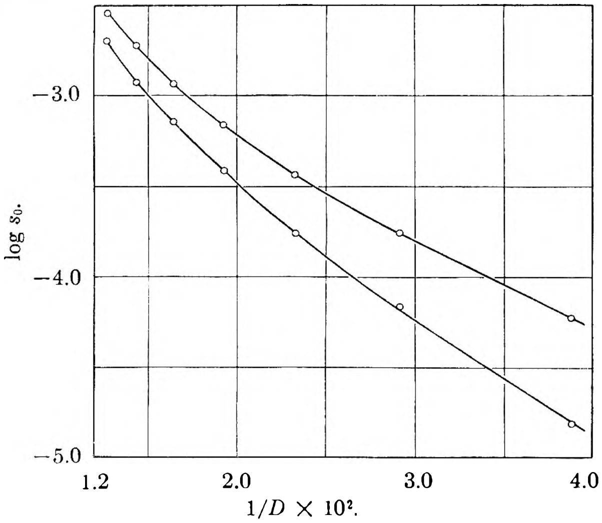

Fig. 1.—Solubility of dinitrotetramminecobalt(III) sulfates in dioxane–water: upper curve, *cis*; lower curve, *trans*.

If values of *r* in equation 1 are calculated from the slopes of the curves in Fig. 1, it is found that *r* is of the order of a few Ångström units, is greater for the *cis* than for the *trans* salt, and increases with decreasing dielectric constant for both salts.

Arguing that at least part of the failure of the Born equation in mixed solvents was due to a sorting of the molecules of the solvent by the electrolyte, Ricci and Nesse,[11] applying the treatment of Debye,[12] calculated the ratio of solubilities in water to that in solutions containing 20, 50 and 80% dioxane for 1–1 and 1–2 electrolytes at 25°. Assuming the same radial distances as those used by Ricci and Nesse and using the calculated ratios from their Table V, we obtain the results in Table II.

TABLE II

CALCULATED SOLUBILITIES OF DINITROTETRAMMINECOBALT(III) SULFATES AT 25°, ALLOWING FOR SORTING OF SOLVENT MOLECULES

	Wt. % dioxane	$s_{\mu} = 0 \times 10^3$		Ratio $\frac{\text{calcd.}}{\text{obsd.}}$
		Obsd.	Calcd.[12]	
cis	0	2.86	...	...
	20	1.17	1.79	1.6
	50	0.177	0.41	2.3
trans	0	2.00	...	...
	20	0.713	1.25	1.8
	50	0.070	0.29	4.2

If the simple Born equation is used to calculate solubilities at high dioxane contents from data at low dioxane contents, values are obtained which are much smaller than the observed values. It is seen from Table II that the allowance for the sorting effect brings the calculated solubilities above the observed values; in the language of Ricci and Nesse, it "overcorrects" the Born equation. The magnitude of the overcorrection is about the same as that found by Ricci and Nesse for silver sulfate and zinc and barium iodates in the same solvents. It is perhaps significant that the agreement is slightly better for the unsymmetrical *cis* salt than for the *trans* salt and the 1–2 electrolytes studied by Ricci and Nesse. This might be expected if the sorting effect for spherical ions is not actually as great as the Debye treatment predicts.

An empirical relation between the solubility of a salt and the dielectric constant has been suggested by Ricci and Davis[13] on the basis that the activity coefficient of an electrolyte is a constant at saturation, independent of the dielectric constant of the medium. According to this relationship a straight line of slope 3 should be obtained on plotting log *s* against log *D*, if the limiting law is assumed. Such plots for the data reported here do in fact give straight lines, but the slopes for the *cis* salt are 3.6 and 3.7 at 25 and 15°, respectively, and those for the *trans* salt are 4.2 and 4.3. Better agreement may be obtained if the activity coefficients are calculated allowing for the effect of ion size, but the value required for the mean distance of closest approach is seven ångström units for the *cis* salt, and for the *trans* salt the wholly unreasonable value 25 Å. The Ricci–Davis relation, useful as it is, must therefore be used with caution.

In comparing the change of solubility of the *cis* sulfate with that of the *trans* sulfate, one might attribute the difference to the unsymmetrical character of the *cis* ion as compared to the *trans* ion. Kirkwood[14] has derived an equation for the activity coefficient of an ion of arbitrary charge distribution at infinite dilution as a function of the dielectric constant. If this is rearranged to give the change in solubility of a salt with change in dielectric constant, an equation is obtained in which the first term varies as $1/D$ and contains $1/r$ as in equation 1. Since it is not possible to determine *r* accurately from the measurements, no useful calculations can be made involving the further terms which contain dipole and higher polar moments. Similarly no comparison of the dipole moments of the *cis* and *trans* salts can be made, since the difference in the *r* values of the two salts cannot be accurately assessed.

Calculated values of $\Delta H°$, $\Delta F°$ and $\Delta S°$ for the solution process are given in Table III. In making the calculations the activity coefficients in the saturated solutions were calculated from the limiting law; volume concentrations (moles per liter of solution) were used at both temperatures. The precision of the heat content and entropy values, calculated from a 10° temperature range, is not great. For both salts $\Delta H°$ is positive, indicating that the heat evolved in solvation is not sufficient to overcome that required to break down the crystal lattice. $\Delta H°$ increases with decreasing dielectric constant, pointing to a decrease in solvation

---

[11] J. E. Ricci and G. J. Nesse, *J. Am. Chem. Soc.*, **64**, 2305 (1942).

[12] P. Debye, *Z. physik. Chem.*, Cohen Festband, **56** (1927).

[13] J. E. Ricci and T. W. Davis, *J. Am. Chem. Soc.*, **62**, 407 (1940).

[14] J. G. Kirkwood, *J. Chem. Phys.*, **2**, 351 (1934).

energy as water is diluted with dioxane. The value of $\Delta H°$ for the *cis* salt is only slightly higher than that for the *trans* salt, so that the greater solubility for the former is largely an entropy effect. A more rigid binding of the solvating molecules, and a greater entropy increase would be expected for the unsymmetrical ion, and the larger $\Delta S°$ values for this ion correlate with its greater tendency to sort water from dioxane suggested from the data in Table II. For both salts there is an increase in entropy change with decreasing dielectric constant, conforming to the expectation of a more rigid solvation complex in solutions of higher dioxane content.

TABLE III

HEAT, FREE ENERGY AND ENTROPY OF SOLUTION FOR DINITROTETRAMMINECOBALT(III) SULFATES IN DIOXANE–WATER MIXTURES

	cis			*trans*		
Wt. % dioxane	$\Delta H°$, kcal.	$\Delta F°_{296}$, kcal.	$\Delta S°_{298}$	$\Delta H°$, kcal.	$\Delta F°_{298}$, kcal.	$\Delta S°_{296}$
0	18.7	9.6	31	16.4	10.2	21
10	18.7	10.3	28	15.9	11.5	15
20	19.0	11.2	26	18.9	12.1	23
30	20.8	12.1	29	19.0	13.2	19
40	25.6	13.2	42	22.7	14.6	27
50	30.8	14.5	55	27.1	16.2	37
60	...	16.5	..	...	18.9	..

HEATS OF ADSORPTION OF ARGON ON A SERIES OF CARBON BLACKS GRAPHITIZED AT SUCCESSIVELY HIGHER TEMPERATURES[1]

BY R. A. BEEBE AND D. M. YOUNG[2]

Contribution from the Moore Laboratory of Chemistry, Amherst College, Amherst, Mass.

Received August 3, 1953

The calorimetric heats of adsorption have been measured for argon at −195° on a series of carbon blacks graphitized at the successively higher temperatures, 1000, 1500, 2000 and 2700°. X-Ray and electron microscope studies reported by Schaeffer, *et al.*, indicate a higher degree of graphitization with increasing temperature of heat treatment; this would result in progressively more homogeneous surfaces within the series. Our experimental results illustrate clearly the change in the shape of the heat-coverage curve with increasing degree of surface homogeneity produced by high temperature heat treatment. These results may be correlated with the stepwise isotherms found by Polley, *et al.*, on the same series of blacks.

There is a growing body of experimental data which shows rather sharp differences in the characteristics of physically adsorbed films on heterogeneous and on more homogeneous surfaces. Differences of this sort are especially apparent in the heat-coverage curves for the adsorption of gases on such surfaces. These differences may be illustrated by the work on carbon blacks previously reported from this Laboratory. In particular two non-porous blacks have been extensively studied.[3] One of these, known commercially as Spheron 6, is a rubber reinforcing channel black; the other, designated as Graphon, is produced by heat treatment of the Spheron 6 at electric furnace temperatures, approximately 3000°.

The X-ray studies of Biscoe and Warren[4] have shown that, in contrast to the parent material Spheron, the Graphon possesses a much higher degree of order in its three dimensional structure with indication of a partial graphitization during the above heating process. From the adsorption studies it is apparent that, in comparison with Spheron 6, the Graphon has a relatively homogeneous surface.[3] Probably as a result of this homogeneity and the consequent opportunity for easily observing the effects of lateral interaction between adsorbed molecules, there are characteristic humps in the isotherms and maxima in the heats of adsorption *vs.* coverage curves for both nitrogen and argon.[3]

Schaeffer, Smith and Polley[5] have reported the preparation of a series of carbon blacks starting with Spheron 6 by graphitizing at successively higher temperatures up to 2700°. This provides an interesting series in which there is a gradual change from a heterogeneous surface to successively more homogeneous surfaces.

Polley, Schaeffer and Smith[6] have measured the isotherms for argon on several series of these heat-treated blacks. Their data show a progressive change, with increasing graphitization temperature, from a normal type II isotherm to isotherms of stepwise character. These authors point out that the stepwise isotherms are precisely the type which would be expected for adsorption on homogeneous surfaces, and cite the predictions of Fowler and Guggenheim,[7] of Halsey[8] and of Hill.[9] The humps in the isotherms are attributed to interaction between adsorbed molecules.

Because heat data are more susceptible to theoretical interpretation than are the isotherms alone, we have undertaken a calorimetric study of the series of graphitized Spheron carbon adsorb-

---

[1] Presented before the Division of Physical and Inorganic Chemistry at the 122nd National Meeting of the American Chemical Society in Atlantic City, N. J., September, 1952.

[2] National Research Council, Ottawa, Canada.

[3] R. A. Beebe, B. Millard and J. Cynarski, *J. Am. Chem. Soc.*, **75**, 839 (1953).

[4] J. Biscoe and B. E. Warren, *J. Appl. Phys.*, **13**, 364 (1942).

[5] W. D. Schaeffer, W. R. Smith and M. H. Polley, *Ind. Eng. Chem.*, forthcoming publication.

[6] M. H. Polley, W. D. Schaeffer and W. R. Smith, THIS JOURNAL, **57**, 469 (1953).

[7] R. H. Fowler and E. A. Guggenheim, "Statistical Thermodynamics," Cambridge University Press, Cambridge, 1939, pp. 426–444.

[8] (a) G. D. Halsey, Jr., *J. Am. Chem. Soc.*, **73**, 2693 (1951); (b) *ibid.*, **74**, 1082 (1952).

[9] T. L. Hill, *J. Chem. Phys.*, **15**, 767 (1947).

ents.[10] Moreover the heats of adsorption studies bring out differences in the monolayer, below $V/V_m = 1$, which are not apparent from the work of Polley, *et al.*

Experimental

Materials.—The parent material, Spheron 6, is an essentially non-porous commercial channel black with specific surface area 114 sq. m./g. as determined by nitrogen adsorption. The other four samples which shall be designated as Spheron (1000°), Spheron (1500°), Spheron (2000°) and Spheron (2700°) were prepared by heat treatment of the Spheron 6, at the temperatures indicated, for a period of two hours. The details of preparation and the results of X-ray and electron microscope studies of the structure of the heat-treated carbon blacks have been reported elsewhere.[5] The surface areas of the heat-treated series are given in Table I of the paper by Polley, Schaeffer and Smith[6]; our blacks were identical with the Spheron samples used by these investigators.

The argon used in the adsorption measurements and the helium used in estimating the dead space in the adsorption system were obtained from the Air Reduction Sales Company in the highest degree of purity available. No further purification of these gases was attempted. All the adsorption measurements were made at liquid nitrogen temperature.

Apparatus and Procedure.—The calorimeter and system of gas buret and manometer were identical with those previously used.[3] The calorimeter design was particularly well adapted to the present problem because the inner platinum bucket could be removed for changing samples of adsorbent. Each adsorbent sample was outgassed in the calorimeter at 200° for at least 24 hours prior to the adsorption measurements.[11] With the exception of Spheron (2000°) one complete heat run consisting of from 12 to 15 increments was made for each adsorbent. With the Spheron (2000°) black, one complete run and parts of two other runs were carried out.

As explained in a previous publication,[3] the heats as measured are isothermal heats as defined by Hill[12] and Kington and Aston.[13] Our measured heats would differ from the isosteric heats by a factor $V_G(\partial p/\partial N_s)_T$ where V_G is the volume of the dead space in the calorimeter and $(\partial p/\partial N_s)_T$ is the slope of the isotherm. This term never exceeded 10 cal./mole in any increment of any heat run of the present investigation. Since the quantity $V_G(\partial p/\partial N_s)_T$ is in all cases less than the estimated experimental error ($\pm 3\%$), this quantity has not been subtracted from the calorimetrically measured heats in obtaining the q_{st} values for the isosteric heats shown in Fig. 2.

Results

The results of the experimental work with argon on the four heat-treated carbon blacks are given graphically in Figs. 1 and 2. In Fig. 1 are shown the isotherms for the original Spheron and for the samples treated at 1000 and 2700°. To avoid complication, the isotherms for argon–Spheron (1500°) and argon–Spheron (2000°) have been omitted from Fig. 1. Actually these isotherms fit nicely into the general picture, as the volumes adsorbed at a given pressure up to $p/p_0 = 0.4$ decrease for the different samples in the order Spheron (1000°), Spheron (1500°), Spheron (2000°), and Spheron (2700°). Above $p/p_0 = 0.4$, the volumes adsorbed at a given pressure show an increase in going from Spheron (1000°) through Spheron (1500°) to Spheron (2000°) and finally to Spheron (2700°). These isotherms check with those of Polley, Schaeffer and Smith[6] for the same adsorption system. The heat-coverage curves are shown in Fig. 2. The data on Spheron (untreated material) shown in Figs. 1 and 2 for comparison are taken from previous work in this Laboratory.[3] The heat curve for argon on Spheron 6 is represented by the dotted line in Fig. 2.

Discussion

For the sake of clarity in interpreting the experimental results represented in Fig. 2, the discussion will be divided into a consideration of the various regions of coverage as given below.

1. **Beginning of the First Layer** (V/V_m = **0 to 0.4**).—In this region the differential heats undergo a regular decrease with temperature of graphitization up to 2000°, but no further change in the region between 2000 and 2700°. It has been suggested in a previous publication[3] that the initial high heats found for nitrogen or argon adsorption on Spheron may be due to adsorption in narrow, shallow depressions at the grain boundaries between parallel layer groups in the surface. With graphitization, the growth of the parallel layer groups and the increasing degree of order within these groups would tend to reduce the total length of the above depressions as well as their depth. It is reasonable to believe that such a change would result in increasingly lower initial heats of adsorption with increased graphitization.

Because there is definite evidence of lateral interaction in the second half of the monolayer (see below), it seems probable that this interaction may to some degree be in effect on a relatively bare surface. It may be that without any lateral interaction the heats in the region $V/V_m = 0$ to 0.4 would fall lower than they do experimentally.

2. **Second Part of the First Layer** (V/V_m = **0.4 to 1.0**).—In this region, the arrest in the heat-coverage curves, only slightly apparent for Spheron 6 of Fig. 2, changes into a maximum for the Spheron (1000°) sample and this maximum becomes progressively higher in passing from Spheron (1000°) on up to Spheron (2700°).

In earlier work[3] an attempt has been made to explain the relative behavior of Spheron and Graphon on the assumption that the surface of the former is energetically heterogeneous and that of the latter more homogeneous. On Spheron, the decrease in the heats with increasing coverage would then be attributed to the predominating effect of surface heterogeneity, while on the more homogeneous Graphon, lateral interaction, the effect of which is no longer obscured by that of heterogeneity, is evidenced by the resultant increase in differential heat with coverage, especially at $V/V_m = 0.5$ to 1.0. It is quite reasonable then that the maximum due to this lateral interaction

---

[10] M. H. Polley, W. D. Schaeffer and W. R. Smith[6] have prepared three series of graphitized blacks in addition to the Spheron series which we have studied. In one of these series in particular, which was derived from a furnace black (P-33) the sample graphitized at 2700° appeared to have a considerably more homogeneous surface than that of the Spheron (2700°). Unfortunately the specific surface areas of the P-33 series were too small to give us sufficient definition in the calorimetric values. For that reason we were forced to be content with studying the Spheron series.

[11] M. H. Polley, W. D. Schaeffer and W. R. Smith[6] have shown that the use of outgassing temperatures of 200° and of 1000° resulted in identical isotherms in the case of the heat-treated carbon blacks. They point out that this observation is at variance with that of Gulbransen and Andrew [*Ind. Eng. Chem.*, **44**, 1039 (1952)], in the experiments of the latter investigators with graphite.

[12] T. L. Hill, *J. Chem. Phys.*, **17**, 520 (1949).

[13] G. L. Kington and J. G. Aston, *J. Am. Chem. Soc.*, **73**, 1929 (1951).

should become increasingly prominent as the carbon black becomes more graphite-like with heat treatment.

Crowell and Young[14] have shown that the energy of binding for argon on the basal planes of graphite is virtually the same for all probable positions of the argon atom relative to the surface carbon atoms of the graphite lattice. This means that such a graphite surface would represent a system of non-localized sites for argon adsorption and would tend to permit the formation of a hexagonally close-packed monolayer of argon. It is probable that the Spheron (2700°) surface would approach but would not become identical with such a system of non-localized sites on basal planes of graphite.[15]

Orr[16] has calculated the maximum energy of interaction between an argon atom and its six nearest neighbors in a hexagonally close-packed monolayer adsorbed on a surface of non-localized sites. Using Orr's method as corrected by Young,[17] we obtain 1580 cal./mole for the interaction energy. This is more than twice the increase in the experimentally observed heats in the second half of the monolayer for Spheron (2700°), the most homogeneous member of the series of carbon adsorbents under investigation.

This discrepancy between the theoretical value for interaction and the experimentally observed height of the maximum in the first layer, is probably due to some residual heterogeneity in the graphitized carbon surface. For a valid comparison with the theoretical value we should consider the rise in heats on a homogeneous carbon surface all the way from $V/V_m = 0$ to $V/V_m = 1.0$. High initial heats due to heterogeneity at low coverage would tend to offset the absence of lateral interaction with the result that the observed rise in heats in the region from $V/V_m = 0.4$ to $V/V_m = 1.0$ would not represent the whole of the interaction energy. Moreover any lack of homogeneity in the surface would tend to lower the absolute value of the heats near $V/V_m = 1$ because there would be no sharp separation between the first and second layers.[17]

Mooi, Pierce and Smith[18] have determined the isosteric heats for ethyl chloride on Graphon in the temperature region of −78 to 75°. They comment that in general shape their curve for heats *vs.* volume adsorbed resembles those previously reported for nitrogen on Graphon at −195°,[19–21] but that the maximum in the region of V_m is higher and sharper for ethyl chloride than for nitrogen. It is true that the absolute height of the maximum for ethyl chloride is over twice the height of the maximum in the nitrogen heat curve. However, if we consider the above maxima on a basis *relative* to the total heats of adsorption, we see that the height of the maximum represents a smaller fraction of the

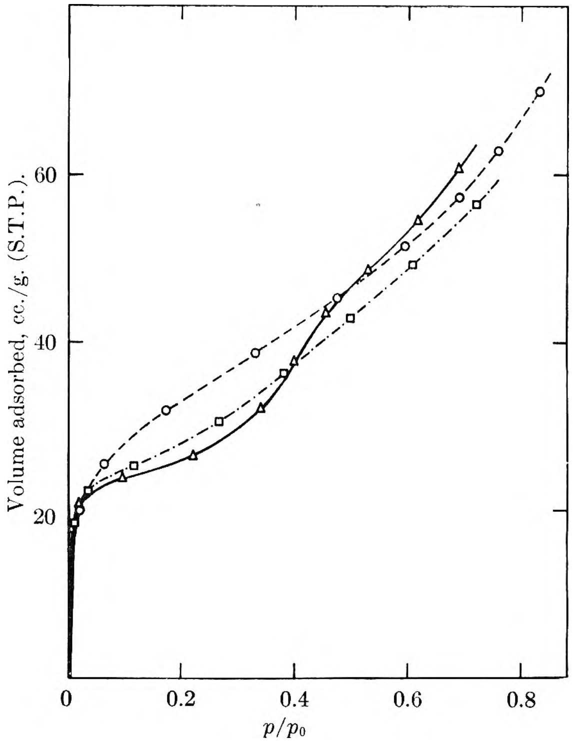

Fig. 1. —, isotherms on carbon blacks at −195°: ----O----, Spheron (untreated); ·—·□·—·, Spheron (1000°); ——Δ——, Spheron (2700°).

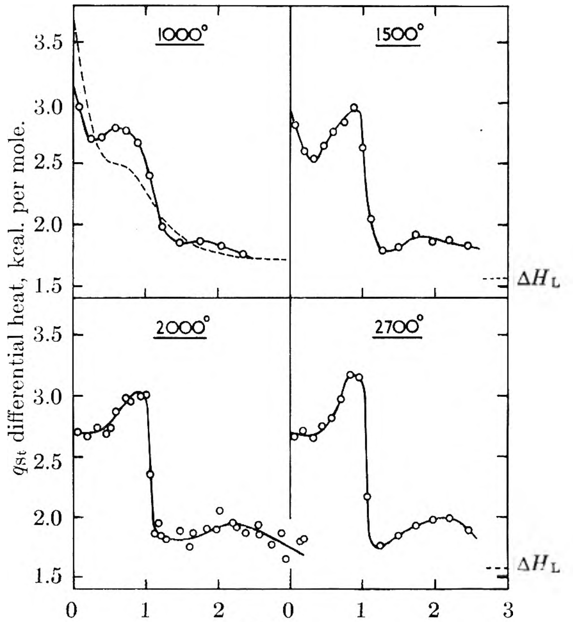

Fig. 2. —, calorimetrically measured heats of adsorption of argon on Spheron carbon blacks at −195°. Dotted line represents untreated black. Temperatures of graphitization are indicated.

---

(14) A. D. Crowell and D. M. Young, *Trans. Faraday Soc.*, forthcoming publication.

(15) The X-ray studies of the series of carbons used in the present investigation show that the samples which were graphitized at the higher temperatures approach graphite in their crystallite structure. With increasing temperature of graphitization the crystallites within the carbon black particles increase in size as well as achieving more nearly perfect ordering of the three dimensional array of carbon atoms.[5] Furthermore, the electron microscope reveals that while the parent Spheron particles are roughly spherical in shape, the graphitized samples such as Spheron (2700°) have developed flat sides due to the growth of the crystallites or parallel layer groups.[5] It seems possible that these flat sides are basal graphite planes, although we have no conclusive evidence that this is true.

(16) W. J. C. Orr, *Proc. Roy. Soc. (London)*, **A173**, 349 (1939).

(17) D. M. Young, *Trans. Faraday Soc.*, **48**, 560 (1952).

(18) J. Mooi, C. Pierce and R. N. Smith, THIS JOURNAL, **57**, 52 (1953).

(19) R. A. Beebe, J. Biscoe, W. R. Smith and C. B. Wendell, *J. Am. Chem. Soc.*, **69**, 95 (1947).

(20) L. G. Joyner and P. H. Emmett, *ibid.*, **70**, 2353 (1948).

(21) T. L. Hill, P. H. Emmett and L. G. Joyner, *ibid.*, **73**, 5102 (1951).

total heat for ethyl chloride than for nitrogen. Such an effect may be due to the higher temperature of the ethyl chloride adsorption or to a less favorable packing of the larger molecules of this adsorbate as suggested by Mooi, *et al.*, in their discussion of the absence of a hump at $2V_m$ in the ethyl chloride isotherm. It would appear that the conditions for observing the effect of lateral interaction on Graphon are less favorable for both ethyl chloride and for nitrogen than they are for argon since the maximum in the heat curve on the relative basis discussed above is highest in the case of argon.

3. The Transition from the First to the Second Layer ($V/V_m = 1$).—Not only is there an increase, with temperature of graphitization, in the heights of the maxima of Fig. 2 at the end of the first layer, but also the slope of the curves near V_m increases with increased graphitization. This evidence points to an increasingly sharp separation between the first and second layers on the increasingly homogeneous samples of graphitized carbon black.

4. The Region above V_m.—A second maximum which becomes more pronounced with degree of graphitization is revealed in Fig. 2, corroborating the results previously obtained in this Laboratory.[3] It is of interest that Mooi, Pierce and Smith[18] have recently reported a low second maximum for ethyl chloride on Graphon.

It is seen from Figs. 1 and 2 that the characteristics of the isotherms and heat-coverage curves have been considerably altered by heat treatment at 1000°. In a previous investigation[19] it was found that the heat treatment at 927° had little effect on either the isotherm or the heat-coverage curve as was attested by the similarity in adsorption characteristics of the Spheron 6 and the "devolatilized" Spheron (927° treated). It was pointed out in the earlier work[19,22] that most of the chemisorbed oxygen on the Spheron 6 had been removed even by heating to 927° and it was inferred that the underlying structure of the black had been little altered by the heat treatment. On the basis of the above observations we may conclude that a considerable change in the physical state of the surface has occurred during heat treatment in the range between 927 and 1000°. Structural changes in the carbon blacks in this temperature range have been discussed by Polley, *et al.*[6] From the work reported by Schaeffer and his co-workers[5] it appears that the major graphitization changes occur between 1000 and 2000°. This temperature range of heat treatment also produces a large change in the adsorption characteristics as is seen from Fig. 2.

Acknowledgment.—Our thanks are due to Mr. W. D. Schaeffer who prepared the new series of blacks and to Dr. W. R. Smith who called them to our attention. We are also indebted to Dr. A. D. Crowell for helpful discussions in the interpretation of our results, and to Miss H. Bienes for assistance in the experimental work.

---

[22] See also R. B. Anderson and P. H. Emmett, THIS JOURNAL, **56**, 753 (1952).

PAMPHLETS

Available for distribution from the office of

CHEMICAL ABSTRACTS

New Titles

A New General System for the Naming of Stereoisomers. A report of the Advisory Committee on Configurational Nomenclature to the Nomenclature Committee of the Division of Organic Chemistry (not official as yet). 50 cents.

Introduction to 1952 Subject Index. This contains a complete list of *organic radicals,* listed by names and formulas, as well as brief indication of organic indexing changes made because of new rulings by the International Union of Pure and Applied Chemistry. 25 cents. (Copies of this Introduction are now included as a part of the booklet entitled "The Naming and Indexing of Chemical Compounds by Chemical Abstracts," as noted below.)

ACS Committee Reports

Definitive Report of the Commission on the Reform of the Nomenclature of Organic Chemistry. Translation with comment and index by Austin M. Patterson	.20
Rules for Naming Inorganic Compounds. Report of the Committee of the International Union of Chemistry for the Reform of Inorganic Chemical Nomenclature, 1940. The committee has provided an American version of the rules	.20
The Pronunciation of Chemical Words. A committee report	.05
Nomenclature of the Hydrogen Isotopes and Their Compounds. A committee report	No charge
The Nomenclature of the Carotenoid Pigments. Report of the Committee on Biochemical Nomenclature of the National Research Council, accepted by the Committee on Nomenclature, Spelling, and Pronunciation of the American Chemical Society	No charge
The Naming of Cis and Trans Isomers of Hydrocarbons Containing Olefin Double Bonds. A committee report	No charge
The Designation of "Extra" Hydrogen in Naming Cyclic Compounds. A committee report	No charge
Avogram. A committee report	No charge
The Naming of Geometric Isomers of Polyalkyl Monocycloalkanes. A committee report	No charge
Commission de nomenclature de chimie inorganique. This relates to the names of new elements or others concerning which there has been controversy as to names. In English	.10
Commission de nomenclature de chimie biologique. A report on nomenclature de vitamines (in French)	.10
Commission de nomenclature de chimie organique. This includes rules on the nomenclature of organosilicon compounds (now covered by "Organosilicon Compounds" below), changes and additions to the Definitive Report, extended examples of radical names, and an extensive list of radical names. All in English	.50
Steroid Nomenclature. Report of the National Research Council's Subcommittee on Steroid Nomenclature (not official as yet)	.50
Arene and Arylene. A committee report	No charge
Halogenated Derivatives of Hydrocarbons. A committee report	.10
Use of "Per" in Naming Halogenated Organic Compounds. A committee report	.10
Use of "H" to Designate Position of Hydrogens in Almost Completely Fluorinated Organic Compounds. A committee report	.10
Organic Compounds Containing Phosphorus. A committee report	.25
Organosilicon Compounds. A committee report	.10
Nomenclature of Natural Amino Acids and Related Substances. A committee report	.25
Carbohydrate Nomenclature. A committee report	.25

Miscellaneous

Directions for Abstractors and Section Editors of Chemical Abstracts. Much concentrated information on nomenclature, symbols, forms, and abbreviations is assembled in this 46-page booklet in form convenient for use .... .25

The Standardization of Chemical Nomenclature. This reprint of an article by the committee chairman contains a list of references to sources of information on chemical literature.......No charge

The Naming and Indexing of Chemical Compounds by Chemical Abstracts. Introduction to the 1945 Subject Index. A comprehensive, 109-page discussion of chemical nomenclature as applied to inorganic as well as organic compounds for systematic indexing, with a classified bibliography, an index, and the following appendixes (lists): (I) Miscellaneous chemical prefixes, (II) Inorganic groups and radicals, (III) Anions, (IV) Organic groups and radicals, (V) Organic suffixes, and (VI) 1945 ring index. Included is an insert of the 6-page 1947 Subject Index Introduction to show changes and additions. 75 cents. With 1952 Introduction (see above "New Title") $1.00

Address all orders to

CHEMICAL ABSTRACTS

The Ohio State University, Columbus 10, Ohio